Giuseppe Etiope

Natural Gas Seepage

The Earth's Hydrocarbon Degassing

Springer

Natural Gas Seepage

Giuseppe Etiope

Natural Gas Seepage

The Earth's Hydrocarbon Degassing

Springer

Giuseppe Etiope
Sezione Roma 2
Istituto Nazionale di Geofisica e
Vulcanologia
Rome
Italy

and

Faculty of Environmental Science
and Engineering
Babes-Bolyai University
Cluj-Napoca
Romania

ISBN 978-3-319-14600-3 ISBN 978-3-319-14601-0 (eBook)
DOI 10.1007/978-3-319-14601-0

Library of Congress Control Number: 2014959122

Springer Cham Heidelberg New York Dordrecht London

Printed on acid-free paper

Springer International Publishing AG Switzerland is part of Springer Science+Business Media (www.springer.com)

Whatever is fluid, soft and yielding will overcome whatever is rigid and hard

Lao-Tzu 600BC

Foreword

Seepage of gases from the Earth and their chemical, physical, and biological interactions in the unsaturated zone prior to flow into the atmosphere is a field of increasing importance. The obvious role of CO_2-rich gases in volcanic and geothermal systems has been an area of specialization within the field of volcanology for a considerable period of time. More subtle flows of CH_4-rich gases have been applied sporadically and with some controversy to the field of petroleum exploration and are usually referred to as "surface geochemistry."

More recently, the environmental aspects of natural gas seepage from the Earth has become of increasing interest. Physical flow of gases to and from the unsaturated zone in response to changing barometric gradients was recognized and is generally understood. The atmospheric science community and ecologists have examined the flow of gases to and from the unsaturated or vadose zone (atmospheric exchange) in the context of biochemical processes that may modify the composition of the boundary layer of the atmosphere. The more subtle geologic processes that may be a source of gases to the atmosphere and imprint upon the recognized biochemical processes have largely been ignored or considered negligible to nonexistent. Dr. Giuseppe Etiope presents in this book a succinct overview of the geologic sources for natural (hydrocarbon-rich) gases and the geochemical processes that exert environmental influences upon atmospheric composition. This subject has been ignored in previous works and Dr. Etiope's book fills this niche. He is in a unique position to bring together this neglected topic.

Two chapters discuss the classification, distribution, and the mechanisms of gas migration in the solid earth. Two chapters discuss the techniques of detection and measurement of gas seepage, and its use for geologic and petroleum exploration. The exploration for petroleum and the recent advancements in hydraulic fracturing ("fracing" or "fracking") have heightened interest in loss of geologic methane to the atmosphere. Methane is a more potent "greenhouse gas" than carbon dioxide which has been the subject of numerous studies of its atmospheric increase in concentration since the Little Ice Age and potential contribution to global warming. Consideration of potential impacts of geologic storage of carbon dioxide and

potential for leakage from over-pressured systems is also relevant to the environmental aspects of gas seepage from the Earth. The relationship of past and present gas seepage to climate change is an important contribution of the book.

A chapter summarizes the abiotic production of gases within the Earth and how the chemical processes relate to the potential for understanding the presence of methane in the martian atmosphere. The last chapter presents an overview of the role of gases in myths of the ancient world and influences during the development of civilizations in the Mediterranean region.

Finally, a personal note: Giuseppe obtained his Ph.D. from the University of Rome, La Sapienza, in 1995. Although Giuseppe was not my student, I consider him my best "student" as he picked up where my research left off on the exchange of gases between the Earth and the atmosphere. Productive collaboration has continued to the present.

Ronald W. Klusman
Emeritus Professor of Chemistry
and Geochemistry
Colorado School of Mines

Acknowledgments

I am indebted to many who have helped me in various ways during the writing of this book. I am especially indebted to my mentors, Prof. Ronald W. Klusman (Colorado School of Mines, USA), Dr. Martin Schoell (Gas-Consult International, Berkeley, USA), and Prof. Michael J. Whiticar (University of Victoria, Canada), who shaped my understandings of gas geochemistry and seepage. Professor Klusman reviewed early drafts of Chaps. 1, 3, and 6. Dr. Schoell and Prof. Whiticar provided precious comments and suggestions for Chaps. 5 and 8. Chapter 4 was carefully reviewed by Arndt Schimmelmann (Indiana University). Dorothy Z. Oehler (NASA Johnson Space Center) reviewed the section in Chap. 7 that focused on potential seepage on Mars. Several important concepts and the data reported in the book benefited from activities, collaborations, and discussions with (in rigorous alphabetic order) Calin Baciu, Antonio Caracausi, Dimitris Christodoulou, Giancarlo Ciotoli, Bethany Ehlmann, Paolo Favali, George Ferentinos, Maurizio Guerra, Charles Holland, Hakan Hosgormez, Elena Ifandi, Artur Ionescu, Francesco Italiano, Stavroula Kordella, Keith Lassey, José Manuel Marques, Giovanni Martinelli, Adriano Mazzini, Dorothy Z. Oehler, George Papatheodorou, Arndt Schimmelmann, Barbara Sherwood Lollar, Liana Spulber, Peter Szatmari, Basilios Tsikouras, Iñaki Vadillo, and Oliver Witasse. Basic concepts and ideas on gas migration and soil-gas stemmed from the teaching of Prof. Salvatore Lombardi, supervisor of my Ph.D. thesis on gas migration in the 1990s. Special thanks go to Alexei Milkov who generously shared his innovative perspective on gas geochemistry and mud volcanoes with me. Thanks to Kimberly Mace for valuable language editing. Photos and images were kindly provided by Calin Baciu, Bethany Ehlmann, Akper Feyzullayev, Luigi Innocenzi, Dorothy Z. Oehler, George Papatheodorou, David Rumsey, Liana Spulber, and Michael J. Whiticar. Not last, I extend special thanks to the publishing editor Stephan A. Klapp, without whom this book could not have been written. Many thanks go to my wife, Olga, who patiently supported me in the journey of producing this book.

Contents

Chapter 1
Introduction

In this introductive chapter, basic concepts concerning natural gas seepage, including the terminology typically adopted for various types of seepage, the origins of gas (microbial, thermogenic, and abiotic), and the significance and implications of gas seepage for petroleum exploration, the environment, planetary geology, and astrobiology are presented. The types of surface gas occurrences that can be considered as "gas seepage" are also clarified, with special reference to the concepts of modern and fossil gas, and to the gas occurring in frozen, polar regions. The implications of natural gas seepage, both offshore and onshore, are summarised by tracing the history of its study via academia and the oil industry, and by arriving at the modern, comprehensive, and holistic view that guides this book. The arguments discussed in successive chapters are also briefly presented.

1.1 Basic Concepts and Definitions

1.1.1 What Gas Seepage Is, What It Is Not

1.1.1.1 Hydrocarbon-Rich Gas

Natural gas seepage is the steady or episodic, slow or rapid, visible or invisible flow of gaseous hydrocarbons from subsurface sources to Earth's surface. In petroleum geology literature, use of the term "seepage" is traditionally restricted to the hydrocarbon-rich gas, composed mainly of methane (CH_4) and subordinately ethane (C_2H_6), propane (C_3H_8), and butane (C_4H_{10}), that is formed in petroleum (oil and gas) prone sedimentary basins through microbial or thermal conversions of organic matter in source rocks, generally shales or limestones (e.g., Hunt 1996). As a result of its derivation from biological compounds, mainly the lipids and carbohydrates liberated by marine (sapropelic) and terrestrial (humic) organic matter, the gas is cumulatively termed "biotic". Non-hydrocarbon gases, such as CO_2, N_2, He, and H_2S, are generally also present as minor constituents. Thus, seepage does not

G. Etiope, *Natural Gas Seepage*, DOI 10.1007/978-3-319-14601-0_1

refer to geothermal or volcanic H_2O- or CO_2-rich gas manifestations (e.g., fumaroles, mofettes, and geysers) where hydrocarbons are a minor component.

In most cases, since it is almost always produced by the dewatering of coal strata and induced by mining activity, methane seepage from coal-beds is not considered to be a natural phenomenon. However, natural thermogenic gas seepage has been associated with coal-bearing strata in the Ruhr Basin (Germany), apparently unrelated to mining (Thielemann et al. 2000). In addition, Judd et al. (2007) reported extensive methane-derived authigenic carbonates associated with the coal-bearing Carboniferous rocks of the Irish Sea. Therefore, the existence of significant natural seepage related to coal-beds cannot be excluded.

Methane-rich gas can also seep from igneous or metamorphic formations such as ophiolites (mantle ultramafic rocks obducted onto continents), orogenic peridotite massifs (ultramafic rocks emplaced into mountain belts), batholiths (igneous intrusions), and crystalline shields. In these environments, methane and other hydrocarbons may have an abiotic origin not related to the degradation of organic matter (Etiope and Sherwood Lollar 2013). Abiotic gas seepage is discussed in Chap. 7.

1.1.1.2 Geological, Fossil, and Modern Methane

The methane produced in deep source rocks is "fossil", radiocarbon (^{14}C) free (i.e., carbon older than 50,000 years BP) and can be termed "geological" (Fig. 1.1). Geological methane is the natural gas humankind uses today for energy and that, together with oil, largely influences the global economy. The seepage associated

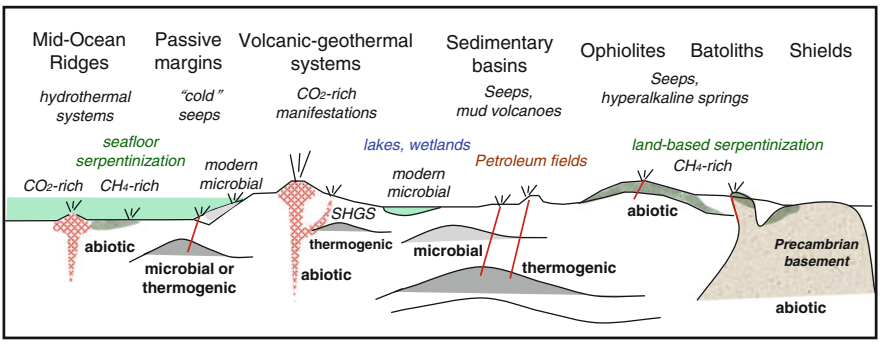

Fig. 1.1 The various geological environments for methane production on Earth. In this book, seepage refers to the surface migration of fossil methane-rich gas, including biotic (microbial and thermogenic) gas in sedimentary basins and abiotic gas from land-based serpentinisation systems. CO_2-rich volcanic and geothermal manifestations, where hydrocarbons are a minor component, as well as emissions of modern microbial methane from wetlands and shallow sediments, are not considered seepage in petroleum geology. *SHGS* Sediment-Hosted Geothermal Systems, where thermogenic methane can be transported to the surface by magmatic-hydrothemal fluids

with this fossil gas should not be confused with that of the more recent (late Pleistocene and Holocene) methane produced within shallow sediments in estuaries, deltas, bays, or trapped beneath permafrost. Some scholars may also wish, however, to consider this "recent" gas as "geological". In any case, geological gases should not be confused with those produced by very recent and contemporary microbial activity in peatlands, wetlands, lakes, and oceans. Seepage does not include these sources of gas. The distinction is particularly important when dealing with natural sources of methane in the atmosphere. Since they constitute different source strengths in inventories, have very different process-based models, and different emission factors and aerial distributions, geological and modern biochemical sources must be treated separately.

1.1.1.3 Seepage in Frozen Regions

Seepage in polar frozen regions must be given specific treatment. Methane has been extensively reported in permafrost, glaciers, and frozen lakes, and in the seafloor in Arctic regions. Gas emissions have been widely attributed to ice melting, cryosphere disintegration, and hydrate decomposition (i.e. global warming, e.g., Walter et al. 2006). In general, this methane is modern and microbially produced in very shallow sediments or aquatic systems. Most permafrost can, in fact, be considered "frozen" wetlands. When permafrost melts, gas leaks to the surface and enters the atmosphere. Based on the information provided above, such emissions should not be called seepage. However, in many instances the gas in frozen regions has been discovered to be "geological" or "fossil". Perennially frozen, ice-saturated ground and massive glacial overburden may form a low permeability cap for methane migrating from the subsoil. If the cap melts, gas leaks to the surface; this type of emission can be defined as seepage. Also, some deeper permafrost containing thermogenic methane (e.g., Collett and Dallimore 1999) may be considered to be a sort of "frozen seepage". Polar regions have petroleum systems just as non-polar regions and are not special places for geological gas generation and seepage; but places where seepage can be temporarily "blocked" and released in a shifting balance between endogenic (gas pressure build-up, geothermal heat flow, and fracturing) and exogenic (climate and meteorology) factors. Recent studies have observed and measured unblocked seepage (e.g., Walter Anthony et al. 2012). Since no observations were obtained until 20–30 years ago, it is not easy to determine whether or not this type of seepage is the result of present, post-industrial climate change. An alternative is an ancient, pre-industrial natural change, or a change as recent as the accepted end of the "Little Ice Age" (approximately 1850). At this point in time, it is even possible that the process is only partially driven by cryosphere changes.

1.1.2 A Jungle of Names: Seeps, Macroseeps, Microseepage, Microseeps, and Miniseepage

In all cases of biotic and abiotic gas, seepage can lead to visible, focused gas manifestations or invisible but widespread exhalations from the soil. Focused manifestations are called "seeps" or "macro-seeps" (rarely written as "macroseeps") while widespread dispersed exhalation is called "microseepage" (more rarely written as "micro-seepage"). The first category includes mud volcanoes, not to be confused with traditional, magmatic volcanoes. There are, however, additional seepage types and names, such as microseeps and miniseepage, that are sometimes improperly used in the scientific literature, creating some confusion. All of the terminology, as well as typical flux values by name type, are provided in Chap. 2. In general, the term "seep" should only be used to indicate a point source (vent type, with a flow rate measurable as mass/time e.g., grams/day). The suffix "-page" is provided to indicate an areal source (exhalation type, with flow rate measured as mass/area/time, e.g., grams m^{-2} day^{-1}), or the phenomenon in general. "Seep" is also used for oil (liquid petroleum or, more generally, liquid range hydrocarbons); so there are "oil seeps" or "oil macroseeps" and "oil microseeps", but there is no "oil microseepage".

1.1.3 Seepage id est Migration

Gas seepage implies the long-distance movement of gas that can be on the order of several kilometers. Two main categories of fluid migration mechanisms exist: (1) diffusion, ruled by Fick's Law, where gas moves by concentration gradients; and (2) advection, ruled by Darcy's Law, where movement is determined by pressure gradients. Both mechanisms are described in Chap. 3. Advection is the leading mechanism for seeps and microseepage. The velocity of movement is determined by the permeability of rock crossed by the gas and the pressure gradients induced by gas pressure at the starting point of migration (source rock or secondary accumulations). Seepage, therefore, reflects the permeability of the subsurface and may provide considerable information for structural geology. Gas, in fact, follows preferential pathways of movement (less resistance paths), as determined by fractures and faults. Thus, a seep is frequently an indication of a fault (Chap. 5).

1.1.4 Microbial, Thermogenic, and Abiotic Methane

At this point it is useful to recall the basic geochemical concepts and features that characterize methane and other gaseous hydrocarbons of "geological" origin. Natural gas geochemistry based on the molecular and isotopic composition of

methane, ethane, propane, and butane is widely described in books (e.g., Tissot and Welte 1984; Hunt 1996) and articles, beginning with the pioneering works of Stahl (1977), Bernard et al. (1978), Sackett (1978), Schoell (1980), Rice and Claypool (1981), Whiticar et al. (1986), Faber (1987), Chung et al. (1988) and Schoell (1988) to the recent fundamental works and models of Berner and Faber (1996), Lorant et al. (1998), Whiticar (1999), Tang et al. (2000), Mango (2001), and Milkov (2011). The list above is not exhaustive (apologies to those who are not cited) but includes the most referenced works for origin interpretations of natural gas related to petroleum. Additional studies have focused on the abiotic origin of natural gas, typically found in igneous rocks. For up-to-date information, the reader is referred to recent review articles by Etiope and Sherwood Lollar (2013), McCollom (2013), and Etiope and Schoell (2014).

Here, for those without specialized knowledge of natural gas geochemistry, a brief summary is provided of the main definitions and interpretative criteria that allow the differentiation of the three main classes of natural gas (microbial, thermogenic, and abiotic) that are the object of seepage. Basic genetic diagrams are provided in Fig. 1.2. The application of such criteria to gas seeps in petroleum system assessments is discussed in Chap. 5.

Microbial (or biogenic) gas is produced during the diagenesis of sediments (see Hunt 1996) by specialised microbial communities (Archaea) at relatively low temperatures (typically up to 60–80 °C; or up to 120 °C or more by extremophiles in special hydrothermal systems). Microbes predominantly produce methane, subordinately ethane and, likely, trace amounts of propane (Formolo 2010). The term "bacterial methane" is also used in the literature. However, it should be remembered that *Bacteria* do not produce methane, only *Archaea*. Microbial gas is very dry, i.e., it consists almost entirely of methane. Generally (but not always), such a gas indicates relatively shallow gas source rocks and reservoirs. Thermogenic gas is produced in deeper rocks by the thermal cracking of organic matter (catagenesis) or oil at higher temperatures, typically up to 190–200 °C (Hunt 1996). Thermogenic gas can be independent from or associated with oil reservoirs and can have variable amounts of ethane, propane, butane, and condensate (C_{5+} hydrocarbons). As anticipated and as a result of its derivation from biological compounds, microbial and thermogenic gas is cumulatively termed "biotic". Abiotic gas, instead, is produced by chemical reactions that do not require the presence of organic matter. These reactions include magmatic processes and gas-water-rock reactions (for example Fischer Tropsch type reactions) occurring over a wide range of temperatures (see Etiope and Sherwood Lollar 2013). Trace amounts of abiotic hydrocarbons (typically parts per million by volume) occur in volcanic and geothermal fluids, but considerable amounts of methane, reaching orders of 80–90 vol.%, have been discovered in an increasing number of sites in Precambrian crystalline shields and serpentinised ultramafic rocks in mid-ocean ridges and in land-based ophiolites, peridotite massifs, and igneous intrusions. The details are discussed in Chap. 7.

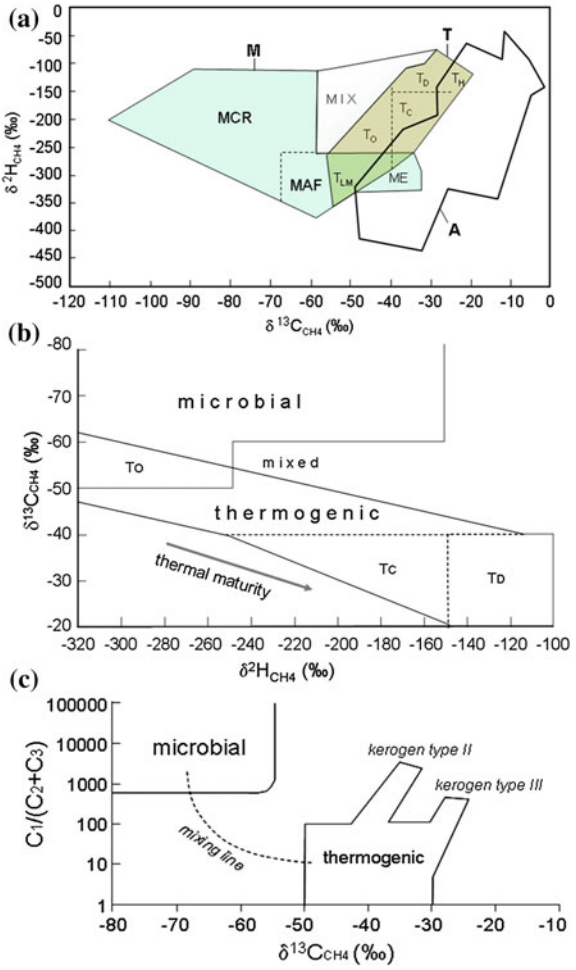

Fig. 1.2 The basic geochemical tools to determine the origin of natural gas. **a** and **b** are two recent versions of Schoell's plot, or C and H isotope diagrams (redrawn from Etiope and Sherwood Lollar 2013 and Etiope et al. 2013b, based on Schoell 1980 and new empirical data). Also see Fig. 7.4. **c** is the Bernard diagram (redrawn from Bernard et al. 1978). *M* microbial; *T* thermogenic; *A* abiotic; *MCR* microbial carbonate reduction; *MAF* microbial acetate fermentation; *ME* microbial in evaporitic environment; T_O thermogenic with oil; T_C thermogenic with condensate; T_D dry thermogenic; T_H thermogenic with high-temperature CO_2–CH_4 equilibration; and T_{LM} thermogenic low maturity

The first step for identifying the origin of natural gas is to analyse the composition of the stable isotopes of carbon ($^{13}C/^{12}C$) and hydrogen ($^{2}H/^{1}H$) in methane (expressed as $\delta^{13}C$ and $\delta^{2}H$ in ‰ (per mil) relative to Vienna Pee Dee Belemnite, VPDB, and Vienna Standard Mean Ocean Water, SMOW, standards; e.g., Schoell (1980)). Results are typically plotted in a "Schoell's diagram", an empirical diagram that differentiates the genetic fields of microbial, thermogenic, and abiotic methane. Two modern versions of this diagram are presented in Fig. 1.2a, b. Worldwide, occurrences of thermogenic and microbial gases have a well-defined distribution in regards to carbon and hydrogen isotopes. Microbial methane is generally characterized by $\delta^{13}C$ values lower than −50 ‰. Thermogenic methane is

typically plotted in the range between −50 and −30 ‰, but highly mature gas can reach values of −20 ‰. Abiotic CH_4 has a wide range of $\delta^{13}C$ and $\delta^{2}H$ values and, although overlapping with parts of both the microbial and thermogenic fields, is characterised by an overall shift towards more ^{13}C-enriched and more ^{2}H-depleted values (Chap. 7).

The second step in identification is to check the relative abundance of methane (C_1), ethane (C_2), and propane (C_3) using the Bernard ratio, $C_1/(C_2 + C_3)$. Microbial gas generally has a Bernard ratio >500. Use of this ratio in relation to $\delta^{13}C$ is beneficial for determining the mixing between microbial and thermogenic gas (Fig. 1.2c) that frequently occurs in many reservoirs. The wetness of the gas, expressed as $\Sigma C_{2-5}/\Sigma C_{1-5}$ (i.e., Jenden et al. 1993), is another useful parameter for assessing mixing processes and the level of gas maturity. During the first stages of catagenesis, at relatively low temperatures (low maturity), gas is "wet" (i.e. rich in alkanes heavier than methane, ethane C_2, to pentane C_5). Wetness can range between 10 and 100. With increasing temperature and maturity gas becomes "dry", less rich in C_2–C_5 due to the thermal cracking of heavy alkanes. Wetness can drop to values below one. If the carbon isotopic composition is not evaluated, this type of dry thermogenic gas can be confused with microbial gas that generally has a wetness <0.1.

Additional important interpretative steps include those based on the relationship between the $\delta^{13}C$ of methane and ethane with the maturity of source rocks (Berner and Faber 1996) and those based on the isotopic composition of non-hydrocarbon gases (especially CO_2 and N_2). In Chap. 5, specific examples are provided for determining gas origins and secondary alterations in seeps. However, it is important for geochemical data to always be interpreted in the geological context. For understanding the origin of a given gas species (or the reason why a gas species is abundant within a given system), a detailed examination of associated gases and a verification of all possible local geological controls is required. Similar geochemical parameters may in fact refer to different origins or processes if the geological context is different.

1.2 Significance of Seepage and Implications

1.2.1 Seepage and Petroleum Exploration

In general, gas seepage results from the vertical migration of gas from subsurface accumulations of hydrocarbons or reservoirs, whether or not they are commercially significant. For this reason, seepage has historically been an important driver of global petroleum exploration. Many large oil and gas fields in North America, Europe, the Caspian Basin, Asia, and the Caribbean were, in fact, discovered after drilling in the vicinity of seeps (Link 1952; Macgregor 1993; Abrams 2005).

The link between seeps and hydrocarbon reservoirs has been verified by multiple lines of evidence, including geochemical analyses and seismic profiles. A recent compilation of papers edited by Aminzadeh et al. (2013) focused on the use of new technologies designed to image seeps for exploration and field development applications. In the past, microseepage was investigated for hydrocarbon exploration with alternate outcomes and opinions (Philp and Crisp 1982; Price 1986; Klusman 1993; Tedesco 1995). Today, it is studied using new gas detection techniques, the details of which are provided in Chaps. 4 and 5.

1.2.2 Marine Seepage on the Crest of the Wave

Gas seepage was and is still today the object of a wide body of research within the marine environment. Since the discovery by King and MacLean (1970) of peculiar gas seepage features on the seabed called "pockmarks", countless oceanographic cruises have reported the widespread occurrence of "cold seeps", including carbonate mounds and chimneys and mud volcanoes on continental shelves (e.g., Judd and Hovland 2007). These types of seeps were revealed to have enormous significance for biology, as they fuel chemosynthesis-based benthic organisms and represent specific, unique ecosystems and habitats. Since they may be sensitive to seismicity and may induce seabed instability and slope failures, cold seeps can also be important for geohazard monitoring in the petroleum industry. Over the past three decades, studies of seeps within the marine environment, with the involvement of leading marine research institutes in Europe, the Americas, and Asia, have been dominant in terms of information. Due to the vast literature produced by marine institutes, the term "gas seepage" has almost exclusively been associated with the marine environment (e.g., Judd 2000; Kvenvolden et al. 2001). With the exception of some large mud volcanoes, onshore seeps have received little attention in the scientific literature and have remained within the domain of interest of the oil industry. A consequence of this trend is that in review papers focused on global methane emissions to the atmosphere (e.g., Crutzen 1991) and in early reports, from 1990 to 2007, of the Intergovernmental Panel on Climate Change (IPCC (Prather et al. 2001)), geological gas sources were missing or included only as submarine seeps and related gas hydrates (see Sect. 6.4.1.1). The first review article on methane sources that also discussed onshore seepage was Lacroix (1993). Because marine studies provided very few data points for gas fluxes entering the atmosphere (and there were no onshore seepage studies), geological methane emissions were globally ranked as a minor source as compared with other natural sources. Within the past few years this view has drastically changed, thanks to a long series of seepage studies on land beginning with the pioneering work of Prof. Ronald Klusman of the Colorado School of Mines.

1.2.3 From Sea to Land

Ronald Klusman was one of the first scholars to apply the closed-chamber method for gas flux measurements in petroleum geology, a technique more widely employed in biological soil respiration studies (the details are discussed in Chap. 4). Since the 1930s, the occurrence of methane and light alkanes adsorbed in soils or present as a free gas in soil pore space (soil-gas) has been extensively utilized by geologists and geochemists as a tool for oil and gas exploration (e.g., Laubmeyer 1933; Horvitz 1969; Jones and Drozd 1983; Schumacher and Abrams 1996). However, studies such as those listed above have focused exclusively on the detection of anomalous concentrations of hydrocarbons (and associated geophysical or other geochemical indicators). Due to increased complexity as compared to simple compositional measurements, soil–atmosphere flux measurements were not performed. Understanding the impact on the atmosphere was not an objective. However, as it provides dynamic information of the seepage system's activity and response to gas pressure potentials, Klusman et al. (2000) suggested that knowing the gas flux is also useful for petroleum exploration. As discussed in Chap. 5, by utilizing both the molecular and isotopic composition of gas, flux can be a formidably informative parameter for understanding petroleum systems.

Klusman indirectly recognised an important phenomenon, intrinsically obvious for petroleum geologists but ignored by experts in soil and atmospheric greenhouse gas emissions, as follows: dry soil is not always a methane sink (Klusman et al. 1998). In general, soil that is not flooded or that does not have relevant quantities of water within its pores, such as grasslands or forest soils in temperate climates, absorbs methane from the atmosphere as a result of methanotrophic oxidation by CH_4-consuming bacteria. Therefore, the soil-atmosphere methane flux is negative (i.e., methane flows from the atmosphere to the soil). In seepage areas, the amount of methane migrating from the subsoil to the soil may overcome methanotrophic consumption and net gas flux becomes positive, from the soil to the atmosphere. As discussed in Chap. 6, that microseepage is quite common and pervasive within all petroliferous and sedimentary basins is now evident, making it a globally important source of methane to the atmosphere (Etiope and Klusman 2010).

Today, a vast gas flux dataset from seeps and microseepage is available from the hydrocarbon-prone sedimentary basins of Europe, North America, and Asia (e.g., Etiope 2009; Etiope et al. 2011, 2013a; and references therein). The characteristic fluxes of the various types of seepage (emission factors), as well as their geographic distribution, are now known. Notwithstanding the uncertainties inherent in extrapolations and bottom-up estimation procedures, mainly related to the uncertainties associated with the actual global area of microseepage, today, onshore seepage is considered to be a major source of methane to the atmosphere. As discussed in greater detail in Chap. 6, and as recently outlined in the assessment reports of the US-EPA (2010) and the IPCC in 2013 (Ciais et al. 2013), total geological methane emissions, including onshore and offshore seepage and geothermal manifestations, are the second most important natural source of methane after wetlands (e.g., Etiope 2012).

1.2.4 A New Vision

Today, we have a more complete picture of the various types of seepage, its global distribution, either on land or in the marine environment, and gas chemistry. A new and important concept is that of the Petroleum Seepage System (PSS) introduced in the 2000s. The PSS is defined as (Abrams 2005) "the interrelationships among total sediment fill, tectonics (migration pathway), hydrocarbon generation (source and maturation), regional fluid flow (pressure regime and hydrodynamics), and near-surface processes (zone of maximum disturbance)". The PSS is part of the Total Petroleum System (TPS), a term used in petroleum geology (Magoon and Schmoker 2000) to describe the entire hydrocarbon-fluid system in the lithosphere (that can be mapped), including the essential elements and processes required for oil and gas accumulations, migrations, and seeps. The concept presumes that migration pathways must exist, either now or in the past, connecting the provenance with accumulations. Seeps are not an exception, but a common, integral component of a TPS. The PSS would then be the connection between the TPS and Earth's surface. Abrams (2005) also indicated that "Understanding the Petroleum Seepage System, hence petroleum dynamics of a basin, is key to understanding and using near-surface geochemical methods for basin assessment and prospect evaluation." TPS and PSS concepts call attention to the fact that petroleum accumulations are not totally closed, isolated, and sealed compartments. Gas (and oil) frequently leak from reservoirs through cap rocks, even in large and productive fields, implying that perfect sealing is not necessary for having a commercial reservoir. Seeps are not a problem, but an opportunity.

Today, we understand that the importance of seepage is not limited to petroleum exploration and sea-floor biology, and that, as a source of methane to the atmosphere, onshore seepage is likely more important than seeps within the marine environment. Natural gas seepage has a wider range of social, economic, and environmental implications, some of which have already been mentioned. The entire picture is summarized in the following and in Fig. 1.3, with references to several of the arguments discussed within this book.

(a) In field geology, seeps are effective indicators of tectonic discontinuities and rock formations with enhanced secondary permeability (Sect. 5.1).
(b) In petroleum exploration, seeps can be used as a natural "window" to subsurface petroleum systems; specifically, the geochemical (molecular and isotopic) features of seeping gas may allow investigators to assess, prior to drilling, the nature and quality of hydrocarbon reservoirs and related source rocks (Sects. 5.2 and 5.3).
(c) As a result of the explosive and toxicological properties of methane and hydrogen sulphide, and due to mud eruptions and the degradation of the geotechnical properties of soil foundations, certain gas seeps can represent hazards for humans and buildings (Sect. 6.1).

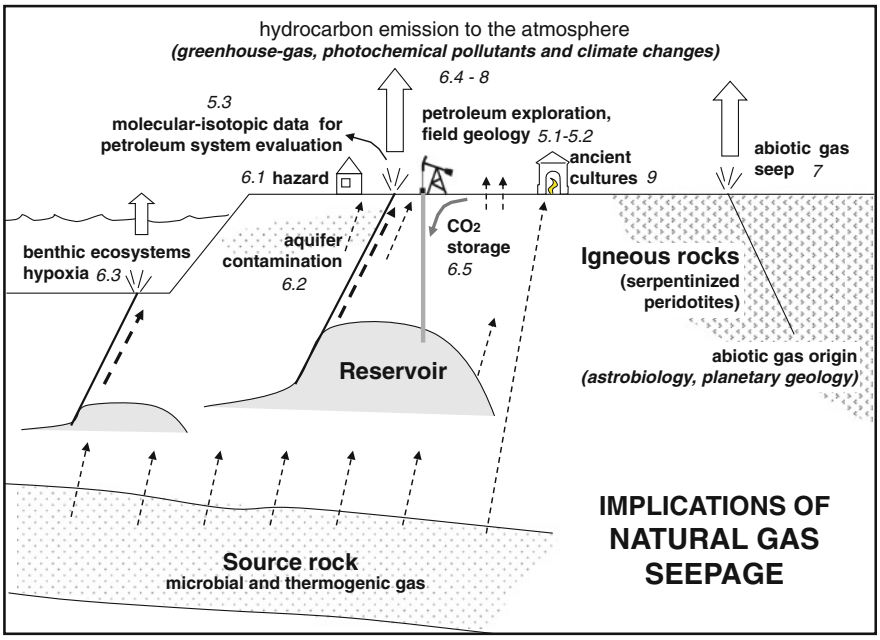

Fig. 1.3 Summary of the implications of natural gas seepage as discussed in this book. Numbers indicate the specific chapters in which particular processes are addressed

(d) In environmental impact studies, knowledge of gas seepage is essential for determining natural versus anthropogenic causes of aquifer or soil pollution (stray gas), as for the recent and controversial case of shale-gas production (Sect. 6.2).

(e) Gas seepage in marine and lake environments can reduce the amount of oxygen dissolved within the water column (hypoxia), with consequent impacts on aquatic ecosystems and fisheries (Sect. 6.3).

(f) The significant impact of gas seepage on contemporary atmospheric budgets of hydrocarbons has been established and is not limited to the greenhouse gas (methane) but also includes photochemical pollutants (ethane and propane) (Sect. 6.4).

(g) In the geological disposal of CO_2 in deep sedimentary rocks, microseepage may reveal permeable pathways that can be used by the injected CO_2 to again escape to the surface; more important, the injection of CO_2 in depleted petroleum fields increases the reservoir's fluid pressure which may trigger a new seepage of gaseous hydrocarbons to the atmosphere (Sect. 6.5).

(h) Abiotic gas seepage from serpentinised igneous rocks seems to be more widespread than previously understood. Understanding the environments and mechanisms of abiotic CH_4 generation may improve models of the origin of life (Sect. 7.1). One of the possible origins of abiotic methane, in fact, refers to

the Sabatier reaction between CO_2 and H_2 producing CH_4 and H_2O considered to be the fundamental transition from inorganic to organic chemistry that preceded biologic evolution. In the study of the origin and occurrence of hydrocarbons on other planets (e.g., methane on Mars), abiotic gas seepage can be considered to be a terrestrial analog; Sect. 7.2).

(i) Methane seepage may have played a role in past climate change (Chap. 8). Seepage may have contributed to the variations in atmospheric methane concentrations and the consequent greenhouse-gas effect on various geological time scales. Such an outcome is suggested by several proxies and has been hypothesised in recent models that re-evaluate the role of buried organic carbon and thermogenic methane production in atmosphere-ocean-biosphere-geosphere interactions.

(j) Finally, gas and oil seeps have had a peculiar role in ancient cultures, driving mythological legends, religious traditions, and contributing to human civilization (Chap. 9).

Important to understand is that the story begins and ends with a fundamental learning: gas seepage is more common and diffuse than generally considered. Gas seepage is a planetary process, widespread worldwide, that influences and conditions all of Earth's external "spheres", whether hydrosphere, atmosphere, cryosphere, biosphere, or anthroposphere. Recalling Greek and oriental philosophical visions of nature, seepage is like "pneuma" or "Tao", permeating most of Earth's systems. On a more technical level it can be considered to be "Earth's hydrocarbon degassing", alluding to the degassing of the crust. The role of the deep parts of the planet and the mantle are likely negligible. However, wide-ranging is the debate on the origin and migration of mantle abiotic hydrocarbons (Etiope and Sherwood Lollar 2013). The broader concept of Earth's degassing must not be limited to volcanoes and CO_2-rich geothermal manifestations. In this "holistic" perspective, gas seepage and its implications can only be fully understood through transdisciplinary and multidisciplinary scientific research. Such a vision may have far-reaching implications, of which, at the time of this writing, we understand only a portion.

References

Abrams MA (2005) Significance of hydrocarbon seepage relative to petroleum generation and entrapment. Mar Pet Geol 22:457–477

Aminzadeh F, Berge T, Connolly D, O'Brien G (eds) (2013) Hydrocarbon Seepage: from source to surface. AAPG/SEG Special Publication, Geophysical Developments No. 16, 256 pp

Bernard BB, Brooks JM, Sackett WM (1978) Light hydrocarbons in recent Texas continental shelf and slope sediments. J Geophys Res 83:4053–4061

Berner U, Faber E (1996) Empirical carbon isotope/maturity relationships for gases from algal kerogens and terrigenous organic matter, based on dry, open-system pyrolysis. Org Geochem 24:947–955

Ciais P, Sabine C, Bala G, Bopp L, Brovkin V, Canadell J, Chhabra A, DeFries R, Galloway J, Heimann M, Jones C, Le Quéré C, Myneni RB, Piao S, Thornton P (2013) Carbon and other biogeochemical cycles. In: Stocker TF et al. (eds) Climate change 2013: the physical science basis. Contribution of working group I to the fifth assessment report of IPCC. Cambridge University Press, Cambridge, UK and New York, NY, USA

Chung HM, Gormly JR, Squires RM (1988) Origin of gases hydrocarbons in subsurface environments: theoretical considerations of carbon isotope distribution. Chem Geol 71:97–104

Collet TS, Dallimore SR (1999) Hydrocarbon gases associated with permafrost in the Mackenzie Delta, Northwest Territories, Canada. Appl Geochem 14:607–620

Crutzen PJ (1991) Methane's sinks and sources. Nature 350:380–381

Etiope G (2009) Natural emissions of methane from geological seepage in Europe. Atmos Environ 43:1430–1443

Etiope G (2012) Methane uncovered. Nat Geosci 5:373–374

Etiope G, Drobniak A, Schimmelmann A (2013a) Natural seepage of shale gas and the origin of "eternal flames" in the Northern Appalachian Basin, USA. Mar Pet Geol 43:178–186

Etiope G, Ehlmann B, Schoell M (2013b) Low temperature production and exhalation of methane from serpentinized rocks on Earth: a potential analog for methane production on Mars. Icarus 224:276–285

Etiope G, Klusman RW (2010) Microseepage in drylands: flux and implications in the global atmospheric source/sink budget of methane. Glob Plan Change 72:265–274

Etiope G, Nakada R, Tanaka K, Yoshida N (2011) Gas seepage from Tokamachi mud volcanoes, onshore Niigata Basin (Japan): origin, post-genetic alterations and CH_4-CO_2 fluxes. Appl Geochem 26:348–359

Etiope G, Schoell M (2014) Abiotic gas: atypical but not rare. Elements 10:291–296

Etiope G, Sherwood Lollar B (2013) Abiotic methane on Earth. Rev Geophys 51:276–299

Faber E (1987) Zur Isotopengeochemie gasförmiger Kohlenwasserstoffe. Erdöl Erdgas Kohle 103:210–218

Formolo M (2010) The microbial production of methane and other volatile hydrocarbons. In: Kenneth N (ed) Timmis handbook of hydrocarbon and lipid microbiology, Springer, New York. pp 113–126

Horvitz L (1969) Hydrocarbon geochemical prospecting after 20 years. In: Heroy W (ed) Unconventional methods in exploration for petroleum and natural gas. Southern Methodist University Press, Dallas, pp 205–218

Hunt JM (1996) Petroleum geochemistry and geology. W.H. Freeman and Co, New York, 743 pp

Jenden PD, Drazan DJ, Kaplan IR (1993) Mixing of thermogenic natural gases in northern Appalachian basin. AAPG Bull 77:980–998

Jones VT, Drozd RJ (1983) Predictions of oil and gas potential by near-surface geochemistry. AAPG Bull 67:932–952

Judd AG (2000) Geological sources of methane. In: Khalil MAK (ed) Atmospheric methane: its role in the global environment. Springer-Verlag, New York, pp 280–303

Judd AG, Croker P, Tizzard L, Voisey C (2007) Extensive methane-derived authigenic carbonates in the Irish Sea. Geo-Mar Lett 27:259–268

Judd AG, Hovland M (2007) Seabed fluid flow: impact on geology, biology and the marine environment. Cambridge University Press, Cambridge

King LH, MacLean B (1970) Pockmarks on the Scotian shelf. Geol Soc Am Bull 81:3141–3148

Klusman RW (1993) Soil Gas and Related Methods for Natural Resource Exploration. Wiley, Chichester, p 483

Klusman RW, Jakel ME, LeRoy MP (1998) Does microseepage of methane and light hydrocarbons contribute to the atmospheric budget of methane and to global climate change? Assoc Petrol Geochem Explor 11:1–55

Klusman RW, Leopold ME, LeRoy MP (2000) Seasonal variation in methane fluxes from sedimentary basins to the atmosphere: results from chamber measurements and modeling of transport from deep sources. J Geophys Res 105D:24,661–24,670

Kvenvolden KA, Lorenson TD, Reeburgh W (2001) Attention turns to naturally occurring methane seepage. EOS 82:457

Lacroix AV (1993) Unaccounted-for sources of fossil and isotopically enriched methane and their contribution to the emissions inventory: a review and synthesis. Chemosphere 26:507–557

Laubmeyer G (1933) A new geophysical prospecting method, especially for deposits of hydrocarbons. Petrol Lond 29:14

Link WK (1952) Significance of oil and gas seeps in world oil exploration. AAPG Bull 36: 1505–1540

Lorant F, Prinzhofer A, Behar F, Huc AY (1998) Isotopic (^{13}C) and molecular constraints on the formation and the accumulation of thermogenic hydrocarbon gases. Chem Geol 147:249–264

Macgregor DS (1993) Relationships between seepage, tectonics and subsurface petroleum reserves. Mar Pet Geol 10:606–619

Magoon LB, Schmoker JW (2000) The total petroleum system—the natural fluid network that constraints the assessment units. U.S. Geological Survey World Petroleum Assessment 2000, description and results: USGS digital data series 60, World Energy Assessment team, p 31

Mango FD (2001) Methane concentrations in natural gas: the genetic implications. Org Geochem 32:1283–1287

McCollom TM (2013) Laboratory simulations of abiotic hydrocarbon formation in Earth's deep subsurface. Rev Miner Geochem 75:467–494

Milkov AV (2011) Worldwide distribution and significance of secondary microbial methane formed during petroleum biodegradation in conventional reservoirs. Org Geochem 42:184–207

Philp RP, Crisp PT (1982) Surface geochemical methods used for oil and gas prospecting. A review. J Geochem Explor 17:1–34

Prather M, Ehhalt D, Dentener F, Derwent RG, Dlugokencky E, Holland E, Isaksen ISA, Katima J, Kirchhoff V, Matson P, Midgley PM, Wang M (2001) Chapter 4. Atmospheric chemistry and greenhouse gases. In: Houghton JT et al (eds) Climate change 2001: the scientific basis, Cambridge University Press, Cambridge. pp 239–287

Price LC (1986) A critical overview and proposed working model of surface geochemical exploration. Unconventional methods in exploration for petroleum and natural gas IV, Southern Methododist University Press, pp 245–309

Rice DD, Claypool GE (1981) Generation, accumulation, and resource potential of biogenic gas. AAPG Bull 65:5–25

Sackett WM (1978) Carbon and hydrogen isotope effects during the thermocatalytic production of hydrocarbons in laboratory simulation experiments. Geochim Cosmochim Acta 42:571–580

Schoell M (1980) The hydrogen and carbon isotopic composition of methane from natural gases of various origins. Geochim Cosmochim Acta 44:649–661

Schoell M (ed) (1988) Origins of Methane in the Earth. Chem Geol 71, 265 pp

Schumacher D, Abrams MA (1996) Hydrocarbon migration and its near surface expression. AAPG Memoir 66:446 pp

Stahl WJ (1977) Carbon and nitrogen isotopes in hydrocarbon research and exploration. Chem Geol 20:121–149

Tang Y, Perry JK, Jenden PD, Schoell M (2000) Mathematical modeling of stable carbon isotope ratios in natural gases. Geochim Cosmochim Acta 64:2673–2687

Tedesco SA (1995) Surface geochemistry in petroleum exploration. Chapman & Hall, New York, pp 206

Thielemann T, Lucke A, Schleser GH, Littke R (2000) Methane exchange between coal-bearing basins and the atmosphere: the Ruhr Basin and the Lower Rhine Embayment, Germany. Org Geochem 31:1387–1408

Tissot BP, Welte DH (1984) Petroleum formation and occurrence. Springer, New York

US Environmental Protection Agency - EPA (2010) Methane and nitrous oxide emissions from natural sources. EPA Rep. 430-R-10-001, Off. of Atmos. Programs, Washington, DC

Walter KM, Zimov SA, Chanton JP, Verbyla D, Chapin FS III (2006) Methane bubbling from Siberian thaw lakes as a positive feedback to climate warming. Nature 443:71–75

Walter Anthony KM, Anthony P, Grosse G, Chanton J (2012) Geologic methane seeps along boundaries of Arctic permafrost thaw and melting glaciers. Nat Geosci 5:419–426

Whiticar MJ, Faber E, Schoell M (1986) Biogenic methane formation in marine and freshwater environments: CO_2 reduction versus acetate fermentation - isotope evidence. Geochim Cosmochim Acta 50:693–709

Whiticar MJ (1999) Carbon and hydrogen isotope systematics of bacterial formation and oxidation of methane. Chem Geol 161:291–314

Chapter 2
Gas Seepage Classification and Global Distribution

The surface expressions of natural gas seepage can be classified on the basis of spatial dimension, visibility, and fluid typology, as summarised in the following scheme:

- Macro-seeps
  - Focused flow
    - Gas seeps (*gas only*)
    - Oil seeps (*gas and oil*)
    - Gas-bearing springs (*dissolved gas*)
    - Mud volcanoes (*gas, water and sediments*)
  - Diffuse flow — Miniseepage (invisible)
- Microseepage
  - Diffuse flow — (invisible, independent from macro-seeps)

Macro-seeps (or seeps) are "channelled" flows of gas, typically related to fault systems. Gas flux is expressed in terms of mass/time (e.g., kg/day or tons/year). Microseepage is the pervasive, widespread exhalation of gas throughout relatively large areas, conceptually independent from seeps, even if also enhanced along faults. Gas flux is expressed in terms of mass/area/time (for methane it is usually in mg m^{-2} day^{-1}). Sometimes the term "micro-seeps" is used in the scientific literature, especially in the marine environment (e.g., Hovland et al. 2012) to define relatively smaller seeps, not observable, for example, by hydroacoustic methods. However, the term can be misleading as it may be confused with microseepage. The classification in the above scheme is, in theory, valid for either subaerial (land-based) or underwater (marine and lake) environments. As discussed in Sect. 2.3, the marine environment can have specific gas-seepage structures.

G. Etiope, *Natural Gas Seepage*, DOI 10.1007/978-3-319-14601-0_2

2.1 Macro-Seeps

2.1.1 Gas Seeps

Gas seeps are fluid manifestations that release only a gaseous phase (Figs. 2.1 and 2.2). They can also be called "dry seeps". Gas may vent from outcropping rocks, through the soil horizon, or through river/lake beds. Since surface water is only crossed by gas flow, gas bubbling from groundwater filled wells, or other shallow water bodies, should be considered dry seeps. Gas seeps may also manifest with strong odours, an absence of vegetation, wet bubbly ground, abnormal snow-melt patterns, and may lead to soil temperature anomalies. As discussed in greater detail in Sect. 5.3, the origin of the gas is mainly thermogenic (and abiotic in special cases, see Chap. 7), and subordinately microbial and mixed.

Methane-rich gas flowing through rocks and dry soil can self-ignite and produce so-called "eternal fires", the presence of a continuous flame as reported in historical records. However, any dry gas seep with a sufficiently focused and intense CH_4-rich gas flow can burn by artificial ignition, for example, with a lighter. "Eternal flames", such as those of Yanardag in Azarbaijan, Baba Gurgur in Iraq, or Chimaera in Turkey (Fig. 2.2), have particular charm and as discussed in Chap. 9 are frequently associated with ancient religious traditions and myths.

Methane fluxes, either from individual vents or from an entire macro-seepage area (including miniseepage), may span a wide range of values, on the order of 10^{-1}–10^{3} tonnes/year. Table 2.1 presents methane fluxes directly measured in the field from gas seeps (and oil seeps, springs, and mud volcanoes, as described below). Methane flux from large seep fires, such as Yanardag or Baba Gurgur, may exceed 10^{3} tonnes/year (the Yanardag flux provided in Table 2.1 refers only to a small portion of the miniseepage surrounding the large flames; see Fig. 2.2). For gas vents with a diameter <1 m, the flux is typically between 0.1 and 100 tonnes/year.

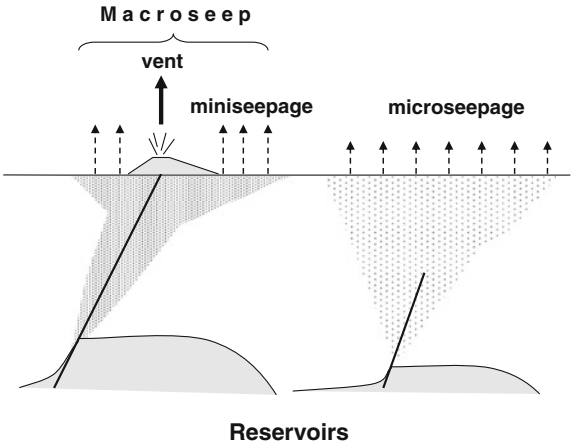

Fig. 2.1 Conceptual sketch of macro-seeps, miniseepage, and microseepage

Fig. 2.2 Examples of gas seeps and "eternal fires". **a** Deleni, Romania; **b** Yanardag, Azerbaijan; **c** Giswil, Switzerland; **d** Baba Gurgur, Iraq; **e** Chimaera, Turkey; and **f** Faros-Katakolo, Greece. (*Photo credits* **a**, **c**, **e**, and **f** G. Etiope; **b** L. Innocenzi; **d** http://www.en.wikipedia.org/wiki/File:P3110004.jpg)

The flux is generally constant over time and only weaker gas seeps, with fluxes below 1 tonnes/year, show variations in their activity in response to seasonal, meteorological, and additional factors (e.g., aquifer conditions).

A main characteristic of seep fires is that because the size of the flame is proportional to gas flow (F in g/s) according to the following equations (Delichatsios 1990;

Table 2.1 Methane flux from seeps, as measured by closed-chambers or the inverted funnel systems described in Chap. 4

Country	Type	Seep-site name	CH_4 flux (ton/year)	References
Azerbaijan	Gas	Yanardag (*miniseepage only*)	>68	Etiope et al. (2004)
	MV	Lokbatan	342	Etiope et al. (2004)
	MV	Kechaldag	94	Etiope et al. (2004)
	MV	Dashgil	843	Etiope et al. (2004)
	MV	Bakhar	45	Etiope et al. (2004)
Greece	Gas	Katakolo Faros	68	Etiope et al. (2013a)
	Gas	Katakolo Harbour	21	Etiope et al. (2013a)
	Gas	Killini	1.4	Etiope et al. (2006)
	Gas	Patras Coast	1.2	Etiope et al. (unpublished)
Italy	Gas	Montechino	100	Etiope et al. (2007)
	Gas	Miano	200	Etiope et al. (2007)
	Gas	M.Busca fire	9.2	Etiope et al. (2007)
	Gas	Censo fire	6.2	Etiope et al. (2007)
	Gas	Occhio Abisso	2.7	Etiope et al. (2007)
	MV	Rivalta	12	Etiope et al. (2007)
	MV	Regnano	34	Etiope et al. (2007)
	MV	Nirano	32.4	Etiope et al. (2007)
	MV	Ospitaletto	1.4	Etiope et al. (2007)
	MV	Dragone	0.3	Etiope et al. (2007)
	MV	Bergullo	1	Etiope et al. (2007)
	MV	Pineto	2.7	Etiope et al. (2007)
	MV	Astelina (Cellino Attanasio)	0.5	Etiope et al. (2007)
	MV	Frisa Lanciano	1.9	Etiope et al. (2007)
	MV	Serra de Conti	3.3	Etiope et al. (2007)
	MV	Offida	1.8	Etiope et al. (2007)
	MV	S.Vincenzo la Costa	0.02	Morner and Etiope (2002)
	MV	Puianello	0.12	Etiope (unpublished)
	MV	Rotella	0.1	Etiope (unpublished)
	MV	Vallone	0.05	Etiope (unpublished)
	MV	Maccalube Aragona	394	Etiope et al. (2002)
	MV	Paternò Stadio	2.1	Etiope et al. (2002)
	Oil	Madonna dell'Olio Bivona	0.02	Etiope et al. (2002)
	Spring	Tocco da Casauria	0.01	Etiope (unpublished)
Japan	MV	Murono Tokamachi	>20	Etiope et al. (2011b)
	MV	Kamou (Gamo) Tokamachi	3.7	Etiope et al. (2011b)

(continued)

Table 2.1 (continued)

Country	Type	Seep-site name	CH_4 flux (ton/year)	References
Romania	Gas	Andreiasu	50	Etiope et al. (2004)
	Gas	Bacau Gheraiesti	40	Baciu et al. (2008)
	Gas	Bazna	0.4	Spulber et al. (2010)
	Gas	Praid	4.4	Spulber et al. (2010)
	Gas	Deleni	~20	Spulber et al. (2010)
	Gas	Sarmasel	595	Spulber et al. (2010)
	MV	Fierbatori	37	Etiope et al. (2009)
	MV	Paclele Mari	730	Etiope et al. (2009)
	MV	Paclele Mici	383	Etiope et al. (2009)
	MV	Beciu	>260	Etiope et al. (2009)
	MV	Homorod	1	Spulber et al. (2010)
	MV	Monor	16	Spulber et al. (2010)
	MV	Valisoara	0.03	Spulber et al. (2010)
	MV	Filias	0.4	Spulber et al. (2010)
	MV	Porumbeni	0.5	Spulber et al. (2010)
	MV	Cobatesti	1.6	Spulber et al. (2010)
	MV	Boz	0.2	Spulber et al. (2010)
Switzerland	Gas	Lago Maggiore Ten	71	Greber et al. (1997)
	Gas	Giswil	>16	Etiope et al. (2010)
Taiwan	Gas	Suei-huo-tong-yuan	0.97	Yang et al. (2004)
	Gas	Chu-Ho	75.7	Hong et al. (2013)
	MV	Luo-shan	0.1	Yang et al. (2004)
	MV	Chunglun (CL#02)	1.43	Yang et al. (2004)
	MV	Kuan-tze-ling	0.08	Yang et al. (2004)
	MV	Yan-chao	0.7	Yang et al. (2004)
	MV	Gung-shuei-ping	1.1	Yang et al. (2004)
	MV	Diang-kuang	0.7	Yang et al. (2004)
	MV	Hsiao-kung-shuei	1	Hong et al. (2013)
	MV	Hsin-yang-nyu-hu	2.2	Hong et al. (2013)
	MV	Wu-shan-ding	35	Hong et al. (2013)
Ukraine	MV	Boulganack	40	Herbin et al. (2008)
USA California	Gas + Oil	Ojai Valley seeps	3.6	Duffy et al. (2007)
New York	Gas	Chestnut Ridge Park	0.3	Etiope et al. (2013b)
Colorado	Gas	Raton Basin seep Apogee 643	908	LTE (2007)
Colorado	Gas	Raton Basin seep Apogee 644	86	LTE (2007)

In most cases, the flux includes emissions from vents and from surrounding miniseepage (*Gas* gas seeps; *MV* mud volcanoes; *Oil* oil seeps)

Hosgormez et al. 2008; Etiope et al. 2011c), they provide visual information regarding the amount of gas released:

$$F = \frac{Q}{Hc} \tag{2.1}$$

$$Q = \left(\frac{Z_f}{0.052}\right)^{3/2} * P \tag{2.2}$$

where Q is the heat release rate (kW or kJ/s), Hc is the heat of combustion (kJ/g), Z_f is the flame height, and P is the flame perimeter (P = 4D in m; D is estimated at the base of the flame). Theoretical results obtained using this correlation are fairly consistent with those of direct flux measurements obtained from several seep fires investigated in Turkey, Greece, Italy, Romania, and Switzerland (Etiope et al. 2006, 2007, 2010, 2011c). Significant uncertainties may be associated with visual estimates of Z_f and D, and additional factors may influence flame height (e.g., cross winds). The correlation used is, therefore, less valid for very large and turbulent flames (once the turbulent regime is reached, flame height does not change with increasing flow rate). For the worst conditions, however, the method provides an estimate for the order of magnitude of the gas emissions, attributing at least a range of possible fluxes to each flame. For example, a flame approximately 50 cm high with a diameter above 10 cm is typically related to a gas flux higher than 15 kg/day; a small flame of 10 × 5 cm is typical related to a flux below 5 kg/day.

2.1.2 Oil Seeps

Oil seepage is not the object of this book but it is considered here because oil is frequently accompanied by a gaseous phase, especially when oil and gas coexist within a reservoir. The amount of gas in oil seeps decreases during oil exposure to the atmosphere, with subsequent oxidation, biodegradation, and solidification. Asphalts and tars (solid seeps) do not generally contain significant quantities of gas. The gas associated with oil is typically thermogenic and particularly rich in alkanes heavier than methane, from ethane to butane, with a wetness, $\Sigma C_{2-5}/\Sigma C_{1-5}$ (see the notation in Chap. 1), generally higher than 5–10 %. As a result, oil seeps are special natural sources of atmospheric ethane and propane, which, as discussed in Chap. 6, are photochemical pollutants and ozone precursors. Oil seeps may form black oil-filled pools, or produce oil that flows from rocks or soils or oil-impregnated terrains where the oil flow is episodic. In aquatic environments, oil is visible as drops, surrounded by iridescences, slicks (layers of buoyant oil), oily patches, or as diffuse iridescences. Oil is also released from mud volcano structures (see below) and for these cases oil emission points are an integral part of the mud volcano seepage system. For inventory purposes, these oil manifestations should not be considered as independent seeps.

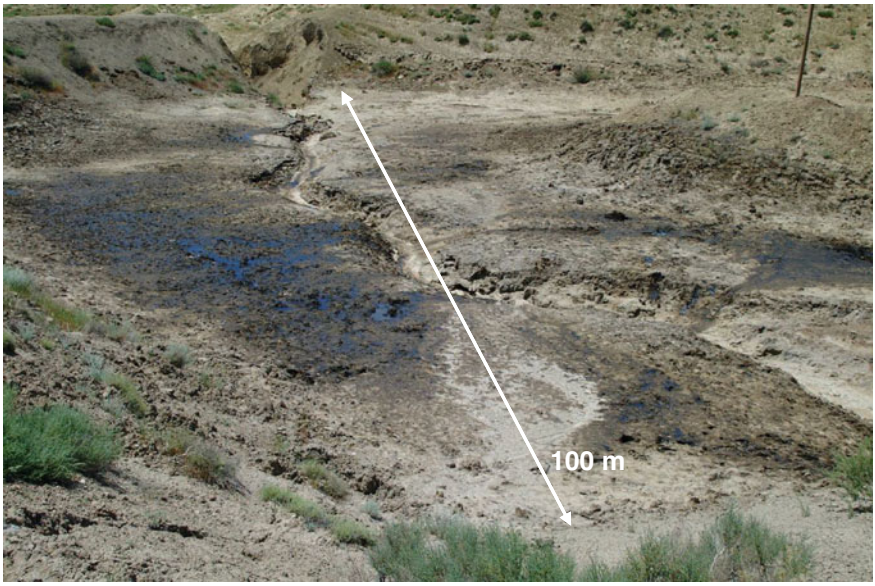

Fig. 2.3 The oil seep at Dashgil, Azerbaijan (*photo* by L. Innocenzi, INGV)

Geological evidence indicates that many historical oil seeps have disappeared today or that their fluid activity has been strongly reduced due to vigorous petroleum extraction that began in the 1800s (see Chap. 8). The decrease of oil flow is a result of the decrease of fluid pressures inside reservoirs. A large number of oil manifestations from the Alpine–Himalayan, Pacific Ocean, and Caribbean sedimentary belts, as described in the 20th century's petroleum geology literature (e.g., Link 1952), no longer exist. Nevertheless, almost all petroleum basins currently contain active oil seeps, numbering in the thousands. Some of the most active and large onshore oil seeps can currently be observed in Azerbaijan (near Dashgil, Fig. 2.3), Alaska (Samovar Hills), California (e.g., the McKittrick and Sargent oil fields), Pulkhana (Iraq), Kuwait (e.g., Burgan), and New Zealand (Kōtuku).

2.1.3 Gas-Bearing Springs

Freshwater springs and shallow aquifers may contain variable concentrations of dissolved methane originating from modern, microbial processes. As discussed in Chap. 1, this background methane should not be labelled seepage. In theory, this type of background methane should only occur when groundwater conditions are sufficiently reducing, with very low dissolved oxygen (DO) concentrations; otherwise the gas is rapidly oxidised limiting the presence of "non-seepage" methane in confined aquifers. In practice, microbial methane can be found in any type of aquifer (e.g.,

Darling and Gooddy 2006), with concentrations ranging from 0.05 μg/L (a typical lower detection limit) to mg/L levels. Unravelling this background methane and eventual seeping methane is only possible using analyses of the C and H isotopic composition of CH_4 and additional dissolved alkanes (ethane, propane, etc.).

For the case of seeping gas, groundwater from the springs of mineral waters and artesian aquifers may release an abundant gaseous phase to the atmosphere (Table 2.1, Fig. 2.4). Water may have a deep origin and may have interacted with gas during its ascent to the surface. Due to depressurization and water turbulence, degassing mainly occurs at the spring outlet. Mineral water springs have often been neglected as the vehicle of hydrocarbons from subsurface accumulations and few data (concentrations and/or degassing fluxes) for dissolved gases are available for petroleum-bearing sedimentary basins. Studies on the environmental impact of petroleum production, especially with reference to hydraulic fracking for shale-gas production within the United States, have recently provided new datasets indicating that groundwater containing natural methane (on the order of tens of mg/L) is more common than previously thought (e.g., Kappel and Nystrom 2012; Warner et al. 2013; also see Sect. 6.2). Due to possible links with subsurface petroleum accumulations, gas-bearing springs have also been the object of recent research in Europe, in particular in Italy and Romania (e.g., Ionescu 2015).

A useful example is that of the Tocco da Casauria spring, located in the Apennine Mountains of central Italy (Fig. 2.4). The spring is historically known for

Fig. 2.4 The gas and oil bearing spring of Tocco da Casauria, Central Italy (*photo* by G. Etiope)

episodic releases of oil, visible as iridescences in the water. The molecular composition and flux of the evolved gas from the water was measured on site using a portable spectrometer (a Fourier Transform Infrared, FTIR) linked to a closed-chamber (also see Chap. 4). The spring outlet was found to release more than 20 g of CH_4 per day, with a flux that gradually decreased along the water stream. Flowing water releases gas tens of meters from the spring. The soil surrounding the spring also exhales gas with CH_4 fluxes on the order of 10^1–10^2 mg m^{-2} day^{-1}, and heavier alkanes (ethane, propane, butane, and pentane) and benzene were also detected. Laboratory analyses confirmed that the gas has a dominant thermogenic origin, likely with a minor microbial component (the "Bernard ratio $C_1/(C_2 + C_3)$ was determined to be 23 and the stable carbon isotopic composition of CH_4, $\delta^{13}C$, was −57 ‰; see the notations in Chap. 1 and Fig. 1.2). The hydrocarbons likely migrate from productive reservoirs in Miocene reef limestones (Reeves 1953).

A discussion is provided in Chap. 7 regarding springs in serpentinised ultramafic rocks that may carry methane of abiotic origin.

2.1.4 Mud Volcanoes

Mud volcanoes are the largest surface expression of the migration of hydrocarbon fluids in petroleum bearing sedimentary basins (Fig. 2.5). Geology and formation mechanisms are described in a wide array of scientific literature (e.g., Milkov 2000; Kopf 2002; Dimitrov 2002a). Only some of the basic concepts are outlined here.

Mud volcanoes are cone shaped structures produced over faults by the upwelling of sediments (mud) fluidised by gas and water; and may develop as single isolated cones and craters or, more frequently, as groups of cones and crater systems. The diameter of single craters may range from a few cm to several tens of meters and conical structures can be several hundreds of meters high, as for the giant mud volcanoes of Azerbaijan (Fig. 2.5).

Gas is typically released from craters, gryphons (gas-mud vents generally occurring at the flanks of a main dome or crater; Fig. 2.6), or bubbling pools and small lakes (salses; Fig. 2.7) and, as for other types of macro-seeps, through the diffuse exhalation (miniseepage) of muddy ground (Table 2.1). Some mud volcanoes are characterised by intense and continuous degassing through gryphons and salses while others have low or absent venting activity but higher eruptive potential. Eruptions of gas and mud can be explosive and can represent a hazard for local communities and infrastructures (see Chap. 6). From 1810 until present, more than 250 eruptions of 60 mud volcanoes have been observed in Azerbaijan. Some have released tens of thousands of tonnes of CH_4 within a few hours (e.g., Guliyev and Feizullayev 1997).

Mud volcanoes are formed in sedimentary basins and involve the mobilisation of sedimentary rocks, mainly shales. Accordingly, they can be considered as a type of "sedimentary volcano" (not to be confused with traditional volcanoes, which are related to magmatic processes). Some confusion, however, exists within the

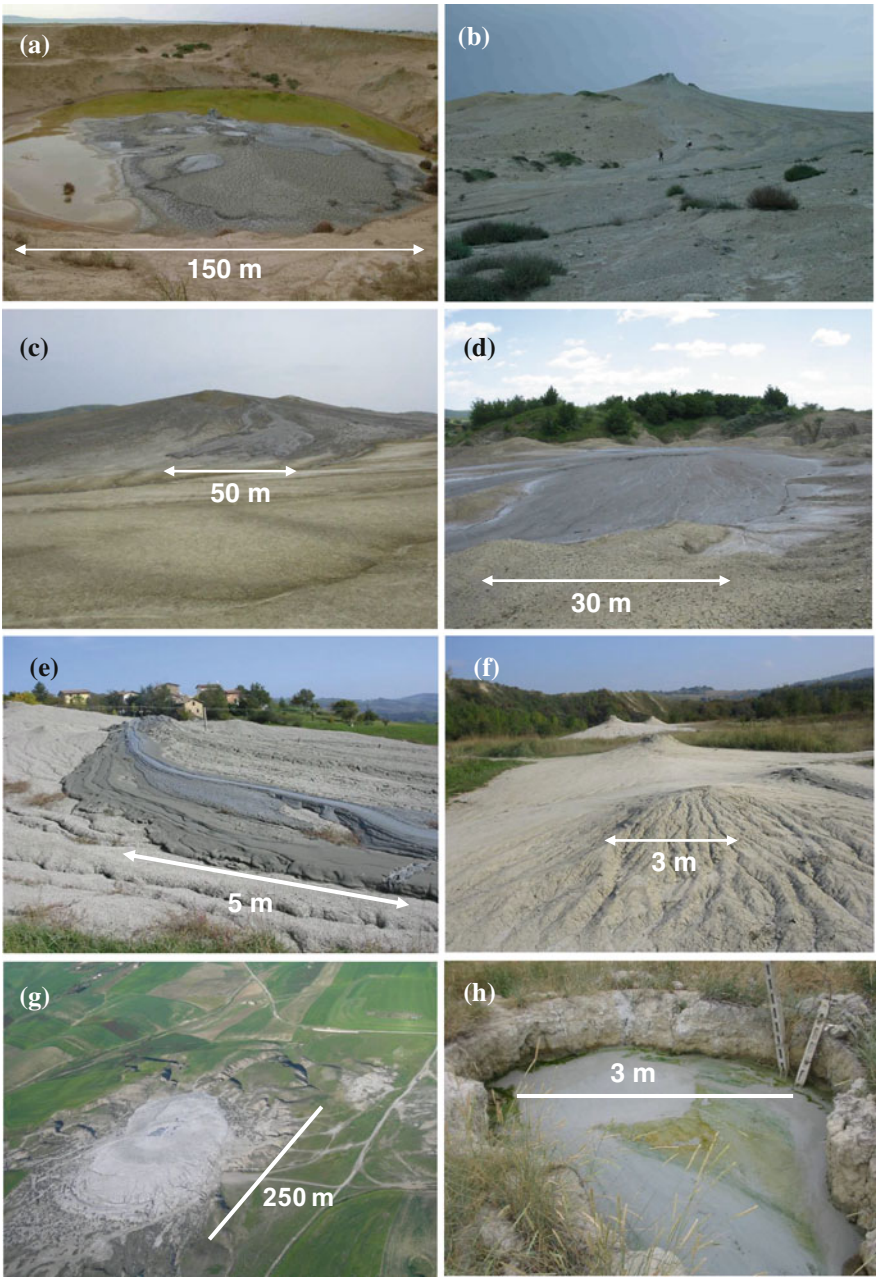

Fig. 2.5 Mud volcanoes **a**, **b** Bakhar New and Bakhar, Azerbaijan; **c** Paclele Mari, Romania; **d** Fierbatori, Romania; **e** Regnano, North Italy; **f** Nirano, North Italy; **g** Maccalube, Sicily, Italy; and **h** Pineto, Central Italy. (*Photos credits* **a**, **b** L. Innocenzi INGV; **c**, **d**, **e**, **f** and **h** G. Etiope; **g** courtesy of www.iloveagrigento.it)

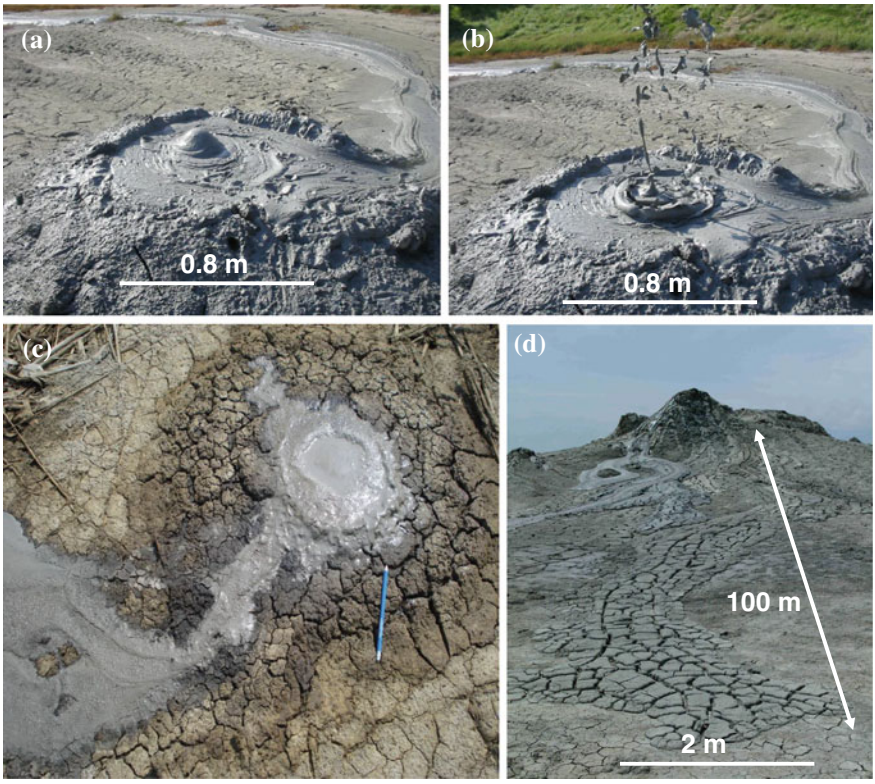

Fig. 2.6 Craters and gryphons in mud volcanoes **a**, **b** Regnano, Italy; **c** Murono, Tokamachi, Japan, **d** Bakhar, Azerbaijan (*Photos credits* **a**, **b**, **c**: G. Etiope; **d**: L. Innocenzi, INGV)

scientific literature, as some muddy gas manifestations, not hydrocarbon-rich or related to sedimentary volcanism, are improperly called mud volcanoes. For example, many vapour-rich or CO_2-vents related to geothermal or hydrothermal systems (e.g., the Salton Sea gas manifestations in California; Sturz et al. 1992 and Mazzini et al. 2011; or the LUSI eruption in Indonesia; Mazzini et al. 2012) have been referred to as mud volcanoes. The term "mud volcano" should not be used for any gas manifestation resembling a mud pool or for areas where extrusive mud gives rise to a conical edifice. The issue is not only a semantics problem. Mud volcanism implies the existence of a series of specific geological processes and features, and, not insignificant, the generation of gas and water related to hydrocarbon diagenetic as well as catagenetic production and accumulation processes. In true mud volcanoes, the water is "fossil', saline, and stems from hydrocarbon reservoirs or from the illitization of clay minerals in shales. A global dataset indicates that in 80 % of terrestrial mud volcanoes methane is thermogenic; microbial gas is less common (Etiope et al. 2009). In special cases, gas can be dominated by CO_2 or N_2. Such mud volcanoes can occur in hydrocarbon systems close to subducting slabs and geothermal environments (e.g., Motyka et al. 1989),

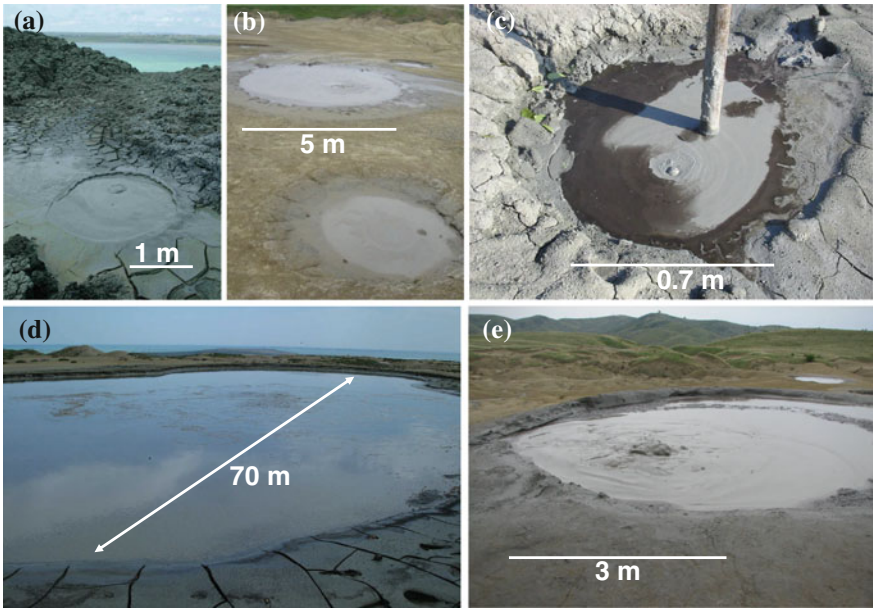

Fig. 2.7 Bubbling pools and lakes in mud volcanoes **a** Kechaldag, Azerbaijan; **b** Paclele Mari, Romania; **c** Pujanello, Italy; **d** Dashgil, Azerbaijan; **e** Paclele Mici, Romania (*Photos credits* **a** and **d** L. Innocenzi; **b**, **c**, **e** G. Etiope)

or are related to fractionated gas systems (i.e. with post-genetic enrichments of non-hydrocarbon gases with respect to methane) and to the final stages of natural gas generation (e.g., Etiope et al. 2011a). However, they can always be associated with a Total Petroleum System (as defined in Chap. 1). A tentative list of the diagnostic and distinctive elements required for a mud volcano is as follows (e.g., Etiope and Martinelli 2009):

- The discharge of a three phase system (gas, water, and sediment).
- Gas and saline water related to a diagenetic or catagenetic hydrocarbon production system.
- The involvement of sedimentary rocks with a gravitative instability resulting from rapid sedimentation, leading to the formation of diapirs or diatremes (see the definitions in Kopf 2002).
- The presence of breccia within the discharged material.

Thus, it is clear that misuse of the term "mud volcano" can lead to misinterpretations and misplaced expectations (Etiope and Martinelli 2009), in particular, in planetary geology when discussing, for example, mud volcanism on Mars (Skinner and Mazzini 2009).

2.1.5 Miniseepage

Use of the term "miniseepage" was proposed by Klusman (2009) and readapted by Etiope et al. (2011b) to define the invisible, diffuse exhalation of gas surrounding visible seeps within a macro-seepage zone. Before 2010, the diffuse exhalation in macro-seeps was named microseepage (e.g., Etiope 2009a). But it is useful to distinguish miniseepage, as it is conceptually different from the exhalation that is far or independent from seeps (for which the term "microseepage" should be reserved). Methane miniseepage flux is typically higher than microseepage, generally on the order of 10^3–10^5 mg m^{-2} day^{-1} versus units of hundreds of mg m^{-2} day^{-1} (e.g., Etiope et al. 2004; Etiope and Klusman 2010).

Miniseepage is a sort of halo that surrounds a channelled seep (Figs. 2.1 and 2.2). The concept is very important because it makes a clear distinction between the visible point of gas emission (a crater, a vent, or a flame) and the surrounding soil. A transition area exists where gas flux gradually decreases, dropping to "zero" after tens or hundreds of meters. Measurements of gas flux along profiles within the soil surrounding gas vents suggest that miniseepage can spread over tens of thousands of square meters and that the total, integrated, output of gas to the atmosphere may be higher than that from focused, visible emissions. The Tokamachi mud volcanoes in Japan provide a relevant example (Etiope et al. 2011b). In this area, invisible gas emissions from the muddy ground surrounding bubbling craters was determined to be almost three times higher than the flux obtained from visible bubble plumes. Positive CH_4 fluxes, from tens to thousands of mg m^{-2} day^{-1}, were recorded in soil patches throughout the investigated area, $\sim$4,900 m^2, up to 90 m from the mud volcano crater. The total methane output from macro-seepage (the sum of emissions measured from all vents) was estimated to be approximately 5 tonnes/year. Total gas output from the diffuse exhalations of soil, derived using spatial interpolations between individual gas measurements (e.g., using the "natural neighbour" interpolation technique), yielded an output of approximately 16 tonnes CH_4 per year. Therefore, more than 75 % of total methane emissions occurred from invisible and diffuse seepage surrounding visible mud volcano vents. What is invisible may be more important than what is visible.

Due to the flooding of soil with gas, miniseepage can be unveiled by patches of stressed or dying vegetation and/or by small bubbling when the ground is saturated with water, for example after a rainfall event. Soil temperature anomalies may be several meters deep and blue-gray haze during winter inversions may also be observed (Klusman 2009).

2.1.6 The Global Distribution of Onshore Macro-Seeps

The exact global number of onshore seeps is unknown but appears to exceed 10,000 (Clarke and Cleverly 1991; Etiope et al. 2008), distributed throughout the petroliferous basins of all continents. Mud volcanoes, in particular, follow oil and gas

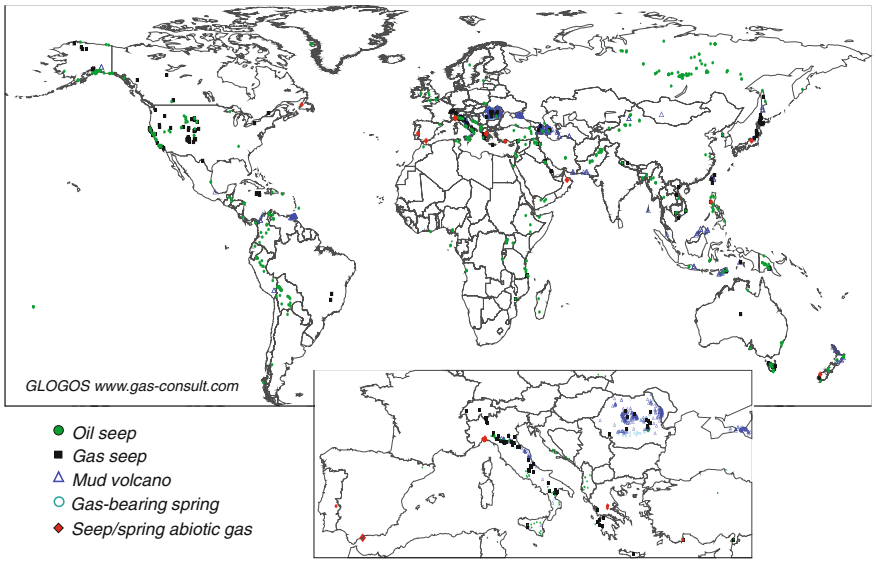

Fig. 2.8 Global map of onshore seeps (from the GLOGOS dataset, Version 2014, www.gas-consult.com)

reservoirs located within the Alpine-Himalayas, the Pacific Ocean, and the Caribbean geological belts (Etiope and Milkov 2004). A recent database, named GLOGOS (Global Onshore Gas-Oil Seeps; Etiope 2009b; www.gas-consult.com), reports 2,100 documented seeps from 89 countries, distinguished as gas seeps, oil seeps, mud volcanoes, or gas-bearing springs (Fig. 2.8). Table 2.2 summarises the dataset for each continent, as well as the number of seeps by type and country.

The dataset represents only a portion of the total onshore seeps on Earth but likely includes all of the largest seeps, because they are more easily documented and attract attention for scientific research, petroleum exploration, and natural heritage protection. Small or inactive seeps tend to be less observed and reported. Although the derived statistics may be under-represented, the dataset indicates (Table 2.2; Fig. 2.9) that the number of oil seeps, gas seeps, and mud volcanoes globally is more or less similar (634, 694, and 652, respectively) and that gas-bearing springs are subordinate (120). The recognition of a spring as a "hydrocarbon seep" is, in fact, not immediate and, in general, is the result of focused investigations (the 120 springs were actually documented largely due to specific studies in Italy and Romania). The actual global number of mineral springs that carry hydrocarbons to the surface may be considerably higher.

On several continents, the relative amounts of seep typologies are variable and depend on the type of petroleum provinces (gas or oil prone) with active tectonics capable of forming seepage systems. Active burning gas seeps, with more or less permanent flames, have been documented in Azerbaijan, Canada, Greece, India, Indonesia, Iraq, Italy, Jamaica, Nepal, New Zealand, the Philippines, Romania, Switzerland, Taiwan, Turkey and the United States (in California and New York

Table 2.2 Summary of the number of countries and related seeps contained within the GLOGOS dataset (Version 2014.2; www.gas-consult.com)

Continent	Countries	Oil seeps	Gas seeps	Mud Volcanoes	Springs	Total seeps
Europe	19	207	239	534	111	1,091
Asia	31	123	62	57	7	249
Africa	14	36	5	0	0	41
North America	2	115	363	3	2	483
Central South America	19	107	6	30	0	143
Oceania	4	46	19	28	0	93
Total	89	634	694	652	120	2,100

Europe Albania, Armenia, Azerbaijan, Croazia, Denmark, Georgia, Greece, Ireland, Italy, Poland, Portugal, Romania, Russia, Spain, Sweden, Switzerland, Turkey, United Kingdom, Ucraine
Asia Bahrain, Bangladesh, Brunei, Cambodia, China, India, Indonesia, Iran, Iraq, Israel, Japan, Jordan, Korea North, Kuwait, Kyrgyzstan, Laos, Malaysia, Mongolia, Myanmar, Nepal, Oman, Pakistan, Philippines, Syria, Taiwan, Thailand, Timor-Leste, Turkmenistan, United Arab Emirates, Vietnam, Yemen
Africa Angola, Egypt, Ethiopia, Ghana, Madagascar, Morocco, Mozambique, Nigera, Sao Tome, Somalia, Tanzania, Tunisia, Uganda, Zaire
North America Canada, United States of America (including 17 States: Alabama, Alaska, California, Colorado, Illinois, Kentucky, Michigan, Montana, Nevada, New Mexico, New York, Oregon, South Dakota, Texas, Utah, Washington, Wyoming)
Central South America Argentina, Barbados, Belize, Bolivia, Brasil, Chile, Colombia, Costa Rica, Dominican Republic, Ecuador, Guatemala, Jamaica, Mexico, Nicaragua, Panama, Perù, Puerto Rico, Trinidad, Venezuela
Oceania Australia, New Zealand, Papua New Guinea, Tonga

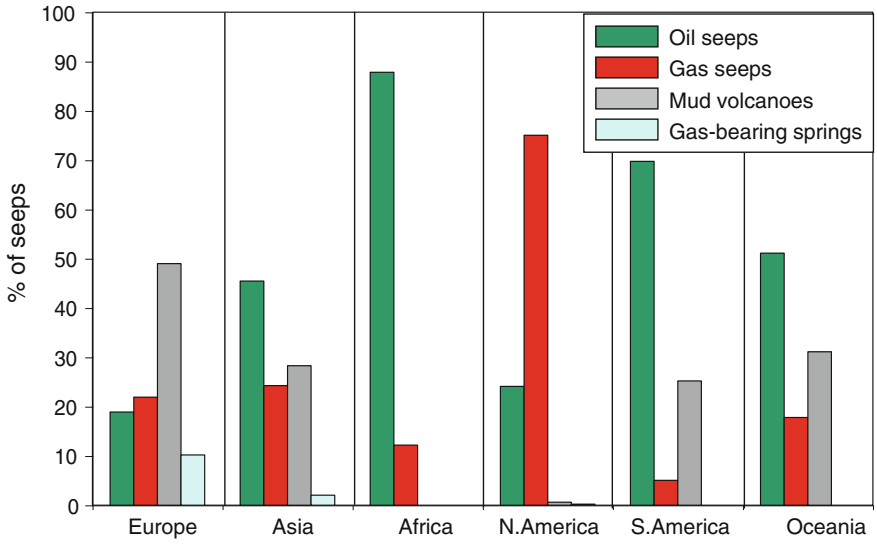

Fig. 2.9 The relative percentages of various types of seeps on the continents as documented by the GLOGOS dataset (2,100 seeps from 89 countries, dataset Version 2014; www.gas-consult.com). Europe includes Azerbaijan

State). The GLOGOS onshore seep dataset also indicates that mud volcanoes are located in at least 26 countries in Europe, Asia, and the Americas and Oceania; none have been located in Africa. Mud volcanoes are particularly widespread in Romania, with 214 structures, most relatively small and a few meters wide. In Azerbaijan, 180 structures have been located, most of which are hundreds of meters in height covering individual areas of several km^2. In Italy, 87 structures have been determined (e.g., Etiope et al. 2007; Martinelli et al. 2012). Most are small mud cones (with muddy ground up to a few square meters wide) with the exception of the large Maccalube in Sicily that is approximately 0.7 × 0.5 km wide. A few to a few tens of mud volcanoes are located (in alphabetical order) in Alaska, China, Colombia, Georgia, India (Andaman), Indonesia, Iran, Japan, Malaysia, Mexico, Mongolia, Myanmar, New Zealand, Pakistan, Papua New Guinea, Perù, Russia (Taman), Taiwan, Timor Leste, Trinidad, Turkmenistan, Ukraine (Kerch), and Venezuela. All of these mud volcano sites correspond to sedimentary basins with mobilised shales, heavily tectonised and faulted.

No apparent relationship exists between seep location and type of climate, latitude, or surface ecosystem. Seeps are located in deserts, forests, wetlands, or grasslands. As discussed in Chaps. 3 and 5, the occurrence of seepage appears to be determined only by petroleum and structural geology, in other words, hydrocarbon sources and faults.

2.2 Microseepage

Microseepage is the slow, continual, or episodic loss of methane and light alkanes from gas-oil-prone sedimentary basins. Microseepage is basically the pervasive, diffuse exhalation of gas from soil, independent of the presence of macro-seeps. Microseepage is assumed to be a general phenomenon driven by the buoyancy of the gas phase relative to connate waters (see Chap. 3). Such invisible seepage can easily be detected using soil-gas analyses, revealing anomalous concentrations of gaseous hydrocarbons in the soil, and using a closed-chamber technique that allows determinations of gas flux to the atmosphere. Indirect methods, such as microbial prospecting (e.g., Tucker and Hitzman 1996; Wagner et al. 2002), remote sensing (e.g., van der Meer et al. 2002), and magnetic measurements (e.g., Liu et al. 2004) can also detect microseepage inside large areas. These techniques are described in Chap. 4. Field measurements have indicated that microseepage is enhanced along faults, especially those produced by neotectonics, and can have strong seasonal variations (Klusman 1993, 2003; Etiope and Klusman 2010).

In dry soils (i.e. in the absence of water saturated soils), the methane flux is generally negative, indicating that methane flows from the atmosphere to the soil where it is consumed by bacterial methanotrophic oxidation. Due to this biological activity, dry lands are considered to be a net sink of atmospheric methane, absorbing approximately 30 Mt (million tonnes) CH_4 per year on a global scale, with local fluxes generally on the order of −5 to −1 mg m^{-2} day^{-1} (Dong et al. 1998). Microseepage is responsible for less negative or positive fluxes of methane,

indicating that soil consumption can be lower than the input from underground sources. During the summer, methanotrophic activity increases and microseepage flux decreases. The opposite is true in the winter. Positive methane fluxes are typically a few units or tens of mg m^{-2} day^{-1}, but may be hundreds of mg m^{-2} day^{-1} over wide tectonised and faulted areas corresponding to hydrocarbon fields. Values are comparable with biological CH_4 emissions in wet, anaerobic ecosystems, typically in the range of 1–500 mg m^{-2} d^{-1} (Batjes and Bridges 1994). In soils where the microbial production of CH_4 is possible (wet soils, soils with peat layers, and soils above shallow aquifers or paleo-lakes), the microseepage of fossil gas can only be recognised using CH_4 isotope analyses and, if possible, the identification of anomalous concentrations of heavier alkanes (C_{2+}).

Examples of microseepage methane fluxes are provided in Table 2.3.

The global coverage of microseepage is unknown. However, as shown by innumerable surveys performed for petroleum exploration (for example Schumacher and Abrams 1996; Saunders et al. 1999; Wagner et al. 2002; Etiope 2005; Khan and Jacobson 2008; Tang et al. 2010; Sechman 2012) all petroleum basins contain microseepage. Microseeping areas include all of the sedimentary basins contained in dry climates with petroleum and gas generation processes at depth, estimated to be 43,366,000 km^2 (Klusman et al. 1998). Available flux data suggest that microseepage closely corresponds to the spatial distribution of oil-gas fields, coal measures, and portions of sedimentary basins where methanogenic (diagenetic) and thermogenic (catagenetic) processes take place. Etiope and Klusman (2010) assumed that microseepage occurs within the Total Petroleum System (TPS), as defined in Chap. 1). On Earth, 42 countries produce 98 % of total petroleum and 70 countries produce 2 % (the remaining ~90 countries produce 0 %). So, the TPS and, consequently, the potential for microseepage, occur in 112 countries. Based on a careful analysis of onshore TPS map and GIS datasets, the global area of potential microseepage (Fig. 2.10) has been estimated to be on the order of 8×10^6 km^2 (Etiope and Klusman 2010). The area may exclude wide zones of coal measures and portions of sedimentary basins that experience thermogenesis. However, the area represents approximately 15 % of Earth's dry land area. Here, it must be emphasised that the estimate refers to the potential area of microseepage. The actual microseepage area may be significantly smaller.

2.3 Marine Seepage Manifestations

Seepage occurring in the marine environment deserves an additional and separate discussion. A plethora of books and articles have been written about submarine seeps (see for example, Hovland and Judd 1988; Hovland et al. 1993; Judd and Hovland 2007; Suess 2010; and recent reviews by Valentine 2011; Anka et al. 2012; Hovland et al. 2012 and Boetius and Wenzhöfer 2013). The objective of this section is to offer a quick overview for unspecialised readers, recalling some key definitions and concepts that are specific to submarine seepage manifestations.

Table 2.3 Microseepage flux data in hydrocarbon-prone areas. All of the measurements provided were obtained using the closed-chamber technique described in Chap. 4 [with the exception of Balakin et al. (1981)]

	References	No. of sites	Area (km^2)	Flux range (mg m^{-2} day^{-1})
United States				
Denver-Julesburg basin (Colorado)	Klusman et al. (2000)	84	70,250	−41 to 43.1
Piceance (Colorado)	Klusman et al. (2000)	60	12,130	−6.0 to 3.1
Powder River (Wyoming)	Klusman et al. (2000)	78	62,820	−14.9 to 19.1
Railroad Valley (Nevada)	Klusman et al. (2000)	120	3,370	−6.1 to 4.8
Rangely (Colorado) winter	Klusman (2003a,b)	59	78	−8.60 to 865
Rangely (Colorado) summer	Klusman (2003a,b)	59	78	−4.02 to 145
Teapot Dome (Wyoming) winter	Klusman (2006)	39	42	−0.48 to 1.14
Russia-Georgia-Azerbaijan				
Great Caucasus	Balakin et al. (1981)	na	na	430
Lesser Caucasus	Balakin et al. (1981)	na	na	12
Kura depression	Balakin et al. (1981)	na	na	8
Romania				
Transylvania, Tarnaveni-Bazna	Etiope (2005)	5	5	2 to 64
Transylvania, Media	Spulber et al. (2010)	2	na	0 to 20
Transylvania, Ludu	Spulber et al. (2010)	2	na	0 to 30
Transylvania, Cucerdea	Spulber et al. (2010)	1	na	416
Italy				
Abruzzo-Marche Adriatic coast				
Vasto	Etiope (2005)	30	2	−5 to 142
Pescara	Etiope (2005)	5	1	−4 to 13
Regional survey (6000 km^2)	Etiope and Klusman (2010)	45	6,000	−3 to 190
Miglianico field	See Chap. 5	55	75	−3 to 300
China				
Talimu Basin, Yakela Oil-Gas Field				
Oil-gas interface Sector	Tang et al. (2010)	5	50 m^2	2.4 to 3.5
Luntai Fault	Tang et al. (2007)	16	800 m profile	4.4 to 11

na not available. *Note* Each of the sites in Klusman et al. (2000), Klusman (2003a, b), and Klusman (2005; 2006) consisted of triplicate measurements. For all of the basin studies and the Rangely Field, repeated measurements were obtained at the same locations and for various seasons. Only one survey during the winter of 2004 was conducted at the Teapot Dome Field. Measurements in Europe were conducted using 10 L chambers during the spring and summer seasons

Marine seeps are traditionally called "cold seeps" to distinguish them from hot and CO_2-rich hydrothermal vents, which are generally related to submarine volcanic and mid-ocean ridge systems. Cold seeps occupy passive continental shelves and slopes, up to depths of ~3,000 m below the sea surface. Many of these

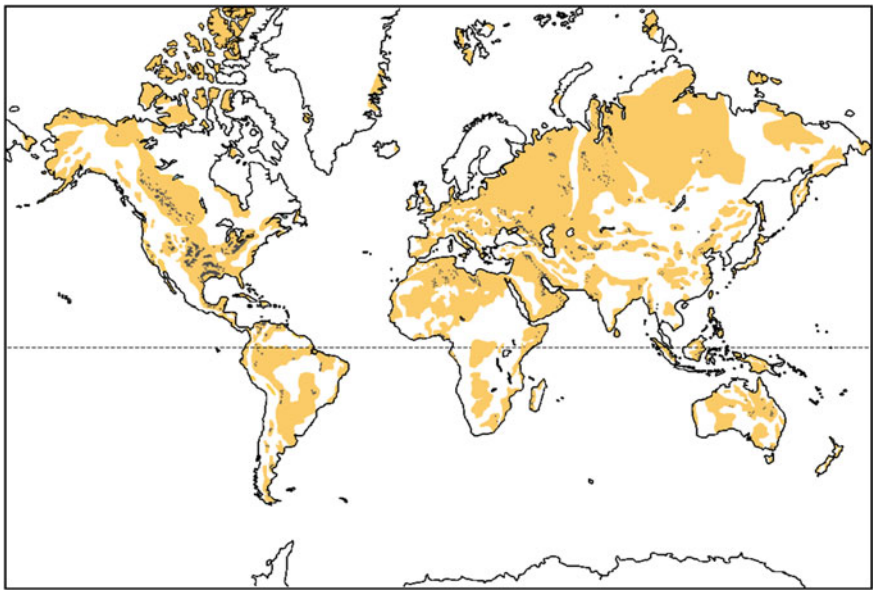

Fig. 2.10 Global distribution of onshore sedimentary basins (*sand brown*) and the main petroleum fields (*grey areas* and *dots*). The potential microseepage area is a portion of the sedimentary basins surrounding the petroleum-producing areas defined by Total Petroleum Systems (based on data and maps from St. John (1980), Masters et al. (1998); USGS World Petroleum Assessment, http://energy.usgs.gov/OilGas/)

sedimentary areas host Total Petroleum Systems (i.e. offshore petroleum fields). Cold seeps are biologically important because they fuel chemosynthesis-based benthic communities consisting of invertebrates containing bacterial symbionts that depend on H_2S or CH_4. Over the last 45 years and since the pioneering discoveries of "pockmarks" by King and MacLean (1970), thousands of cold seeps have been detected in continental margins around the world. On the basis of wide exploration, seafloor seep manifestations can be classified as follows:

(a) pockmarks
(b) carbonate slabs and chimneys
(c) sediment holes and bacterial mats
(d) submarine mud volcanoes
(e) gas hydrate mounds
(f) gas-charged sediments

(a) Pockmarks are cone-shaped depressions in soft seafloor sediments produced from the "blow-out" of gas and water. Gas emissions are generally episodic and may follow cyclic phases of charge (the accumulation of gas beneath the seabed, the inflation of sediments, and the formation of a dome) and discharge (gas released in

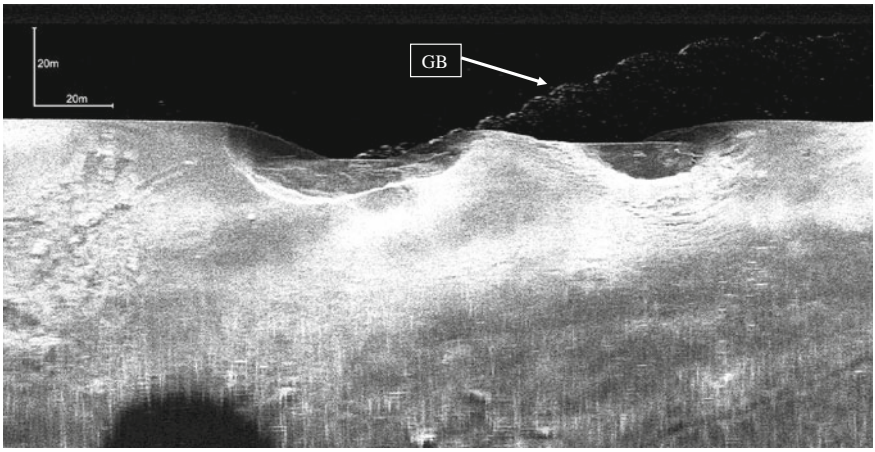

Fig. 2.11 An example of the pockmarks within the Patras Gulf (Greece) at water depths of 30 m as detected by side scan sonar (sonograph). The *image* indicates gas bubbles (GB) rising in the water column from an active pockmark, 40 m in diameter. The sonograph was collected by an EG&G dual frequency (100 and 500 kHz) side scan sonar system at a frequency of 100 kHz (courtesy of G. Papatheodorou)

the water with suspensions of fine-grained sediments). Gas escape is more vigorous during initial cycles; the gas flux then gradually decreases as gas overpressures dissipate. Pockmark size ranges from less than one meter to several hundreds of meters in diameter. Depressions can be several tens of meters deep. Giant pockmarks with diameters of 100–200 m have been reported in Belfast Bay, Maine (Kelley et al. 1994) and in the Barents Sea, Norway (Solheim and Elverhoi 1997). Other areas of pockmarks have been found within the eastern Canadian continental shelf, the Black Sea, offshore of north-western Spain, the Adriatic Sea (Italy), the Patras and Corinth Gulf (Greece; Fig. 2.11), the Skagerrak coast (Denmark), the Scotian Shelf (U.K.), the Norwegian Channel, the Stockholm archipelago (Sweden), the Arabian Gulf, the Northern Congo Fan, and the Arctic Ocean (see Etiope and Klusman 2002 or Judd and Hovland 2007 for relevant references).

(b) Carbonate slabs and chimneys, also named "Methane-derived Authigenic Carbonate" (MDAC), are diagenetic deposits of Mg-calcite, aragonite, or dolomite with variable shapes, planar crusts, mounds, or columns. Their size is also quite variable, from millimeter concrections to several meter high chimneys and 100 meter wide pavements. They were first identified in the North Sea in 1983 (Hovland and Judd 1988). The carbon isotopic composition of the carbonate is ^{13}C-depleted (δ^{13}C often <-20 ‰ VPDB, in contrast to values of approximately 0 ‰ for normal sedimentary carbonates) because it is derived from methane, not from seawater or sediment porewater (e.g., Peckmann et al. 2001). Carbonate deposits, in fact,

represent the remnants of contemporary or ancient methane seepage. Carbonate precipitation, expressed in the following form:

$$CH_4 + SO_4^{2-} \rightarrow HCO_3^- + HS^- + H_2O$$

is due to increased alkalinity driven by the microbial anaerobic oxidation of methane (AOM), which is driven by a consortium of archaea (engaged in reverse methanogenesis) and sulphate reducing bacteria (e.g., Boetius et al. 2000; Thiel et al. 2001). Unless there are other indicators of active seepage (e.g., bacterial mats or gas bubbles), MDAC does not necessarily imply that seepage is on-going. However, MDAC may indicate that seepage has occurred over a prolonged period of time.

(c) Gas is also frequently released through small (a few centimetres in width) holes or fractures located within the seabed, often identified by black patches or brown to white bacterial mats. The bacteria (generally *Beggiatoa*) oxidise the H_2S derived from bacterial sulfate reduction that accompanies hydrocarbon oxidation when oxygen is depleted in sediments (Sassen et al. 1993). Examples of gas-bearing holes and fractures are those located in the shallow waters of Katakolo harbour in western Greece (Fig. 2.12). A wide area with at least 133 bubble emissions from holes and microbial white patches was recently reported in the Southern Ocean, off the sub-Antarctic island of South Georgia (Römer et al. 2014).

(d) More than 300 mud volcanoes have been reported on the continental shelves, and more than 1,000 may occur in deep-water areas (Milkov 2000). The list, likely not exhaustive, includes the Norwegian Sea, the Mediterranean Sea, the Black Sea, the Caspian Sea, the Persian Gulf, the trenches adjacent to Japan, New Zealand, the Aleutian Islands, offshore areas of California and Costa Rica, the Gulf of Mexico, the Caribbean Sea, and areas offshore of Nigeria. Submarine mud volcanoes are being continuously discovered, year after year, thanks to the increasing efficiency of geophysical remote sensing and acoustic imaging. One of the best studied submarine mud volcanoes is Haakon Mosby, discovered in 1989 on the Southwest Barents Sea slope at a water depth of 1,270 m (Crane et al. 1995; Milkov et al. 2004). Haakon Mosby has a diameter of $\sim$1 km and an elevation of $\sim$10 m above the surrounding seafloor. The emitted methane is of mixed microbial and thermogenic origin. The volcanic structure is a heterogeneous system of different types of gas seepage and related ecosystems, including focused vents, authigenic carbonates, and gas hydrates; in other words, a real natural laboratory for studying all of the main geochemical and biological processes related to gas seepage within the marine environment.

(e) In many cases gas is simply stored in shallow sediments, without evidence of morphological structures located on the seafloor. Gas-charged sediments can be revealed by hydro-acoustic surveys as acoustic anomalies, i.e. acoustic turbid zones, gas pockets, enhanced reflectors, columnar disturbances, and acoustic wipe outs (attenuation). In Pleistocene sediments and deltaic environments, gas is typically microbial and recent, and produced in the sediment itself. True seepage of deeper microbial and thermogenic gas is almost always associated with faults so

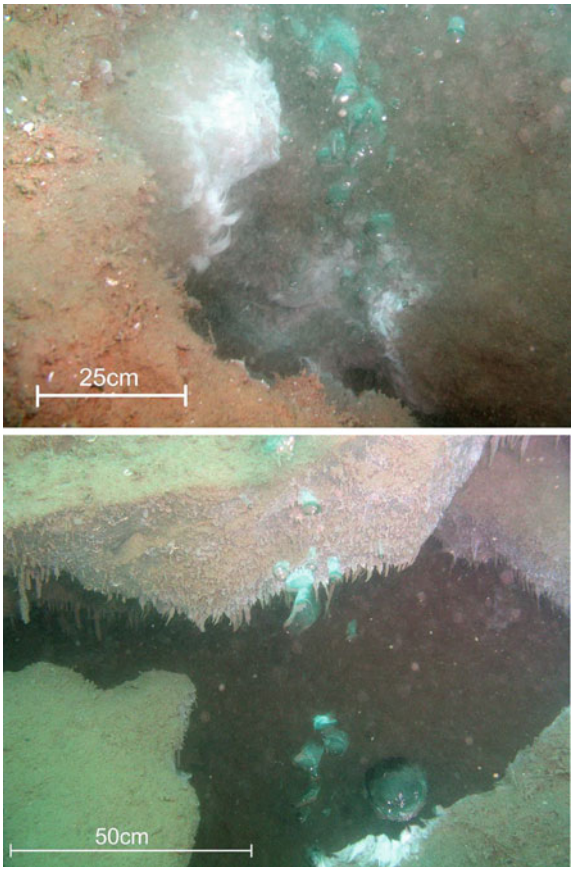

Fig. 2.12 Underwater photos showing *bubbles* (up to 20 cm in diameter) rising from seabed fissures at Katakolo Harbour (western Greece, Ionian Sea), at a water depth of 7 m. The rim of the seabed fissures is covered by *white* bacterial mats (courtesy of G. Papatheodorou)

that gas-charged sediments are distributed along strips or elliptical areas (e.g., Papatheodorou et al. 1993).

(f) Finally, gas hydrates or clathrates occur in deep-sea sediments or shallow seabeds in Arctic regions (e.g., Milkov 2004) and are an enormous potential seepage source. Hydrates likely contain one order of magnitude more methane than the 220 Gt of carbon estimated to occur in all conventional gas reservoirs (Milkov 2004; Archer et al. 2009). Gas hydrates are ice-like crystalline solids composed of rigid cages of water molecules that enclose guest gas molecules, and form in the pores of seabed sediments when at least 5–10 % of gaseous methane is present. One cm^3 of hydrate may contain 160 cm^3 of methane. These solid structures are stable under specific pressure and temperature conditions. When these conditions change (e.g., seawater warming or landslides along the slopes), gas can be liberated (e.g., Dillon et al. 2001). Gas-hydrates may form mounds with thicknesses of several hundreds meters. The mounds can then be eroded, collapse, or decay due to chemical dissolution, leading to the floatation of gas-rich hydrates. Hydrates, however, are not only a potential source of seepage but often a result of seepage.

Thermogenic gas hydrates, in particular, entrap gas ascending from subsurface accumulations (e.g., Sassen et al. 1999). As suggested by the considerable amounts of thermogenic gas hydrates in the Gulf of Mexico alone, up to 500 Gt (Milkov and Sassen 2001), the contribution of thermogenic gas seepage to global hydrate reservoirs is likely underestimated.

In all of the cases listed above, gas can ascend the water column as single bubble trains or bubble plumes that are often intermittent or episodic. Large, continuous, and long-lasting bubble plumes indicate strong pressure gradients and source potential, and, in fact, typically indicate the presence of thermogenic gas. Examples include areas offshore of California (Coal Oil Point; Hornafius et al. 1999), within the Black Sea (Golden Sands; Dimitrov 2002b), and along the Ionian coast of Peloponnesus in Greece (Katakolo; Etiope et al. 2013a). Whether or not methane can reach the sea surface and enter the atmosphere is discussed in Chap. 6.

When gas flow is weak and most of the gas is in solution within sediment porewater, methane is more easily oxidised and consumed by diverse communities of bacteria and archaeal metanotrophs (e.g., Boetius and Wenzhöfer 2013). In this respect, the seabed represents a biological sink for methane. Therefore, weak exhalations of microseepage are rapidly and completely consumed and destroyed.

References

Anka Z, Berndt C, Gay A (2012) Hydrocarbon leakage through focused fluid flow systems in continental margins. Mar Geol 332–334:1–3

Archer D, Buffet B, Brovkin V (2009) Ocean methane hydrates as a slow tipping point in the global carbon cycle. Proc Nat Acad Sci U.S.A 106:20,596–20,601

Baciu C, Etiope G, Cuna S, Spulber L (2008) Methane seepage in an urban development area (Bacau, Romania): origin, extent and hazard. Geofluids 8:311−320

Balakin VA, Gabrielants GA, Guliyev IS, Dadashev FG, Kolobashkin VM, Popov AI, Feyzullayev AA (1981) Test of experimental study of hydrocarbon degassing of lithosphere of South Caspian basin and adjacent mountains systems, using laser gas-analyzer "Iskatel-2". Dokl Akad Nauk SSSR 260(1):154–156 (in Russian)

Batjes NH, Bridges EM (1994) Potential emissions of radiatively active gases from soil to atmosphere with special reference to methane: development of a global database (WISE). J Geophys Res 99(D8):16,479–16,489

Boetius A, Wenzhöfer F (2013) Seafloor oxygen consumption fuelled by methane from cold seeps. Nat Geosci 6:725–734

Boetius A, Ravenschlag K, Schubert CJ, Rickert D, Widdel F, Gieseke A, Amann R, Jørgensen BB, Witte U, Pfannkuche O (2000) A marine microbial consortium apparently mediating anaerobic methane oxidation. Nature 407:623–626

Clarke RH, Cleverly RW (1991) Leakage and post-accumulation migration. In: England WA, Fleet AJ (eds) Petroleum migration, vol 59. Geological Society Special Publication, London, pp 265–271

Crane K, Vogt PR, Sundvor E, Shor A, Reed T IV (1995) SeaMARC II investigations in the northern Norwegian-Greenland Sea. Meddelelser Norsk Polarinstitutt 137:32–140

Darling WG, Gooddy DC (2006) The hydrogeochemistry of methane: evidence from english ground waters. Chem Geol 229:293–312

Delichatsios MA (1990) Procedure for calculating the air entrainment into turbulent pool and jet fires. J Fire Prot Engin 2:93–98

Dillon WP, Nealon JW, Taylor MH, Lee MW, Drury RM, Anton CH (2001) Seafloor collapse and methane venting associated with gas hydrate on the Blake Ridge—causes and implications to seafloor stability and methane release. In: Paull CK, Dillon WP (eds) Natural gas hydrates: occurrence, distribution, and detection. American Geophysical Union, Washington, pp 211–233

Dimitrov L (2002a) Mud volcanoes—the most important pathway for degassing deeply buried sediments. Earth-Sci Rev 59:49–76

Dimitrov L (2002b) Contribution to atmospheric methane by natural gas seepages on the Bulgarian continental shelf. Contin Shelf Res 22:2429–2442

Dong Y, Scharffe D, Lobert JM, Crutzen PJ, Sanhueza E (1998) Fluxes of CO_2, CH_4 and N_2O from temperate forest soil: the effect of leaves and humus layers. Tellus 50B:243–252

Duffy M, Kinnaman FS, Valentine DL, Keller EA, Clark JF (2007) Gaseous emission rates from natural petroleum seeps in the Upper Ojai Valley, California. Environ Geosci 14:197–207

Etiope G (2005) Mud volcanoes and microseepage: the forgotten geophysical components of atmospheric methane budget. Ann Geophys 48:1–7

Etiope G (2009a) Natural emissions of methane from geological seepage in Europe. Atm Environ 43:1430–1443

Etiope G (2009b) GLOGOS, A new global onshore gas-oil seeps dataset. Search and discovery, Article #70071, AAPG online journal. http://www.searchanddiscovery.net. Accessed Dec 2014

Etiope G, Klusman RW (2002) Geologic emissions of methane to the atmosphere. Chemosphere 49:777–789

Etiope G, Klusman RW (2010) Microseepage in drylands: flux and implications in the global atmospheric source/sink budget of methane. Glob Plan Change 72:265–274

Etiope G, Martinelli G (2009) "Pieve Santo Stefano" is not a mud volcano: comment on "Structural controls on a carbon dioxide-driven mud volcano field in the Northern Apennines" (by Bonini 2009). J Struct Geol 31:1270–1271

Etiope G, Milkov AV (2004) A new estimate of global methane flux from onshore and shallow submarine mud volcanoes to the atmosphere. Environ Geol 46:997−1002

Etiope G, Caracausi A, Favara R, Italiano F, Baciu C (2002) Methane emission from the mud volcanoes of Sicily (Italy). Geophys Res Lett 29, doi:10.1029/2001GL014340

Etiope G, Feyzullaiev A, Baciu CL, Milkov AV (2004) Methane emission from mud volcanoes in eastern Azerbaijan. Geology 32:465–468

Etiope G, Papatheodorou G, Christodoulou D, Ferentinos G, Sokos E, Favali P (2006) Methane and hydrogen sulfide seepage in the NW Peloponnesus petroliferous basin (Greece): origin and geohazard. AAPG Bull 90:701–713

Etiope G, Martinelli G, Caracausi A, Italiano F (2007) Methane seeps and mud volcanoes in Italy: gas origin, fractionation and emission to the atmosphere. Geophys Res Lett 34:L14303. doi:10.1029/2007GL030341

Etiope G, Lassey KR, Klusman RW, Boschi E (2008) Reappraisal of the fossil methane budget and related emission from geologic sources. Geophys Res Lett 35:L09307. doi:10.1029/2008GL033623

Etiope G, Feyzullayev A, Baciu CL (2009) Terrestrial methane seeps and mud volcanoes: a global perspective of gas origin. Mar Pet Geol 26:333–344

Etiope G, Zwahlen C, Anselmetti FS, Kipfer R, Schubert CJ (2010) Origin and flux of a gas seep in the Northern Alps (Giswil, Switzerland). Geofluids 10:476–485

Etiope G, Baciu C, Schoell M (2011a) Extreme methane deuterium, nitrogen and helium enrichment in natural gas from the Homorod seep (Romania). Chem Geol 280:89–96

Etiope G, Nakada R, Tanaka K, Yoshida N (2011b) Gas seepage from Tokamachi mud volcanoes, onshore Niigata Basin (Japan): origin, post-genetic alterations and CH_4-CO_2 fluxes. Appl Geochem 26:348–359

Etiope G, Schoell M, Hosgormez H (2011c) Abiotic methane flux from the Chimaera seep and Tekirova ophiolites (Turkey): understanding gas exhalation from low temperature serpentinization and implications for Mars. Earth Planet Sci Lett 310:96–104

Etiope G, Christodoulou D, Kordella S, Marinaro G, Papatheodorou G (2013a) Offshore and onshore seepage of thermogenic gas at Katakolo Bay (Western Greece). Chem Geol 339:115–126
Etiope G, Drobniak A, Schimmelmann A (2013b) Natural seepage of shale gas and the origin of "eternal flames" in the Northern Appalachian Basin, USA. Mar Pet Geol 43:178–186
Greber E, Leu W, Bernoulli D, Schumacher ME, Wyss R (1997) Hydrocarbon provinces in the Swiss southern Alps—a gas geochemistry and basin modelling study. Mar Pet Geol 14:3–25
Guliyev IS, Feizullayev AA (1997) In: All about mud volcanoes. NAFTA-Press, Baku Pub, House, p 120
Herbin JP, Saint-Germès M, Maslakov N, Shnyukov EF, Vially R (2008) Oil seeps from the "Boulganack" mud volcano in the Kerch Peninsula (Ukraine—Crimea), study of the mud and the gas: inferences for the petroleum potential. Oil Gas Sci Technol Rev IFP 63:609–628
Hong WL, Etiope G, Yang TF, Chang PY (2013) Methane flux of miniseepage in mud volcanoes of SW Taiwan: comparison with the data from Europe. J Asian Earth Sci 65:3–12
Hornafius JS, Quigley D, Luyendyk BP (1999) The world's most spectacular marine hydrocarbon seeps (Coal Oil Point, Santa Barbara Channel, California): quantification of emissions. J Geophys Res 20(C9):20,703–20,711
Hosgormez H, Etiope G, Yalçın MN (2008) New evidence for a mixed inorganic and organic origin of the Olympic Chimaera fire (Turkey): a large onshore seepage of abiogenic gas. Geofluids 8:263–275
Hovland M, Judd AG (1988) Seabed pockmarks and seepages: impact on geology, biology and the marine environment. Graham and Trotman, London, 293 pp
Hovland M, Judd AG, Burke RA Jr (1993) The global flux of methane from shallow submarine sediments. Chemosphere 26:559–578
Hovland M, Jensen S, Fichler C (2012) Methane and minor oil macro-seep systems—their complexity and environmental significance. Mar Geol 332–334:163–173
Ionescu A (2015) Geogenic methane in petroliferous and geothermal areas in Romania: origin and emission to the atmosphere. Dissertation, Babes-Bolyai University, Cluj-Napoca
St. John B (1980) Sedimentary basins of the world and giant hydrocarbon accumulations. Tulsa, AAPG, Map and Accompanying Text, 26 pp
Judd AG, Hovland M (2007) Seabed fluid flow: impact on geology, biology and the marine environment. Cambridge University Press, Cambridge
Kappel WM, Nystrom EA (2012) Dissolved methane in New York groundwater. U.S. Geological Survey Open-File Report 2012–1162, 6 pp. http://pubs.usgs.gov/of/2012/1162/
Kelley JT, Dickson SM, Belknap DF, Barnhardt WA, Henderson M (1994) Giant sea-bed pockmarks: evidence for gas escape from Belfast Bay. Mar Geol 22:59–62
Khan SD, Jacobson S (2008) Remote sensing and geochemistry for detecting hydrocarbon microseepages. GSA Bull 120:96–105
King LH, MacLean B (1970) Pockmarks on the Scotian shelf. GSA Bull 81:3141–3148
Klusman RW (1993) Soil gas and related methods for natural resource exploration. Wiley, Chichester 483 pp
Klusman RW (2003a) Rate measurements and detection of gas microseepage to the atmosphere from an enhanced oil recovery/sequestration project, Rangely, Colorado, USA. App Geochem 18:1825–1838
Klusman RW (2003b) A geochemical perspective and assessment of leakage potential for a mature carbon dioxide-enhanced oil recovery project and as a prototype for carbon dioxide sequestration, Rangely field, Colorado. AAPG Bull 87:1485–1507
Klusman RW (2005) Baseline studies of surface gas exchange and soil–gas composition in preparation for CO_2 sequestration research: Teapot Dome, Wyoming USA. AAPG Bull 89:981–1003
Klusman RW (2006) Detailed compositional analysis of gas seepage at the National Carbon Storage Test Site, Teapot Dome, Wyoming USA. App Geochem 21:1498–1521
Klusman RW (2009) Geochemical detection of gas microseepage from CO_2 sequestration AAPG/SEG/SPE Hedberg Conference. "Geological Carbon Sequestration: Prediction and Verification" August 16–19, 2009, Vancouver, BC Canada

Klusman RW, Jakel ME, LeRoy MP (1998) Does microseepage of methane and light hydrocarbons contribute to the atmospheric budget of methane and to global climate change? Ass Pet Geochem Explor Bull 11:1–55

Klusman RW, Leopold ME, LeRoy MP (2000) Seasonal variation in methane fluxes from sedimentary basins to the atmosphere: results from chamber measurements and modeling of transport from deep sources. J Geophys Res 105D:24,661–24,670

Kopf AJ (2002) Significance of mud volcanism. Rev Geophys 40:1–52

Link WK (1952) Significance of oil and gas seeps in world oil exploration. AAPG Bull 36:1505–1540

Liu Q, Chan L, Liu Q, Li H, Wang F, Zhang S, Xia X, Cheng T (2004) Relationship between magnetic anomalies and hydrocarbon microseepage above the Jingbian gas field, Ordos basin, China. AAPG Bull 88:241–251

LTE (2007) Phase II raton basin gas seep investigation las animas and huerfano counties, Colorado, Project #1925 oil and gas conservation response fund. http://cogcc.state.co.us/Library/Ratoasin/Phase%20II%20Seep%20Investigation%20Final%20Report.pdf

Martinelli G, Cremonini S, Samonati E (2012) Geological and geochemical setting of natural hydrocarbon emissions in Italy. In: Advances in natural gas technology, InTech e Open Access Publisher, RIJEKA, pp 79–120 http://cdn.intechopen.com/pdfs/35288/InTech-Geological_and_geochemical_setting_of_natural_hydrocarbon_emissions_in_italy.pdf

Masters CD, Root DH, Turner RM (1998) World conventional crude oil and natural gas: identified reserves, undiscovered resources and futures. U.S. Geol Survey Open-File Report 98–468

Mazzini A, Svensen H, Etiope G, Onderdonk N, Banks D (2011) Fluid origin, gas fluxes and plumbing system in the sediment-hosted Salton Sea Geothermal System (California, USA). J Volc Geoth Res 205:76–83

Mazzini A, Etiope G, Svensen H (2012) A new hydrothermal scenario for the 2006 Lusi eruption, Indonesia. Insights from gas geochemistry. Earth Planet Sci Lett 317–318:305–318

Milkov AV (2000) Worldwide distribution of submarine mud volcanoes and associated gas hydrates. Mar Geol 167:29–42

Milkov AV (2004) Global estimates of hydrate-bound gas in marine sediments: how much is really out there? Earth Sci Rev 66:183–197

Milkov AV, Sassen R (2001) Estimate of gas hydrate resource, northwestern Gulf of Mexico continental slope. Mar Geol 179:71–83

Milkov A, Vogt PR, Crane K, Lein AY, Sassen R, Cherkashev GA (2004) Geological, geochemical, and microbial processes at the hydrate bearing Håkon Mosby mud volcano: a review. Chem Geol 205:347–366

Morner NA, Etiope G (2002) Carbon degassing from the lithosphere. Global Planet Change 33:185–203

Motyka RJ, Poreda RJ, Jeffrey WA (1989) Geochemistry, isotopic composition, and origin of fluids emanating from mud volcanoes in the Copper River basin Alaska. Geochim Cosmochim Acta 53:29–41

Papatheodorou G, Hasiotis T, Ferentinos G (1993) Gas-charged sediments in the Aegean and Ionian Seas, Greece. Mar Geol 112:171–184

Peckmann J, Reimer A, Luth U, Luth C, Hansen BT, Heinicke C, Hoefs J, Reitner J (2001) Methane-derived carbonates and authigenic pyrite from the northwestern Black Sea. Mar Geol 177:129–150

Reeves F (1953) Italian oil and gas resources. AAPG Bull 37:601−653

Römer M, Torres M, Kasten S, Kuhn G, Graham AGC, Mau S, Little CTS, Linse K, Pape T, Geprägs P, Fischer D, Wintersteller P, Marcon Y, Rethemeyer J, Bohrmann G, shipboard scientific party ANT-XXIX/4 (2014) First evidence of widespread active methane seepage in the Southern Ocean, off the sub-Antarctic island of South Georgia. Earth Planet Sci Lett 403:166–177

Sassen R, Roberts HH, Aharon P, Larkin J, Chinn EW, Carney R (1993) Chemosynthetic bacterial mats at cold hydrocarbon seeps, Gulf of Mexico continental-slope. Org Geochem 20:77–89

Sassen R, Joye S, Sweet ST, DeFreitas DA, Milkov AV, MacDonald IR (1999) Thermogenic gas hydrates and hydrocarbon gases in complex chemosynthetic communities, Gulf of Mexico continental slope. Org Geochem 30:485–497

Saunders DF, Burson KR, Thompson CK (1999) Model for hydrocarbon microseepage and related nearsurface alterations. AAPG Bull 83:170–185

Schumacher D, Abrams MA (1996) Hydrocarbon migration and its near surface expression. AAPG Memoir 66:446 pp

Sechman H (2012) Detailed compositional analysis of hydrocarbons in soil gases above multi-horizon petroleum deposits—a case study from western Poland. App Geochem 27:2130–2147

Skinner JA Jr, Mazzini A (2009) Martian mud volcanism: terrestrial analogs and implications for formational scenarios. Mar Pet Geol 26:1866–1878

Solheim A, Elverhoi A (1997) Gas-related sea-floor depressions. In: Glaciated continental margins, Chapman and Hall, London

Spulber L, Etiope G, Baciu C, Malos C, Vlad SN (2010) Methane emission from natural gas seeps and mud volcanoes in Transylvania (Romania). Geofluids 10:463–475

Sturz AA, Kamps RL, Earley PJ (1992) Temporal changes in mud volcanoes, Salton Sea Geothermal Area. In: Kharaka YK, Maest AS (eds) Water-rock interaction. Balkema, Rotterdam, pp 1363–1366

Suess E (2010) Marine cold seeps. In: Kenneth N (ed) Handbook of hydrocarbon and lipid microbiology. Springer, Timmis, pp 185–203

Tang J, Bao Z, Xiang W, Gou Q (2007) Daily variation of natural emission of methane to the atmosphere and source identification in the Luntai Fault region of the Yakela condensed oil/gas field in the Talimu basin, Xinjiang, China. Acta Geol Sinica 81:771–778

Tang J, Yin H, Wang G, Chen Y (2010) Methane microseepage from different sectors of the Yakela condensed gas field in Tarim Basin, Xinjiang, China. App Geochem 25:1257–1264

Thiel V, Peckman J, Richnow HH, Luth U, Reitner J, Michaelis W (2001) Molecular signals for anaerobic methane oxidation in Black Sea seep carbonates and microbial mat. Mar Chem 73:97–112

Tucker J, Hitzman D (1996) Long-term and seasonal trends in the response of hydrocarbon-utilizing microbes to light hydrocarbon gases in shallow soils. In: Schumacher D, Abrams MA (eds) Hydrocarbon migration and its near-surface expression. AAPG Mem 66:353–357

Valentine DL (2011) Emerging topics in marine methane biogeochemistry. Ann Rev Mar Sci 3:147–171

van der Meer F, van Dijk P, van der Werff H, Yang H (2002) Remote sensing and petroleum seepage: a review and case study. Terra Nova 14:1–17

Wagner M, Wagner M, Piske J, Smit R (2002) Case histories of microbial prospection for oil and gas, onshore and offshore northwest Europe. In: Schumacher D, LeSchack LA (eds) Surface exploration case histories: applications of geochemistry, magnetics and remote sensing, AAPG studies in geology no 48 and SEG Geophys Ref Series no 11, pp 453–479

Warner NR, Kresse TM, Hays PD, Down A, Karr JD, Jackson RB, Vengosh A (2013) Geochemical and isotopic variations in shallow groundwater in areas of the Fayetteville Shale development, north-central Arkansas. App Geochem 35:207–220

Yang TF, Yeh GH, Fu CC, Wang CC, Lan TF, Lee HF, Chen CH, Walia V, Sung QC (2004) Composition and exhalation flux of gases from mud volcanoes in Taiwan. Environ Geol 46:1003–1011

Chapter 3
Gas Migration Mechanisms

The basic principles and laws governing the migration of natural gases and their seepage to Earth's surface are provided in this chapter by examining the geological factors or processes that influence physical parameters within transport equations. To offer a simple reference framework of seepage processes to readers without specialised knowledge of gas dynamics, migration mechanisms, diffusion and advection in their various forms are summarised without complex mathematics and using carefully controlled terminology. Additional details, retracing the history of gas migration studies, may be obtained from Illing (1933), Muskat (1946), MacElvain (1969), Bear (1972), Pandey et al. (1974), Malmqvist and Kristiansson (1985), Price (1986), and Brown (2000), as well as in the review paper by Etiope and Martinelli (2002). Oil migration is not the focus of this chapter.

3.1 Fundamentals

3.1.1 Sources and Pathways

Gas migration and seepage to the surface are strictly related to the existence of two geological features, a gas migration source and a preferential route for gas motion. The concepts are linked to the Petroleum Seepage System (PSS) introduced in Chap. 1.

The migration source (the starting point of migration) is not necessarily the gas source, in other words, where the gas is generated (source rock). Accumulations of gas (reservoirs) are common migration sources. However, it is possible that gas seeping to Earth's surface may also come directly from source rocks (e.g., shales) without reservoir intermediation, as considered in recent theoretical models (Berbesi et al. 2014) and suspected in a seep located in the State of New York, USA (Etiope et al. 2013). As discussed in Chap. 5, this argument is fundamental for assessing petroleum systems.

G. Etiope, *Natural Gas Seepage*, DOI 10.1007/978-3-319-14601-0_3

The preferential routes of gas flow are zones of enhanced permeability such as sand horizons within a clayey sequence (mainly horizontal migration), and tectonic discontinuities such as faults and fracture networks (mainly vertical migration). Permeability is the basic parameter controlling gas flow through porous and fractured media (porosity only determines the gas volume stored within a rock). Permeability is a constant determined only by the media's structure and independent of the nature of the fluid passing through the media (Muskat 1946). Hence, water permeability and gas permeability are the same for dry media. For a two-phase system, gas permeability decreases as water content increases because the space available for gas is reduced.

In practice, secondary permeability due to the fracturing and faulting induced by tectonic movements is the leading factor driving gas seepage. The shape, size, and local distribution of macro-seeps, as well as gas injection tests (e.g., Ciotoli et al. 2005) and "chimneys" in seismic images (e.g., Heggland 1998; Loseth et al. 2009), indicate that gas typically follows channels of enhanced permeability (i.e. of minor resistance to gas motion), and that once the preferential pathway (the 'channel') is activated, gas flow only occurs along this channel and is insensitive to the permeability of contiguous rock volumes. The process is also known as "fracture flow" (Loseth et al. 2009). The channel provides minimum dissipation for gas energy and the conservation of pressure and flow rate. Basically, seepage does not occur throughout the fault line but only in some portions, forming spotty seeps on the surface. Channels may then "migrate" horizontally and change their position along faults due to, for example, fracture self-sealing and fracture propagation. In fact, it is not rare to observe seeps (vents and craters) that change their location by a few meters or tens of meters year after year.

3.1.2 Diffusion and Advection

Depending on the source and the surrounding permeabilities, gas movement can be induced by two types of force fields, concentration gradients and pressure gradients. In the first case, the spreading of gas molecules in a direction that tends to equalise the concentrations in all parts of a rock system occurs as gas "diffusion". In the second case, the entire gaseous mass tends to move from a zone of high pressure to a zone of low pressure; this mass transport is called "advection".

In the scientific literature, the terms "mass transport", "viscous flow", "fluid flow", "air flow", "non-diffusive transport", and "effusion" (e.g., Harbert et al. 2006) are also used for advection. However, some authors have improperly used the term "convection" to indicate pressure-driven transport (e.g., Mogro-Campero and Fleischer 1977). "Convection" is advective movement with a pressure gradient generated by thermal gradients. Since it disperses more rapidly and consequently become lighter, a warmer gas ascends (i.e., at constant volume, a warmer gas is more pressurised). In other words, "convection" is a form of advection driven by temperature gradients. Changing the perspective from temperature to pressure is

possible using the equation of state. It is incorrect, however, to name as "convective" something that is not linked to temperature effects, such as normal gas flows linked to buoyancy or to hydrostatic and lithostatic gradients. Convective flows are more typical of geothermal systems.

Diffusion and advection can be examined using transport equations without complex mathematics, i.e. assuming realistic limitations (those frequently adopted to solve practical problems) on the nature of fluid and porous media. In Muskat (1946), Wickoff outlines the inadequacy of applying the rigorous mathematical solutions of certain physical laws to complex geological settings.

Diffusion is the movement of a chemical species from a volume of high concentration of that species to a volume of lower concentration. The movement is described by Fick's Law, in which the gas flux is directly related to the concentration gradient and a constant, as follows:

$$F = -D_m \nabla C \qquad (\nabla = \delta/\delta x + \delta/\delta y + \delta/\delta z) \tag{3.1}$$

or for a one-dimensional form along the z axis, as follows:

$$F = -D_m dC/dz \tag{3.2}$$

where D_m is the molecular diffusion coefficient (m^2/s) and dC is the variation in gas concentration (kg/m^3) along dz (m). The molecular diffusion coefficient is a constant for the specific gas and it is controlled by molecular size and shape. The lighter the hydrocarbon, the greater the coefficient. The coefficient only changes with temperature, pressure, and the physical nature of the substance through which molecular motion occurs. In rock pores, this substance is generally water or air (or a gas mixture). Therefore, for each gas, the diffusion coefficient in water (D_{mw} or simply D_w) must be distinguished from the diffusion coefficient in air (D_{ma} or simply D_m). Furthermore, in porous media the volume through which gas diffuses is reduced and the average path length between two points is increased (i.e. tortuosity). Interstitial diffusion is then defined by the "effective" diffusion coefficient (D_e), as follows:

$$D_e = D_m n \tag{3.3}$$

where n is the effective porosity of the media (%) and describes diffusion by considering the motion of a gas molecule through a porous structure. Global diffusion is defined by the "apparent" diffusion coefficient (D), also known in the literature as the "true" or "bulk" coefficient; it includes the effects of the porosity and tortuosity of the media. For soil, most authors agree to define this coefficient, as follows (e.g., Lerman 1979):

$$D = D_e n = D_m n^2 = D_m n/\tau \tag{3.4}$$

where τ is the tortuosity of the media. In conclusion, $D_m > D_e > D$.

In practice, a gas diffusing over time t will cover a diffusive distance (Z_d) based on the following equation:

$$Z_d = (D\ t)^{0.5} \tag{3.5}$$

The equation indicates that methane diffusing in still water (D_w: 1.5×10^{-5} cm^2/s) will cover 1.1 cm in 1 day, 22 cm per year, 6.9 m in 1000 years, etc. Ethane, propane, and butane will be progressively slower, as the diffusion coefficient of each hydrocarbon is 1.23 times that of its next heavier homolog (e.g., Witherspoon and Saraf 1965).

The term advection refers to the movement of matter under the influence of external forces, namely pressure gradients. In a broader sense, all of the following movements due to "global" forces are advective (Lerman 1979): atmospheric precipitation, evaporation, wind, the deposition of sediments, groundwater flow, and the movement of crustal plates.

A gas with a concentration C (kg/m^3) and a velocity v (m/s) results in the following flux:

$$F = C\ v \tag{3.6}$$

Velocity depends on the pressure gradient and on a mobility coefficient that is related to the geometry of the media and gas viscosity. In the case of advection through dry porous media, the mobility coefficient depends on the intrinsic permeability of the media, according to Darcy's Law:

$$v = -k\nabla P/\mu \quad (\nabla = \delta/\delta x\ + \delta/\delta y\ + \delta/\delta z) \tag{3.7}$$

or in a one-dimensional form, along the z axis, and for a short distance:

$$v = k\Delta P/(\mu Z) \tag{3.8}$$

where v is the gas velocity (m/s), k is the intrinsic permeability (m^2), μ is the dynamic gas viscosity ($kg\ m^{-1}\ s^{-1}$), and ΔP is the pressure difference ($kg\ m^{-1}\ s^{-2}$) between two points spaced at a distance Z (m).

An estimate of advective gas velocity through a planar fissure may be obtained using the following formula (Gascoyne and Wuschke 1992):

$$v = (b^2/12\mu)(dP/dz) \tag{3.9}$$

where ($b^2/12$) is the fissure permeability, b is the fissure width, and μ is the gas viscosity.

For estimating gas velocity through fractured media (a system of intersecting fissures), "cubic law" (Schrauf and Evans 1986) can apply, as follows:

$$v = (b^3/6d\mu)(dP/dz) \tag{3.10}$$

where d is the mean distance between intersecting fissures (m).

Advective processes can occur within the subsurface whenever pressure gradients between two points occur. Such gradients can be induced by tectonic stresses, variations in lithostatic loading, rock fracturing, localised gas generation, the recharge and discharge of aquifers and deep fluid reservoirs, and, near the surface, by barometric pressure pumping. Also, the natural tendency of lighter gases (e.g., helium, hydrogen) to ascend due to low density is an advective phenomenon. In fact, a gas with a density ρ_1, moves upward if it is bounded by a gaseous phase with a density $\rho_2 > \rho_1$. The lighter gas is subjected to a pressure gradient $\rho_2 g$ and the following equation is valid:

$$v = k\ g(\rho_2 - \rho_1)/\mu \tag{3.11}$$

with g acceleration of gravity, and the term $g\ (\rho_2 - \rho_1)$ is equivalent to a pressure gradient. The very existence of a naturally occurring background pressure gradient in the Earth is an index of continuous outgassing.

In the geological environment, diffusion and advection almost never act separately; thus, formally, the movement of gas should be ascribed to them in combination. By combining the diffusion and advection terms, the total flux of gas, in a one-dimensional form, is:

$$F = [-n\ D_m(dC/dz)] + [v\ C] \tag{3.12}$$

where $[-n\ D_m\ (dC/dz)]$ is the diffusive term and [v C] is the advective term.

Depending on the assumptions and limitations adopted, the general equation of transport, in terms of mass conservation, may be written in more or less complex forms. In most cases, for practical problems, migration models and their relevant equations can follow criteria of simplicity and acceptable approximation. Therefore, it is possible to consider one-dimensional equations for laminar and steady-state flows through dry, homogeneous, and isotropic porous media.

Hence, the following general transport equation, common in fluid mechanics, can be obtained:

$$n\ D_m\left(d^2C/dz^2\right) - v(dC/dz) + (\alpha - \omega) = 0 \tag{3.13}$$

where α is the generation rate of the gas and ω is the rate of removal of the gas from the stream (as a result of adsorption by rocks, the dissolution by groundwater, or microbiological consumption). In practice, several variants of the equation exist.

3.2 Actual Mechanisms and Migration Forms

For a seepage system especially, the velocity and spatial scales of advective movements are much higher than the diffusive ones. Diffusion is only important in capillaries or small-pore rocks, indicating that within a petroleum seepage system diffusion is the prevailing mechanism of "primary migration" (Hunt 1996) in gas source rocks (shales and limestones), after or during the generation of hydrocarbons. Thus, the diffusion coefficients of methane and heavier alkanes in water (mentioned above) should be considered. Frequently, the generation of hydrocarbons is concurrent with the diagenesis of clays such as smectites to illite, resulting in water being simultaneously driven out as an advective process. Some gas can then be transported in solution by water. The passage of gas from source to external rocks to trapped reservoir rocks (secondary migration), and from one reservoir to another or to Earth's surface (tertiary migration) is largely driven by pressure gradients (Fig. 3.1). Advection assumes an exclusive role in larger pores or in fractured media outside of source rocks.

However, depending on the physical-geological conditions that the gas encounters, the nature of the driving force can change during gas ascent. Furthermore, sedimentary basins and their constituent rocks are subjected to basin loading, compaction with water loss, extensional and compressional stresses, and other tectonic forces that change the driving force of gas flow. Finally, variations in temperature, pressure, mechanical stress, chemical reactions, and mineral precipitation change the gas-bearing properties of geological formations. Interactions between all of these factors may lead to time-dependent fluid transport for which gas seepage may be quite variable on daily, seasonal, and geological time scales.

Depending on gas-water-rock system conditions, gas advection can have different forms (Fig. 3.2). In dry porous or fractured media, gas flows through interstitial or fissure space and is defined as gas-phase advection. Equation (3.7) can

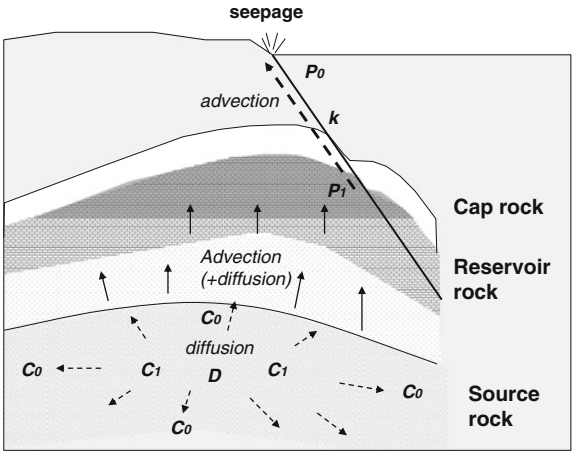

Fig. 3.1 The main factors controlling gas migration from source rocks to reservoirs and to the surface (*P* gas pressure; *k* permeability; *D* gas diffusion coefficient; and *C* gas concentration)

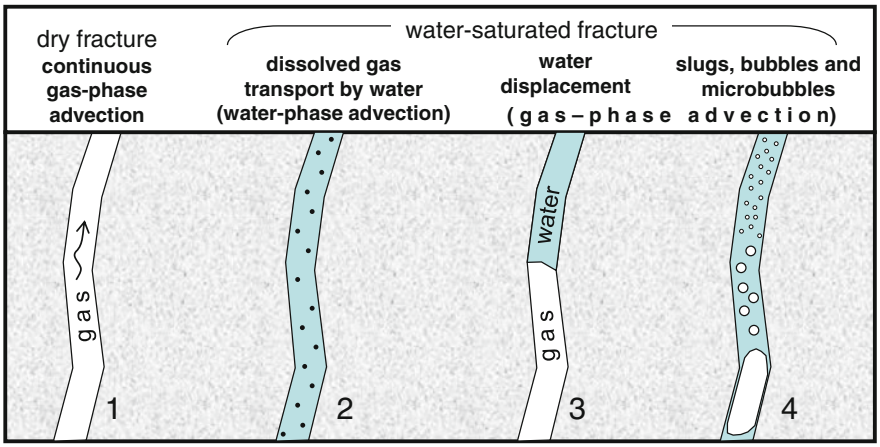

Fig. 3.2 A schematic picture of gas advection forms in dry and water-saturated fractured media. *1* Pressure-driven continuous gas-phase flow through dry fractures. *2* The water-phase transport of gas in solution. *3* A pressure-driven or density-driven continuous gas-phase displacing water in saturated fractures. *4* The buoyant movement of gas bubbles in aquifers and water-filled fractures, either as slugs or microbubbles

be applied. For saturated porous media, three possible phenomena may occur, as follows:

(a) Gas dissolves and is transported by groundwater (water-phase advection);
(b) Gas flows and displaces water (gas-phase advection); and
(c) Gas flows as bubbles.

In water-phase advection (a), the gas, being in solution, moves at the same velocity as water; hence, Darcy's equation, in the following form used in hydrogeology, is valid:

$$v = K\, i \tag{3.14}$$

where K is the hydraulic conductivity of the media (in darcy units) and i is the hydraulic gradient.

For gas-phase advection through water-saturated media, gas must have a pressure (Pg) above the sum of hydrostatic pressure (Pw) plus a capillary pressure (Pc). Hydrostatic pressure is given by the height of the piezometric surface (Hw) from the point considered ($Pw = \rho_\omega\, g\, H_w$). Capillary pressure is linked to the interfacial tension of water (σ) and to the pore throat radius (r) according to the Laplace equation ($Pc = 2\sigma/r$). When $Pg < (Pw + Pc)$, gas only enters the media by diffusion. When $Pg > (Pw + Pc)$ two-phase flow occurs, with water displaced by gas. If $Pg = Pfr >> (Pw + Pc)$ gas fractures the rock (Pfr is the pressure at which the fracture begins and roughly corresponds to the lithostatic pressure). When the gas pressure Pg reaches Pfr, gas flows through the fracture planes generated. If, however, $Pfr < (Pw + Pc)$, gas flow only occurs in the fracture and there is no

migration of gas within the rock matrix. The pressure can rise and bring about the propagation of the fracture network. If, on the contrary, Pfr > (Pw + Pc), gas will flow in the fracture and from the fracture towards the matrix. Here, it should be noted that both hydrostatic and lithostatic pressure can operate on the gas (as occurs in a "gas cap") to serve as a driving force for the gas itself.

As a result, water displacement (b) occurs when Pg > (Pw + Pc) and can be at a different scale depending on the dimension of the advancing front of the gas with respect to the type of water-bearing media (homogenous porous media, single fracture, etc.). For example, within a saturated fissure, gas totally displaces water if the gas strip front has a size similar to the fissure width (Gascoyne and Wuschke 1992). Equation (3.9) can be used by considering the difference of density between gas and water as the pressure gradient. On the contrary, if gas moves as a tiny strip, with a size less than that of the fracture width, or moves as an intermittent flow (i.e. Pg varies in time from values above to values below the displacement threshold = Pw + Pc) or, finally, exsolves from water by oversaturation, then gas bubbles form (c). The bubble flow mechanism is considered to be a common form of gas movement in the subsurface, so deserves a separate discussion.

3.2.1 Bubble and Microbubble Flow

Bubble and microbubble buoyancy is a commonly proposed mechanism for gas seepage, including microseepage (Price 1986; Klusman and Saeed 1996; Saunders et al. 1999; Brown 2000). The phenomenon has been studied in its two main stages, bubble formation and bubble motion.

Bubbles in a liquid can originate from two main mechanisms: (a) the supersaturation of a solution of a gas or (b) direct introduction into a liquid (i.e. mechanical entrainment; Teller et al. 1963). Saturation depends on gas solubility, which is, in turn, influenced by temperature and pressure (as well as by pH and ionic strength). Temperature increases and pressure decreases lead to water degassing. In the subsurface, depressurisation can occur when moving groundwater meets fractures, when the hydrostatic or lithostatic pressure drops (e.g., after erosion, landslides, or mining), or when pumping effects are induced by tectonic stress or aquifer charging and discharging. Increasing temperatures can be linked to variations in the thermal conductivity of rocks (i.e., water crosses rocks with different thermal conductivities) or to variations within the local geothermal gradient resulting from hydrogeological or tectonic phenomena. The appearance of a bubble requires a gas nucleus as a void in the liquid. The nucleus may be in the form of a nanoscopic bubble or of a solid carrying adsorbed gas. Such "heterogeneities" act as catalysts for the degassing induced by T and P variations. For example, bubble formation is made easier by energetic particles produced during the "alpha" decay of radioactive minerals (Malmqvist and Kristiansson 1985). Obviously, a solution also becomes oversaturated when gas is locally generated by microbiological or

chemical reactions. For further details on bubble nucleation and formation, the reader may refer to Frenkel (1955), Mesler (1986), and Tsuge (1986).

Bubbles and microbubble streams can form when a fault crosses an aquifer, with gas coming from depth along the fault itself. The growth of a gas bubble in water is controlled by the diffusion of the gas dissolved in water, and by the decompression of gas within the bubble as the hydrostatic pressure decreases. With bubble growth, buoyancy forces become more important and at a certain moment overcome the drag forces that tend to keep the bubble stationary. A bubble in water can then move in accordance with Stokes' Law, as follows:

$$v = d^2 g\left(\rho_w - \rho_g\right)/18\mu_w, \tag{3.15}$$

where v is the bubble velocity (m s^{-1}), d is the bubble diameter (m), g is the gravity acceleration (m s^{-2}), ρ_w and ρ_g are the water and gas density, respectively (kg m^{-3}), and μ_w is the water viscosity (kg m^{-1} s^{-1}). The equation indicates that the velocity of a bubble is directly related to the square of its diameter. When hydrostatic pressure decreases, d increases and bubbles accelerate with respect to the surrounding water. The equation, so written, is the general form of Stokes' Law. The equation must be properly modified for porous media. First, parameter d must have an upper limit somehow related to the structure of the media. Explicitly, it is expected that the maximum size of bubbles is controlled by the minimum transverse section of the migration path through porous media. For a fractured rock, bubble size may be related to the minimum distance between the fissure walls. Using the following equation, Várhegyi et al. (1986) described a theoretical model for estimating the size of a bubble (d_B) and its velocity as a function of media porosity (n) and grain diameter (d_G):

$$d_B = 1.26\, d_G\, n(n + 0.21) \tag{3.16}$$

Using this formula, it is possible to derive the maximum velocity (with the bubble size being equal to the pore space) of gas bubbles through homogeneous and equigranular porous media, although this kind of media is only rarely found in nature. In theory, the relationship between d_G and the true grain size distribution is very difficult to investigate. However, for the case of a wide grain size distribution, it is likely that d_G (equivalent to mean grain size) is shifted towards finer sizes and that the cross section available for bubble flow is reduced (Várhegyi et al. 1986). To estimate the order of magnitude of microbubble velocity in geologic media, the modified Stokes' equation (3.16) may be used, although the model was developed by considering the generic Stokes' Law of bubble motion using bubble diameter as a function of rock porosity. For fractured media, the fracture or fissure width determines the maximum bubble diameter required for Varhegyi's equation. Since it does not take into account a number of factors that occur under real conditions, the simple model must be considered as a first approach for bubble velocity derivations in geological environments. The velocity given by Stokes' equation should refer to single bubbles in "unbounded" water conditions, when the motion and

shape of a given bubble is not perturbed by other bubbles or the wall effect induced by the fracture. By increasing gas fluxes, bubbles can coalesce to produce vertically elongated bubbles called "slugs", then continuous gas streams within the fracture.

In short, depending on the gas flux and fracture size for which the velocity of gas bubbles must be examined, the following bubble flow patterns can be identified as those possibly occurring in natural rock fractures:

1. Bubbles with a negligible fracture wall effect. Classic equations of single bubble motion can be used by assuming that there is no perturbation of bubble flow by the fracture walls. Such a condition can occur for microbubbles in relatively larger fractures and rock voids.
2. Bubbles rising along a typically narrow fracture whose walls influence bubble rise (the fracture width close to the bubble diameter). The bubble velocity (v_w), normalized to Stokes' velocity (v), depends on the ratio of the bubble's radius (r) to the half width (b) of the fracture (approximated by parallel plates) according to Brown (2000), as follows:

$$\frac{v_w}{v} = 1 - 1.004\left(\frac{r}{b}\right) + 0.418\left(\frac{r}{b}\right)^3 - 0.21\left(\frac{r}{b}\right)^4 - 0169\left(\frac{r}{b}\right)^5 \tag{3.17}$$

3. Long bubble-trains and slugs ($r > b$). By increasing gas flux and/or reducing the fracture aperture, bubbles become elongated (slugs) forming a typical bubble-train flow.
4. Bubble plumes in larger rock voids ($r << b$). Due to bubble turbulence, an additional upwelling fluid velocity should be considered (variable from 10 to 40 cm/s) (Clift et al. 1978). In large joint systems, water-filled cavernous zones, and sinkholes in karst environments, intense bubble plumes can rise without significant wall friction.

At higher gas pressures and fluxes, slugs can be replaced by connected gas streams driven by pressure gradients. In particular, bubbles coalescing within a subsequent gas stream can occur if the pressure-driven velocity is higher than the buoyancy-driven velocity. Bubble-trains and slug flow can be due to intermittent gas leakages through reservoir–cap rock systems or to the transmission of pressure pulses created by crack propagation due to tectonic (seismic) stresses. Continuous phase flow may exist only if the fracture is continuously invaded by large amounts of gas, with pressures above hydrostatic plus capillary pressures (e.g., leakage from geothermal or hydrocarbon pressurized reservoirs). Any reduction of gas pressure or fracture width will interrupt the flow, and slugs or trains of bubbles will form. As a bubble rises, its radius increases and can be occluded within the fracture. As bubbles occlude, they again coalesce to form longer slugs and then continuous phase gas columns.

3.2.2 Gas Seepage Velocity

Obtaining the velocity of gas migration is an important task in gas seepage studies. Theoretical gas velocity as a function of fracture width can be calculated using Eq. (3.9) for continuous gas-phase flow between parallel plates and Eq. (3.15) for bubble flow in the Stokes regime, by assuming that the bubble diameter is smaller than the fracture width. In Fig. 3.3, velocity curves were plotted for reference conditions corresponding to a subsurface depth of 1,000 m (i.e., 38 °C and 10 MPa; a water density of 1,000 kg/m^3; a water viscosity of 0.0009 Pa; a gas density of 100 kg/m^3; and a gas viscosity of 0.000015 Pa). Due to the simple buoyancy of gas in water, the pressure gradient is assumed to be density-driven. Bubble velocity was computed both with and without the wall effect (Eqs. 3.15 and 3.17, respectively).

Experimental data on in situ gas velocity are very difficult to obtain. Very few examples that include fracture data are available within the literature. Those that are available come primarily from studies on the sealing properties of gas storage reservoirs (e.g., Jones and Thune 1982), or from field gas injection tests (generally performed as a part of studies on the geological disposal of radioactive wastes; e.g., Lineham et al. 1996; Ciotoli et al. 2005) where the injected gas has a pressure equal to the hydrostatic pressure plus a capillary pressure. Studies of leakage from gas storage reservoirs and controlled experiments suggest gas velocities of hundreds of

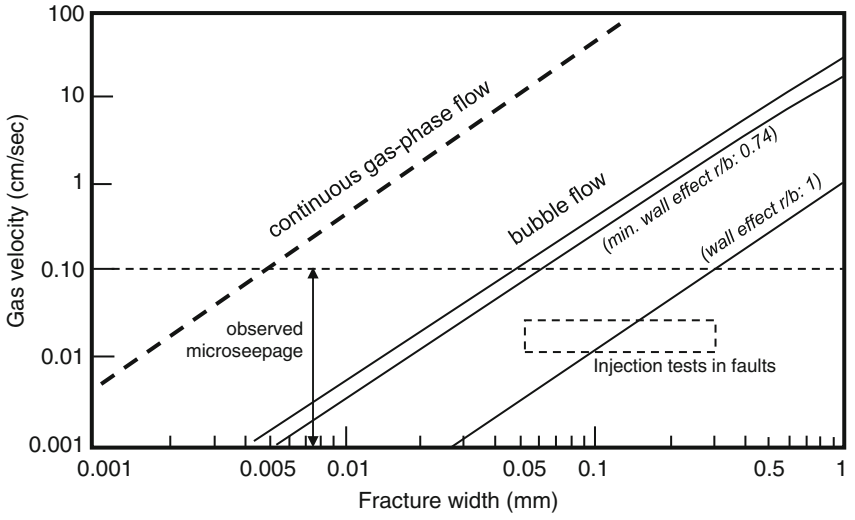

Fig. 3.3 Plot of gas velocity as a function of fracture width (redrawn from Etiope and Martinelli 2002). The theoretical velocities of continuous gas-phase flow and bubble flow were computed for fluid properties at a depth of 1,000 m (see text). The wall-effect bubble velocity was computed for $r/b = 0.74$ and r/b = 1. The *rectangle* represents experimental values from a gas injection test along a fault (Ciotoli et al. 2005). The range of observed microseepage velocities was obtained from Brown (2000)

centimeters per day, orders of magnitude greater than those driven by diffusion alone (Jones and Thune 1982; Harbert et al. 2006). Some conservative estimates for velocity, using an unknown fracture aperture, were made by evaluating the effects of subsurface pressure changes on the surface geochemical signatures of hydrocarbon seepage (Brown 2000). In special cases related to gas vents, velocities can be estimated by measuring the flux of the gas emitted; 150–300 m/day was conservatively estimated for gas rising through mud volcanoes (Martinelli and Ferrari 1991).

Theoretically, as demonstrated by Brown (2000), continuous phase gas migration is the fastest mechanism. In fact, the velocity of continuous phase flow is controlled by the viscosity of gas (Eq. 3.7). The viscosity controlling bubble ascent is that of water, which is approximately 60 times that of gas using the assumed reference conditions. For fractures of a few millimetres, bubble velocity ranges from 0.001 to 10–20 cm/s. Microbubbles of colloidal size (radii below 1 μm), considered by MacElvain (1969) and Price (1986) to be a favourable mechanism for hydrocarbon gas transport, should have low velocities on the order of 10^{-6}–10^{-5} cm/s. Instead, observed gas velocities range on the order of 10^{-4}–10^{0} cm/s (0.1–2,000 m/day). Figure 3.3 suggests that these velocities can easily be reached by continuous phase flows at any fracture width and by bubbles within fractures larger than 0.01 mm. For larger fracture apertures and voids on the order of cm, microbubble plumes may reach velocities on the order of 10^{4} m/day. Depending on the wall effect, bubble-trains and slugs can have velocities intermediate between microbubbles and continuous gas flow. Heinicke and Koch (2000) observed that hydrogeochemical earthquake signals can be due to CO_2 slugs rising through water-filled faults at velocities of approximately 7–8 cm/s (6,000–7,000 m/day). The conclusion of Brown (2000), that gas-bubble ascent cannot account for observed microseepage velocities, is, therefore, only valid for bubbles of colloidal size.

Overall, field and laboratory gas injection tests (e.g., Etiope and Lombardi 1996; Ciotoli et al. 2005) indicate that aquifers do not constitute a barrier for gas migration or reduce gas velocity. In fact, due to the higher buoyancy that develops between gas and water (Eq. 3.15) as compared to that between gas and gas (Eq. 3.11), under the same injection pressure gas in saturated rock moves faster than gas in dry rock.

3.2.3 Matter Transport by Microbubbles

It was suggested, even if experimental data are still scarce, that during their ascent in fractured rocks microbubbles can transport gaseous and solid material, including metallic minerals and radionuclides. This process is generally described as “matter transport by geogas” (Malmqvist and Kristiansson 1984; Kristansson et al. 1990; Hermansson et al. 1991; Etiope 1998). Since the particles may include precious minerals, such as gold, copper and zinc, and radioactive elements, such as uranium, radium and cesium, this phenomenon may have several implications both in ore

prospecting and in underground nuclear or toxic waste repositories. Bubble can take (strip) gaseous and solid material from the surrounding rocks and transport them through four types of physical mechanisms (Fig. 3.4; Hermansson et al. 1991; Etiope 1998): (a) flotation (lifting of solid particles inside the bubble); (b) binding on the gas–water interface of active elements; (c) aerosol transport; (d) transport of volatile compounds dissolved in the carrier gas.

Flotation is a well known physical process (e.g., Aplan 1966) due to the fact that the specific surface energy is higher between water and gas than between minerals and gas. Thus a microbubble stream crossing crushed rocks can lift fine particles and transport them upward. Laboratory observations effectively proved that gas bubbles in porous media can transport argillaceous particles (Goldenberg et al. 1989), and fine powder of metallic elements and radionuclides (Etiope and Lombardi 1996).

Transport of active elements on gas–water interface is due to the lower energy level provided by the interface itself than that occurring in solution. Many elements, mainly radionuclides, tend to attach and concentrate on bubble surfaces (Peirson et al. 1974; Pattenden et al. 1981). It has been shown, for example, that a substantial enrichment of elements can take place on surfaces of bubbles of air that pass through seawater. It was found that foam on the surface water contains up to 600 times more plutonium per unit volume than the sea water (Walker et al. 1986).

Aerosol transport may occur by dispersion of solid and/or liquid particles induced by rapid movement of gas pockets through the rocks. This mechanism is also know as "geoaerosol transport" (Holub et al. 2001) and aerosol sampling from

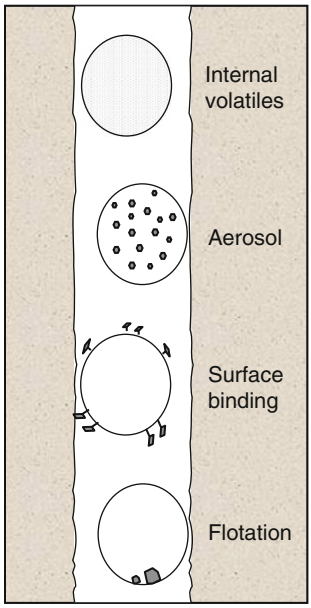

Fig. 3.4 The four mechanisms of matter transport by gas microbubbles along rock fractures

rock fissures has been used in mineral exploration (Kristiansson et al. 1990; Krcmár and Vylita 2001).

Finally, volatile compounds can be mixed inside the bubble gas. They may include both gaseous molecules and volatile compounds such as mercury and arsenic. If such compounds are formed in the fractures of the rocks, they may dissolve in the geogas and be transported to the surface.

These bubble transport mechanisms, especially flotation, appear to be also important for the rapid migration of liquid hydrocarbons and oil. In many mud volcanoes it is not rare to observe oil droplets and iridescences around bubble plumes (Fig. 3.5). Specific studies are however necessary to better understand and model the phenomenon.

3.2.4 The Concept of Carrier Gas and Trace Gas

Another important physical concept regarding gas migration is that of the transport of trace gases by a carrier gas. Advective migration discussed above, either as continuous gas flow or microbubbles, requires a stream of "free gas", i.e. gravitative forces act only on gases which occur at sufficiently large concentrations (gas domain). To form a stream of a particular gaseous species, an immense number of molecules of that species must be available at the same location at the same time. In many cases the amount of heavy gaseous alkanes (especially propane, butane and pentane) and noble gases, such as helium (He) and radon (Rn), occurring in the subsurface is many orders of magnitude too small (orders of ppmv or 10^{-10} ppm for Rn) to form a macroscopic quantity of gas which can react to pressure gradients and flow autonomously by advection (pure radon or helium bubbles do not exist!). Such gases must be carried by a macroscopic flow of another gas which is moving upwards, i.e. a "carrier gas", able to form large gaseous domains. Carrier gas is generally CH_4, CO_2 or N_2, depending on the specific geological environment. Anomalous concentrations of helium in soil-gas (discussed in Chap. 5), for example, can only be explained by an ascending carrier gas, and in fact helium in soil or groundwater is always associated to a major gas, such as CH_4, N_2 or CO_2. The long-distance transport of radon is another phenomenon due to carrier gas advection (e.g., Malmqvist and Kristiansson 1984; Etiope and Martinelli 2002). Radon (^{222}Rn) is an unstable nuclide with a short half-life (3.8 days), so its concentration rapidly decreases during the slow diffusion in the rocks. In order for radon to reach the surface from deep sources (uranium or radium bearing rocks or fluids) before decaying, it must be transported upwards at a rapid rate, which, in itself, is possible only if a rapidly ascending carrier gas exists.

This concept is quite important when applied to the evaluation of sources of the several hydrocarbons occurring in a seeping gas. The minor hydrocarbon compounds that may occur at trace levels (ppmv or ppbv) in a surface seep, such as butane, pentane or olefins (i.e., alkenes, such as ethene, propene, butene) cannot move rapidly and for long distances autonomously. In a gaseous flow system

Fig. 3.5 Oil layers and iridescences around bubbles in mud volcano craters (**a** Kechaldag, Azerbaijan; *photo* by L. Innocenzi, INGV; **b** Paclele Mici, Berca, Romania; *photo* by L. Spulber)

methane is always their carrier gas. This implies that their origin (source rock) cannot be very distant from that of methane, and in most case it is the same. Such a type of evaluation is important to assess the origin of the gas, the possible mixing of compounds from different sources and, thus, the petroleum system, as discussed in Chap. 5.

References

Aplan FF (1966) Flotation. In: Kirk-Othmer (ed) Encyclopedia of chemical technology, 2nd edn. Wiley-Interscience Publications, New York

Bear J (1972) Dynamics of fluids in porous media. Elsevier, New York

Berbesi LA, di Primio R, Anka Z, Horsfield B, Wilkes H (2014) Methane leakage from evolving petroleum systems: masses, rates and inferences for climate feedback. Earth Planet Sci Lett 387:219–228

Brown A (2000) Evaluation of possible gas microseepage mechanisms. AAPG Bull 84:1775–1789

Ciotoli G, Etiope G, Guerra M, Lombardi S, Duddridge GA, Grainger P (2005) Migration and behaviour of gas injected into a fault in low-permeability ground. Q J Eng Geol Hydroge 38:305–320

Clift R, Grace JR, Weber ME (1978) Bubbles, drops and particles. Academic Press, New York

Etiope G (1998) Transport of radioactive and toxic matter by gas microbubbles in the ground. J Environ Radioact 40:11–13

Etiope G, Lombardi S (1996) Laboratory simulation of geogas microbubble flow. Environ Geol 27:226–232

Etiope G, Martinelli G (2002) Migration of carrier and trace gases in the geosphere: an overview. Phys Earth Planet In 129:185–204

Etiope G, Drobniak A, Schimmelmann A (2013) Natural seepage of shale gas and the origin of "eternal flames" in the Northern Appalachian Basin, USA. Mar Pet Geol 43:178–186

Frenkel J (1955) Kinetic theory of liquids. Dover, New York

Gascoyne M, Wuschke DM (1992) Gas flow in saturated fractured rock: results of a field test and comparison with model predictions. In: "Gas generation and release from Rad.Waste Rep.", Proceedings of the NEA Workshop, Aix en Provence, 23–26 Sept 1991

Goldenberg LC, Hutcheon I, Wardlaw N (1989) Experiments on transport of hydrophobic particles and gas bubbles in porous media. Transport Porous Med 4:129–145

Harbert W, Jones VT, Izzo J, Anderson TH (2006) Analysis of light hydrocarbons in soil gases, Lost River region, West Virginia: relation to stratigraphy and geological structures. AAPG Bull 90:715–734

Heggland R (1998) Gas seepage as an indicator of deeper prospective reservoirs. A study on exploration 3D seismic data. Mar Pet Geol 15:1–9

Heinicke J, Koch U (2000) Slug flow—a possible explanation for hydrogeochemical earthquake precursors at Bad Brambach, Germany. Pure Appl Geophys 157:1621–1641

Hermansson HP, Sjoblom R, Akerblom G (1991) Geogas in crystalline bedrock. Statens Kärnbränsle Nämnd (SKN) report 52, Stockholm

Holub RF, Hovorka J, Reimer GM, Honeyman BD, Hopke PK, Smrz PK (2001) Further investigations of the 'Geoaerosol' phenomenon. J Aerosol Sci 32:61–70

Hunt JM (1996) Petroleum geochemistry and geology. W.H. Freeman and Co, New York, 743 pp

Illing VC (1933) Migration of oil and natural gas. Inst Petrol Technol J 19:229–274

Jones VT, Thune HW (1982) Surface detection of retort gases from an underground coal gasification reactor in steeply dipping beds near Rawlins, Wyoming. In: Society of Petroleum Engineers, SPE paper 11050, p 24

Klusman RW, Saeed MA (1996) A comparison of light hydrocarbon microseepage mechanisms. In: Schumacher D, Abrams MA (eds) Hydrocarbon migration and its near surface effects. AAPG Memoir 66:157–168

Krcmár B, Vylita T (2001) Unfilterable "geoaerosols", their use in the search for thermal, mineral and mineralized waters, and their possible influence on the origin of certain types of mineral waters. Environ Geol 40:678–682

Kristiansson K, Malmqvist L, Persson W (1990) Geogas prospecting: a new tool in the search for concealed mineralizations. Endeavour 14:28–33

Lerman A (1979) Geochemical Processes, water and sediment environments. Wiley Interscience Publications, New York

Lineham TR, Nash PJ, Rodwell WR, Bolt J, Watkins VMB, Grainger P, Heath MJ, Merefield JR (1996) Gas migration in fractured rock: results and modelling of a helium gas injection experiment at the Reskajeage Farm Test Site, SW England, UK. J Contam Hydrol 21:101–113

Loseth H, Gading M, Wensaas L (2009) Hydrocarbon leakage interpreted on seismic data. Mar Pet Geol 26:1304–1319

MacElvain R (1969) Mechanics of gaseous ascension through a sedimentary column. In: Heroy WB (ed) Unconventional methods in exploration for petroleum and natural gas. Southern Methodist University Press, Dallas, pp 15–28

Malmqvist L, Kristiansson K (1984) Experimental evidence for an ascending microflow of geogas in the ground. Earth Planet Sci Lett 70:407–416

Malmqvist L, Kristiansson K (1985) A physical mechanism for the release of free gases in the lithosphere. Geoexploration 23:447–453

Martinelli G, Ferrari G (1991) Earthquake forerunners in a selected area of northern Italy: recent developments in automatic geochemical monitoring. Tectonophysics 193:397–410

Mesler R (1986) Bubble nucleation. In: Cheremisinoff NP (ed) Gas-liquid flows, Encyclopedia of fluid mechanics, vol 3, Gulf Pub Co

Mogro-Campero A, Fleischer RL (1977) Subterrestrial fluid convection: a hypothesis for long-distance migration of radon within the Earth. Earth Planet Sci Lett 34:321–325

Muskat M (1946) The flow of homogeneous fluids through porous media. Edwards Inc., Ann Arbor, Michigan

Pandey GN, Rasintek M, Katz DL (1974) Diffusion of fluids through porous media with implication in petroleum geology. AAPG Bull 58:291–303

Pattenden NJ, Cambray RS, Playford K (1981) Trace elements in the sea-surface microlayer. Geochim Cosmochim Ac 45:93–100

Peirson DH, Cawse PA, Cambray RS (1974) Chemical uniformity of airborne particulate material and a maritime effect. Nature 251:675–679

Price LC (1986) A critical overview and proposed working model of surface geochemical exploration. In: Unconventional methods in exploration for petroleum and natural gas IV, Southern Methodist University Press, pp 245–309

Saunders D, Burson KR, Thompson CK (1999) Model for hydrocarbon microseepage and related near-surface alterations. AAPG Bull 83:170–185

Schrauf TW, Evans DD (1986) Laboratory studies of gas flow through a single natural fracture. Water Resour Res 22:1038–1050

Teller AJ, Miller SA, Scheibel EG (1963) Liquid-gas systems. In: Perry JH (ed) Chemical Engineers' Handbook, McGraw-Hill Book Co, New York

Tsuge H (1986) Hydrodynamics of bubble formation from submerged orifices. In: Cheremisinoff NP (ed) Encyclopedia of fluid mechanics, vol 3. Gulf Publishing Co., Houston

Várhegyi A, Baranyi I, Somogyi G (1986) A model for the vertical subsurface radon transport in "geogas" microbubbles. Geophys Trans 32:235–253

Walker MI, McKay WA, Pattenden NJ, Liss PS (1986) Actinide enrichment in marine aerosols. Nature 323:141–143

Witherspoon PA, Saraf DN (1965) Diffusion of methane, ethane, propane, and n-Butane in water from 25 to 43. J Phys Chem 69:3752–3755

Chapter 4
Detecting and Measuring Gas Seepage

This chapter provides a representative overview of current methodologies for detection of gas seepage on Earth's surface, both on land and in aquatic environments (rivers, lakes, oceans). Most of the techniques described can be utilised to discover gas seepage independent of the study objective (i.e. whether for petroleum exploration, geo-hazards, or environmental studies). Most of these techniques can also be used to measure anthropogenic gas leaks, such as fugitive emissions from petroleum production and distribution facilities. Applications to petroleum exploration, as well as related interpretative tools and limits, with references to microseepage detection, are discussed in Chap. 5.

The goal of this chapter is not (and cannot be) an exhaustive manual or review for all of the currently available surface seepage prospecting methods. As outlined in the sections below, several traditional techniques have been described in review papers. Here, a synthetic and synoptic picture for several currently available methodologies is provided, including the latest techniques and capabilities offered by new generation instruments. The discussion provided here focuses on direct gas detection methods. The use of gas seepage in petroleum exploration is outlined in Chap. 5. Indirect methods, including geophysical techniques and measurements of chemical, physical, or microbiological parameters in soils, water, rocks, or vegetation, modified by the presence of hydrocarbons, are briefly illustrated. Specific references, as well as a few case histories, are provided for those interested in a deeper reading of the technical details of sensing principles and instrumentation design. The detection of oil is not the objective of this book.

4.1 Gas Detection Methods

As illustrated in Fig. 4.1, gas seepage can be detected above the ground (atmospheric measurements), in the ground (soils and well head-space), and in water bodies (shallow aquifers, springs, rivers, bogs, lakes, and seas). Several of the methodologies are visually reviewed in the tree diagram shown in Fig. 4.2.

G. Etiope, *Natural Gas Seepage*, DOI 10.1007/978-3-319-14601-0_4

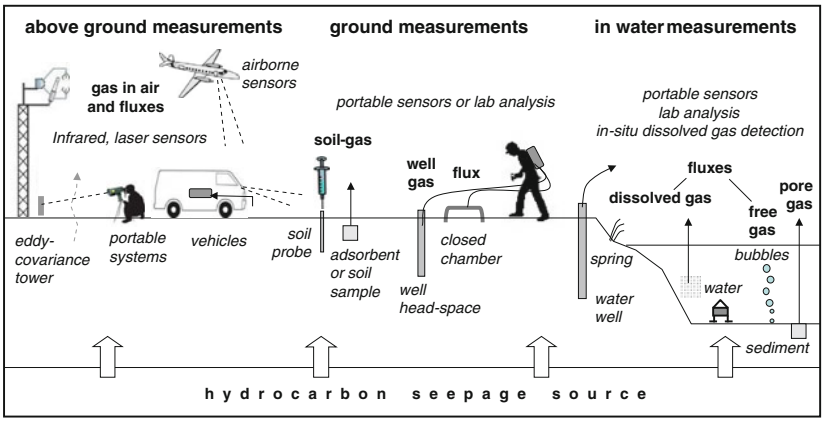

Fig. 4.1 Primary techniques used for direct gas seepage detection, sampling, and analysis in the atmosphere, in the ground or at the ground-atmosphere interface, and in aquatic systems (springs, lakes, bogs, rivers, and seas)

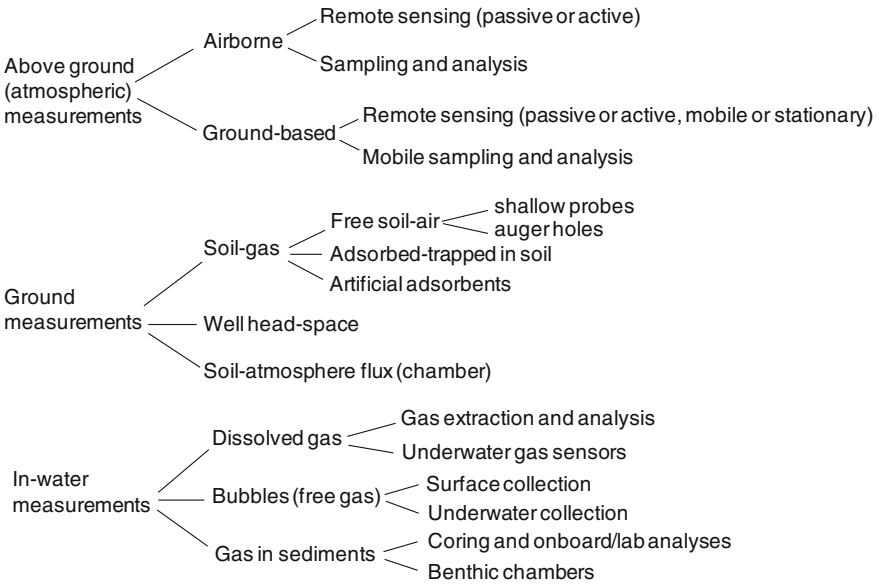

Fig. 4.2 Main methodologies of seepage detection using direct gas measurements

4.1.1 Above-Ground (Atmospheric) Measurements

Detecting hydrocarbons above the ground's surface has several advantages but also comes with substantial drawbacks. Measuring gas in the atmosphere may not require special permits; soils, either in natural or agricultural fields, are not disturbed, and

gas samples representing average signals from large areas can be sampled rapidly. However, depending on the distance from the seepage source, wind and advective mixing in the atmosphere can significantly decrease a gas seepage signal's strength. As a result, detecting seeping gas strongly depends on weather conditions. In many cases, methane dispersion, even for intense seepage to the atmosphere, may lead to column average concentrations that are very close to or only slightly above background levels. Any specific gas concentration anomaly should be verified and confirmed based on ground-based and local measurements. Hydrocarbons detected in the atmosphere can, in fact, result from anthropogenic or natural sources not related to gas seepage (e.g., wetlands, landfills, fossil fuel plants, and leaking pipelines). However, technological improvements over the last twenty years have led to an increase in the capability for detecting trace amounts of gases from/in the atmosphere. Airborne methods are only of practical use for detecting relatively large gas emissions from macro-seeps. Microseepage is more easily detected using ground-based measurements.

Gas detection instrumentation can be divided into two main classes, remote sensing and air-sampling systems, and both can be operated from airborne or ground-based platforms or vehicles.

4.1.1.1 Remote Sensing

The remote sensing of gas in the lower atmosphere is based on analyses of radiation absorbed and emitted by gas molecules. Thus, instruments are generally based on absorption optical spectroscopy. Methane has strong rotational-vibrational transitions that cause absorption in the near-infrared (NIR, 0.78–3 μm wave length) and mid-infrared (MIR, 3–50 μm) spectral ranges, at wave lengths of 1.65, 2.35, and 3.4 μm. Remote sensing can be passive (observations of radiation naturally reflected by gas molecules) or active (observations of radiation reflected or backscattered by gas molecules following laser beam scanning), and can be obtained from satellites (remote sensing from space), aircraft, helicopters, drones (airborne remote sensing), ground-based vehicles, or portable hand-held sensors. At present, available satellite-based remote sensing systems (e.g., SCIAMACHY and GOSAT; Buchwitz et al. 2010) are only capable of detecting continental-scale variations in CH_4 (and other non-hydrocarbon gases such as CO_2 and N_2O). These systems have spatial resolutions up to 10 km (GOSAT), too large for the detection of near-surface local emissions or gas plumes from concentrated point sources. As a result, they are not effective for local scale gas seepage detection. Airborne systems have a much higher resolution and are capable of determining local scale emissions. Recent examples of passive airborne imaging spectrometry applied to gas seepage include the Airborne Visible/Infrared Imaging Spectrometer (AVIRIS) (Bradley et al. 2011; Thorpe et al. 2013) and the Methane Airborne MAPper (MAMAP) instrument (Gerilowski et al. 2010), working in the short-wave infrared (SWIR) and near-infrared (NIR) portions of the electromagnetic spectrum. AVIRIS has been applied to marine and terrestrial seeps in California including the Coal Oil Point marine

seep field (Bradley et al. 2011). In the study of Bradley et al. (2011), remote sensing seep anomalies were found to be consistent with the rising bubble plumes observed on site. The technique is well-suited for the detection of methane seepage from point sources over large areas, but false positives can result from surfaces with strong absorptions at the same wave lengths as those for methane, such as carbonates (2.35 μm).

Active systems for gas seepage detection are based on LIDAR (light detection and ranging) systems (e.g., Zirnig 2004; Thomas et al. 2013) used either in airborne or ground-based platforms, and portable open-path tunable diode laser (TDL) sensors that can easily be handled by one operator. Differential Absorption LIDAR (DIAL), in particular, uses a pulsed laser operating at two wavelengths, one strongly absorbed by the gas (MIR at 3.4 μm) and one weakly absorbed. Differential absorption is proportional to the gas concentration. DIAL was successfully used to detect gas leaks from pipelines (Zirnig et al. 2004). Examples of portable open-path laser sensors are the Boreal Laser's GasFinder (e.g., http://www.epa.gov/etv/pubs/01_vs_boreal.pdf) and Lasermethane™ (Tokyo Gas Engineering and Anritsu Corp.) which is based on wavelength modulation absorption spectroscopy (Iseki 2004). The Lasermethane™ sensor was used to rapidly detect microseepage methane anomalies in air (>2 ppmv), a few cm above the soil, by manually directing a laser beam across tens of meters in the field (Fig. 4.3). Wide areas can be scanned over a short period of time (a 0.3 km^2 field can be scanned within 1 h), by recognising the existence of microseepage in wide zones, with anomalies of up to 40–50 ppmv of methane approximately 10–20 cm above the soil (Etiope and Klusman 2010). Using the ground as a reflector, the instrument has also been used to detect gas leaks from soils or rocks (Etiope et al. 2006).

Fig. 4.3 Detection of anomalous concentrations of methane in the air a few centimetres above the ground using a portable laser sensor (Fierbatori seepage area, Berca oil-field, Romania; photo by C. Baciu)

4.1.1.2 In Situ Sampling-Analysis Systems

Aircraft, helicopters, or ground vehicles can mount "sniffing" devices that collect and pump atmospheric air towards gas sensors. High resolution spectrometers based on Cavity Ring-Down Spectroscopy (CRDS), NonDispersive InfraRed (NDIR), Off-Axis Integrated Cavity Output Spectroscopy (OA-ICOS), and Tunable Diode Laser Absorption Spectroscopy (TDLAS) (e.g., Hirst et al. 2004; Chen et al. 2010; Baer et al. 2012) are capable of detecting trace amounts (ppbv or ppmv) of light hydrocarbons (mainly methane and ethane) in excess of background atmospheric concentrations. Air samples can also be collected and stored for laboratory analyses. The sampling location is recorded by a Global Positioning System (GPS) navigation system that is generally interfaced to the gas analyzer or sampler. As for remote sensing, wind and ground conditions can strongly dilute hydrocarbon flow to the atmosphere and humidity can delay or reduce the gas rising to flight altitudes. Examples of atmospheric ground-based surveys for gas seepage detection can be found in LTE (2007) and Hirst et al. (2004). By driving along roads for 4,490 km in the Raton Basin in Colorado, 67 seep locations were found by analysing air with a fast IR analyser mounted at approximately half a meter from the ground in the rear of a car while recording atmospheric CH_4 anomalies of up to 700 ppmv (LTE 2007).

Stationary atmospheric measurements are typically made using micrometeorological towers, such as those employed for the Eddy-Covariance (EC) method (Burba et al. 2010). The EC method allows estimations of gas flux from the ground to the atmosphere based on rapid sequential gas measurements (by high-resolution infrared sensors), vertical temperature gradients, and air velocities measured in three-dimensions using a sonic anemometer. The method is mainly employed in studies of biological CO_2, CH_4 and ammonia (NH_3) emissions and surface ecosystem budgets, and rarely used to investigate geological gas emissions (e.g., Lewicki et al. 2009).

Mobile surveys based on air sampling and gas chromatography/mass spectrometric (GC/MS) laboratory analyses are described in Petron et al. (2012). The study was not aimed at detecting natural seepage but at assessing man-made hydrocarbon emissions at petroleum production and processing sites. The air-sampling approach may allow the simultaneous detection and quantification of a large number of gas species released by natural seepage (virtually all gaseous hydrocarbons and associated non-hydrocarbon gases), and, for a better understanding of their origin, different types of isotopic analyses. Data points obtained in this manner are obviously discontinuous and widely spaced and could miss seepage signals occurring at non-sampled sites, which could be captured using continuous measurements.

4.1.2 Ground Measurements

Ground measurements include all of the methods capable of detecting gas in the soil or the shallow sub-soil, and at the soil-atmosphere interface (Fig. 4.1). These measurements also include gas in well head-space, and gas flux from soil to the

atmosphere. Gas in all of these systems can be analysed in the laboratory following convenient and economical storage of gas in vials or bags, or analysed directly on site using portable hand-held sensors. In addition to traditional portable gas-chromatographs (with Flame Ionization Detectors, FID, or Thermal Conductivity Detectors, TCD), today, fast and sensitive analysers based on closed-path IR lasers or cavity enhanced absorption sensors are available for detecting methane at sub-ppmv levels. Measuring gas directly on site allows the immediate recognition of seepage and drives surveying strategies, leading to the selection of measurement points. Ground measurements are the most effective method for detecting and characterising low gas exhalations related to microseepage.

4.1.2.1 Soil-Gas or Subsoil Pore-Gas Analysis

Measuring gas composition and concentration in the soil is likely the most employed method for detecting and characterising hydrocarbon seepage. Measurements can be performed on the free gas in soil pores (soil-air), or on the gas trapped in poorly permeable soil or adsorbed to soil minerals or artificial adsorbents that are inserted into soils or sediments.

Free soil-gas can be accessed via shallow (generally around 1 m) metal probes manually inserted into the soil, or via deeper auger holes (generally up to depths of 3–4 m). The gas can be extracted using syringes or manual pumps, and analysed on site using portable sensors or stored in bags or vials for subsequent laboratory analyses. Shallow probe sampling is much more rapid and economical, as may allow complete gas sampling/analysis within a few minutes. However, the shallower the sampling and the higher the soil's porosity and permeability (as for dry sands), the lower the amounts of hydrocarbon gas that can be detected since soil-air may become diluted by advected atmospheric air. Deeper holes almost always encounter water, which also influences the collection of free gases. Water-logged soil and mud should be avoided. The concentration of seeping gas in soil-air is then controlled by meteorological factors such as atmospheric pressure, temperature, and precipitation, as discussed in a wide array of scientific literature (e.g., Klusman and Webster 1981; Hinkle 1994; Wyatt et al. 1995).

Hydrocarbons are generally also trapped in small soil pores or loosely bound to soil grains, organics, or minerals, and cannot be quantitatively extracted using soil probes. Soil samples can be directly collected using special containers that, after heating or shaking, form a head-space from which gas can be sampled and analysed. The main problem with this approach is limited sample integrity and gas lost during drilling and laboratory treatments. In agricultural fields, samples may also be contaminated by fertilizers, herbicides and insecticides containing hydrocarbon-based additives that may confound the search of heavy hydrocarbons related to natural seepage.

Hydrocarbons reaching the B-horizon in soil can adsorb onto clays or become occluded within carbonate cements. Desorption through heating and acid extraction procedures allow hydrocarbon GC analyses that can detect more than a hundred

different compounds, generally from C_5 to C_{20}, at the ppb and ppt levels (e.g., Philp and Crisp 1982, and references therein). However, results strongly depend on the type of soil sampled, the presence of diagenetic carbonates that may release hydrocarbons independent of seepage, and humidity and pH conditions. Acidic soils do not produce carbonate cement, so hydrocarbons cannot be occluded.

An alternative to soil sampling is provided by artificial adsorbents, such as activated carbon (e.g., Klusman 2011) or microporous materials housed in chemically inert, hydrophobic, polytetrafluoroethylene (Teflon®) membranes (e.g., http://www.epa.gov/etv/pubs/01_vr_goresorber.pdf). Adsorbents are typically installed at a depth of 0.5–1 m and passive soil-gas sampling may last for several weeks. The lightest detectable hydrocarbon is ethane. Methane cannot be adsorbed. The main advantage of this technique is that it integrates the gas concentration over long periods by removing the variability caused by atmospheric changes.

Soil-gas prospections for gas seepage detection have been widely documented in the scientific literature. Jones and Drozd (1983), Richers et al. (1986), Richers and Maxwell (1991), Dickinson and Matthews (1993), Jones et al. (2000), Harbert et al. (2006), Klusman (2006), Mani et al. (2011), and Sechman (2012) are just a few examples of peer-reviewed publications.

4.1.2.2 Well Head-Space Analyses

Wells drilled for different purposes, such as shallow explorations, stratigraphic boreholes, water wells, or piezometers, can be used for local collection of gas from seepage. If the well-head is accessible (by opening the cap or valves), the head-space above the water table can be sampled for laboratory analyses or directly analysed on site using portable sensors. The head-space may contain hydrocarbon gases exsolved from the water, or those crossing the aquifer and the water column in the well, as bubbles. Within the Po Basin in northern Italy, numerous wells have high hydrocarbon concentrations within the well head-space and some have been used to assess the origin of gas seepage in the region (e.g., Etiope et al. 2007).

4.1.2.3 Soil-Atmosphere Gas Flux Measurements

The flux of natural gas from the soil to the atmosphere is an important parameter in seepage studies because in addition to information on the presence of gas seepage it provides an indication of intensity and persistence, reflecting underground gas pressures, gas flux, and accumulation potential. The main technique adopted for measuring gas flux in the ground is that of the closed or accumulation chamber, a well-established, economical, and straightforward technology (Fig. 4.4).

The technique allows gas flux calculations by measuring gas concentration build-up (accumulation) over time inside a chamber that is firmly positioned on the surface. If the rate of change of gas concentration is constant (steady emission, i.e., ppmv versus time is linear) then linear regression can be used in order to calculate

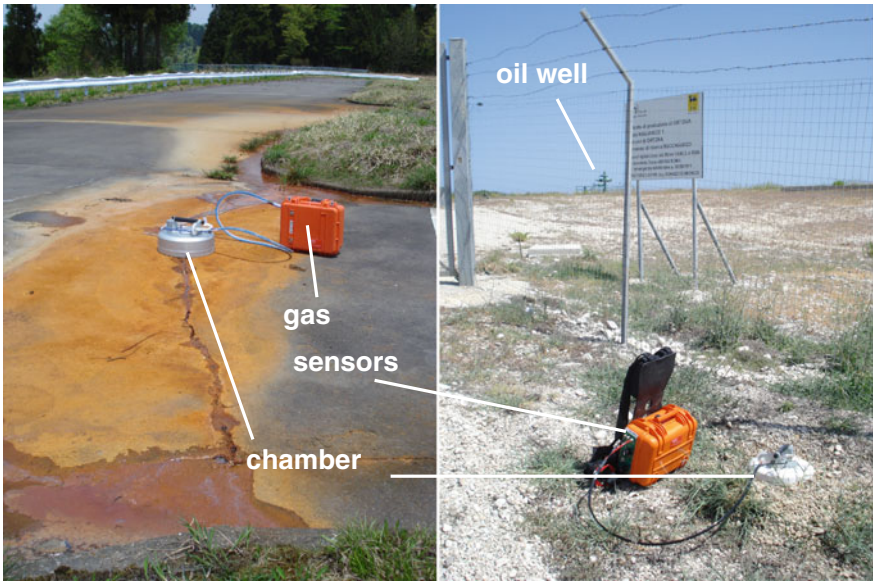

Fig. 4.4 Examples of gas flux measurements using the closed-chamber method with portable gas sensors. *Left* gas seepage through the asphalt at Tokamachi (Niigata Basin, Japan); *Right* a microseepage measurement at the Miglianico oil field in central Italy (also see Sect 5.2 and Fig. 5.2). Photos by G. Etiope

the slope of concentration versus time. The slope of the line reflects the gas flux. The flux, Q, is obtained by multiplying the slope by the chamber height (m), and is generally expressed in terms of mg m^{-2} day^{-1}, as follows:

$$Q = \frac{V_{FC}}{A_{FC}} \cdot \frac{c_2 - c_1}{t_2 - t_1} \left[\frac{mg}{m^2 * d}\right]$$

where V_{FC} (m^3) is the volume of the chamber, A_{FC} (m^2) is its area, and c_1 and c_2 (mg/m^3) are the methane concentrations at times t_1 and t_2 (days). Measurement times are chosen depending on the gas flux and the sensitivity of the analyser. The lower the gas flux, the higher the time required to obtain a measurable gas concentration. The lower the height of the chamber, the lower the time required to measure a given flux. For example, for a sensor with a resolution and a lower detection limit of 1 ppmv CH_4, a methane flux of 100 mg m^{-2} d^{-1} can be measured in 1 min using a chamber with a height of 10 cm; 30 s for a chamber of 5 cm.

Methane concentrations can be measured in the laboratory after a gas is collected in vials or bags, or on site using portable sensors. On-site analyses with portable flow-through sensors allow for continuous recording of concentration build-up. Imperfect sealing of the chamber's bottom against the ground may lead to underestimations of flux measurements. Uncertainty for measurements is, therefore, related to the errors (accuracy and reproducibility) of the analyser itself and to the

actual volume of air enclosed by the chamber, which depends on how deep within the soil the chamber is actually positioned.

Closed-chambers can be used for short-term measurements and spatial surveys, and for long-term monitoring in fixed positions. Several authors have provided basic recommendations and guidelines regarding the use of closed-chambers (e.g., Mosier 1989). The main potential problems include temperature perturbations (influencing biological activity and gas adsorption into soil minerals) and pressure perturbations induced by wind (causing deviations in mass flow in and around the chamber). Such problems can be minimised using insulated, reflective chambers equipped with a capillary hole capable of equilibrating the internal and external air pressure.

Closed-chambers were initially developed for studies of the exchange of carbon and nitrogen bearing gases at the soil-atmosphere interface, such as for soil respiration (e.g., Hutchinson and Livingston 1993; Norman et al. 1997). The technique was then applied to detect methane microseepage in petroliferous basins (Klusman et al. 2000; LTE 2007) and coal mines (Thielemann et al. 2000), and gas exhalations in geothermal or volcanic areas (e.g., Hernandez et al. 1998; Etiope 1999; Cardellini et al. 2003). A wide array of reports of chamber measurements for methane fluxes in mud volcanoes and other types of seeps are currently available (e.g., Etiope et al. 2004a, b; 2011a, b; 2013; Hong et al. 2013). Such studies have allowed the recognition of invisible miniseepage (see the definition in Chap. 2) surrounding vents at macro-seepage sites (Fig. 4.4). The closed-chamber method has also been fundamental for assessing the typical methane fluxes for various types of seeps, as described in Chap. 2, and, based on the procedures described in Chap. 6 , for deriving local, regional, and global bottom-up estimates of geological methane emissions to the atmosphere.

4.1.3 Measurements in Aqueous Systems

Hydrocarbons in the waters of lakes, bogs, rivers, springs, shallow aquifers, and seas can occur in solution (as a dissolved gas) or as a free-phase (bubbles). Seeping gas is then present within sediments.

4.1.3.1 Dissolved Gas

Water samples from aqueous environments can be collected in glass bottles properly sealed with hydrocarbon-free septa and secured with aluminium caps. Deep waters in lakes and seas can be collected using Nansen or Niskin bottles then stored in glass bottles. The addition of a microbicide (e.g., mercuric chloride, $HgCl_2$) is useful for limiting methane oxidation. Dissolved gases can then be extracted either on site or in the laboratory using head-space and/or stripping methods (McAuliffe 1969; Capasso and Inguaggiato 1998).

In offshore petroleum exploration areas, seawater can be pumped from a ship through deep towed sample inlets at depths of 100–200 m and carried to an onboard analysis system (e.g., Sackett 1977; Philp and Crisp 1982; Gasperini et al. 2012). Gases in solution can then be stripped from seawater samples and analysed via gas-chromatography or other sensors.

Methane can also be directly analysed in solution using special underwater sensors that employ a semi-permeable membrane that allows gas permeation into an internal head-space in contact with a detector, generally a solid-state, optical sensor or spectrometer. Such instruments are typically employed in the marine environment, in vertical casts, in horizontal profilers, or in benthic platforms (e.g., Marinaro et al. 2006; Camilli and Duryea 2007; Newman et al. 2008; Krabbenhoeft et al. 2010; Gasperini et al. 2012; Embriaco et al. 2014). A review of the present technology is provided in Boulart et al. (2010).

4.1.3.2 Gas Bubble Collection

Bubble trains observable at the surface of lakes, rivers, bogs, seawater and in water pools of mud volcanoes can be captured using special funnels ("bubble traps") or floating accumulation chambers that can also measure gas flux (e.g., Cole et al. 2010; Etiope et al. 2013). Bubble traps are initially purged using water that is progressively displaced by gas. Since the volume of the funnel is known, the time bubbling gas takes to displace water can provide a good estimate of the gas flow rate. In vents not accessible for direct measurements, the order of magnitude of the gas flux to the atmosphere from bubbles can be visually estimated by examining the size and frequency of individual bubble trains (Etiope et al. 2004a, b). For example, the gas output of a single train of spherical bubbles with diameters of 1 cm (0.5 mL), having 80 % CH_4 and bursting each second, is in the order of 40 L per day.

Bubbles can be collected underwater, along the water column or on the floor, by a diver (e.g., Etiope et al. 2006) or by remotely operating vehicles equipped with arms and special sampling tools (e.g., Bourry et al. 2009). In all cases, the sampled gas can then be analysed in the laboratory for a complete molecular and isotopic composition. However, due to the exchange of gas species between the bubbles and seawater, as outlined in Chap. 6, it is important to understand that the gas composition of bubbles at the sea or lake surface, having travelled several tens or hundreds of meters along the water column, may be different from the original gas issuing from the sea or lake bottom.

4.1.3.3 Underwater Sediment Analyses

Gas-charged sediments located on the bottom of lakes, rivers, and seas can be sampled using several types of tools based on gravity driven or rotary mechanical penetration (e.g., Hopkins 1964; Abrams 2013). Gravity corers consist of a hollow tube (the barrel with a core liner) attached to an external weight. Mechanical coring devices use rotary

drilling or vibracoring to facilitate the penetration of the barrel into sediments. Vibracorers, in particular, are effective in sampling compacted and slightly cemented sediments that cannot be penetrated using conventional gravity driven devices (Abrams 2013). Once a sediment sample is retrieved onboard a ship, it must be quickly processed and stored for successive laboratory analyses. Since they can be rapidly lost, volatile hydrocarbons (C_1–C_{12}) and non-hydrocarbon gases require special handling. Sediments are typically stored in non-coated metal cans or clear plastic jars. Seawater and an inert gas (helium) or air are added to create a head-space. To prevent hydrocarbon oxidation by microbes, anti-microbial agents, such as sodium azide or mercuric chloride, must be added before closing the can or jar. Technical details regarding sediment sampling and analyses have been reported in a wide array of scientific literature and reviews, including Bernard et al. (1978), Logan et al. (2009), Abrams and Dahdah (2010), Abrams (1996, 2013), and references therein.

Benthic chambers have also been used to detect gas seepage from lakes or marine sediments (e.g., Caprais et al. 2010). These chambers work like soil-atmosphere flux chambers and use sampling cells that collect small amounts of water at predetermined intervals. Chambers can be deployed and recovered using remotely operated vehicles or divers in shallower waters.

4.2 Indirect Methods

Indirect methods for seepage detection are based on the recognition of chemical, physical, and biological changes in soils, sediments, rocks, vegetation, or water, that are induced by the presence of hydrocarbons or other gases related to seepage. Changes include those associated with microbiology, minerals, acoustics, electrochemistry, radioactivity, and vegetation anomalies. The synoptic tree diagram provided in Fig. 4.5 summarises the main methods, briefly described below. The scheme refers to gas seepage detection, not oil detection or underground reservoir research. For technical details, applications, and case histories, the reader should consult the references provided below.

Although indirect methods alone are not sufficient for identifying underground hydrocarbon resources of commercial importance, most, especially those based on remote sensing, have allowed us to discover hydrocarbon seepage throughout large areas in sedimentary basins, suggesting that microseepage is a ubiquitous process in petroleum systems as discussed in Chap. 2.

4.2.1 Chemical-Mineralogical Alterations of Soils

Hydrocarbons can modify certain chemical and mineralogical features of soils. Microbial biodegradation entails hydrocarbon oxidation, particularly of methane, and may produce diagenetic carbonates, typically calcite. The process is the same as

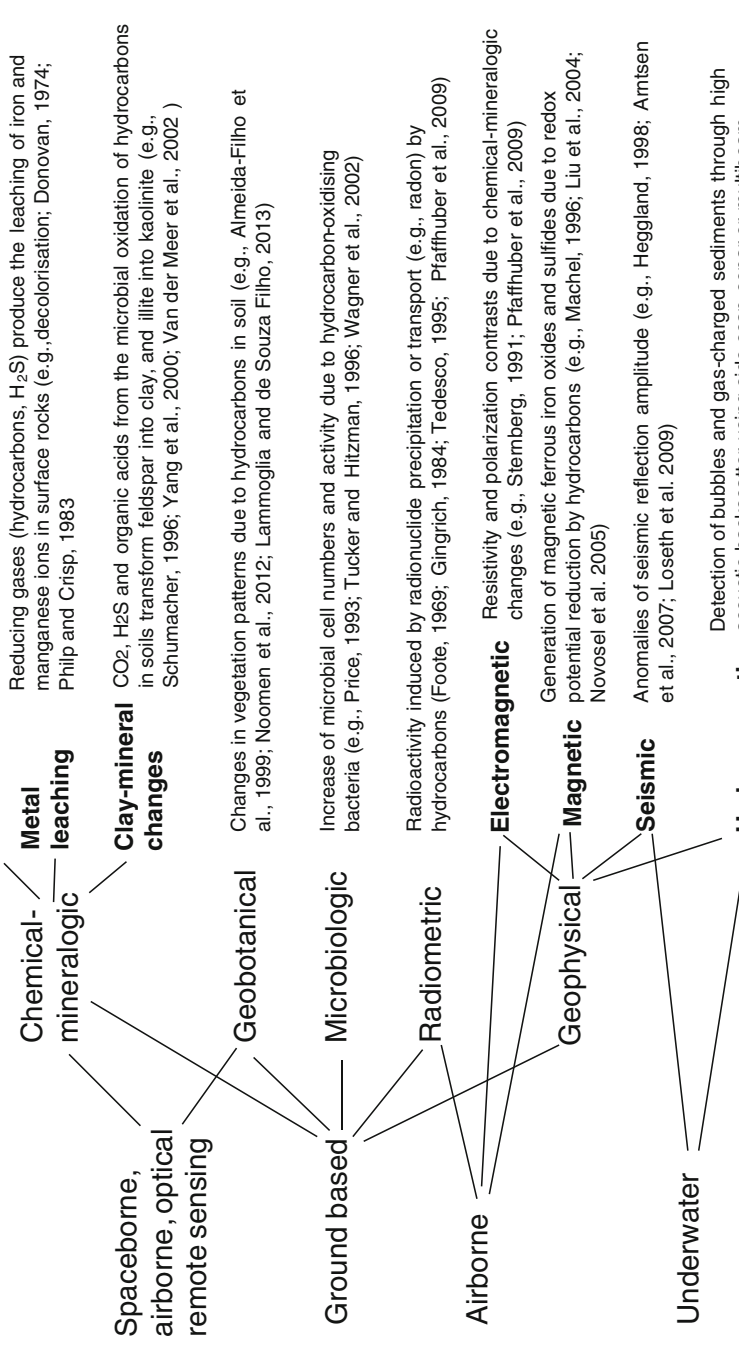

Fig. 4.5 Main indirect methods of natural gas seepage detection

the one described in Chap. 2 that produces carbonates on the seafloor. Calcite fills soil pores and the oxidation is generally aerobic, as follows:

$$CH_4 + 2O_2 + Ca^{2+} = CaCO_3 + H_2O + 2H^+$$

The reaction evolves via the production of carbon dioxide that reacts with water to form bicarbonate. The produced bicarbonate precipitates as carbonate or carbonate cement with a $^{13}C/^{12}C$ isotopic ratio (expressed as $\delta^{13}C$ value along the VPDB carbon isotopic scale in permil) that is related to that of the biodegraded parent hydrocarbon. Calcite formed in this manner typically has an isotopic composition more negative than –20 ‰ that is much lower than the traditional calcite derived from the atmosphere, freshwater, or marine environments (of approximately –10 to +5 ‰). Diagenetic methane-derived carbonates in soils are widespread, in correspondence with many petroleum fields in North America, as documented, for example, by Donovan et al. (1974) and Schumacher (1996).

Additionally, hydrocarbons and associated hydrogen sulphide (H_2S) can reduce ferric oxide (hematite) and manganese ions in soil minerals and sandstones, forming bleaching red beds, or, in general, the decolorisation of rock. Sandstones are generally unaltered, reddish-brown, outside the boundary of petroleum fields, and may become pink, yellow, and white along the faults of productive anticlines (Donovan 1974). CO_2, H_2S, and organic acids from the microbial oxidation of hydrocarbons in soils can also transform feldspar into clay, and illite to kaolinite (e.g., Schumacher 1996). Alterations can effectively be detected using optical remote sensing techniques such as aerial photography, radar, a Landsat Multispectral Scanner, a Landsat Thematic Mapper, or airborne multispectral scanner data (Yang et al. 2000; van der Meer et al. 2002).

However, it is important to understand that although the mechanisms of the soil alterations induced by seeping hydrocarbons are well established, the cause of soil and sediment alteration in a given area may not be due to hydrocarbon seepage. Many factors other than seepage can induce near-surface anomalies. Hydrocarbons can be an indirect cause, but are not always the most likely cause. Therefore, the prospection methods outlined below are not conclusive, but are useful for reconnaissance surveys. In association with direct gas detection methods, these methods can effectively support and complete interpretations derived using traditional geophysical techniques of petroleum exploration.

4.2.2 Vegetation Changes (Geobotanical Anomalies)

Hydrocarbons in the soil may impact vegetation growth and health, and can be detected through the analysis of reflectance spectra (Almeida-Filho et al. 1999; Noomen et al. 2012; Lammoglia and de Souza Filho 2013). The reflectance of healthy vegetation can be observed using visible light based on the absorption features caused by plant pigments such as chlorophyll and carotenoids, and in the

near infrared (NIR) and shortwave infrared (SWIR) using adsorption bands related to internal leaf structure, water content, and leaf area. The cause of vegetation modification is generally related to oxygen depletion in soil induced by the presence of hydrocarbons, but plant growth can also be directly affected by hydrocarbons when ethane concentrations within the soil are greater than 0.7 vol.% (Noomen et al. 2012). The two main biological indicators of gas seepage are decreases in chlorophyll abundance and leaf area.

4.2.3 Microbiological Analyses of Soils

Hydrocarbon-oxidising bacteria are specialised microorganisms that take energy from hydrocarbon gases and liquids. Microorganisms can use extremely low concentrations of hydrocarbons and are typically found living within soils and seabed sediments above hydrocarbon reservoirs (e.g., Price 1993; Tucker and Hitzman 1996; Wagner et al. 2002). Wherever small traces of hydrocarbons occur during a period of several years in the soil, there is a significant occurrence of specialised bacteria (Hanson and Hanson 1996). Onshore sampling is performed using a hand auger at a depth of $\sim$150 cm. Offshore samples are obtained using a vibracorer or grab sampler, at approximately 30 cm below the top of the sediment. Samples are then packed in airtight sterile bags and transported to the laboratory for the incubation and specific analyses of total cell counts and microbial activity (consumption of hydrocarbons using gas chromatography and pressure measurements, and biological CO_2 formation rates). Numerous case-histories exist for microbiological prospections devoted to petroleum exploration (see, for example, Wagner et al. 2002 and references therein).

4.2.4 Radiometric Surveys

The occurrence of radionuclides, such as uranium and radium, in hydrocarbons is widely documented within the petroleum geochemistry literature (e.g., Durrance 1986; Hunt 1996). Radionuclides accumulate in petroleum deposits due to anoxic environments and chelation by organic molecules. Of sedimentary rocks, productive petroleum-bearing shales contain the highest levels of radioactivity. Hence, hydrocarbon fluids can be more radioactive than other fluids, leading to an assumption that hydrocarbon seepage can be detected by relatively high concentrations of radionuclides within the near surface which is only partially true. Petroleum accumulations almost never produce high radioactivity at the surface. To be more precise, the total gamma radiation produced is not necessarily high above hydrocarbon accumulations. Only concentrations (or better the activity) of radon-222, the gaseous radionuclide in the nuclear decay chain of uranium-235, are typically higher in soils above petroleum fields (Gott and Hill 1953; Foote 1969;

Gingrich 1984; Pfaffhuber et al. 2009). The relative concentration of different radionuclides, whose behaviour (and migration capability) is different in relation to the redox conditions in rocks, is important. A column of rocks impacted by hydrocarbon seepage is, in fact, a reducing environment. Rocks without hydrocarbons generally exist under oxidising conditions. Some radionuclides are mobile under reducing conditions while others are not. The use of radioactivity for petroleum exploration has always been controversial, mainly because past measurements were based on total gamma radiation without differentiating various radionuclides. Therefore, although the method still has some proponents and has apparently been used with some success in Russia, it has met with little acceptance in the petroleum industry due to an insufficient understanding of its technical basis and because different techniques did not work consistently. That radiometric survey should be executed with spectrometers capable of measuring total radioactivity and differentiating radionuclides, and not radiometers, which provide only total gamma radiation, is important. Knowing specific ratios between selected radionuclides is, in fact, necessary for revealing the presence of seepage in soils or seabed sediments.

During hydrocarbon gas microseepage, micro-sized bubbles of gas seep near-vertically through a network of water filled joints and bedding planes immediately above hydrocarbon deposits. Carbonic and organic acids transform the clay minerals, primarily illite, that contain potassium and uranium. As a result, these elements are released and leached away by groundwater. The uranium may not leach away entirely but is chemically reduced to uraninite and precipitate, resulting in some build-up of uranium in surface sediments. The result explains the muted loss of uranium relative to potassium in the system. Thorium appears to be immune to these processes. Chemical reduction processes can also result in the development of magnetic minerals, leading to coincident "micromagnetic" anomalies. Radioelement anomalies over hydrocarbon microseepages typically have the following characteristics (e.g., Saunders 1993): 1. Potassium is significantly diminished. 2. Uranium is somewhat diminished and often variable. 3. Thorium remains relatively constant.

Additionally, a sort of electrochemical cell develops above reduced bodies (hydrocarbon accumulations) producing a very high contrast in the "oxidation suite" of minerals, including uranium and thorium. Apical radiometric anomalies may form over faults that act as a conduit for waters that contain radioactive minerals. However, halo anomalies are also found above the edges of reducing body (cathodes), with a central low over the centre of the body (anode).

Two processes, microseepage and the development of electrochemical cells (redox), produce low radionuclide responses over petroleum fields and/or high radionuclide responses surrounding the edges. In most cases, redox processes seem to prevail. Thus, the acquisition of high-resolution gamma ray spectrometer data, and careful data processing and enhancement for discriminating alteration effects from host lithologies, can provide viable exploration techniques. In summary, when subsurface hydrocarbons are absent, uranium's intrinsic migratory ability and its greater specific radioactivity cause it to be a significant contributor to the radiation detected at the surface. When hydrocarbons are present, geochemical interactions

constrain or arrest uranium's movement, causing a decrease in the gamma flux detected over petroleum deposits. As such, low radiation flux patterns are distinguishable from the random gammas observed in areas barren of hydrocarbons. A decrease in total gamma-ray intensity, often observed over oil fields, may then be due to depletion in one or all three of the main radionuclides (^{40}K, ^{232}Th, and ^{238}U).

4.2.5 Geophysical Techniques

A wide set of geophysical methods can be used to detect seepage (not necessarily underground hydrocarbon accumulations), including electromagnetic, magnetic, seismic, and hydro-acoustic techniques, either onshore or offshore, from airborne, ground-based, or underwater systems (see Fig. 4.5). Due to the extent of the topic, this section is not exhaustive. Reviews are provided in Schumacher (1996) and Aminzadeh et al. (2013) and specific literature sources are found in Fig. 4.5. Only some of the basic concepts are provided here.

Magnetic and electromagnetic methods detect surface anomalies related to the mineralogical changes discussed above; for example, the production of magnetic ferrous iron oxide. These techniques are a natural complement of those that examine the ground's tonal anomalies. The link between hydrocarbons and magnetic anomalies was recognized at the beginning of the last century (Harris 1908), but extensive investigations have only been conducted in the USA since the late 1970s when a direct relationship between aeromagnetic anomalies and oil microseepage was determined over the Cement oil field in Oklahoma (Donovan 1974). In general, low magnetization is attributed to seepage. In fact, the reducing environment induced by seepage results in the diagenesis and transformation of highly magnetic minerals such as magnetite into nearly non-magnetic pyrite (Novosel et al. 2005).

Seismic methods, based on anomalies of seismic reflection amplitudes (e.g., Loseth et al. 2009), are a powerful tool for uncovering crustal seepage chimneys. In particular, 3D seismic data can provide 3-dimensional images of fluid flow shapes and their spatial distributions, including the seepage root (reservoir) and top (near surface or surface sediment modifications). Sesimic anomalies can be distinguished into the following two types: (1) permanent deformations of the primary bedding of sedimentary strata (e.g., mud mobilisations and sand injections) and the formation of surface or subsurface "syn-leakage" features (e.g., pockmarks, bioherms), and (2) acoustic changes due to the replacement of formation water by hydrocarbon fluids. Details and case-histories are well described by Heggland (1998) and Loseth et al. (2009), among others.

Finally, hydro-acoustic methods refer to the detection of acoustic backscatter related to gas bubbles (gas plumes or gas flares) rising within the water column, or to gas-charged sediments in rivers, lakes, or seas. Side-scan sonars and multibeam echosounders are typically employed and numerous examples exist for submarine seepage detection (e.g., Papatheodorou et al. 1993; Orange et al. 2002; Rollet et al. 2006; Judd and Hovland 2007; Weber et al. 2014 and references therein). These

techniques allowed the development of important theoretical models for the transfer of methane from the seabed to the atmosphere and determined that, in general, gas only reaches the sea surface if the seep is shallower than 300–400 m (Schmale et al. 2005; McGinnis et al. 2006). Bubble acoustic scattering was also modelled in order to estimate the gas flux of a bubble plume, either from ship-based remote sensing (Weber et al. 2014) or from benthic landers (such as *GasQuant* or *BOB*, or the Bubble OBservatory module; Greinert 2008; Bayrakci et al. 2014). Benthic devices are particularly useful for monitoring seepage variations over time.

References

Abrams MA (1996) Distribution of subsurface hydrocarbon seepage in near-surface marine sediments. In: Schumacher D, Abrams MA (eds) Hydrocarbon migration and its near-surface expression. AAPG Memoir, vol 66. PennWell Publishing, Tulsa, pp 1–14

Abrams MA (2013) Best practices for the collection, analysis, and interpretation of seabed geochemical samples to evaluate subsurface hydrocarbon generation and entrapment. In: Offshore technology conference, Houston, 6–9 May 2013, OTC-24219

Abrams MA, Dahdah NF (2010) Surface sediment gases as indicators of subsurface hydrocarbons—examining the record in laboratory and field studies. Mar Pet Geol 27:273–284

Almeida-Filho R, Miranda FP, Yamakawa T (1999) Remote detection of a tonal anomaly in an area of hydrocarbon microseepage, Tucano basin, north-eastern Brazil. Int J Remote Sens 20:2683–2688

Aminzadeh F, Berge TB, Connolly DL (eds) (2013) Hydrocarbon seepage: from source to surface. AAPG/SEG Special Publication, Geophysical Developments No. 16, American Association of Petroleum Geologists, Tulsa, 256 pp

Arntsen B, Wensaas L, Løseth H, Hermanrud C (2007) Seismic modelling of gas chimneys. Geophysics 72:251–259

Baer D, Gupta M, Leen JB, Berman E (2012) Environmental and atmospheric monitoring using off-axis integrated cavity output spectroscopy (OA-ICOS). Am Lab 44:10

Bayrakci G, Scalabrin C, Dupré S, Leblond I, Tary J-B, Lanteri N, Augustin J-M, Berger L, Cros E, Ogor A, Tsabaris C, Lescanne M, Géli L (2014) Acoustic monitoring of gas emissions from the seafloor. Part II: a case study from the Sea of Marmara. Mar Geophys Res. doi:10.1007/s11001-014-9227-7

Bernard BB, Brooks JM, Sackett WM (1978) Light hydrocarbons in recent Texas continental shelf and slope sediments. J Geophys Res 83:4053–4061

Boulart C, Connelly DP, Mowlem MC (2010) Sensors and technologies for in situ dissolved methane measurements and their evaluation using technology readiness levels. TrAC Trends Anal Chem 29:186–195

Bourry C, Chazallon B, Charlou JL, Donval JP, Ruffine L, Henry P, Geli L, Çağatay MN, Inan S, Moreau M (2009) Free gas and gas hydrates from the Sea of Marmara, Turkey. Chemical and structural characterization. Chem Geol 264:197–206

Bradley ES, Leifer I, Roberts DA, Dennison PE, Washburn L (2011) Detection of marine methane emissions with AVIRIS band ratios. Geophys Res Lett 38:L10702

Buchwitz M, Bovensmann H, Burrows JP, Schneising O, Reuter M (2010) Global mapping of methane and carbon dioxide: from SCIAMACHY to CarbonSat. In: Proceedings ESA-iLEAPS-EGU conference on earth observation for land-atmosphere interaction science, ESA Special Publications SP-688, ESRIN, Italy, 3–5 Nov 2010

Burba G, Anderson D (2010) A brief practical guide to Eddy Covariance measurements: principles and workflow examples for scientific and industrial applications. Li-Cor Biosciences, Lincoln, p 214

Camilli R, Duryea A (2007) Characterizing marine hydrocarbons with in-situ mass spectrometry. Oceans 2007. doi:10.1109/OCEANS.2007.4449412

Capasso G, Inguaggiato S (1998) A simple method for the determination of dissolved gases in natural waters. An application to thermal waters from Vulcano island. Appl Geochem 13:631–642

Caprais JC, Lanteri N, Crassous P, Noel P, Bignon L, Rousseaux P, Pignet P, Khripounoff A (2010) A new CALMAR benthic chamber operating by submersible: first application in the cold-seep environment of Napoli mud volcano (Mediterranean Sea). Limnol Ocean Meth 8:304–312

Cardellini C, Chiodini G, Frondini F, Granieri D, Lewicki J, Peruzzi L (2003) Accumulation chamber measurements of methane fluxes: application to volcanic-geothermal areas and landfills. Appl Geochem 18:45–54

Chen H, Winderlich J, Gerbig C, Hoefer A, Rella CW, Crosson ER, Van Pelt AD, Steinbach J, Kolle O, Beck V, Daube BC, Gottlieb EW, Chow VY, Santoni GW, Wofsy SC (2010) High-accuracy continuous airborne measurements of greenhouse gases (CO_2 and CH_4) using the cavity ring-down spectroscopy (CRDS) technique. Atmos Meas Tech 3:375–386

Cole JJ, Bade DL, Bastviken D, Pace ML, Van de Bogert M (2010) Multiple approaches to estimating air-water gas exchange in small lakes. Limnol Ocean Meth 8:285–293

Dickinson RG, Matthews MD (1993) Regional microseep survey of part of the productive Wyoming-Utah thrust belt. AAPG Bull 77:1710–1722

Donovan TJ (1974) Petroleum microseepage at Cement, Oklahoma: evidence and mechanism. AAPG Bull 58:429–446

Donovan TJ, Friedman I, Gleason JD (1974) Recognition of petroleum-bearing traps by unusual isotopic compositions of carbonate-cemented surface rocks. Geology 2:351–354

Durrance EM (1986) Radioactivity in geology. principles and applications. Horwood Ltd., Chichester

Embriaco D, Marinaro G, Frugoni F, Monna S, Etiope G, Gasperini L, Polonia A, Del Bianco F, Çağatay MN, Ulgen UB, Favali P (2014) Monitoring of gas and seismic energy release by multi-parametric benthic observatory along the North Anatolian Fault in the Sea of Marmara (NW Turkey). Geophys J Int. doi:10.1093/gji/ggt436

Etiope G (1999) Subsoil CO_2, and CH_4 and their advective transfer from faulted grassland to the atmosphere. J Geophys Res 104:16889–16894

Etiope G, Klusman RW (2010) Microseepage in drylands: flux and implications in the global atmospheric source/sink budget of methane. Global Planet Change 72:265–274

Etiope G, Baciu C, Caracausi A, Italiano F, Cosma C (2004a) Gas flux to the atmosphere from mud volcanoes in eastern Romania. Terra Nova 16:179–184

Etiope G, Feyzullaiev A, Baciu CL, Milkov AV (2004b) Methane emission from mud volcanoes in eastern Azerbaijan. Geology 32:465–468

Etiope G, Papatheodorou G, Christodoulou D, Geraga M, Favali P (2006) The geological links of the ancient Delphic Oracle (Greece): a reappraisal of natural gas occurrence and origin. Geology 34:821–824

Etiope G, Martinelli G, Caracausi A, Italiano F (2007) Methane seeps and mud volcanoes in Italy: gas origin, fractionation and emission to the atmosphere. Geophys Res Lett 34:L14303. doi:10.1029/2007GL030341

Etiope G, Nakada R, Tanaka K, Yoshida N (2011a) Gas seepage from Tokamachi mud volcanoes, onshore Niigata Basin (Japan): origin, post-genetic alterations and CH_4-CO_2 fluxes. Appl Geochem 26:348–359

Etiope G, Schoell M, Hosgormez H (2011b) Abiotic methane flux from the Chimaera seep and Tekirova ophiolites (Turkey): understanding gas exhalation from low temperature serpentinization and implications for Mars. Earth Planet Sci Lett 310:96–104

Etiope G, Christodoulou D, Kordella S, Marinaro G, Papatheodorou G (2013) Offshore and onshore seepage of thermogenic gas at Katakolo Bay (Western Greece). Chem Geol 339:115–126

Foote RS (1969) Review of radiometric techniques. In: Heroy WE (ed) Unconventional methods in exploration for petroleum and natural gas. Southern Methodist University, Dallas, pp 43–55
Gasperini L, Polonia A, Del Bianco F, Etiope G, Marinaro G, Favali P, Italiano F, Cağatay MN (2012) Gas seepages and seismogenic structures along the North Anatolian Fault in the Eastern Marmara Sea. Geochem Geophys Geosys 13:Q10018. doi:10.1029/2012GC004190
Gerilowski K, Tretner A, Krings T, Buchwitz M, Bertagnolio P, Belemezov F, Erzinger J, Burrows JP, Bovensmann H (2010) MAMAP—a new spectrometer system for column-averaged methane and carbon dioxide observations from aircraft: instrument description and performance assessment. Atmos Meas Tech Discuss 3:3199–3276
Gingrich JE (1984) Radon as a geochemical exploration tool. J Geochem Explor 21:19–39
Gott GB, Hill JW (1953) Radioactivity in some oil fields of Southeast Kansas. USGS Bull 988E:69–112
Greinert J (2008) Monitoring temporal variability of bubble release at seeps: the hydroacoustic swath system GasQuant. J Geophys Res 113:C07048. doi:10.1029/2007JC004704
Hanson RS, Hanson TE (1996) Methanotrophic bacteria. Microbiol Rev 60:439–471
Harbert W, Jones VT, Izzo J, Anderson TH (2006) Analysis of light hydrocarbons in soil gases, Lost River region, West Virginia: relation to stratigraphy and geological structures. AAPG Bull 90:715–734
Harris GD (1908) Salt in Louisiana, with special reference to its geologic occurrence, part II—localities south of the Oligocene. La Geol Surv Bull 7:18–27
Heggland R (1998) Gas seepage as an indicator of deeper prospective reservoirs. A study on exploration 3D seismic data. Mar Pet Geol 15:1–9
Hernandez P, Perez N, Salazar J, Nakai S, Notsu K, Wakita H (1998) Diffuse emission of carbon dioxide, methane, and helium-3 from Teide volcano, Tenerife, Canary Islands. Geophys Res Lett 25:3311–3314
Hinkle ME (1994) Environmental conditions affecting concentrations of He, CO_2, O_2 and N_2 in soil gases. App Geochem 9:53–63
Hirst B, Gibson G, Gillespie S, Archibald I, Podlaha O, Skeldon KD, Courtial J, Monk S, Padgett M (2004) Oil and gas prospecting by ultra-sensitive optical gas detection with inverse gas dispersion modelling. Geophys Res Lett 31(L12115):1–4
Hong WL, Etiope G, Yang TF, Chang PY (2013) Methane flux of miniseepage in mud volcanoes of SW Taiwan: comparison with the data from Europe. J Asian Earth Sci 65:3–12
Hopkins TL (1964) A survey of marine bottom samplers. In: Seers M (ed) Progress in oceanography, vol 2. Pergamon-MacMillan, New York, pp 213–256
Hunt JM (1996) Petroleum geochemistry and geology. Freeman and Co, New York 743 pp
Hutchinson GL, Livingston GP (1993) Use of chamber systems to measure trace gas fluxes. In Harper L et al (eds) Agricultural ecosystem effects on trace gases and global climate change, ASA Special Publication 55, ASA, CSSA, SSSA, Madison, pp 63–78
Iseki T (2004) A portable remote methane detector using an InGaAsP DFB laser. Environ Geol 46:1064–1069
Jones VT, Drozd RJ (1983) Prediction of oil or gas potential by near-surface geochemistry. AAPG Bull 67:932–952
Jones VT, Matthews MD, Richers DM (2000) Light hydrocarbons for petroleum and gas prospecting. In: Hale M (ed) Handbook of exploration geochemistry, vol 7. Elsevier Science Publishers, Amsterdam, pp 133–212
Judd A, Hovland M (2007) Seabed fluid flow: the impact on geology, biology and the marine environment. Cambridge University Press, Cambridge, 475 pp
Klusman RW (2006) Detailed compositional analysis of gas seepage at the National Carbon Storage Test Site, Teapot Dome, Wyoming, USA. App Geochem 21:1498–1521
Klusman RW (2011) Comparison of surface and near-surface geochemical methods for detection of gas microseepage from carbon dioxide sequestration. Int J Greenhouse Gas Control 5:1369–1392
Klusman RW, Webster JD (1981) Meteorological noise in crustal gas emission and relevance to geochemical exploration. J Geochem Explor 15:63–76

Klusman RW, Leopold ME, LeRoy MP (2000) Seasonal variation in methane fluxes from sedimentary basins to the atmosphere: results from chamber measurements and modeling of transport from deep sources. J Geophys Res 105D:24661–24670

Krabbenhoeft A, Netzeband GL, Bialas J, Papenberg C (2010) Episodic methane concentrations at seep sites on the G.L. upper slope Opouawe Bank, southern Hikurangi Margin, New Zealand. Mar Geol 272:71–78

Lammoglia T, de Souza Filho CR (2013) Unraveling hydrocarbon microseepages in onshore basins using spectral-spatial processing of advanced spaceborne thermal emission and reflections radiometer (ASTER) data. Surv Geophys 34:349–373

Lewicki JL, Hilley GE, Fischer ML, Pan L, Oldenburg CM, Dobeck L, Spangler L (2009) Eddy covariance observations of surface leakage during shallow subsurface CO_2 releases. J Geophys Res 114:D12302. http://dx.doi.org/10.1029/2008JD011297

Liu Q, Chan L, Liu Q, Li H, Wang F, Zhang S, Xia X, Cheng T (2004) Relationship between magnetic anomalies and hydrocarbon microseepage above the Jingbian gas field, Ordos basin, China. AAPG Bull 88:241–251

Logan GA, Abrams MA, Dahdah N, Grosjean E (2009) Examining laboratory methods for evaluating migrated high molecular weight hydrocarbons in marine sediments as indicators of subsurface hydrocarbon generation and entrapment. Org Geochem 40:365–375

Loseth H, Gading M, Wensaas L (2009) Hydrocarbon leakage interpreted on seismic data. Mar Pet Geol 26:1304–1319

LTE (2007) Phase II Raton Basin Gas Seep Investigation Las Animas and Huerfano Counties, Colorado, Project #1925 Oil and Gas Conservation Response Fund. http://cogcc.state.co.us/Library/Ratoasin/Phase%20II%20Seep%20Investigation%20Final%20Report.pdf

Machel HM (1996) Magnetic contrasts as a result of hydrocarbon seepage and migration. In: Schumacher D et al. (eds) Hydrocarbon Migration and Its Near-Surface Expression. AAPG Memoir, vol 66. PennWell Publishing, Tulsa, pp 99–109

Mani D, Patil DJ, Dayal AM (2011) Stable carbon isotope geochemistry of adsorbed alkane gases in near-surface soils of the Saurashtra Basin, India. Chem Geol 280:144–153

Marinaro G, Etiope G, Lo Bue N, Favali P, Papatheodorou G, Christodoulou D, Furlan F, Gasparoni F, Ferentinos G, Masson M, Rolin JF (2006) Monitoring of a methane-seeping pockmark by cabled benthic observatory (Patras Gulf, Greece). Geo-Mar Lett. doi: 10.1007/s00367-006-0040-4

McAuliffe C (1969) Determination of dissolved hydrocarbons in subsurface brines. Chem Geol 4:225−233

McGinnis DF, Greinert J, Artemov Y, Beaubien SE, Wüest A (2006) Fate of rising methane bubbles in stratified waters: how much methane reaches the atmosphere? J Geophys Res 111: C09007

Mosier A (1989) Chamber and isotope techniques. In: Andreae M, Schimel DS (eds) Exchange of trace gases between terrestrial ecosystems and the atmosphere. Report of the Dahlem Workshop, Berlin. Wiley, New York, pp 175–188

Newman KR, Cormier MH, Weissel JK, Driscoll NW, Kastner M, Solomon EA, Robertson G, Hill JC, Singh H, Camilli R, Eustice R (2008) Active methane venting observed at giant pockmarks along the U.S. mid-Atlantic shelf break. Earth Planet Sci Lett 267:341–352

Noomen MF, van der Werff HMA, van der Meer FD (2012) Spectral and spatial indicators of botanical changes caused by long-term hydrocarbon seepage. Ecol Inform 8:55–64

Norman JM, Kucharik CJ, Gower ST, Baldocchi DD, Crill PM, Rayment M, Savage K, Striegl RG (1997) A comparison of six methods for measuring soil surface carbon dioxide fluxes. J Geophys Res 102:28,771–28,777

Novosel I, Spence GD, Hyndman TRD (2005) Reduced magnetization produced by increased methane flux at a gas hydrate vent. Mar Geol 216:265–274

Orange DL, Yun J, Maher N, Barry J, Greene G (2002) Tracking California seafloor seeps with bathymetry, backscatter and ROVs. Cont Shelf Res 22:2273–2290

Papatheodorou G, Hasiotis T, Ferentinos G (1993) Gas charged sediments in the Aegean and Ionian Seas, Greece. Mar Geol 112:171–184

Pétron G, Frost G, Miller BR, Hirsch AI, Montzka SA, Karion A, Trainer M, Sweeney C, Andrews AE, Miller L, Kofler J, Bar-Ilan A, Dlugokencky EJ, Patrick L, Moore CT Jr, Ryerson TB, Siso C, Kolodzey W, Lang PM, Conway T, Novelli P, Masarie K, Hall B, Guenther D, Kitzis D, Miller J, Welsh D, Wolfe D, Neff W, Tans P (2012) Hydrocarbon emissions characterization in the Colorado Front Range: A pilot study. J Geophys Res 117:D04304

Pfaffhuber AA, Monstad S, Rudd J (2009) Airborne electromagnetic hydrocarbon mapping in Mozambique. Explor Geophys 40:1–9

Philp RP, Crisp PT (1982) Surface geochemical methods used for oil and gas prospecting: a review. J Geochem Explor 17:1–34

Price LC (1993) Microbial-soil surveying—preliminary results and implications for surface geochemical exploration. Ass Petrol Geochem Explor Bull 9:81–129

Richers DM, Maxwell LE (1991) Application and theory of soil gas geochemistry in petroleum exploration. In: Merrill RK (ed) Source and migration processes and evaluation techniques. AAPG Treatise of Petroleum Geology, Tulsa, pp 141–208

Richers DM, Jones VT, Matthews MD, Maciolek JB, Pirkle RJ, Sidle WC (1986) The 1983 Landsat soil gas geochemical survey of the Patrick Draw area, Sweetwater County, Wyoming. AAPG Bull 70:869–887

Rollet N, Logan GA, Kennard JM, O'Brien PE, Jones AT, Sexton M (2006) Characterisation and correlation of active hydrocarbon seepage using geophysical data sets: an example from the tropical, carbonate Yampi Shelf, Northwest Australia. Mar Pet Geol 23:145–164

Sackett WM (1977) Use of hydrocarbon sniffing in offshore exploration. J Geochem Explor 7:243–254

Saunders DF (1993) Relation of thorium-normalized surface and aerial radiometric data to subsurface petroleum accumulations. Geophysics 58:1417–1427

Schmale O, Greinert J, Rehder G (2005) Methane emission from high-intensity marine gas seeps in the Black Sea into the atmosphere. Geophys Res Lett 32:L07609

Schumacher D (1996) Hydrocarbon-induced alteration of soils and sediments, hydrocarbon migration and its near-surface expression. In: Schumacher D, Abrams MA (eds) Hydrocarbon migration and its near-surface expression. AAPG Memoir, vol 66. PennWell Publishing, Tulsa, pp 71–89

Sechman H (2012) Detailed compositional analysis of hydrocarbons in soil gases above multi-horizon petroleum deposits—a case study from western Poland. App Geochem 27:2130–2147

Sternberg B (1991) A review of some experience with the induced polarization/ resistivity method for hydrocarbon surveys: successes and limitations. Geophysics 56:1522–1532

Tedesco SA (1995) Surface geochemistry in petroleum exploration. Chapman & Hall, New York, p 206

Thielemann T, Lucke A, Schleser GH, Littke R (2000) Methane exchange between coal-bearing basins and the: the Ruhr Basin and the Lower Rhine Embayment, Germany. Org Geochem 31:1387–1408

Thomas B, David G, Anselmo C, Coillet E, Rieth K, Miffre A, Cariou JP, Rairoux P (2013) Remote sensing of methane with broadband laser and optical correlation spectroscopy on the Q-branch of the $2\nu_3$ band. J Mol Spetcrosc 291:3–8

Thorpe AK, Roberts DA, Bradley ES, Funk CC, Dennison PE, Leifer I (2013) High resolution mapping of methane emissions from marine and terrestrial sources using a cluster-tuned matched filter technique and imaging spectrometry. Remote Sens Environ 134:305–318

Tucker J, Hitzman D (1996) Long-term and seasonal trends in the response of hydrocarbon-utilizing microbes to light hydrocarbon gases in shallow soils. In: Schumacher D, Abrams MA (eds) Hydrocarbon migration and its near-surface expression. AAPG Memoir, vol 66. AAPG, Tulsa, pp 353–357

van der Meer F, van Dijk P, van der Werff H, Yang H (2002) Remote sensing and petroleum seepage: a review and case study. Terra Nova 14:1–17

Wagner M, Wagner M, Piske J, Smit R (2002) Case histories of microbial prospection for oil and gas, onshore and offshore northwest Europe. In: Schumacher D, LeSchack LA (eds) Surface exploration case histories: applications of geochemistry, magnetics and remote sensing. AAPG

Studies in Geology No. 48 and SEG Geophys Ref Series No. 11. American Association of Petroleum Geologists, Tulsa, pp 453–479

Weber TC, Mayer L, Jerram K, Beaudoin J, Rzhanov Y, Lovalvo D (2014) Acoustic estimates of methane gas flux from the seabed in a 6000 km^2 region in the Northern Gulf of Mexico. Geochem Geophys Geosyst 15:1911–1925. doi:10.1002/2014GC005271

Wyatt DE, Richers DM, Pirkle RJ (1995) Barometric pumping effects on soil gas studies for geologic and environmental characterization. Environ Geol 25:243–250

Yang H, Zhang J, van der Meer F, Kroonenberg SB (2000) Imaging spectrometry data correlated to hydrocarbon microseepage. Int J Remote Sens 21:197–202

Zirnig W (2004) Helicopter-borne laser methane detection system—a new tool for efficient gas pipeline inspection. IGRC 2004, Vancouver, Canada, 1–4 Nov 2004, http://www.gerg.eu/publications/confer_papers/2004/zirnig_vancouv04.pdf

Chapter 5
Seepage in Field Geology and Petroleum Exploration

As discussed in Chap. 3 the following basic preconditions are required for a seepage area to develop: (1) rock permeability to gas, mainly secondary permeability along faults and fractures, and (2) a gas source (source or reservoir rocks). As discussed below, seepage can then provide information regarding the location and nature of the source and the migration pathway. In the modern fossil fuel industry, especially in the 1900s, natural hydrocarbon seepage provided the first clues for petroleum and natural gas explorations. Although some surface seeps are not directly linked with economic petroleum reservoirs, many large hydrocarbon fields have been discovered after drilling within and adjacent to seeps with gas and oil that leaked and migrated from active petroleum seepage systems (see the definition in Chap. 1). The first oil well in North America, the Drake well in Pennsylvania, was actually drilled on a macro-seep. Roughly 70 % of the world's hydrocarbon reserves have been discovered on the basis of seep observations, including large fields in the Middle East such as the Burgan Field in Kuwait (e.g., Hunt 1996). Therefore, assessments for the origin and magnitude of seeping gas prior to drilling may be important for understanding subsurface hydrocarbon potentials and gas genesis and quality (e.g., the presence of shallow microbial gas, deeper thermogenic accumulations, oil biodegradation, and non-hydrocarbon risk gases). New instrumental and interpretative tools, based on a holistic approach that assists petroleum exploration, can be used to detect and interpret gas seepage.

When integrated with geophysical and geological surveys, seepage detection is particularly useful for petroleum exploration. The justifications, potentials, critics, and advantages and disadvantages of surface geochemical prospection for petroleum exploration are discussed elsewhere (e.g., Klusman 1993; Tedesco 1995; Schumacher and Abrams 1996; Abrams 2005, and references therein).

G. Etiope, *Natural Gas Seepage*, DOI 10.1007/978-3-319-14601-0_5

5.1 Seepage and Faults

Link (1952) was one of the first geologists to describe specific relationships between seeps and underground rock stratigraphy and structural geology. He distinguished five types of seeps (Fig. 5.1), as follows:

Type 1. Seeps on a homocline (i.e., simple outcrops of inclined oil-bearing homocline beds). Whether or not these "oil-bearing beds" were sources or reservoir rocks was not clear. However, even if they are not prolific, this type of system is more suitable for oil seeps.

Type 2. Seeps caused by the crushing and fracturing of shallow source rocks. This type of system would be the case for near surface source rocks (e.g., shale) that liberate hydrocarbons only after crushing or fracturing (for example, by neotectonics). Apparently, Link (1952) anticipated the concept of "natural fracking" of shales, as recently hypothesised for a gas seep in New York state (Etiope et al. 2013b) and as discussed in Sect. 5.3.2.

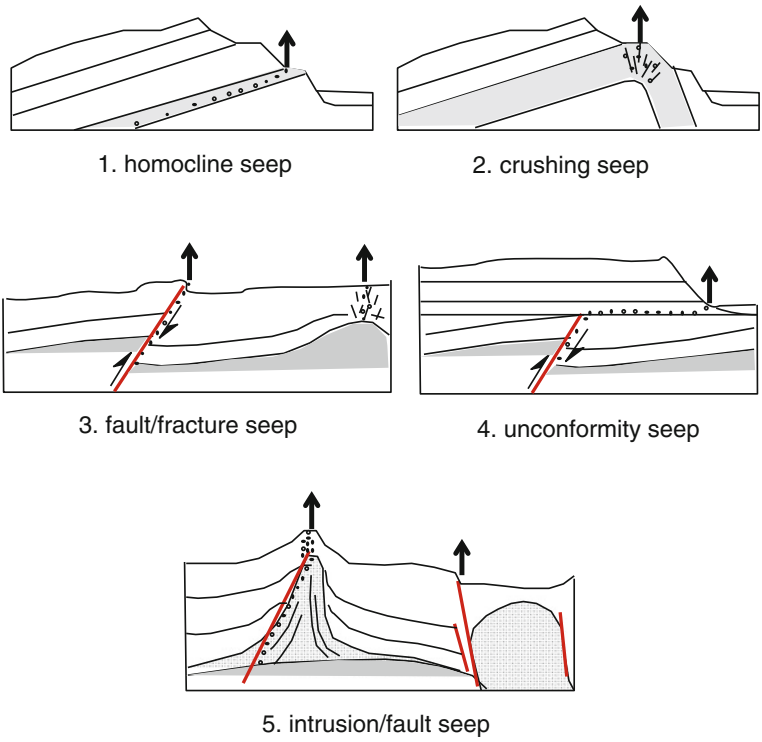

Fig. 5.1 The five types of hydrocarbon seeps proposed by Link (1952) in relation to stratigraphic and structural settings. Seep *Types 1–2* are specific for oil. *Types 3–5* are more characteristic of gas seepage, but may also include oil seepage. *Type 5* is found in mud volcanoes

Type 3. Seeps from hydrocarbon accumulations along normal or thrust faults, or fractured or eroded cap rocks. This type of system is the most common type of gas seepage system. Gases can find two types of pathways: faults, especially when the reservoir is relatively deep, and, in the case of cap rocks (typically evaporites or clays) that have locally lost their sealing capacity, random fractures of relatively high permeable rocks overlying the reservoir.

Type 4. Seeps over an unconformity overlying faulted or eroded reservoirs. The main pathway to the surface is stratigraphic (the unconformity) and brings the fluid from a buried fault (connected to the reservoir) or directly from an eroded reservoir. Basically, permeable beds collect hydrocarbons from a buried Type 3 seepage system.

Type 5. Seeps associated with intrusions such as shale diapirs, salt diapirs, serpentine nappes, or igneous intrusions. Mud volcanoes belong in this category. However, intrusions, especially mobilised shales, generally follow fault systems so there would not be much difference in this type and Type 3. The intrusion would just be an additional element.

In practice, because they are more "stratigraphically" controlled, Types 1 and 2 are specific for oil seeps (and solid hydrocarbons, tar, bitumen, and asphalt) with relatively shallow (or even outcropping) sources or reservoirs. Types 3, 4, and 5 (with Type 5 considered to be a sub-category of Type 3) imply a leading role for tectonic discontinuities, faults, and fracture networks ("tectonically" controlled), and are typical of gas seepage.

On a worldwide statistical basis, McGregor (1993) found that seeps are associated with all types of faults, either in compressive or extensional tectonic regimes, and uplifted basins fractured by neotectonic unloading and release joints. He noted, in particular, that seeps are more frequent on the surface intersects of permeable fractures or other seal breaches. Such has been confirmed in recent seepage and seismic reflection studies where seeps, especially mud volcanoes, occur at the intersection of two or more faults (e.g., Medialdea et al. 2009; Bonini 2013; Etiope et al. 2013a). Fault intersections clearly produce higher permeability and act as a "channel", a preferential pathway for gas migration, as discussed in Chap. 3. Accordingly, gas seepage can be a formidable indicator of tectonic discontinuities where intersections are buried and not observable from the surface. In the absence of visible seeps, the detection of anomalous concentrations of gases within soil-air has been revealed to be particularly useful for tracing buried faults, and has also been found to be independent of hydrocarbon gases (e.g., Gregory and Durrance 1985; Duddridge et al. 1991; Klusman 1993; Baubron et al. 2001; Guerra and Lombardi 2001; Fu et al. 2005). In many instances, soil-gas anomalies have been used in clay basins where, due to the homogeneity and plastic behaviour of the clayey cover, fault recognition is often a problem (Ciotoli et al. 1999; Etiope and Lombardi 1995). The target is the detection of soil concentrations of endogenous gases such as CH_4, CO_2, Rn, and He higher than a reference level (soil-gas anomalies vs. background). Depending on the type of gas, the reference level can be the atmospheric concentration, the typical biologic production level in soil, or, for radon, the normal concentration induced by the decay of the uranium-radium

naturally present in soil minerals. Soil-gas anomalies are often found to be linearly distributed along fault lines, more or less marking the direction and position of the fault plane. More frequently, however, anomalies are found in isolated spots along the fault, indicating that gas only migrates along focused channels in the absence of fault intersections as a result of the spatial heterogeneity of fault permeability. Soil-gas anomalies, however, even in the presence of active and permeable faults, may be absent if the gas source is weak or if the gas flow pathway is laterally displaced, even by several km, by the horizontal flow of aquifer groundwater. As discussed in Chap. 3, aquifers can be rapidly crossed by vertical streams of gas bubbles and microbubbles, without significant lateral deviation in gas flow. However, this only occurs when gas input is substantial and methane bubbles are not completely dissolved in water.

In some cases, seeps can also provide useful information on the geodynamics of the basin. Several types of seeps occurring within the same basin can, in fact, serve as indicators of local tectonic deformation. For example, in the Northern Apennine thrust wedge (Italy), mud volcanoes mark the compressional sector of the basin, with tectonic compaction and fluid overpressures at depth, while dry seeps mainly characterise the extensional sector (Bonini 2013). Basically, the compression-to-extension transition revealed by earthquake focal mechanism solutions corresponds to the spatial switch between mud volcanism and dry-seepage. Dry seeps, it seems, do not require intense compressional stresses. Gas pressure and permeability are enough. Shale mobilization and water plus gas expulsion in mud volcanism, instead, requires tectonic compaction. As a result, mud volcanism has been extensively studied in relation to its sensitivity to seismic activity (e.g., Mellors et al. 2007).

5.2 Microseepage Applied to Areal Petroleum Exploration

Since the 1930s, the occurrence of methane, light alkanes, and rare gas (helium, radon) anomalies in dry soils has been extensively used by geologists and geochemists as a tool for oil and gas exploration, with pioneering studies in the Soviet Union (Sokolov 1933), Germany (Laubmeyer 1933), and the USA (Hoffman 1939). A nice collection of historical bibliographic references on surface geochemistry applied to petroleum exploration, updated to 2006 by Saunders and Davidson (2006), is currently available at http://www.lib.utexas.edu/taro/smu/00014/smu-00014.html.

From the 1980s, microseepage, in several petroleum basins in North America and Europe, has been the object of modelling and measurements (e.g., Jones and Drozd 1983; Davidson 1986; Klusman 1993; Tedesco 1995; Matthews 1996; Schumacher and Abrams 1996; Schumacher and LeSchack 2002; Abrams 2005; Sechman 2012, as a few examples). As described in Chap. 4, such studies allowed the refinement of direct and indirect gas measurements methods.

The idea of prospecting for oil and gas by geochemical means is still viewed with scepticism by many scholars and petroleum explorers. Nevertheless, all studies,

independent of the method employed, have confirmed that microseepage is quite common and pervasive within all petroliferous and sedimentary basins, preferably along faults and fracture zones, consistent with the theory of gas migration discussed in Chap. 3 and Sect. 5.1. Surface geochemistry has undoubtedly been historically successful in reducing exploration risk, especially in dry holes. Schumacher (2010) reported the following: "Of wells drilled on prospects associated with positive microseepage anomalies 82 % were completed as commercial discoveries. In contrast, only 11 % of wells drilled on prospects without an associated microseepage anomaly resulted in discoveries".

The problem is that, using current methods, some seepage signatures are not distinguishable from background soil or sediment signals, and some seepage, even if well-defined with high gas concentrations, does not necessarily correspond to productive hydrocarbon accumulations. Indeed, a very small fraction, likely a few percent by volume of the hydrocarbons generated in source rocks, is sequestered in commercial fields, with the remaining gas dispersed and migrating toward the surface (Hunt 1996). The relationships between seepage and subsurface petroleum generation and entrapment are often complex. The guidelines (or best-practices), that should be considered for detecting and interpreting microseepage, are based on the studies of Price (1986) and Saunders et al. (1999), and the multi-year research of Jones et al. (2000), Abrams (2002, 2005), Klusman (2006), and Etiope and Klusman (2010), and references therein.

5.2.1 Which Gas Can Be Measured?

Microseepage prospection for petroleum exploration has traditionally been based on the analyses of a wide range of hydrocarbons (HCs, alkanes and aromatics) and non-hydrocarbon gases (e.g., helium, radon, etc.). Many oil companies have focused their attention on complex volatile hydrocarbons, considered to be unequivocal tracers of petroleum deposits. For example, since they can derive from several sources other than petroleum (gas and/oil) deposits, methane anomalies in soils have been considered ambiguous. Such is particularly true for marine sediments, but, as described below, not for methane detection in the normally dry soils of temperate climates. However, since they require highly specialised personnel and may not be feasible in poorly accessible areas, the sampling and analyses of heavy HCs in soils are generally based on procedures (e.g., auger hole drilling at 2–4 m below the soil) that are quite expensive and time consuming. The effectiveness of methane and light alkanes, ethane and propane, was re-evaluated in the early 2000s. Indeed, several studies have indicated that the most important variables for predicting gas and oil are methane and propane, respectively (e.g., Seneshen et al. 2010). Methane is a good tracer for gas fields, is more mobile and abundant than other hydrocarbons, and has an isotopic composition (a fundamental parameter for determining gas origins) that is measurable in the field using modern portable spectrometers. Measurements regarding the flux of methane are discussed in Sect. 5.2.2.

In temperate climates, due to methanotrophic consumption, the methane concentration in soil pores is generally lower than that in the atmosphere (1.8–1.9 ppmv). As a result, values exceeding several ppmv, coupled with stable carbon isotopic determinations (as well as the concentration of other gases), can easily be attributed to subsurface sources. Since other natural or man-made sources can contribute to hydrocarbon anomalies in the soil, the origin of CH_4 must always be assessed using C and H isotope analyses.

Helium (He) is another historical tracer for petroleum deposits (e.g., Dyck 1976; Pogorsky and Quirt 1981; Klusman 1993; Tedesco 1995). Helium is produced by radioactive decay processes (the alpha decay of U-238, U-235, and Th-232), mainly in igneous and metamorphic rocks, and accumulates with petroleum in reservoirs below rock strata with very low permeabilities. Helium is chemically inert, physically stable, and highly mobile. During degassing, helium mixes with other more abundant gases (carrier gases such as methane or carbon dioxide) and is more easily transported towards the surface. The constant helium concentration in the atmosphere (5,220 ppbv, parts per billion by volume) results from the dynamic equilibrium between terrestrial sources and the helium escaping to outer space. As a result, atmospheric helium is considered to be a reference standard, and soil-gas helium results are expressed in ppbv as the difference between the sample and atmospheric concentrations. Helium anomalies (i.e., hundreds to thousands of ppbv in excess of the atmospheric concentrations) have been reported, in correspondence with gas-oil fields, in the USA and Australia (e.g., Roberts 1981; Tedesco 1995; Seneshen et al. 2010), Germany (Van Den Boom 1987), and Italy (Ciotoli et al. 2004). No significant studies have been reported in recent years and there are no case histories indicating that helium surveys have contributed to the discovery of petroleum fields. Rather, as frequently observed in geothermal, tectonic, and seismic areas (e.g., Gregory and Durrance 1985), helium anomalies can easily be produced by the migration of deep gases, not related to hydrocarbon accumulations.

Recently, use of the helium isotopic ratio ($^3He/^4He$) and the noble gas (Ne, Ar, Kr, Xe) content of soil-air has been proposed as a tracer for microseepage (Mackintosh and Ballentine 2012). Soil-gas analyses performed within the Teapot Dome oil field in Wyoming indicated that He anomalies were coupled with high concentrations of CH_4, with a $^3He/^4He$ ratio comparable to that of the deep reservoir. The $^4He/CH_4$ ratio has also been determined to be similar to subsurface sources, demonstrating the conservative nature of helium as a tracer. However, groundwater rather than soil gas may provide better results (Mackintosh and Ballentine 2012).

For all gases, seepage can be verified by examining the areal distribution of gas concentration anomalies. Such a result is possible if surveys are based on a large number of sampling points homogeneously distributed over a given area. The larger the number of sampling points, the better the response of statistical elaborations in helping to unravel backgrounds and anomalies (e.g., Howarth 1993; Tedesco 1995). Data population analyses, histogram distributions, data variations using probability plots, and pattern recognition are typically employed (Tedesco 1995). The sampling strategy is also fundamental. An improperly-spaced grid with too small or too large a sample spacing can result in a cursory and rough assessment of seepage

distributions. In all cases, geochemical data should be used in conjunction with available geological and geophysical data. The likelihood of finding petroleum within an area characterised by surface gas anomalies, may only be ascertained using strict correlations with local geological structures.

5.2.2 Microseepage Methane Flux Measurements

In the past, because of increased complexity as compared to simple compositional measurements within the soil-air in traditional exploration surveys, soil–atmospheric flux measurements were never performed. However, since it provides dynamic information for seepage system activity and a response to gas pressure potentials, knowing the gas flux is useful for petroleum exploration (e.g., Klusman et al. 2000). Flux measurements based on the closed-chamber technique are described in Chap. 4. By utilizing both the molecular and isotopic composition of gases, flux can be an informative parameter for understanding petroleum systems. Measurements of methane microseepage flux to the atmosphere began in late 1990s in the USA (Klusman et al. 1998, 2000; Klusman 2006), and in the 2000s in Europe (Etiope et al. 2002, 2004a, b, 2006) and Asia (Tang et al. 2010). The approach is based on the concept that under normal dry soil conditions the methane flux is negative as a result of methanotrophic consumption (dry soil is, in fact, a sink for atmospheric methane). Positive methane fluxes, associated with C and H isotopic analyses, may indicate active seepage from underground sources. Measurements performed in the Denver-Julesburg Basin (Colorado) have revealed thermogenic CH_4 fluxes, up to 43 mg m^{-2} day^{-1} during winter periods. In summer, warm periods, methanotrophic activity in soils increases and CH_4 flux decreases (Klusman et al. 2000). Seasonal variations of microseepage have also been observed in other countries (e.g., Tang et al. 2010). Seasonal changes of atmospheric and soil conditions are a fundamental factor to consider in areal explorations, especially when CH_4 flux values are on the order of a few units or tens of mg m^{-2} day^{-1}. In more fractured and tectonised basins, the methane flux is substantially higher and the seasonal methanotrophic filter is less influential. The results of microseepage flux surveys within the Yakela Field in China indicated a correlation between the intensity of the methane flux, the type of hydrocarbon accumulation (gas or oil), and the lateral variability of gas pressure in condensed gas pools (Tang et al. 2010). CH_4 fluxes were pervasive in all sectors. Therefore, only a portion of the CH_4 migrating from deep oil–gas reservoirs was consumed in the soil by methanotrophic oxidation. CH_4 fluxes were higher (values >10 mg m^{-2} day^{-1}) in an area characterised by multiple fault lines, lower in correspondence with the gas–oil interface of the field, and much lower in correspondence with the oil–water sector and the area outside field boundaries.

Figure 5.2 provides an example of the regional microseepage distribution assessed using reconnaissance surveys based on closed-chamber measurements within a petroleum basin located in central Italy. The data refer to the methane flux from the soil (an average of two measurements at the same site) measured over an area of

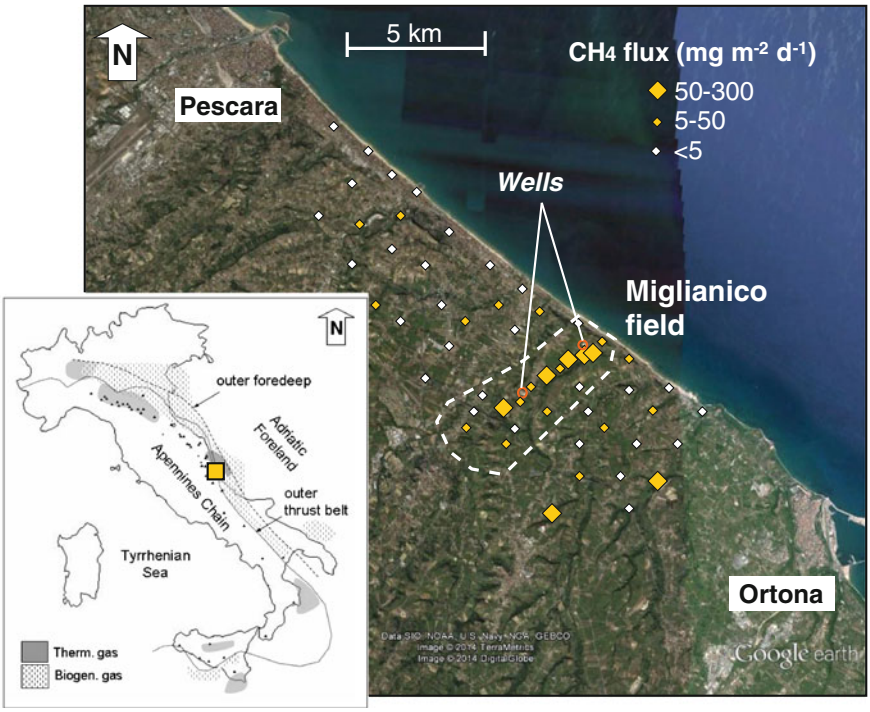

Fig. 5.2 A seepage survey performed using the closed-chamber method within and around the Miglianico petroleum field located in central Italy. *Diamonds* indicate measurements points (executed in duplicate). The map on the *left* provides the location of the area in the framework of thermogenic and microbial hydrocarbon basins in Italy. *Small dots* indicate gas and oil seeps (from the GLOGOS data-base; Etiope 2009, and http://hydrocarbonseeps.blogspot.it/p/hysed.html)

approximately 75 km^2 within and surrounding the Miglianico Oil Field. At 55 sites, 31 yielded a negative or non-detected methane flux (<5 mg m^{-2} day^{-1}), normal for dry soil; while 24 sites yielded fluxes above 5 mg m^{-2} day^{-1}, with seven exceeding 50 mg m^{-2} day^{-1} and producing values up to 300 mg m^{-2} day^{-1}. The highest flux sites were located within the boundary of the oil field, in the vicinity of productive wells, corresponding to the top of an anticline. Although many more measurements are needed for a rigorous statistical evaluation of the data, this quick survey, which was completed in 2 days, indicated the existence of considerable gas seepage corresponding to the hydrocarbon field. Isotopic analyses of two gas samples collected from the chamber confirmed that the CH_4 is thermogenic ($\delta^{13}C$: −39 and −41 ‰).

The stable carbon isotopic composition of the CH_4 accumulating within the closed chamber was also investigated in the Yakela Field in China (Tang et al. 2010), in a coal basin in Germany (Thielemann et al. 2000), and for the microseepage of abiotic gases above ultramafic rocks in Turkey and Spain (Etiope et al. 2011a, 2014b). The analyses generally indicated that, over time, the $\delta^{13}C_{CH4}$ value increases with the CH_4 concentration. For the Yakela Field seepage, for example,

methane became progressively ^{13}C-enriched beginning with values of approximately −47 ‰ (atmospheric CH_4) up to −43 ‰ (with 7 ppmv of CH_4 after ~1 h). The increasing $\delta^{13}C$ trend was compatible with the seepage of thermogenic CH_4 occurring in deep Yakela reservoirs ($\delta^{13}C$ of −42 to −31 ‰; Tang et al. 2010). For the case of abiogenic gas seepage from an ophiolite in Turkey, the CH_4 concentration increased up to 23 ppmv after 15 min and $\delta^{13}C$ increased from −47 to −30 ‰. A two-endmember mixing model fit the seepage profile for CH_4, with a $\delta^{13}C$ of −15 ‰, a value similar to gas that is known to seep abundantly in the region (the Chimaera gas; Etiope et al. 2011c). Basically, thermogenic or abiotic CH_4 microseeping and accumulating in a chamber is more enriched in ^{13}C than atmospheric air or any microbial gas that may be produced in the soil. The microseepage of fossil microbial gas cannot be distinguished from the modern microbial CH_4 eventually produced in wet soils or shallow peat sediments. The phenomenon is illustrated in Fig. 5.3.

As discussed in the sub-chapter that follows, knowing the molecular and isotopic composition of seeping gas is always fundamental for assessing gas origin and potential source rocks.

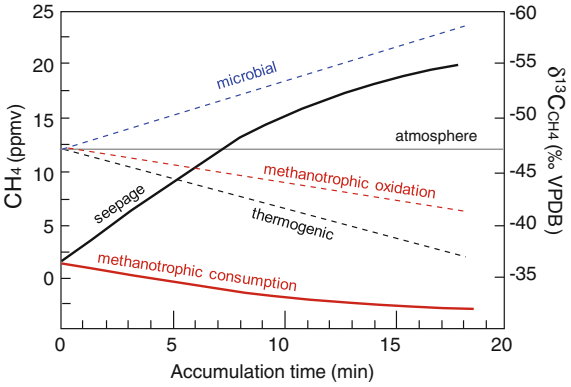

Fig. 5.3 Examples of the CH_4 concentrations and the $\delta^{13}C_{CH4}$ patterns observed using microseepage flux measurements by the closed-chamber technique. The continuous *black* (seepage) and *red* (consumption) *lines* indicate the variation of methane concentrations within the chamber. Thermogenic gas seepage was recorded using simultaneous increases of $\delta^{13}C$ (the *dashed black line*) and concentrations (the *continuous black line*) of CH_4. Increases in $\delta^{13}C_{CH4}$ within the chamber could also be due to methanotrophic oxidation (bacteria preferentially consume ^{12}C), but, in the absence of seepage, a corresponding decrease in CH_4 concentrations should be observed (the *continuous red line*). For the case of the seepage of microbial gas, an increase in CH_4 concentrations is associated with a $\delta^{13}C_{CH4}$ decrease (the *dashed blue line*)

5.3 Seep Geochemistry for Petroleum System Evaluation

Analyses of the molecular and isotopic composition of seeping gas is a key task for understanding subsurface hydrocarbon potential, genesis, and quality (e.g., by discriminating shallow microbial gas from deeper thermogenic accumulations, and suggesting the presence of oil and undesirable non-hydrocarbon gases, such as CO_2, N_2 and H_2S). Gas seeps can also indicate subsurface petroleum biodegradation, which has an important impact on hydrocarbon quality and may influence exploration and production strategies. Thus, seeping gas geochemistry can contribute to assessing, prior to or without drilling, a petroleum system, which is particularly useful in frontier or unexplored areas.

5.3.1 Recognising Post-genetic Alterations of Gases

Due to post-genetic or secondary alteration processes that operate after gas formation and during its migration to the surface, seeping gas and original reservoir gas may, however, display differences. Recognising these processes and how they can impact the seeping gas observed at the surface is important, otherwise geochemical signatures can be misinterpreted and wrong attributions can be given to the gas source.

Six main types of post-genetic processes can be distinguished, as follows:

(a) microbial (aerobic and anaerobic) oxidation of methane;
(b) abiogenic oxidation of methane;
(c) isotopic fractionation by diffusion;
(d) molecular fractionation by advection;
(e) gas mixing;
(f) biodegradation of petroleum and secondary methanogenesis.

(a) *Microbial* (*aerobic and anaerobic*) *oxidation of methane*
Since microbes preferentially consume ^{12}C, the oxidation (consumption) of methane induces a decrease in the Bernard ratio ($C_1/(C_2 + C_3)$) and an enrichment in ^{13}C in residual CH_4 (Fig. 5.4). The aerobic microbial oxidation of methane has been studied and documented beginning with the benchmark works of Coleman et al. (1981) and Schoell (1983) (also see Whiticar 1999 and references therein). Comparisons between seep and reservoir gases (Deville et al. 2003; Etiope et al. 2007, 2009a) indicate that microbial oxidation may occur in some mud volcanoes. The anaerobic oxidation of methane has been extensively documented in submarine mud volcanoes and is responsible for significant methane consumption on the seafloor (e.g., Niemann et al. 2006). For terrestrial mud volcanoes, only a few investigations have been conducted, with different results. The presence of anaerobic methane oxidation was reported in a mud volcano in Romania (Alain et al. 2006) but not in Taiwan (Chu et al. 2007). However, the existence of diffuse microseepage throughout the muddy cover of land-based mud volcanoes (e.g., Hong et al. 2012) suggests that

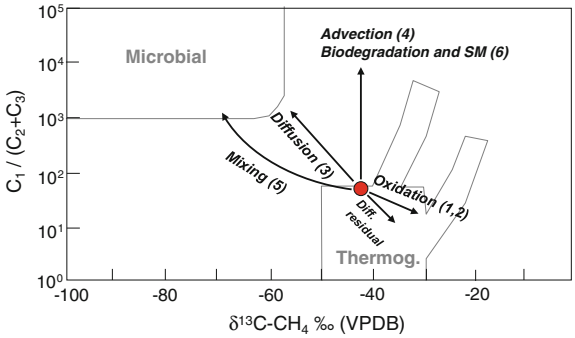

Fig. 5.4 Post-genetic modifications of natural gas composition and carbon isotopes of methane. *Arrows* indicate the possible variations of the Bernard ratio ($C_1/(C_2 + C_3)$) and the $\delta^{13}C$ of CH_4 due to six alteration processes (see text) following the generation of a thermogenic gas indicated by a *circle*

methane consumption, if any, is not pervasive and could only be significant in focused, localised zones.

(b) *Abiogenic oxidation of methane*

Abiogenic oxidation of methane generally refers to thermochemical sulphate reduction (TSR) or oxidation by hematite, magnetite, and other ferric (Fe^{3+})-bearing minerals (e.g., Pan et al. 2006; Kiyousu and Imaizumi 1996). These processes occur at relatively high temperatures (approximately 80–400 °C) and can be invoked in very deep reservoirs (and in high heat flow regions). Abiogenic oxidation may produce high H_2S concentrations (usually >5 %) and increase the $\delta^{13}C$ and $\delta^{2}H$ values of C_1–C_5 hydrocarbons. Such conditions can be met in seepage systems adjacent to geothermal or volcanic systems (or in sediment-hosted hydrothermal systems). A particular case of abiogenic oxidation occurs in a seep (Homorod, a small mud volcano) located at the eastern margin of the Transylvania Basin, in Romania (Etiope et al. 2011a). The methane released by this seep was found to have a deuterium concentration, $\delta^{2}H_{CH4}$, of up to +124 ‰ that far exceeds the values reported for any terrestrial gas, while $\delta^{13}C_{CH4}$ was only slightly ^{13}C enriched (maximum value of −25.7 ‰). With respect to the original CH_4, the ^{2}H versus ^{13}C enrichment ratio ($\Delta H/\Delta C$) was approximately 20, typical of abiogenic oxidation, while the ratio produced by microbial oxidation is typically ∼8–9 (Coleman et al. 1981; Kinnaman et al. 2007).

(c) *Isotopic fractionation by diffusion*

Isotopic fractionation by diffusion is a well known phenomenon occurring during primary migration (within source rock) and, subordinately, in secondary migration (between reservoirs), when, as discussed in Chap. 3, slow gas movement is driven by concentration gradients. The result is a depletion of ^{13}C in diffusing CH_4 and ^{13}C enrichment in the residual gas (Fig. 5.4). However, diffusion is not important in seeps where advection is the dominant gas migration mechanism. The comparison between seep and reservoir gases in different basins, in fact, indicates that isotopic fractionation by diffusion does not significantly affect the seeping gas and generally

leads to a slight difference in $\delta^{13}C_{CH4}$, not exceeding 5 ‰ (Deville et al. 2003; Etiope et al. 2007, 2009a).

(d) *Molecular fractionation by advection*
Molecular fractionation by advection is a sort of distillation or the differential segregation of light hydrocarbon molecules as a function of their adsorption and solubility properties. The effect is that gas seeping to the surface has less ethane and propane (i.e., it is dryer, with a higher $C_1/(C_2 + C_3)$ ratio) than the original (Fig. 5.4). By comparing seep and reservoir gas it has been observed that molecular fractionation is typical of slow degassing mud volcanoes, whereas ascending gas significantly interacts with water and sediments, and typical of gas seeps with a relatively low flux. In this sense a low flux mud volcano or seep can be considered as a "natural refinery". Vigorous gas seeps, instead, have the same molecular composition as reservoir gas. In fact, an inverse proportionality exists between gas flux and molecular fractionation, the higher the flux the lower the Bernard ratio (Etiope et al. 2011a). Not considering this alteration mechanism may lead to severe mistakes in interpretations of gas origin. For example, if one only looks at the relative C_1–C_3 composition (the Bernard ratio) and $\delta^{13}C_{CH4}$ is not analysed, the high CH_4 content (for example, above 95 vol.%) relative to ethane and propane, may lead one to think that the gas is microbial. In fact, many mud volcanoes have a Bernard ratio typical of microbial gas (>500), but isotopic data and petroleum system evaluations clearly indicate that the gas is, instead, thermogenic (e.g., Etiope et al. 2009a). As a result, since it does not always reflect the original gas composition, the "Bernard" parameter may be misleading when applied to mud volcanoes or low flux seeps.

(e) *Gas mixing*
Based on the statistics of 260 seeps worldwide, less than 20 % of seeps release gas with features of mixing between thermogenic and microbial methane (Etiope et al. 2009a, b). Mixing can occur during the ascent of gas through the sedimentary horizons of the seepage system, whereas microbial gas pools may exist at shallower depths. The attribution of mixing is, however, not immediate and due to other secondary post-genetic processes the values of the carbon isotopes of CH_4 alone can be misleading. The recognition of mixing should mainly be based on $\delta^{13}C_{CH4}$ versus $C_1/(C_2 + C_3)$ (Fig. 5.4) and $\delta^{13}C_{CH4}$ versus $\delta^{13}C_{C2H6}$ diagrams (e.g., Etiope et al. 2011c).

(f) *Biodegradation of petroleum and secondary methanogenesis*
Oil can be biodegraded by living microorganisms (bacteria, yeasts, molds, and fungi) at the surface and at shallow depths, typically at up to 2 km and at temperatures of approximately 80 °C. Biodegradation gradually destroys n-paraffins (n-alkanes or normal alkanes) followed by loss of acyclic isoprenoids (e.g., norpristane, pristine, phytane, etc.). When biodegradation occurs within an oil reservoir, API gravities decrease. As a result, the value and producibility of oil accumulation decreases. Petroleum biodegradation is a phenomenon that was neglected in the past. Today, it is considered to occur in most conventional oil reserves (Head et al. 2003). Biodegradation is undetectable by geophysical methods and is typically chemically

diagnosed after the drilling and recovery of hydrocarbon samples. Seeps can help in the detection of subsurface biodegradation prior to drilling.

Due to the preferential degradation of C_3 and n-alkanes, reservoir gases associated with anaerobic biodegradation processes have a typical fingerprint characterised by large isotopic separations between successive n-alkanes and high C_2/C_3 (ethane/propane) and iC_4/nC_4 (iso-butane/normal-butane) ratios (Pallasser 2000; Milkov and Dzou 2007). Biodegradation is then typically followed by the microbial production of methane (secondary methanogenesis), microbial gas generated in reservoir (not in source rocks) and associated with liquid hydrocarbons. Secondary microbial methane is, however, isotopically indistinguishable from thermogenic methane (i.e., it is more ^{13}C enriched than normal microbial methane; Brown 2011; Milkov 2011). Secondary methanogenesis follows a CO_2 reduction pathway, whereas CO_2 is produced earlier by oil biodegradation. Residual CO_2 has an increased ^{13}C content, and $\delta^{13}C$ values are typically positive, exceeding +5 ‰. CO_2 of this type is often named "heavy CO_2". The presence of heavy CO_2 associated with ^{13}C enriched propane in gas seeps indicates that the hydrocarbon accumulations feeding the seepage are biodegraded, as observed in a large number of seeps worldwide (e.g., Etiope et al. 2009b, 2013a, 2014a).

5.3.2 Assessing Gas Source Type and Maturity

Taking secondary modifications into account, seeping gas can be used to better assess gas origins and source rocks, in other words understanding subsurface petroleum systems. The genetic diagrams of Schoell and Bernard (Fig. 1.2) can be used to consider (or verify, if possible) potential molecular and isotopic alterations. Statistical analyses of the global data-set of onshore seeps (the GLOGOS data-set; see Chap. 2) indicate that for over 403 seeps (including 168 gas seeps, 199 mud volcanoes, and 36 gas-rich springs), 60 % of the seeping gas is dominantly thermogenic ($\delta^{13}C_1 > -50$ ‰) while only 11 % is dominantly microbial ($\delta^{13}C_1 < -60$ ‰; Fig. 5.5). The results are consistent with the prevailing occurrence of thermogenic gas accumulations which account for approximately 80 % of the world's natural gas resources (Rice 1993). The results are also consistent with processes and environments leading to seepage and mud volcanism. Mud volcanoes, in particular, are almost always connected with deep hydrocarbon pools whose sources are predominantly located below the oil window. Exceptions are those seeps and mud volcanoes in rapidly subsiding sedimentary basins, where deep reservoirs can still be microbial (e.g., the Transylvania Basin, the Adriatic Basin, and the Gulf of Mexico). Examples of thermogenic and microbial gas seeps are reported in Table 5.1. As a general rule, because they are more often perturbed by tectonics in orogenic belts and rift systems frequently crossed by active and permeable faults, seepage is mainly related to thermogenic reservoirs. Younger and shallower microbial gas reservoirs, like those in poorly tectonised foreland basins, are generally more preserved.

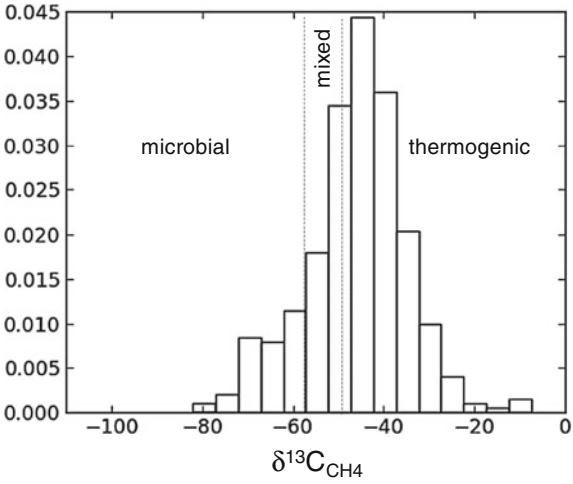

Fig. 5.5 A frequency distribution histogram of the $\delta^{13}C$ of methane from 403 seeps worldwide (based on the GLOGOS dataset, version 2014)

Applying geochemical models that are capable of estimating the types of kerogen in source rocks (Type I, II, or III, i.e., marine or terrestrial organic matter) and its maturity, generally expressed in terms of vitrinite reflectance (see Hunt 1996), is possible. A good practice is combining the maturity model of Berner and Faber (1996), empirically derived from pyrolysis experiments, with theoretical thermogenic gas generation modelling, such as the one developed by Tang et al. (2000) that can predict gas and oil generation, including the primary carbon isotopic composition of alkanes. Currently, by knowing the $\delta^{13}C$ of methane (C_1), ethane (C_2), or propane (C_3), there two independent ways exist for estimating the maturity of source rocks and gas formation temperatures. For additional information regarding the details, meaning, and limits of the models, the reader is referred to the above mentioned studies. In practice, by assuming a series of $\delta^{13}C$ values for the original carbon existing in the petroleum system under investigation, it is possible to draw "maturity lines" in a $\delta^{13}C_1$ versus $\delta^{13}C_2$ or $\delta^{13}C_2$ versus $\delta^{13}C_3$ diagram (Fig. 5.6) using the Berner-Faber model.

A line exists for each kerogen type and for each $\delta^{13}C$ value. In the diagram, seeping gas will eventually fall on or close to a given line. The line represents the most likely source rock. In the example provided in Fig. 5.6, theoretical lines for Types II and III kerogens, with different $\delta^{13}C$ values are shown; seeping gas falls on a line related to kerogen Type II with a vitrinite reflectance (maturity) of approximately 1.8 Ro for source rocks having a $\delta^{13}C$: −27.8 ‰. The result can be verified using thermogenic gas generation modelling and a similar $\delta^{13}C_1$ versus $\delta^{13}C_2$ or $\delta^{13}C_2$ versus $\delta^{13}C_3$ diagram, where the kerogen lines (I, II, or III) are independent of the original $\delta^{13}C$ of kerogen, but depend on the heating rate considered for gas generation during catagenesis (for example, 5 °C for a million years; see Tang (2000) for details). The use of a maturity plot, or combined maturity and gas formation modelling, in gas seeps allowed assessments of source rocks in petroleum systems in Japan (Etiope et al. 2011b), Greece (Etiope et al. 2013a), Italy (Etiope

Table 5.1 Examples of the carbon ($\delta^{13}C$, VPDB) and hydrogen ($\delta^{2}H$, VSMOW) isotopic composition of methane in thermogenic and microbial gas seeps in Europe (data selected from the GLOGOS data-set; Etiope 2009a, b; http://www.gas-consult.com)

Country	Seep name	Gas origin	$\delta^{13}C$	$\delta^{2}H$	References
Greece	Katakolo Faros	T	−34.3	−136	Etiope et al. (2013a)
	Katakolo Harbour	T	−31.2	−135.5	Etiope et al. (2013a)
	Killini	T	−49	−174	Etiope et al. (2006)
	Kaiafas	T	−47.5	−166.5	Etiope et al. (2006)
	Patras Coast	M	−73.9	−210.9	Etiope et al. (unpublished)
	Kotychi	M	−69.7	−202.3	Etiope et al. (unpublished)
	Trifos	Mix	−66.7	−175	Etiope et al. (unpublished)
Italy	Tocco da Casauria	T	−57	−267	Etiope (unpublished)
	Lavino	T	−50	−260	Etiope (unpublished)
	Tramutola	T	−42.12	−193.8	Etiope et al. (2007)
	Montechino	T	−33.98	−132.6	Etiope et al. (2007)
	Miano	T	−39.38	−168.4	Etiope et al. (2007)
	M. Busca fire	T	−35.81	−160.9	Etiope et al. (2007)
	Corporeno	M	−65.98	−174.1	Etiope et al. (2007)
	Comacchio	M	−76.14	−223	Cremonini et al. (2008)
	Censo fire	T	−35.1	−146	Etiope et al. (2002)
	Pietramala	T	−42.6	−188	Tassi et al. (2012)
Romania	Andreiasu	T	−34.49	−147.6	Etiope et al. (2009a)
	Bacau Gheraiesti	T	−49.42	−173.4	Baciu et al. (2008)
	Deleni (Zugo)	M	−66.11	−189.6	Etiope et al. (unpublished)
	Praid	T	−28.99	−193.6	Etiope et al. (2009a)
	Sarmasel	M	−67.42	−192.2	Etiope et al. (2009a)
Switzerland	Lago Maggiore Ten	M	−61.1	−243	Greber et al. (1997)
	Lago Maggiore Ver	M	−66.9	−211	Greber et al. (1997)
	Lago Maggiore Bol	M	−67.3	−228	Greber et al. (1997)
	Lago Maggiore Ala	M	−63.6	−238	Greber et al. (1997)
	Rivapiana	M	−62.8	−177	Greber et al. (1997)
	Stabio N.Bagni	T	−49.4	−186	Greber et al. (1997)
	Stabio S2	T	−42.9	−162	Greber et al. (1997)
	Ponte Falloppia	T	−37.3	−125	Greber et al. (1997)
	Giswil	T	−35.5	−159.3	Etiope et al. (2010)
Turkey	Kumluca	M	−65	−209	Etiope et al. (unpublished)

T Thermogenic; *M* Microbial

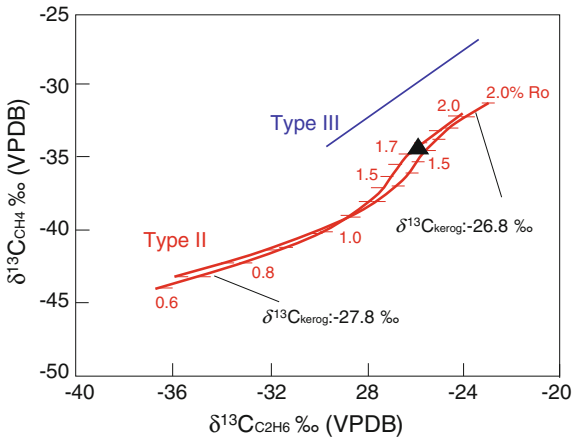

Fig. 5.6 Example of the application of a maturity plot, based on the model by Berner and Faber (1996), for seeping gas (thermogenic seepage of Katakolo, Western Greece; Etiope et al. 2013a). The source of the seeping gas was unknown, but maturity lines were drawn by considering candidate source rocks along the Ionian Coast and their kerogen stable carbon isotope composition. The seep (*black triangle*) has a combined $\delta^{13}C$ value of methane and ethane that fits a kerogen *Type II* with a maturity (vitrinite reflectance) of 1.8 Ro for kerogen, with $\delta^{13}C$: −27.8 ‰, or a 1.6 Ro for a kerogen with $\delta^{13}C$: −26.8 ‰ (modified and redrawn from Etiope et al. 2013a)

et al. 2014a), and Indonesia (in relation to the famous "Lusi" mud eruption site; Mazzini et al. 2012).

An interesting case of source identification based on an analysis of seeping gas is that of the natural flame at Chestnut Ridge Park in New York State (USA). The seep is a spectacular "eternal flame", a regional tourist attraction since it shines from behind the veil of a cascading waterfall (Fig. 5.7).

Fig. 5.7 The "eternal flame" at Chestnut Ridge Park located in New York State. The gas is thermogenic and is directly released from fractured shale source rocks (photo by G. Etiope)

The seep, as usual, is located along a fault-controlled creek, releases approximately 1 kg of methane per day, and seems to feature the highest ethane and propane ($C_2 + C_3$) concentration ever reported for a natural gas seep: ~35 vol.% (Etiope et al. 2013b). Closed-chamber measurements allowed discovery of the fact that gas is also released through nearby invisible and diffuse seepages from the ground. While seeping gas generally arises from conventional pressurised reservoirs that guarantee, especially when the gas flux is considerable, the necessary pressure gradient to support the seep for a long period of time, the burning Chestnut gas seep gas appears to directly migrate from source rocks (i.e., shales). By combining molecular and isotopic data for seeps and reservoir gases in the region, the stratigraphy of the underlying shales indicated that thermogenic gas originates from Upper Devonian shales without the intermediation of a conventional reservoir (Etiope et al. 2013b). The results suggest that tectonically fractured shales seem to express "naturally fracked" characteristics and may provide convenient targets for hydrocarbon exploration. As a result, gas production from "tectonically fracked" systems may not require extensive artificial fracking.

5.3.3 The Presence of Undesirable Gases (CO_2, H_2S, N_2)

The occurrence of non-hydrocarbon gases such as carbon dioxide (CO_2), hydrogen sulphide (H_2S), and nitrogen (N_2) within a reservoir reduces the economic value of the deposit. These gases lower the heating value of natural gas (the energy released upon combustion of a unit of mass or volume), may be corrosive, and must be separated from the hydrocarbons and properly disposed of prior to gas use. Production costs significantly increase with the presence of these gases and encountering high concentrations of these gases is considered a risk for an oil company. As a result, detecting these gases in seeps that represent the composition of a reservoir is of critical importance.

In some cases, CO_2 may be so abundant, exceeding 20 vol.%, rendering a prospect uneconomic. High CO_2 reservoirs have been found in the South China Sea, in the Malay Basin and the Gulf of Thailand, in the Central European Pannonian Basin, in the Colombian Putumayo Basin, in the Iblean platform in southern Italy, in the Taranaki Basin in New Zealand, in the North Sea South Viking Graben, and in the Australian Cooper-Eromanga Basin (Thrasher and Fleet 1995). CO_2 may originate, as follows:

(i) during the same thermogenic stage forming the hydrocarbons, in particular, through kerogen decarboxylation,
(ii) during the bacterial degradation of petroleum,
(iii) during thermochemical sulphate reduction (TSR), although
(iv) larger amounts derive from volcanic-geothermal processes, such as magma degassing and the contact metamorphism of carbonates.

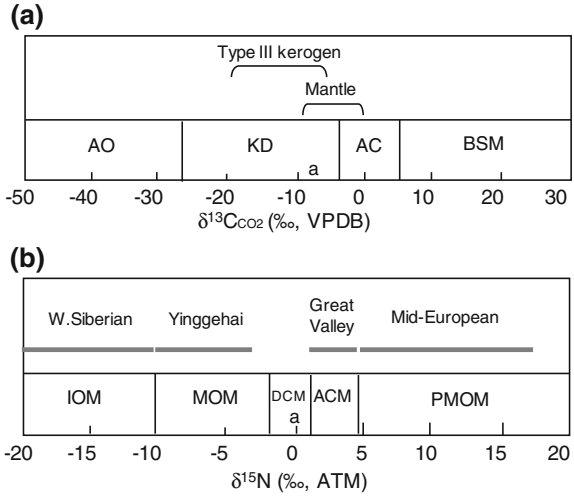

Fig. 5.8 **a** Carbon dioxide isotopic zonation after Jenden et al. (1993) and Kotarba (2001). *AO* Aerobic hydrocarbon oxidation; *KD* Kerogen decarboxylation; *AC* Alteration of marine carbonates; *BSM* Biodegradation and secondary methanogenesis; *a* atmosphere. **b** Nitrogen isotopic zonation after Zhu et al. (2000). *IOM* Immature organic matter (Ro ≤ 0.6 %), typical of the West Siberian Basin; *MOM* Mature and high-mature organic matter (Ro = 0.6–2 %), e.g., the Yinggehai Basin in China; *DCM* Deep crust and mantle; *ACM* Ammonium clay minerals and mudrock during metamorphism (e.g., California Great Valley); *PMOM* Post-mature organic matter (Ro > 2 %) (e.g., Mid-European Basins)

The stable carbon isotope composition of CO_2 (Fig. 5.8a) and the isotopic composition of associated helium can help in distinguishing sources (e.g., Jenden et al. 1993; Cathles and Schoell 2007). High CO_2 concentrations (exceeding 20 vol.%) in hydrocarbon seeps have been found in petroleum systems in the vicinity of geothermal or volcanic systems, such as in the Sidoarjo Basin, in East Java (Mazzini et al. 2012), and in some mud volcanoes in Ukraine (up to 64 vol.%), Russia (up to 29 vol.%), and Trinidad (up to 25 vol.%) (Etiope et al. 2009b and references therein).

H_2S is highly corrosive, it destroys well equipment (pumps, casing, and rods), and, as described in Chap. 6, toxic. H_2S typically originates from microbial sulphate reaction (BSR), the thermal decomposition of sulfur compounds in kerogen or oil, or, more frequently, via thermochemical sulphate reaction (TSR) which takes place when hydrocarbons are in contact with salts (Noth 1997). TSR is the only process able to produce large amounts of H_2S (>5 vol.%) and is dominant in the presence of evaporites, in contact with limestones at temperatures generally above 80 °C (Noth 1997) or 120 °C (Warden and Smalley 1996). High H_2S seeps have been found, for example, along the Ionian coast of western Greece, at Katakolo and Killini, where thermogenic gas carries up to 1.4 vol.% H_2S to the surface, with a sulphur isotopic composition ($\delta^{34}S$: +2 ‰) that suggests an origin related to thermochemical sulfate reduction or to the thermal decomposition of sulfur compounds in kerogen or oil (Etiope et al. 2013a).

In a reservoir, N_2 concentrations can overcome those of methane and other hydrocarbons when source rocks provide gases that originated during the late, overmaturity stage (vitrinite reflectance Ro > 4). N_2-rich gases are released during the final stage of gas generation, after CH_4 formation has ceased (Krooss et al. 1995). However, large N_2 amounts are likely produced by the metamorphism of clayey, ammonium-containing, sedimentary rocks (Zhu et al. 2000; Etiope et al. 2011a). Magmatic sources can also provide N_2 when the petroleum system is in the vicinity of volcanic systems. Relative N_2 concentrations with respect to hydrocarbons can then increase by TSR that destroys light alkanes. Examples of N_2-rich seeps are found in Papua New Guinea (≤76 vol.%; Baylis et al. 1997) and in Romania (up to 98 vol.%; Etiope et al. 2011a). The isotopic composition of N_2 ($\delta^{15}N$) can help in assessing the origin of gases (Fig. 5.8b).

5.3.4 Helium in Seeps… for Connoisseurs

The only non-hydrocarbon gas that has economic benefit is helium (He). Helium is a beneficial chemical element in technology and industry. He is indispensable in frontier technologies involving space, atomic energy, and superconductivity, and in many types of advanced research, including fusion and low temperature physics. Although it makes up 25 % of the universe, helium is a rare gas in our atmosphere (5 ppmv) and is only found in significant concentrations, exceeding 0.1 vol.%, in natural gas fields and geothermal fluids. Helium is conventionally only derived from petroleum gas deposits. The geographic distribution of helium-rich natural gas deposits is uneven. Approximately 90 % of helium-rich natural gas reserves are concentrated in North America, particularly in the Hugoton-Panhandle fields in Kansas, Oklahoma, and Texas (the largest North American gas field), and the Tip-Top Field in Wyoming, with an average helium concentration of 0.6–0.8 vol.%. Beyond the USA, helium is only extracted in Poland, Russia, China, Algeria, and Canada, and in small quantities in the Netherlands and Qatar. The average concentration of helium in the fields of these countries ranges between 0.18 and 0.9 vol.%. Helium is conveniently only produced in gas fields containing a minimum of 0.3 vol.% (Gage and Driskill 2004). Helium enrichment generally results from the exsolution of the gas phase from water during basin uplift (Ballentine and Sherwood Lollar 2002; Brown 2005).

In general, helium is not particularly abundant in seeps and concentrations are typically on the order of units to hundreds of ppmv. However, a single seep was discovered in 2010 in Romania that contained He concentrations of up to 1.48 % by volume (Etiope et al. 2011a), well above the average level occurring within commercial reservoirs inside the USA. The seep may reveal the presence of a He-rich reservoir. Today, surface seepage surveys rarely include the detection of helium, although it has been used as a tracer for hydrocarbon exploration for many years

(see Sect. 5.2.1). Attention will focus on He, not only as tracer but also as a target, when global demand and market price begin to grow considerably in the near future (http://www.theballooncouncil.org).

References

Abrams MA (2002) Surface geochemical calibration research study: an example of research partnership between academia and industry. In: New insights into petroleum geoscience research through collaboration between industry and academia. Geological Society, London, UK, 8–9 May 2002

Abrams MA (2005) Significance of hydrocarbon seepage relative to petroleum generation and entrapment. Mar Pet Geol 22:457–477

Alain K, Holler T, Musat F, Elvert M, Treude T, Kruger M (2006) Microbiological investigation of methane- and hydrocarbon-discharging mud volcanoes in the Carpathian Mountains, Romania. Environ Microbiol 8:574–590

Baciu C, Etiope G, Cuna S, Spulber L (2008) Methane seepage in an urban development area (Bacau, Romania): origin, extent and hazard. Geofluids 8:311−320

Ballentine CJ, Sherwood Lollar B (2002) Regional groundwater focusing of nitrogen and noble gases into the Hugoton-Panhandle giant gas field, USA. Geochim Cosmochim Acta 66:2483–2497

Baubron J-C, Rigo A, Toutain J-P (2001) Soil gas profiles as a tool to characterize active tectonic areas: the Jaut Pass example (Pyrenees, France). Earth Planet Sci Lett 196:69–81

Baylis SA, Cawley SJ, Clayton CJ, Savell MA (1997) The origin of unusual gas seeps from onshore Papua New Guinea. Mar Geol 137:109–120

Berner U, Faber E (1996) Empirical carbon isotope/maturity relationships for gases from algal kerogens and terrigenous organic matter, based on dry, open-system pyrolysis. Org Geochem 24:947–955

Bonini C (2013) Fluid seepage variability across the external Northern Apennines (Italy): structural controls with seismotectonic and geodynamic implications. Tectonophysics 590:151–174

Brown A (2005) Origin of high helium concentrations in dry gas by water fractionation. In: AAPG research conference abstracts, origin of petroleum, 18 June 2005, Calgary, Alberta, Canada

Brown A (2011) Identification of source carbon for microbial methane in unconventional gas reservoirs. AAPG Bull 95:1321–1338

Cathles LM, Schoell M (2007) Modeling CO_2 generation, migration and titration in sedimentary basins. Geofluids 7:441–450

Chu PH, Wu JJ, Cheng TW, Lin LH, Chen KC, Wang PL (2007) Evaluating the potential of anaerobic methane oxidation in terrestrial mud volcanoes of southern Taiwan. In: Proceedings of the 9th international conference gas geochemistry, National Taiwan University, p 154

Ciotoli G, Etiope G, Guerra M, Lombardi S (1999) The detection of concealed faults in the Ofanto Basin using the correlation between soil-gas fracture surveys. Tectonophysics 301:321–332

Ciotoli G, Lombardi S, Morandi S, Zarlenga F (2004) A multidisciplinary statistical approach to study the relationships between helium leakage and neo-tectonic activity in a gas province: The Vasto Basin, Abruzzo-Molise (Central Italy). AAPG Bull 88:355–372

Coleman DD, Risatti JB, Schoell M (1981) Fractionation of carbon and hydrogen isotopes by methane-oxidizing bacteria. Geochim Cosmochim Acta 45:1033–1037

Cremonini S, Etiope G, Italiano F, Martinelli G (2008) Evidence of possible enhanced peat burning by deep originated methane in Po river delta (Italy). J Geol 116:401–413

Davidson JJ (ed) (1986) Unconventional methods in exploration for petroleum and natural gas-IV. Southern Methodist University, Dallas, Texas, 350 pp

Deville E, Battani A, Griboulard R, Guerlais SH, Herbin JP, Houzay JP, Muller C, Prinzhofer A (2003) Mud volcanism origin and processes. New insights from Trinidad and the Barbados

Prism. In: Van Rensbergen P, Hillis R, Maltman AJ, Morley C (eds) Surface sediment mobilization, vol 216. Special Publication of the Geological Society, London, pp 475–490
Duddridge GA, Grainger P, Durrance EM (1991) Fault detection using soil gas geochemistry. Quat J Eng Geol 24:427–435
Dyck W (1976) The use of helium in mineral exploration. J Geochem Explor 5:3–20
Etiope G (2009) GLOGOS, A new global onshore gas-oil seeps dataset. Search and discovery, Article #70071, 28 September 2009. AAPG online journal. http://www.searchanddiscovery.net
Etiope G, Lombardi S (1995) Soil gases as fault tracers in clay basin: a case history in the Siena basin (Central Italy). In: Dubois C (ed) Gas geochemistry. Science Reviews, Northwood, pp 19–29
Etiope G, Klusman RW (2010) Microseepage in drylands: flux and implications in the global atmospheric source/sink budget of methane. Global Planet Change 72:265−274
Etiope G, Caracausi A, Favara R, Italiano F, Baciu C (2002) Methane emission from the mud volcanoes of Sicily (Italy). Geophys Res Lett 29. doi:10.1029/2001GL014340
Etiope G, Baciu C, Caracausi A, Italiano F, Cosma C (2004a) Gas flux to the atmosphere from mud volcanoes in eastern Romania. Terra Nova 16:179–184
Etiope G, Feyzullaiev A, Baciu CL, Milkov AV (2004b) Methane emission from mud volcanoes in eastern Azerbaijan. Geology 32:465–468
Etiope G, Papatheodorou G, Christodoulou D, Ferentinos G, Sokos E, Favali P (2006) Methane and hydrogen sulfide seepage in the NW Peloponnesus petroliferous basin (Greece): origin and geohazard. AAPG Bull 90:701–713
Etiope G, Martinelli G, Caracausi A, Italiano F (2007) Methane seeps and mud volcanoes in Italy: gas origin, fractionation and emission to the atmosphere. Geophys Res Lett 34. doi:10.1029/2007GL030341
Etiope G, Feyzullayev A, Baciu CL (2009a) Terrestrial methane seeps and mud volcanoes: a global perspective of gas origin. Mar Pet Geol 26:333–344
Etiope G, Feyzullayev A, Milkov AV, Waseda A, Mizobe K, Sun CH (2009b) Evidence of subsurface anaerobic biodegradation of hydrocarbons and potential secondary methanogenesis in terrestrial mud volcanoes. Mar Pet Geol 26:1692–1703
Etiope G, Zwahlen C, Anselmetti FS, Kipfer R, Schubert CJ (2010) Origin and flux of a gas seep in the northern Alps (Giswil, Switzerland). Geofluids 10:476–485
Etiope G, Baciu C, Schoell M (2011a) Extreme methane deuterium, nitrogen and helium enrichment in natural gas from the Homorod seep (Romania). Chem Geol 280:89–96
Etiope G, Nakada R, Tanaka K, Yoshida N (2011b) Gas seepage from Tokamachi mud volcanoes, onshore Niigata Basin (Japan): origin, post-genetic alterations and CH_4-CO_2 fluxes. App Geochem 26:348–359
Etiope G, Schoell M, Hosgormez H (2011c) Abiotic methane flux from the Chimaera seep and Tekirova ophiolites (Turkey): understanding gas exhalation from low temperature serpentinization and implications for Mars. Earth Planet Sci Lett 310:96–104
Etiope G, Christodoulou D, Kordella S, Marinaro G, Papatheodorou G (2013a) Offshore and onshore seepage of thermogenic gas at Katakolo Bay (Western Greece). Chem Geol 339:115–126
Etiope G, Drobniak A, Schimmelmann A (2013b) Natural seepage of shale gas and the origin of "eternal flames" in the Northern Appalachian Basin, USA. Mar Pet Geol 43:178–186
Etiope G, Panieri G, Fattorini D, Regoli F, Vannoli P, Italiano F, Locritani M, Carmisciano C (2014a) A thermogenic hydrocarbon seep in shallow Adriatic Sea (Italy): gas origin, sediment contamination and benthic foraminifera. Mar Pet Geol 57:283–293
Etiope G, Vadillo I, Whiticar MJ, Marques JM, Carreira P, Tiago I (2014b) Methane seepage at hyperalkaline springs in the Ronda peridotite massif (Spain). AGU fall meeting abstracts, December 2014
Fu CC, Yang TF, Walia V, Chen C-H (2005) Reconnaissance of soil–gas composition over the buried fault and fracture zone in Southern Taiwan. Geochem J 39:427–439
Gage BD, Driskill DL (2004) The helium resources of the United States, 2003, Technical Note 415. Bureau of Land Management. BLM/NM/ST-04/002+3745, 35 pp
Greber E, Leu W, Bernoulli D, Schumacher ME, Wyss R (1997) Hydrocarbon provinces in the Swiss southern Alps—a gas geochemistry and basin modelling study. Mar Pet Geol 14:3−25

Gregory RG, Durrance EM (1985) Helium, carbon dioxide and oxygen soil gases: small-scale variations over fractured ground. J Geochem Explor 24:29–49

Guerra M, Lombardi S (2001) Soil–gas method for tracing neotectonic faults in clay basins: the Pisticci field (Southern Italy). Tectonophysics 339:511–522

Head IM, Jones DM, Larter SR (2003) Biological activity in the deep subsurface and the origin of heavy oil. Nature 426:344–352

Hoffman MG (1939) An advance in exploration by soil analysis methods. Oil Gas J 113:23–24

Hong WL, Etiope G, Yang TF, Chang PY (2012) Methane flux of miniseepage in mud volcanoes of SW Taiwan: comparison with the data from Europe. J Asian Earth Sci 65:3–12

Howarth RJ (1993) Statistics and data analysis in geochemical prospecting. In: Govett GJS (ed) Handbook of exploration geochemistry, 2. Elsevier Scientific Publishing Company, Amsterdam, Oxford, New York, pp 44–75

Hunt JM (1996) Petroleum geochemistry and geology. Freeman and Co., New York, 743 pp

Jenden PD, Hilton DR, Kaplan IR, Craig H (1993) Abiogenic hydrocarbons and mantle helium in oil and gas fields. In: Howell DG (ed) The future of energy gases (US geological survey professional paper 1570). United States Government Printing Office, Washington, pp 31–56

Jones VT, Drozd RJ (1983) Predictions of oil or gas potential by near-surface geochemistry. AAPG Bull 67:932–952

Jones VT, Matthews MD, Richers D (2000) Light hydrocarbons in petroleum and natural gas exploration. In: Hale M (ed) Handbook of exploration geochemistry: geochemical remote sensing of the sub-surface, vol 7, Chapter 5. Elsevier Science Publishers, Amsterdam

Kinnaman FS, Valentine DL, Tyler SC (2007) Carbon and hydrogen isotope fractionation associated with the aerobic microbial oxidation of methane, ethane, propane and butane. Geochim Cosmochim Acta 71:271–283

Kiyosu Y, Imaizumi S (1996) Carbon and hydrogen isotope fractionation during oxidation of methane by metal oxides at temperatures from 400 to 530 °C. Chem Geol 133:279–287

Klusman RW (1993) Soil gas and related methods for natural resource exploration. Wiley, Chichester, 483 pp

Klusman RW (2006) Detailed compositional analysis of gas seepage at the National Carbon Storage Test Site, Teapot Dome, Wyoming USA. App Geochem 21:1498–1521

Klusman RW, Leopold (Jakel) ME, LeRoy MP (2000) Seasonal variation in methane fluxes from sedimentary basins to the atmosphere: results from chamber measurements and modeling of transport from deep sources. J Geophys Res 105D:661–670

Klusman RW, Jakel ME, LeRoy MP (1998) Does microseepage of methane and light hydrocarbons contribute to the atmospheric budget of methane and to global climate change? Ass Petrol Geochem Explor Bull 11:1–56

Kotarba MJ (2001) Composition and origin of coalbed gases in the Upper Silesian and Lublin basins, Poland. Org Geochem 32:163–180

Krooss BM, Littke R, Muller B, Frielingsdorf J, Schwochau K, Idiz EF (1995) Generation of nitrogen and methane from sedimentary organic matter: implications on the dynamics of natural gas accumulations. Chem Geol 126:291–318

Laubmeyer G (1933) A new geophysical prospecting method, especially for deposits of hydrocarbons. Petroleum 29:14

Link WK (1952) Significance of oil and gas seeps in world oil exploration. AAPG Bull 36:1505–1540

Macgregor DS (1993) Relationships between seepage, tectonics and subsurface petroleum reserves. Mar Pet Geol 10:606–619

Mackintosh SJ, Ballentine CJ (2012) Using $^{3}He/^{4}He$ isotope ratios to identify the source of deep reservoir contributions to shallow fluids and soil gas. Chem Geol 304−305:142−150

Matthews MD (1996) Hydrocarbon migration—a view from the top. In: Schumacher D, Abrams MA (eds) Hydrocarbon migration and its near-surface expression: AAPG Memoir, vol 66. American Association of Petroleum Geologists, Tulsa, pp 139–155

Mazzini A, Etiope G, Svensen H (2012) A new hydrothermal scenario for the 2006 Lusi eruption, Indonesia. Insights from gas geochemistry. Earth Planet Sci Lett 317–318:305–318

Medialdea T, Somoza L, Pinheiro LM, Fernández-Puga MC, Vázquez JT, León R, Ivanov MK, Magalhães V, Díaz-del-Río V, Vegas R (2009) Tectonics and mud volcano development in the Gulf of Cádiz. Mar Geol 261:48–63

Mellors R, Kilb D, Aliyev A, Gasanov A, Yetirmishli G (2007) Correlations between earthquakes and large mud volcano eruptions. J Geophys Res 112:B04304. doi:10.1029/2006JB004489

Milkov AV (2011) Worldwide distribution and significance of secondary microbial methane formed during petroleum biodegradation in conventional reservoirs. Org Geochem 42:184–207

Milkov AV, Dzou L (2007) Geochemical evidence of secondary microbial methane from very slight biodegradation of undersaturated oils in a deep hot reservoir. Geology 35:455−458

Niemann H, Duarte J, Hensen C, Omoregie E, Magalhaes VH, Elvert M, Pinheiro LM, Kopf A, Boetius A (2006) Microbial methane turnover at mud volcanoes of the Gulf of Cadiz. Geochim Cosmochim Acta 70:5336–5355

Noth S (1997) High H_2S contents and other effects of thermochemical sulfate reduction in deeply buried carbonate reservoirs: a review. Geol Rundsch 86:275–287

Pallasser RJ (2000) Recognising biodegradation in gas/oil accumulations through the $\delta^{13}C$ compositions of gas components. Org Geochem 31:1363–1373

Pan C, Yu L, Liu J, Fu J (2006) Chemical and carbon isotopic fractionations of gaseous hydrocarbons during abiogenic oxidation. Earth Planet Sci Lett 246:70–89

Pogorsky LA, Quirt GS (1981) Helium emanometry in exploring for hydrocarbons, Part I. In: Gottlieb BM (ed) Unconventional methods in exploration for petroleum and natural gas, II. Southern Methodist University Press, Dallas, pp 124–135

Price LC (1986) A critical overview and proposed working model of surface geochemical exploration. In: Davidson MJ (ed) Unconventional methods exploration for petroleum and natural gas—IV. Southern Methodist University Press, Dallas, pp 245–304

Rice DD (1993) Biogenic gas: controls, habitats, and resource potential. In: Howell DG (ed) The future of energy gases—U.S. geological survey professional paper 1570. United States Government Printing Office, Washington, pp 583−606

Roberts HA (1981) Helium emanometry in exploring for hydrocarbons-part II, unconventional methods in exploration for petroleum and natural gas. Dallas, Southern Methodist University, pp 136–149

Saunders DF, Davidson MJ (2006) Articles and scientific papers on surface geochemical exploration for petroleum. DeGolyer Library, Southern Methodist University. http://www.lib.utexas.edu/taro/smu/00014/smu-00014.html

Saunders D, Burson KR, Thompson CK (1999) Model for hydrocarbon microseepage and related near-surface alterations. Ass Petrol Geochem Explor Bull 83:170–185

Schoell M (1983) Genetic characterization of natural gases. AAPG Bull 67:2225–2238

Schumacher D (2010) Integrating hydrocarbon microseepage data with seismic data doubles exploration success. In: Proceedings thirty-fourth annual conference and exhibition, May 2010. Indonesian Petroleum Association, IPA10-G-104

Schumacher D, Abrams MA (1996) Hydrocarbon migration and its near surface expression. AAPG Memoir, vol 66. PennWell Publishing, Tulsa, 446 pp

Schumacher D, LeSchack LA (2002) Surface exploration case histories: applications of geochemistry, magnetics, and remote sensing. AAPG studies in geology, No. 48, SEQ geophysical references series no. 11, 486 pp

Sechman H (2012) Detailed compositional analysis of hydrocarbons in soil gases above multi-horizon petroleum deposits—a case study from western Poland. App Geochem 27:2130–2147

Seneshen DM, Chidsey TC, Morgan CD, Van den Berg MD (2010) New techniques for new hydrocarbon discoveries—surface geochemical surveys in the Lisbon and lightning draw southeast field areas, San Juan County, Utah. Miscellaneous Publication 10-2, Utah Geological Survey, p 62

Sokolov VA (1933) New method of surveying oil and gas formations. Tekhnika nefti 16:163

Tang Y, Perry JK, Jenden PD, Schoell M (2000) Mathematical modeling of stable carbon isotope ratios in natural gases. Geochim Cosmochim Acta 64:2673–2687

Tang J, Yin H, Wang G, Chen Y (2010) Methane microseepage from different sectors of the Yakela condensed gas field in Tarim Basin, Xinjiang, China. App Geochem 25:1257–1264

Tassi F, Bonini M, Montegrossi G, Capecchiacci F, Capaccioni B, Vaselli O (2012) Origin of light hydrocarbons in gases from mud volcanoes and CH4-rich emissions. Chem Geol 294–295:113–126

Tedesco SA (1995) Surface geochemistry in petroleum exploration. Chapman & Hall, New York, 206 pp

Thielemann T, Lucke A, Schleser GH, Littke R (2000) Methane exchange between coal-bearing basins and the: the Ruhr Basin and the Lower Rhine Embayment, Germany. Org Geochem 31:1387−1408

Thrasher J, Fleet AJ (1995) Predicting the risk of carbon dioxide 'pollution' in petroleum reservoirs. In: Grimalt JO, Dorronsoro C (eds) Organic geochemistry: developments and applications to energy, climate, environment and human history—selected papers from the 17th International meeting on organic geochemistry. AIGOA, San Sebastian, pp 1086–1088

Van Den Boom GP (1987) Helium distribution pattern of measured and corrected data around the "Eldingen" Oil Field, NW Germany. J Geophys Res 92b:12547–12555

Whiticar MJ (1999) Carbon and hydrogen isotope systematics of bacterial formation and oxidation of methane. Chem Geol 161:291–314

Worden RH, Smalley PC (1996) H_2S-producing reactions in deep carbonate gas reservoirs: Khuff formation, Abu Dhabi. Chem Geol 133:157–171

Zhu Y, Shi B, Fang C (2000) The isotopic compositions of molecular nitrogen: implications on their origins in natural gas accumulations. Chem Geol 164:321–330

Chapter 6
Environmental Impact of Gas Seepage

Natural gas, with its hydrocarbon and non-hydrocarbon compounds, can be explosive, toxic, a consumer of oxygen, a greenhouse gas, and a photochemical pollutant in the atmosphere. Therefore, its seepage to Earth's surface may have several environmental implications. Recognising and distinguishing natural seepage from anthropogenic gas leaks is fundamental. Only the use of proper detection techniques, as described in Chap. 4, combined with correct concepts and interpretative tools, as outlined in Chap. 5, can make this a reality. As shown in Fig. 1.3, the environmental issues discussed in this chapter include geo-hazards, stray gas, hypoxia in aquatic environments, natural gas emissions to the atmosphere, and the cause and effect of seepage on CO_2 capture and storage in deep geological sequestration. Understanding the sources of atmospheric emissions is the objective of a large number of studies in the framework of atmospheric carbon, as well as the greenhouse-gas budget and related climate change. A wider discussion is, therefore, dedicated to this specific topic.

6.1 Geohazards

Gas seeps can represent a geohazard for humans, buildings, and industries. The hazard may be related to the explosive properties of methane (Sect. 6.1.1), to the toxicity of hydrogen sulphide (H_2S; Sect. 6.1.2), to dangers for people in muddy soils and pools, and to the degradation of the geotechnical properties of soils and sediments (Sect. 6.1.3). As described by the examples provided below, hazards related to gas seepage have been documented in several countries in Europe, North America, and Asia. When the direct social and economic impact is relevant, seeps can be the object of forensic studies (e.g., Nagao et al. 1997; Lundegard et al. 2000) aimed at assessing the exact origin of gas, the cause of seepage (natural or man-made), and possible remedial actions. Such an outcome is typical for "urban seeps", seeps occurring in urbanized centres (from small villages to large cities).

G. Etiope, *Natural Gas Seepage*, DOI 10.1007/978-3-319-14601-0_6

6.1.1 Methane Explosiveness

Methane is a non-toxic gas but high concentrations in ambient air, with consequent oxygen paucity, may induce asphyxia causing headaches, nausea, and dizziness. Long-term exposure to methane-rich air may lead to hypoxia in the blood resulting in brain damage. More importantly, methane can lead to explosions when its concentration is in a range of approximately 5–10 % by volume (vol.%) in the presence of oxygen. A level of 5 vol.% is referred to as the Lower Explosive Limit (LEL). A concentration of 0.5 vol.% CH_4, (i.e., 10 % of the LEL), should be considered the limit above which mitigation measures must be taken. Non-specific methane odour provides no warning, even for dangerous concentrations. Natural gas, with methane concentrations of 80–90 vol.% of CH_4 seeping to the surface, can mix with atmospheric air in shallow ground forming explosive levels. The mixture can occur in pockets below asphalt or cement covers and platforms, and in boreholes. Even small frictional movements and vibrations in the ground, either natural or induced, by processes such as drilling and high temperatures during summer, can result in explosions and sudden flames. For example, explosions occurred in 1972 in a tourist harbour in western Greece named Katakolo, a site with an intense thermogenic gas seepage (Etiope et al. 2005, 2006, 2013a). An eruptive flame blew out from the pavement of the main wharf of the harbour destroying the asphalt cover and a utility pole, a part of the local electric power distribution line. The gas seepage represented a hazard during subsequent drilling projects for an extension and upgrade of the harbour. At present, gas still penetrates and damages asphalt pavement at the harbour (Fig. 6.1).

Fig. 6.1 The damage of asphalt cover due to the seepage of CH_4 and H_2S rich gas at the tourist harbour of Katakolo (western Greece). At the step of the Duty Free Shop's door the H_2S concentration in air a few cm above the ground can reach hundreds of ppmv. The *white box* on the ground is an accumulation chamber for measurements of gas flux. The site on the *right photo* is approximately located where an explosion occurred in 1972 (*photos* by G. Etiope)

In 2003, similar problems occurred near Bacau in Romania when a gas leak was accidentally discovered at the end of construction of a residential area with 248 detached houses. Gas invaded several cellars and burned in shallow wells. The building project was stopped and hundreds of people were forced to leave the houses they had just purchased. Successive investigations demonstrated that gas was seeping from a deep thermogenic reservoir (Baciu et al. 2008).

Another important case of "urban seepage" has occurred in Los Angeles (USA). Gas leaks from plugged and abandoned wells and natural seeps along faults have been reported over the last 40 years, and specific studies have been conducted to unravel possible anthropogenic and natural causes of seepage (Jones 2000; Chilingar and Endres 2005). Natural seepage along a fault was recognised at Belmont High School in downtown Los Angeles. School construction was in progress over the Los Angeles City Oil Field that outcropped at the surface just north of the building site. Soil gas studies revealed that explosive levels of methane and hydrogen sulphide (hundreds of ppmv in air above the soil) were migrating to the surface along faults that extended under several school buildings. To intercept the main avenue of gas migration (the fault) and to divert the direction of gas migration, drilling a slant well was proposed. However, school construction was abandoned after over $175 million dollars (USD) were spent by the Los Angeles Unified School District (Chilingar and Endres 2005).

Abiotic gas related to serpentinisation (Chap. 7) can be particularly rich in hydrogen gas (H_2) that can contribute to the flammability and explosiveness of a seep. An example is the Chimaera seep in Turkey, where CH_4 (87 vol.%) and H_2 (10 vol.%) rich gas is actively burning as it flows from the ground, and many trees have been killed by episodic combustion (Etiope and Schoell 2014; see Sect. 7.1.4).

6.1.2 The Toxicity of Hydrogen Sulphide

Hydrogen sulphide (H_2S) can be associated with methane and other hydrocarbons when it is formed in thermogenic environments in the presence of evaporites such as gypsum and anhydrite in salt diapirs. Since they may form cap rocks or structural traps, evaporites are frequently associated with petroleum systems. The origin of H_2S is described in Chap. 5.3. Hydrogen sulphide is the most dangerous and toxic geological gas and is classified as a chemical asphyxiant because it immediately and chemically interacts with blood haemoglobin to block oxygen from being carried to the body's vital organs and tissues. Hydrogen sulphide has a characteristic rotten-egg smell and is easy to detect at low concentrations. At high concentrations it paralyses the sense of smell and can give someone a false sense of security. In general, a concentration of 10 ppmv of H_2S in air causes eye irritation; a 200–300 ppmv concentration in air causes eye inflammation and respiratory tract irritation after 1 h of exposure; a 500–700 ppmv concentration may lead to a loss of consciousness and possibly death within 30–60 min; and a 1,000 ppmv concentration causes diaphragm paralysis at the first breath and rapid asphyxiation.

An example of high H_2S concentrations in seeps is that of Katakolo in Greece, as mentioned above for methane explosiveness. Thermogenic gas at Katakolo carries hundreds to thousands of ppmv of H_2S that accumulates below asphalt. At the Duty Free Shop building at the tourist harbour at Katakolo (Fig. 6.1), the air half a meter above the ground contains several tens to hundreds of ppmv of H_2S that can be irritating to the eyes. When the barometric pressure is low and then there is enhanced episodic degassing, concentrations in air can increase if the pavement is shattered. Along the same coast, approximately 35 km north of Katakolo, the "thermal" baths of Killini (Etiope et al. 2006) are used by local people for therapeutic use, due to the presumed healing properties of the mud formed around the springs. Nevertheless, up to 900 ppmv of H_2S in the air has been measured above a poorly ventilated bubbling pool (Etiope unpublished data) and the people, although red-eyed, were happy.

6.1.3 Mud Expulsions and the Degradation of Soil-Sediments

Since they can be tens of meters deep and behave like quicksand, some mud volcanoes can have craters and muddy pools that are quite dangerous for people. Even in small mud volcanoes, such as those occurring in northern and central Italy (e.g., Pineto in the Abruzzi Region or Ospitaletto in Emilia Romagna), although craters are less than 1 m wide, the fluid mud is more than 2–3 m deep and can be a lethal trap. In particular, the Pineto and Ospitaletto mud volcanoes are easily accessible a few meters from main busy roads and are not properly enclosed.

As for the case of the village of Serra de' Conti located in the Marche Region of central Italy, small mud volcanoes can also perturb soil foundations and urban facilities (Fig. 6.2). In this village, gas and mud have slowly cracked asphalt cover along roads; a newly born mud volcano was even reported inside the cellar of a house (a rare case of an "indoor" mud volcano!).

Large mud volcanoes can violently release gas and mud, as is the case for many of the mud volcanoes in Trinidad and Azerbaijan, posing a risk for people in surrounding villages or for those visiting the site. For example, the Piparo mud volcano in Trinidad erupted in February 1997 with mud ejections 50 m high and flooded an area of 2.5 km^2 (Fig. 6.3). The sound of rumbling and shaking of the ground alerted residents prior to the eruption, and all managed to escape from their houses before mud spilled into the village and crushed roofs. Luckily, no one was killed. Unfortunately, a tragedy occurred in Italy on 27 September 2014, when two kids 7 and 9 years old, died in a sudden eruption of mud in the Maccalube mud volcano in Sicily (see Fig. 2.5g). The children and their father were just walking along a path open to the public, close to a quiescent crater, when it suddenly erupted producing a mud column several meters high. It was the first time people have been killed, at least in recent times, by a mud volcano in Italy.

Fig. 6.2 A temporary repair undertaken due to rising gas and mud after the plumbing of the ground at a cross road in Serra dé Conti village (central Italy) (*photo* by L. Innocenzi, INGV)

Fig. 6.3 The eruption and damage of the Piparo mud volcano eruption (Trinidad) in 1997. The house on the *right* was pushed over by a wall of mud (*photos* from http://www.vulkaner.no by Jørgen S. Aabech)

Much more violent eruptions of gas and mud are not rare in the mud volcanoes of Azerbaijan, such as that of Lokbatan that occurred in 2001 and 2012 with flames up to 300 m high (Fig. 6.4).

A mud eruption occurred in 2006 in the Sidoarjo district in East Java, Indonesia, when several villages were submerged by hot mud that suddenly ejected from the ground, displacing more than 50,000 people (Mazzini et al. 2012). The eruption site, named LUSI (an acronym for LUmpur, mud, and SIdoarjo, the district name) was considered a newborn mud volcano and different scholars debated the cause of the eruption. Causes included an earthquake trigger or a deep borehole drilled

Fig. 6.4 The spectacular 2001 (**a**) and 2012 (**c**–**d**) eruptions of the Lokbatan mud volcano in Azerbaijan (*photos* kindly provided by Akper Feyzullayev, originally from BP Azerbaijan and news.day.az). **b** Measuring gas inside the Lokbatan crater in 2003 (*photo* by L. Innocenzi, INGV)

nearby. However, successive analyses suggested that rather than a classic mud volcano, LUSI is a manifestation of vapour and CO_2-rich hydrothermal fluids linked to a neighbouring magmatic volcano. The hydrothermal fluids stored under pressure below impermeable covers, carried clays (mud) to the surface as well as some thermogenic gas stored in shallower sources or reservoir rocks (Mazzini et al. 2012). This type of manifestation, a sort of hybrid between cold hydrocarbon seeps and hot geothermal vents, is generally called a "Sediment-Hosted Geothermal System" (SHGS; see also Fig. 1.1).

A much smaller and harmless CO_2-rich eruption of a SHGS occurred in 2013 near the international airport of Rome in the Tiber River delta (Ciotoli et al. 2013). In this case, the eruption was a local manifestation (triggered by shallow drilling) of the pervasive occurrence of gas-charged subsoil within the entire delta. Rather than emissions of mud and CO_2, which were focused in a small, 2–3 m wide crater, in this case, the potential hazard was given by the widespread occurrence of gas in the ground over large areas, tens of km^2 wide. The gas can degrade the geotechnical properties of soil foundations, becoming a critical impediment to the construction of new buildings. Such degradation may perturb the foundations of onshore buildings or offshore platforms and, in the sea, may induce submarine landslides along the slopes of continental shelves. Small amounts of gas bubbles within the soil or

seafloor sediments, as well as gas dissolved in soil pore water, affect the response to loading and unloading, rendering the soil compressible, and enhancing local shearing and pore pressure build-up (Sobkowicz and Morgenstern 1984). The presence of gas in the ground, in particular, reduces foundation performance by increasing compressibility and reducing shear strength, increasing the potential for flow or cyclic liquefaction. Gas issuing in the Tiber delta also has methane concentrations approaching the LEL (2–3 vol.%). The phenomenon is critical as it may also impact the ground inside the compound of Rome's international airport, with eruptions only occurring 700 m from the runway.

6.2 Stray Gas, Natural versus Man-Made

The term "stray gas" indicates natural gas that has migrated into shallow aquifers or into the vadose zone (the zone between groundwater and the surface). When stray gas migrates into a well used for irrigation or drinking water, or into a building, there are potential risks and health issues. Anthropogenic stray gas leaks from hydrocarbon production wells, pipelines, gas storage tanks, landfills, and underground mines. Natural stray gas is related to gas seepage. As a result, it is important to understand if the source of a stray gas is anthropogenic or natural so that appropriate remedial (and sometimes legal) action can be undertaken.

The natural presence of hydrocarbons dissolved in the waters of aquifers or issuing from springs indicates that (i) groundwater has crossed sources or reservoir rocks; (ii) groundwater flew along gas-bearing faults or fracture networks; or, more simply and probably most commonly, (iii) gas migrated into aquifers from deeper sources. Distinguishing these possibilities is only attainable by combining the geochemical features of water and those of several gas species in solution, and knowing the geological context. Elevated methane concentrations are generally associated with sodium and sodium-chloride rich water types that reflect deeper groundwater aquifers and that have experienced longer groundwater residence times, and, therefore, longer rock-water interaction times (e.g., Molofsky et al. 2013). If an aquifer is crossed by a vertical seepage plume (for example along a fault), groundwater can carry the gas horizontally for long distances, towards areas where faults and seeps are not expected.

In some cases, the natural presence of methane in shallow groundwater has been confused with the leakage of gas from petroleum boreholes or production activities. Several reports of burning gas from tap water in houses in the US states of Pennsylvania and New York have been attributed to the fracking of gas shales and have had enormous resonance (the reader my simply google the keywords "burning tap water contamination fracking"). While this scenario has certainly occurred in some areas (i.e., Osborne et al. 2011; Jackson et al. 2013) it has not occurred in others (e.g., Molofsky et al. 2013; Vidic et al. 2013; Warner et al. 2012, 2013; Darrah et al. 2014). For example, extensive geochemical studies performed by Duke University and the USGS Arkansas Water Science Center did not find any

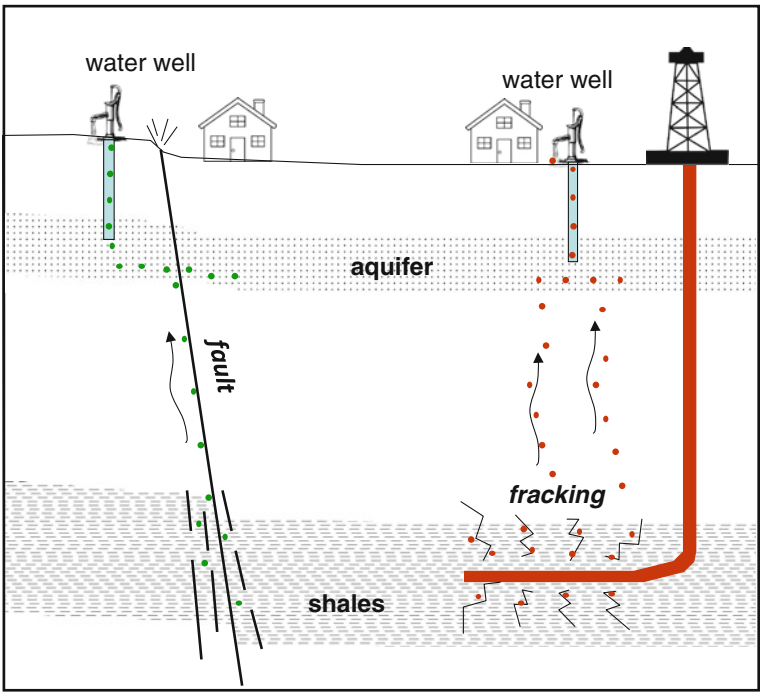

Fig. 6.5 A sketch of the contamination of a shallow aquifer with methane released by shale fracking (*right*), and by seepage from naturally fractured shales (*left*). The seep illustrated in Fig. 5.7 is an example of natural shale-gas migration

direct evidence for the contamination of groundwater wells near shale-gas production sites in Fayetteville (Arkansas, USA). Most of the methane identified in the groundwater had a stable carbon isotopic composition ($\delta^{13}C_{CH4}$) different from the fingerprint of Fayetteville shale-gas (Warner et al. 2013). The reason was a lack of fracture systems that would enable hydraulic connectivity between deep shales and shallow aquifers. Similar results were obtained for the Marcellus and Barnett Shales in Pennsylvania, New York and Texas, where noble gas data (e.g., ^{4}He, ^{20}Ne, ^{36}Ar) ruled out gas contamination from horizontal drilling or hydraulic fracturing (Darrah et al. 2014).

The scenario is illustrated in Fig. 6.5. In general, the possible groundwater impact from shale-gas development differs among sedimentary basins, and variations in both local and regional geology play major roles on hydraulic connectivity and subsurface contamination processes. The Chestnut Park gas seep in New York state (USA), as described in Sect. 5.3.2, is an example of how shale-gas can naturally migrate to the surface without the artificial perturbation of rock permeability. Neotectonic faulting performs natural fracking.

For delicate arguments such as fracking, correct communication by the media should always follow scientific validation. In Romania, for example, this did not

occur when burning gas from a spring in Vaslui County was popularly attributed to shale fracking even though fracking had not been initiated in the region. A reconnaissance study revealed that the entire area surrounding the burning spring is affected by natural seepage, with the presence of small mud volcanoes that have been known in the region for centuries (Baciu et al. unpublished data). Knowing the background conditions (i.e., evaluating the possible presence of natural gas in aquifers and soils before gas and oil production in a given area) is, therefore, extremely important and is a key task that petroleum companies should perform, at least for their own potential future benefit.

6.3 Hypoxia in Aquatic Environments

Hypoxia in water refers to the depletion of oxygen in solution at concentrations below 60 μM (or <2 μg/L; against a normal concentration in air saturated water ≥220 μM or ≥7 mg/L). The condition is critical for biodiversity, ecosystem function, fisheries, aquaculture, and tourism. In many cases, hypoxia in coastal seas, embayments, inlets, and lakes is induced by anthropogenic activities such as the use of agricultural fertilizers, industry, and urbanization. In other cases, it is produced by natural phenomena generally related to variations of hydrodynamic circulation with limited water exchanges. Also, in some cases, submarine gas seepage can induce hypoxia. Since they can be quickly oxidised, reducing gases such as methane and hydrogen sulphide can, in fact, rapidly consume oxygen. Additionally, seepage at the seafloor can trigger the vertical advection of deep water, which is oxygen poor, into the photic zone and the surface mixed layer. The upwelling of hypoxic water can be driven by the density changes induced by gas saturated waters and buoyant two-phase fluids (micro- and macro-bubble plumes). Upwelled waters can have a deleterious effect on fish near the surface.

Hypoxia caused by gas seepage has, in general, been poorly studied. Hypoxia has been reported in the Cariaco Basin (Venezuela), offshore of Namibia, and in the Gulf of Mexico (Kessler et al. 2005, 2011; Emeis et al. 2004; Monteiro et al. 2006); and, more recently, in petroliferous areas in western Greece (Friedrich et al. 2014). In the Cariaco Basin, Kessler et al. (2005) found that 98 % of CH_4 in the hypoxic water column is fossil (geological), seeps from deep sediments, and was likely influenced by a large regional earthquake in the 1960s. In Namibia seawater, the Benguela coastal current upwelling system is one of the most biologically productive regions of the world's ocean, but enhanced releases of hydrogen sulphide perturb coastal waters and near-shore lands. Also verified is that H_2S is associated with eruptions of methane from gas-charged sediments that systematically reduces oxygen availability along the water column (Emeis et al. 2004).

Studies in Greece (Friedrich et al. 2014) indicated that for shallow water conditions and with intense gas seepage, the concentration of dissolved O_2 is locally inversely proportional to the CH_4 concentration. Temporal monitoring and aerial surveys were performed using O_2 and CH_4 underwater sensors located at Katakolo

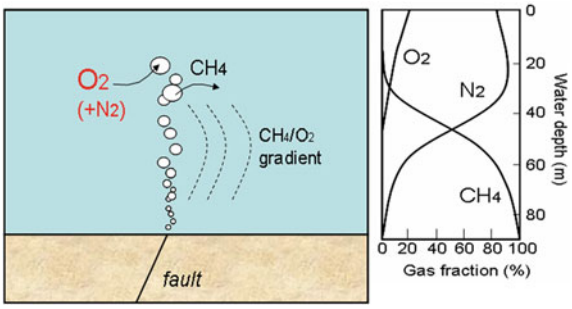

Fig. 6.6 A sketch illustrating the oxygen decrease surrounding a gas bubble plume. The exchange of gases between seawater and bubbles has been modelled, for example, by Mc Ginnis et al. (2006) from which the diagram of gas fraction versus depth was derived. The model refers to changes in gas composition in bubbles with diameters of 0.5 cm. At 70–80 m from the seabed, bubbles do not contain methane anymore but are enriched in oxygen and nitrogen. As discussed in Sect. 6.4, the process is also important for discussions of submarine seepage as a source of methane to the atmosphere

harbour, the site mentioned above for its risk for methane explosiveness and H_2S toxicity. Studies have revealed that even for open sea conditions, enhanced episodes of degassing (vigorous bubbling) produce short-term events of hypoxia (O_2 decreased below 60 μM). At the local seep scale, this process is likely due to either a combination of O_2 oxidation or to the exchange of gases between bubbles and seawater (i.e., N_2 and O_2 from seawater replace the CH_4 inside the bubble). In other words, bubbles strip O_2 from seawater and its concentration in solution decreases (Mc Ginnis et al. 2006). The concept is simplified in Fig. 6.6. If no input of new oxygenated water exists, the site may become hypoxic or even anoxic (the O_2 concentration drops to zero). Similar processes may take place within any submarine site with intense gas seepage, especially if deep-water circulation is low or absent. At the seafloor, microbial sulphate reduction utilising seeping methane as a carbon source can then produce hydrogen sulphide, which further reduces oxygen concentrations.

6.4 Gas Emissions to the Atmosphere

The surface seepage of natural gas containing methane, ethane, and propane implies the injection of these gases into the atmosphere. Methane is a potent greenhouse-gas. Ethane and propane are more important as photochemical pollutants and ozone precursors. Beginning in the 1990s, evaluations of the global emission of these gases, in comparison with other natural and anthropogenic sources, have represented an important topic in global climate change studies. Section 6.4.1 below illustrates the main data and treatments that have led to consideration of the important role of methane seepage in this context. The global dataset related to

geological ethane and propane fluxes is still in its infancy. As discussed in Sect. 6.4.2, only preliminary evaluations have been proposed thus far, deserving future research.

6.4.1 Methane Fluxes and the Global Atmospheric Budget

Methane is the third most important greenhouse gas after H_2O and CO_2, and has a global warming potential that is 28 times higher than that of CO_2 on a 100-year time horizon (Ciais et al. 2013). Methane's concentration has risen from $\sim$0.7 ppmv, its concentration during the pre-industrial period, to a present value of $\sim$1.8 ppmv. Methane is currently responsible for approximately 20 % of the direct radiative forcing from all long-lived greenhouse gases ($\sim$2.3 W/m^2) and for one-third of total radiative forcing, including the indirect effects of CH_4 emissions (3 W/m^2) such as changes in ozone and stratospheric water vapour concentrations (Ciais et al. 2013). Assessments of natural and anthropogenic sources and sinks of methane are, therefore, central to studies of climate change.

6.4.1.1 The Evolution of Methane Emission Inventories and IPCC Reports

Until recently, geological gas seepage has always been considered a negligible or minor contributor to atmospheric methane concentrations as compared to anthropogenic sources (ruminants, energy, rice agriculture, landfills, wastes, and biomass burning), and other natural sources (wetlands, termites, wild animals, oceans, and wild fires; e.g., Lelieveld et al. 1998; Prather et al. 2001; Wuebbles and Hayhoe 2002). The consideration was basically due to the lack of seepage flux data and also the result of a general, and still persistent, attitude within the atmospheric chemistry scientific community of ignoring and understating the role of geological processes in the global methane budget. A wide array of scientific literature, based on theoretical and experimental data beginning in the 1990s (Lacroix 1993; Klusman et al. 1998; Etiope and Klusman 2002; Judd et al. 2002; Kvenvolden and Rogers 2005; Etiope et al. 2008; Etiope 2009, 2010, 2012) has instead indicated that natural gas seepage and geothermal methane emissions are globally important and represent a major natural source of methane to the atmosphere. The latest estimate is $\sim$60 Tg CH_4/y, $\sim$10 % of all methane sources and second only to wetlands (Etiope 2012). Several geological sources, as compared to other natural methane sources, are schematised in Fig. 6.7.

In this regard, it is interesting to follow the evolution of international reports prepared by the agencies in charge of compiling atmospheric gas emission sources and sinks (gas emission inventories), which are references for both academics and politicians.

The European Environment Agency, in its EMEP/CORINAIR Emission Inventory released in 2004 (EEA 2004), only gave minor consideration to

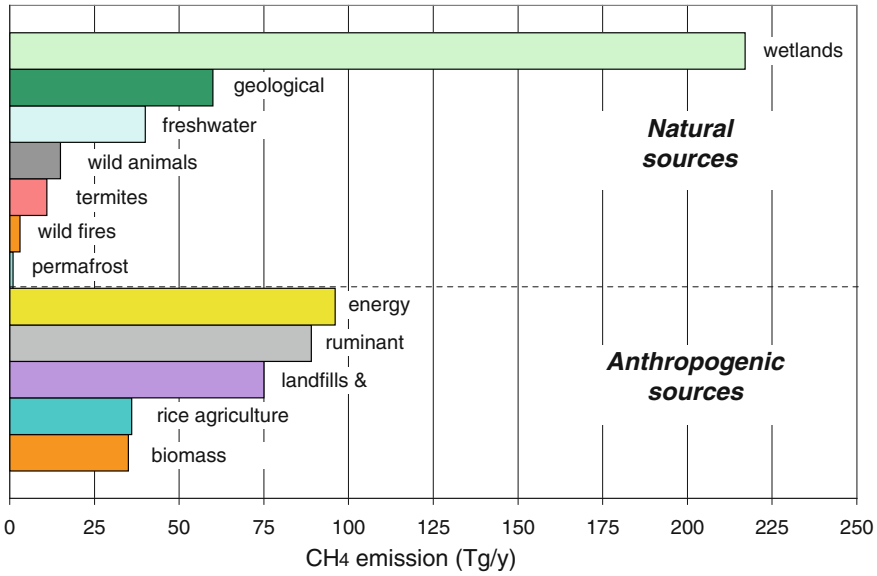

Fig. 6.7 Global sources of methane. Natural and anthropogenic sources were obtained from Ciais et al. (2013), IPCC fifth assessment report. Geological sources were corrected from 54 Tg/year (Ciais et al. 2013) to 60 Tg/year, as considered in this chapter

geological sources, which were mentioned as "Gas seeps" within category Group 11 "Other sources and sinks", without providing emission factors or global emission estimates. The report considered marine seepage exclusively, stating "only seeps under water are easily identified due to formation of gas bubbles". However, thanks to the results of a European project aimed at refining natural methane emissions, including geological ones (the NATAIR project; e.g., Etiope et al. 2007b; Etiope 2009), the successive Emission Inventory Guidebook released in 2009 (EMEP/EEA 2009) endorsed geological seepage as a new natural CH_4 source under the category of "Geological seepage", code 1109. The document was the first to report a comprehensive description for geological processes, classifications, and emission factors for all seepage types, both onshore and offshore. In 2010, an analogous report was issued by the Environmental Protection Agency of the United States (US EPA 2010), with a specific chapter on "Marine and terrestrial geologic sources" that rigorously recalled the wide array of scientific literature published in previous years.

The evolution of reports from the Intergovernmental Panel on Climate Change (IPCC) has been longer. Every 5 or 6 years the IPCC prepares and releases Assessment Reports (AR) which typically include a chapter focused on the carbon budget and methane emissions to the atmosphere. The first three reports, issued in 1990 (AR1), 1995 (AR2), and 2001 (AR3) (see http://www.ipcc.ch), did not consider geological seepage. Only submarine hydrates were mentioned, although there were no studies providing experimental data on hydrate methane emission to

the atmosphere (in particular, see the note in Sect. 6.4.1.3). Geological sources were mentioned for the first time in AR4 in 2007 (Denman et al. 2007), yet old numbers were reported (4–14 Mt/year) that only referred to marine seeps. Finally, the 2013 IPCC report, AR5, (Ciais et al. 2013) included geological emission estimates published in 2008 (54 Mt/year; Etiope et al. 2008). However, oddly, the IPCC table that summarised methane sources placed geological emissions in the same line as ocean sources. Additionally, in the graphic representation (Fig. 6.2 of the 6th chapter in the IPCC AR5 report), geological methane was depicted to stem from volcanoes, which are not important methane sources at all, as discussed below. The picture was a pure schematisation of geological processes, yet it is misleading.

The evolution of official methane emission inventories, endorsing geological sources, has been possible thanks to three fundamental steps, as follows:

(a) the acquisition of a large number of flux data for various seepage types in many countries;
(b) the application of up-scaling and bottom-up procedures that have traditionally been used for other, non-geological, methane sources; and
(c) the top-down verification of global estimates based on the concentration of fossil methane in the atmosphere.

These steps are described in the following sections.

6.4.1.2 Acquiring Methane Flux Data

As previously discussed in Chap. 5, emissions of methane from land-based natural seepage to the atmosphere were studied using direct measurements beginning in the 1990s, with the microseepage studies of Klusman et al. (1998) in the USA. Methane flux measurements from onshore microseepage and macro-seeps were then performed in Europe and Asia, as summarised in Table 6.1. These studies allowed the assessment of specific gas fluxes (the emission factors, as defined below) characteristic of each type of seepage. Flux measurements are generally based on closed-chamber methods (Chap. 4) and various techniques for determining gas output from bubble plumes (e.g., flux-meters, inverted bottles).

Offshore gas emission data are mainly available in the US (the offshore areas of California and the Gulf of Mexico), the North Sea, the Black Sea, the Atlantic coast of Spain and Denmark, various sectors of the Mediterranean Sea, and the Taiwan, Chile, and Japan seas. However, although marine seepage has been the subject of a vast array of scientific literature beginning in the 1980s (e.g., Hovland and Judd 1988; Hovland et al. 1993; Dando et al. 1994; Judd et al. 1997), in most cases, the data only references gas outputs from the seafloor to the water column, while very few studies exist in which the amount of gas entering the atmosphere has actually been measured or estimated (e.g., Hornafius et al. 1999; Judd 2004; Clark et al. 2010; Shakhova et al. 2010; Jessen et al. 2011; Schneider von Deimling et al. 2011; Etiope et al. 2013a). Submarine gas fluxes are generally estimated on the basis of geophysical images (echo-sounders, seismic, sub-bottom profilers, and side-scan

Table 6.1 A summary of the main studies, with methane flux measurements from land-based natural gas seepage (hydrocarbon-rich emissions)

Country	Type of seepage	Reference
Azerbaijan	Gas seeps, mud volcanoes, miniseepage	Etiope et al. (2004), Kopf et al. (2009)
Australia	Gas seeps	Day et al. (2013)
China (PRC)	Microseepage	Tang et al. (2010)
Germany	Microseepage	Thielemann et al. (2000)
Greece	Gas seeps and miniseepage	Etiope et al. (2006, 2013a)
Italy	Gas seeps, mud volcanoes, miniseepage, microseepage	Etiope et al. (2002, 2007a), Etiope and Klusman (2010)
Japan	Mud volcanoes, miniseepage	Etiope et al. (2011a)
Romania	Gas seeps, mud volcanoes, miniseepage	Etiope et al. (2004), Baciu et al. (2008), Spulber et al. (2010), Frunzeti et al. (2012)
Switzerland	Gas seep and miniseepage	Etiope et al. (2010)
Taiwan (ROC)	Mud volcanoes, gas seeps, miniseepage	Yang et al. (2004), Chang et al. (2010), Chao et al. (2010), Hong et al. (2013)
Turkey	Gas seeps, miniseepage, microseepage	Etiope et al. (2011b)
USA—Alaska	Gas seeps	Walter Anthony et al. (2012)
USA—California	Gas seeps	Duffy et al. (2007)
USA—Colorado	Seeps Microseepage	LTE (2007), Klusman and Jakel (1998), Klusman et al. (2000)
USA—Nevada	Microseepage	Klusman et al. (2000)
USA—Wyoming	Microseepage	Klusman et al. (2000)
USA—New York	Gas seep, miniseepage	Etiope et al. (2013b)

sonar records) and bubble parameterization (the size of bubbles and bubble plumes; Weber et al. 2014), sometimes associated with geochemical seawater analyses (for example Judd et al. 1997). As discussed in Chap. 4, recent studies have been proposed using remote sensing techniques based on airborne visible/infrared imaging spectrometry (Bradley et al. 2011).

6.4.1.3 Up-Scaling and Bottom-Up Global Estimates

Global methane emission estimates have been derived using the same procedures typically used for natural and anthropogenic gas sources as recommended by the air pollutant emission guidebook of the European Environment Agency (EMEP-EEA 2009). The procedures are based on the distinction between "point sources" and "area sources", and on the concepts of "activity" and "emission factor". In the case

of gas seepage, a "point source" refers to localised emissions (i.e., a macro-seep with a flux expressed in kg/day or tonnes/year). An "area source" is diffuse seepage (i.e., miniseepage or microseepage, as described in Chap. 2, with a flux of mg m^{-2} day^{-1}). "Activity" is practically the area of diffuse seepage. Each macro-seep includes specific point sources, vents, bubbling pools, and an area source, the miniseepage. Total gas emissions from a seep site (for example, a mud volcano) are, then, the sum of all of the point sources (vents) plus total outputs from the invisible diffuse miniseepage surrounding vents. The "emission factor" is the total emission divided by the area of the seepage (areal emission factor: kg m^{-2} day^{-1}). For macro-seeps, the "emission factor" incorporates emissions from vents and miniseepage, and can also be expressed in terms of a "point emission factor" (kg day^{-1}), a typical total emission of a given type of seep (mud volcanoes, gas seeps, oil seeps, and springs may have different emission factors). In this case, "activity" corresponds to the number of emission points.

In practice, the global methane emission from a given type of macro-seep can be estimated by multiplying the areal emission factor of that type of macro-seep by the global area formed by all macro-seeps, or by multiplying the point emission factor by the global number of those types of macro-seeps. The point emission factor is used for small or focused seeps. For mud volcanoes, the areal emission factor can be considered because the global area of mud volcanoes can be roughly estimated (Etiope and Milkov 2004). Finally, global methane emissions from microseepage are given by the microseepage areal emission factor multiplied by the global microseepage area. The emission factors for several types of seepage and the areas used for global emission estimates are summarised in Table 6.2.

Gas-oil seeps. The order of magnitude of methane emissions from single gas seeps typically ranges from 0.1 to 100 tonnes/year for vents or bubbling pools with a diameter <1 m. In addition to bubble traps and floating accumulation chambers,

Table 6.2 Methane seepage emission factors and "activity" (area or number of point sources) considered in global emission estimates

Type of seepage	Emission factor	Activity	Reference
Gas seeps	300 t/year (average of 66 seeps) ≤30 t/year (79 %); 30–300 t/year (15 %); >300 t/year (6 %)	12,500 seeps Statistical distribution	Etiope et al. (2008)
Mud volcanoes (MV)	Quiescent degassing (QD): 10–10,000 (3,150) t/year	2,880 km^2 930 MV	Etiope et al. (2011a)
	Eruptions: QD × 2		Dimitrov (2002), Etiope and Milkov (2004)
Microseepage	210 mg $m^{-2}day^{-1}$ (3 %) 14.5 mg $m^{-2}day^{-1}$ (12 %) 1.4 mg $m^{-2}day^{-1}$ (34 %)	gas/oil field area: 3.5–4.2 × 10^6 km^2 TPS area: 8 × 10^6 km^2	Etiope and Klusman (2010)

Table 6.3 Global emissions of methane from geological sources

Type of seepage	(Tg yr^{-1})	References
Gas seeps	**3–4**	Etiope et al. (2008)
Mud volcanoes	5–10	Etiope and Klusman (2002)
	10.3–12.6	Dimitrov (2002)
	6–9	Etiope and Milkov (2004)
	10–20	Etiope et al. (2011a)
Microseepage	>7	Klusman et al. (1998)
	10–25	Etiope and Klusman (2010)
Marine seepage	18–48	Hornafius et al. (1999)
	10–30 (**20**)	Kvenvolden et al. (2001)
Geothermal/ volcanic areas	1.7–9.4	Lacroix (1993)
	2.5–6.3	*Volcanoes not included;* Etiope and Klusman (2002)
	<1	*Only volcanoes*; Etiope et al. (2008)
	2.2–7.3	This work (*only volcanoes would be around* 0.015 Tg/year)
Total	13–36	*Microseepage not included*; Judd (2004)
	30–70	Etiope and Klusman (2002)
	45	*Lowest microseepage estimate considered;* Kvenvolden and Rogers (2005)
	42–64	*Best estimate;* Etiope et al. (2008)
	30–80	*Extended range and top-down verification;* Etiope et al. (2008)
	45–76 (60)	Etiope (2012)

The latest global estimate (60 Tg/year) is based on more recent estimates for each seepage type, indicated in bold

the gas flux from bubble trains can be estimated (in terms of orders of magnitude) by bubble parameterization on the basis of bubble sizes and burst frequency (which can be video-recorded), as described in Etiope et al. (2004, 2013a). Fluxes exceeding 1,000 tonnes/year are associated with larger seeps with vigorous degassing, such as those for the everlasting fires in Azerbaijan and Iraq (Fig. 2.2). In general, the invisible miniseepage surrounding vents adds an amount of gas that may be two to three times higher than that released from vents. The methane flux from oil seeps is generally much lower. Global emission estimates from gas-oil seeps (3–4 Tg/year; Table 6.3) were based on a database of fluxes that were measured directly or visually estimated from 66 gas seeps in 12 countries, using an assumption that their flux and size distributions were representative of the global, gas-oil seep population independent of mud volcanism (i.e., at least 12,500 seeps; Etiope et al. 2008). Two procedures were combined. The first procedure considered the average emission factor ($\sim$300 tonnes/year, including miniseepage) and the presumed total number of seeps. The second procedure used the statistical distribution of the flux from 66 seeps, based on three different emission factors, as follows: 79 % of seeps have a flux of up to 30 tonnes/year (low emission factor),

15 % have a flux from 30 to 300 tonnes/year (medium emission factor), and 6 % have a flux >300 tonnes/year (high emission factor). The average flux value for each class roughly corresponds to 10, 100, and 1,000 tonnes/year, respectively.

Mud volcanoes. The single vents or craters of small mud volcanoes (1–5 m high) can release up to tens of tonnes of methane per year. An entire mud volcano (hosting tens or hundreds of vents) can continuously emit hundreds of tonnes of CH_4 per year, and eruptions from mud volcanoes can release thousands of tonnes of CH_4 within a few hours. However, only very approximate and indirect estimates are available for gas outputs during eruptions (e.g., Guliyev and Feizullayev 1997). In all mud volcano areas measured thus far (Italy, Romania, Azerbaijan, Japan, and Taiwan), the specific flux, including vents and miniseepage (excluding eruptions), was between $\sim$100 and 10,000 tonnes km^{-2} $year^{-1}$, with a global average of 3,150 tonnes km^{-2} $year^{-1}$ (Etiope et al. 2011a, and references therein).

Global CH_4 emission estimates from the mud volcanoes shown in Table 6.3 differ slightly, although they were derived from different data sets and approaches. The latest estimates (Etiope and Milkov 2004; Etiope et al. 2011a) were based on direct flux measurements and emission factor approach, including both focused venting and diffuse miniseepage surrounding craters and vents. Estimates were also based on classifications of mud volcano sizes in terms of area, following a compilation of data from 120 mud volcanoes. The most recent estimate (10–20 Tg/year) is based on the updated emission factor analyses mentioned above (Etiope et al. 2011a). The largest uncertainty is related to emissions during eruptions.

Microseepage. The most recent global microseepage emission value (10–25 Tg/year; Table 6.3) was derived on the basis of an accurate estimate of the global area of oil and gas fields and TPS (Total Petroleum Systems, see Chap. 1), and on recognition of the three microseepage emission factors (Table 6.2) derived from a global data set. Based on a GIS dataset from the U.S. Geological Survey World Petroleum Assessment 2000 and related maps, the global area of potential microseepage was assessed using an analysis for the distribution of oil/gas fields within all of the 937 petroleum provinces or basins (Etiope and Klusman 2010). For each province, a polygon was drawn that enclosed gas/oil field points in interactive maps and the area was estimated using graphic software. Using this method, it was determined that significant gas/oil field zones occur in at least 120 provinces. The total area of gas/oil field zones was estimated to be between 3.5 and 4.2 million km^2.

Statistical analyses of 563 microseepage flux measurements, in geographically dispersed areas, (Etiope and Klusman 2010) indicate that positive methane fluxes occur in approximately 49 % of the TPS area and that at least three main levels of microseepage can be considered, as follows:

- Level 1: High microseepage (>50 mg $m^{-2}day^{-1}$)
- Level 2: Medium microseepage (5–50 mg $m^{-2}day^{-1}$)
- Level 3: Low microseepage (0–5 mg $m^{-2}day^{-1}$).

Levels 1 and 2 mainly occur in areas where macro-seeps also exist, in other words, in the presence of "fracture flow" (Chap. 3.1.1) in active and permeable faults in sedimentary basins, in general, during winter. Of over 563 measurements, 276 were positive fluxes (49 %); 3 % were determined within the Level 1 range (a mean of 210 mg $m^{-2}day^{-1}$); 12 % were determined within the Level 2 range (a mean of 14.5 mg $m^{-2}day^{-1}$); and Level 3, common during winter, accounted for approximately 34 % of surveyed sedimentary zones (a mean of 1.4 mg $m^{-2}day^{-1}$). Upscaling to the global microseepage area was based on the average flux from each of the three microseepage levels, by assuming that the percentage of occurrence for the three levels (3, 12, and 34 %) is valid on the global scale. Since the result is not particularly sensitive to changes in unit percentages, the assumption does not yield large errors. Measurements have also been made for all seasons, so seasonal variations have been incorporated into the 563 measurements. Accordingly, the upscaling of all gas/oil field areas resulted in total microseepage on the order of 11–13 Tg $year^{-1}$. Extrapolating to the global potential microseepage area ($\sim$8 million km^2), projected total global emissions on the order of 25 Tg $year^{-1}$. These estimates are coherent with the lower limit of 7 Tg $year^{-1}$ previously suggested by Klusman et al. (1998) and Etiope and Klusman (2002). However, more measurements in various areas and for different seasons are required in order to refine the three-level classification and the actual areas of seepage.

Submarine seeps. As for onshore seeps, methane emissions to the atmosphere from submarine seeps can have a wide range of values. The flux of individual seepage or groups of bubble streams may reach several tonnes per year. Orders of 10^3–10^6 tonnes/year of gas have been estimated over areas of approximately 10^5 km^2 (North Sea; Judd et al. 1997); 47–470 tonnes/year over 0.7 km^2 (Timor Sea seeps; Brunskill et al. 2011); 26 tonnes/year over 0.12 km^2 (the Tommeliten seepage in the North Sea; Schneider von Deimling et al. 2011); and 15,000 tonnes/year over 3 km^2 (the Coal Oil Point seep field, California, Clark et al. 2010). However, flux data acquired for marine seepage are still insufficient for application of the emission factor procedure. As stated above, most studies have focused on methane flux at the seabed and not the flux actually entering the atmosphere (see the review by Judd 2004). Methane bubbles rising along the water column can be partially or completely dissolved and oxidised before reaching the atmosphere. CH_4 decrease, due to gas exchange between seawater and bubbles (Mc Ginnis et al. 2006), from the bottom of the water column to the surface is a well-known process, a phenomenon previously discussed in relation to the local hypoxia induced by gas bubble plumes. The amount of methane lost within the water column largely depends on the depth of the water, the temperature, and the size of the bubbles rising towards the surface. Some observations also suggest that oil coatings on bubbles inhibit gas dissolution and that methane within bubbles can travel longer distances (McDonald et al. 2002; Solomon et al. 2009). However, in general, models and field data indicate that only submarine seeps occurring at depths less than 100–300 m have a significant impact on the atmosphere (e.g., Leifer and Patro 2002; Schmale et al. 2005). In some rare cases, gas bubbles can reach the sea surface from depths >500 m (Solomon et al. 2009) and estimates indicate that only

40 % of methane from concentrated seeps at the seafloor reach the atmosphere (Kvenvolden et al. 2001).

Therefore, for submarine seepage, a theoretical approach was utilized for deriving global methane emission estimates. Kvenvolden et al. (2001) reported a meeting of submarine seepage experts who estimated global methane flux on the basis of both available seep flux data and the amount of geological CH_4 produced and available to seep. The two estimates produced comparable results, 30 and 10 Tg year^{-1}, respectively. The average, $\sim$20 Tg year^{-1}, is considered a realistic value and is still used today as a consensus value, awaiting refinement.

And the gas hydrates? Not clear, however, was whether or not the above estimate by Kvenvolden et al. (2001) considered potential emissions from submarine hydrates. Since a large amount of scientific literature, and even IPCC reports, indicate that gas hydrates are a global source of methane to the atmosphere, with numbers ranging from 2 to 10 Tg/year (Lelieveld et al. 1998; Ciais et al. 2013), a specific discussion should be made regarding this aspect of the data. In actuality, these values are totally speculative, result from misquotations, and are not supported by direct measurements. Instructive to note is that Ciais et al. (2013; the AR5 IPCC report) indicated values of 2–9 Tg/year using a reference of (a) the previous IPCC report (Denman et al. 2007, that indicated 4–5 Tg/year), (b) the work of Dickens (2003), who did not indicate a number (it was a comment to a book), and (c) Shakhova et al. (2010), who reported 10 Tg/year in relation to methane venting from the East Siberian arctic shelf, which may result from seepage that is independent from hydrates (the word "hydrates" is never mentioned in Shakhova et al. (2010)). Denman et al. (2007) referenced the previous IPCC 2001 report (5–10 Tg/year), and Lelieveld et al. (1998; 5–15 Tg/year). Both documents referenced older reports and scientific publications that, in turn, referenced still older publications, arriving, finally, to Cicerone and Oremland (1988), the first article proposing a number (i.e., 5 Tg/year). The value of Cicerone and Oremland (1988), however, was simply hypothetical. No experimental data or estimation procedures were described along the chain of references.

While special events such as submarine slumps may trigger local releases of considerable amounts of gas from hydrates that may reach the atmosphere (Paull et al. 2003), on a global scale, present-day atmospheric methane emissions from hydrates are likely negligible. Observations and model simulations indicate that the majority of gas that escapes from the melting of deep-sea hydrates is dissolved and oxydised in the water column, and fails to enter the atmosphere (Yamamoto et al. 2009). Hydrates may have played a role in the past (as discussed in Chap. 8), and theoretical models predict that a global warming of 3 °C beyond present temperatures would induce a dissociation of 50 % of global hydrates (Archer et al. 2009). However, at present, hydrates do not seem to play any special role in the atmospheric greenhouse gas budget.

Geothermal and volcanic manifestations. As explained in Chap. 1, geothermal and volcanic emissions cannot be considered as seepage. However, in this chapter, since they represent an additional class of geological CH_4 source, they are discussed. Geothermal manifestations, in particular, provide a significant contribution

to global methane emissions to the atmosphere. Volcanoes alone are not a significant CH_4 source (Ryan et al. 2006; Etiope et al. 2007b). Methane concentrations in volcanic gases are generally on the order of a few ppmv or tens of ppmv, with individual emissions, derived on the basis of the compositional CO_2/CH_4 ratio and the CO_2 flux, ranging from a few to tens of tonnes/year (Etiope et al. 2007b). Methane emissions from geothermal fluids, where inorganic synthesis, thermometamorphism, and the thermal breakdown of organic matter are substantial, are more important. The gas composition of geothermal vents, mofettes, and bubbling springs is generally more than 90 vol.% CO_2. The fraction of CH_4 is low, typically 0.1–3 vol.% (in a few cases up to 10–15 vol.%), although the amount of total gas released (orders of 10^3–10^5 tonnes CO_2 year^{-1}) may result in significant emissions of CH_4 (10^1–10^2 tonnes CH_4 year^{-1} from individual vents). The specific flux of soil degassing is generally on the order of 1–10 tonnes km^{-2} year^{-1} (Etiope et al. 2007b). Higher methane fluxes occur in the SHGS (Sediment Hosted Geothermal Systems) described in sect. 6.1.3, where CO_2 of deep magmatic or thermo-metamorphic origin ascends and carries gaseous hydrocarbons that are sourced in shallower sedimentary rocks towards the surface (also see Fig. 1.1).

The first global geothermal CH_4 flux estimates (0.9–3.2 Tg/year) were proposed by Lacroix (1993). A wide dataset was then reported by Etiope and Klusman (2002), who conservatively derived a global geothermal flux between 2.5 and 6.3 Tg/year based on a correlation between gas flux and heat flow. Lacroix (1993) also suggested a global volcanic CH_4 flux of 0.8–6.2 Tg/year. Recent estimates indicate that volcanic emissions do not exceed 1 Tg/year (Etiope et al. 2008). Today, it is possible to re-estimate global emissions using a different approach by considering updated estimates of global CO_2 emissions from volcanic areas (540 Tg/year; Burton et al. 2013), from non-volcanic areas (300–1,000 Mt/year; Morner and Etiope 2002), and a wider dataset on CO_2/CH_4 compositional ratios in both areas (from 28 volcanoes and 90 geothermal manifestations, where the data are mainly derived from Etiope et al. 2007b and Tassi et al. 2012). The average CH_4 concentration in volcanic gases based on this ratio is $\sim$70 ppmv; global volcanic CH_4 emissions are approximately 15,000 tonnes/year. The average CH_4 concentration in geothermal (non-volcanic) gases is $\sim$19,000 ppmv, while global geothermal CH_4 emissions range from 2.2 to 7.3 Tg/year, consistent with previous estimates based on different procedures.

Global. Global geo-CH_4 emission estimates, stemming from mud volcanoes plus gas-oil seeps, plus microseepage, plus submarine emissions, plus geothermal and volcanic emissions, range from 45 to 76 Tg year^{-1} (with a mean of 60 Tg year^{-1}). As mentioned at the beginning of this chapter, the value represents approximately 10 % of total methane emissions from anthropogenic and natural sources. Geological emissions are the second most important natural source of methane after wetlands, and are comparable to several anthropogenic sources (Fig. 6.7). Present geological emission estimates do not include degassing from methane-rich springs, for which available data are quite scarce, and abiotic gas seeps and springs related to the serpentinisation of ultramafic rocks, as discussed in Chap. 7. A specific study should be performed for this type of seepage.

6.4.1.4 Top-Down Verification

Bottom-up emission estimates can be verified using a top-down approach that begins with evaluations of the amount of natural geological CH_4 in the atmosphere. Geological CH_4 is fossil and radiocarbon-free. Also, the methane released from the fossil-fuel industry is obviously fossil. As a result, the atmosphere contains both natural and anthropogenic fossil methane. Fossil methane accounts for 30 ± 5 % of total atmospheric methane (Lassey et al. 2007). The global methane source of 613 Tg/year (an average of 548 Tg/year by top-down and 678 Tg/year by bottom-up estimates; Ciais et al. 2013) implies a fossil source of ~184 Tg $year^{-1}$. Identified anthropogenic-induced fossil emissions aggregate to ~96 Tg/year (up to 123 Tg/year considering top-down evaluations; Ciais et al. 2013). The result would leave a residual natural (geological) fossil source of 61–88 Tg $year^{-1}$. The value can easily accommodate the 60 Tg/year (45–76 Tg/year) estimated using bottom-up approaches.

6.4.1.5 Uncertainties

Uncertainties in global emission estimates largely result from poor knowledge of actual areas of shallow submarine seeps and onshore areas for invisible microseepage. Evident is that all seeps and microseepage zones occur within hydrocarbon provinces, in particular, within Total Petroleum Systems (Chap. 1; Etiope and Klusman 2010), although actual microseepage areas are not known. Three main levels of spatial disaggregation can be defined, with increasing uncertainty, as follows: areas including (encompassing) sites of verified microseepage flux; areas encompassing macroseeps (where microseepage very likely occurs); and areas encompassing oil-gas fields (where microseepage likely occurs). However, the definition of the area used for emission calculations depends on recognition of homogeneous identifiable areas and the spatial variability of the measured flux. Currently, estimations are performed based on the distribution of oil fields by assuming that approximately 50 % of oil field areas have some continuous or seasonal positive flux of CH_4 from soils, as discussed above (Table 6.2). The area identified in oil field maps is then transformed into polygons that are later used in calculations. The polygons drawn are used as a rough method for estimating the emitting area. Additionally, the use of polygons most likely results in over- and/or under-estimations for emitting areas. Somehow, in the overall scenario, since errors in area estimations are balanced, emission values may be closer to reality than one may think. Due to differences in methanotrophic activity (a natural microbial process that removes CH_4 before it can reach the atmosphere) between winter and summer, microseepage is quantitatively understood to be higher in the winter and lower in the summer. Other short-term or seasonal variability is due to meteorology and soil conditions. Longer-time variability (decades, centuries, and millennia) can be induced by endogenic, geological factors (changes in the pressure gradients of rocks, tectonic stress, etc.). For macro-seepage, the main source of uncertainty is

temporal variations in emissions. The largest fraction of emissions occurs during 'individual' events/eruptions that are difficult to simulate, and the resultant emissions are not easily quantifiable. Thus, calculations are normally accomplished using assumptions of continuous gas release from counted vents. The census of vents is also an additional source of uncertainty. Either on land or at sea, the majority of large macro-seeps have been identified and studied, but most of the smaller ones have not been determined, surveyed, or characterised.

Even so, uncertainties for global geoemission estimates are lower than or comparable to those of other natural sources (wetlands, termites, etc.). Further studies, based on direct field measurements (especially for diffuse microseepage and underwater sources) are necessary in order to reduce uncertainties.

6.4.2 *Ethane and Propane Seepage, a Forgotten Potential Source of Ozone Precursors*

Ethane and propane are greenhouse-gases, but, due to their low concentrations in the atmosphere, 0.5–1 ppbv and 0.1–0.5 ppbv, respectively, are of negligible importance (e.g., Kanakidou et al. 1991). Their main role in atmospheric chemistry is related to their reactivity with OH and Cl radicals, inducing photochemical pollution and ozone production in the troposphere (Kanakidou et al. 1991). The main atmospheric sources of ethane and propane are both anthropogenic and natural (i.e. biological, fossil-fuel burning, agricultural waste, biomass combustion, oceans, and plants; Olivier et al. 1996). Based on direct atmospheric measurements and calculated removal rates, total ethane and propane emissions should be on the order of ~15 and 15–20 Tg/year, respectively, although known sources only total ~9.6 Tg/year for each gas (Singh et al. 1994; GEIA-ACCENT database 2005; Stein and Rudolph 2007), indicating that there are missing sources.

Geological emissions were not considered until 2009 (Etiope and Ciccioli 2009). Available data on the relative proportion of methane, ethane, and propane in the various types of seepage (onshore seeps, mud volcanoes, microseepage, marine seeps, and geothermal-volcanic fluids), and the estimated rates of global emissions of methane from each type of seepage, made it possible to derive first order estimates of global geological emissions for ethane and propane (Etiope and Ciccioli 2009). The exercise was quite banal but required careful knowledge of several seepage types with different ethane/methane (C_2/C_1) and propane/methane (C_3/C_1) compositional ratios (Table 6.4).

By considering the average C_2/C_1 and C_3/C_1 ratios for each seepage type, based on 238 seeps and more than 4,000 soil-gas data points geographically dispersed in various countries, the results suggested global emissions on the order of 2–4 Tg/year for ethane and 1–2.4 Tg/year for propane. The values represent 17 and 10 % of total ethane and propane sources, respectively. Here, to check the variability of the results in relation to the input parameters (methane flux and compositional ratios), a

Table 6.4 Global emissions of ethane and propane from geological sources, as compared to other natural and anthropogenic sources (Tg/year)

Type of seepage/ source	Geo-CH_4 emission	Median C_2/C_1	Ethane emission	Median C_3/C_1	Propane emission
Gas seeps	3–4	0.018	0.1	0.009	0.07–0.1
Mud volcanoes	10–20	0.0007	0.01–0.03	0.00008	0.002–0.004
Microseepage	10–25	0.068	1.3–3.2	0.031	0.8–2.13
Marine seepage	20	0.012	0.4	0.017	0.094
Geothermal areas	2.2–7.3	0.013	0.05–0.18	0.0013	0.01–0.03
Volcanoes	0.015	0.02	0.001	0.01	0.0004
Total geologic	45–76 (60)		~2–4		~1–2
Biogenic			*0.80*		*1.63*
Oceans			*0.78*		*1.06*
Anthropogenic			*5.70*		*6.51*
Forest—savanna burning			*2.29*		*0.41*
Total poet			9.57		9.61

Geological emissions were re-calculated from Etiope and Ciccioli (2009), based on the updated global methane emissions provided in Table 6.3. Median ethane/methane (C_2/C_1) and propane/methane (C_3/C_1) ratios were derived from published concentration data (more than 230 gas manifestations and more than 4,000 soil-gas samples), as described in Etiope and Ciccioli (2009). Biogenic, oceanic, anthropogenic, and biomass-burning emissions were obtained from the POET inventory, base year 2000 (GEIA-ACCENT database 2005). Note the low C_2/C_1 and C_3/C_1 ratios for mud volcanoes, which, as discussed in Sect. 5.3, are due to molecular fractionation

global C_2/C_1 and C_3/C_1 ratio average for seeping gas is considered. The ratios are 0.02 and 0.009, respectively, when all of the types of seepage and the data examined by Etiope and Ciccioli (2009) are considered. Using more recent estimates for global averaged methane emissions (~60 Tg/year), the result is 2.5 Tg of ethane and 1.4 Tg of propane per year, values within the previously derived range. Measurement uncertainty depends on (a) the uncertainty of the value for global methane emissions (as discussed above), (b) the statistical significance of the averaged C_2/C_1 and C_3/C_1 ratios which strongly depend on the relative contribution of both the microbial gas, which typically does not contain C_2 and C_3, and the thermogenic gas associated with oil or low maturity source rocks with the highest C_2/C_1 and C_3/C_1 ratios. In fact, the dataset considered by Etiope and Ciccioli (2009) did not include recently discovered seepage with high concentrations of ethane and propane, such as that from shales within the northern Appalachian basin (the Chestnut Ridge Park seep located in New York State, as described in Chap. 5; $C_1 + C_2$: 35 vol.%, equivalent to C_2/C_1 and C_3/C_1 ratios of 0.4 and 0.2, respectively; Etiope et al. 2013b). The addition of this type of $C_2 + C_3$ rich seepage, occurring in several fractured shale basins, will significantly increase global emission estimates.

The addition of geological seepage in atmospheric budgets of ethane and propane would fill, at least partially, the "missing source" gap (Kanakidou et al. 1991; Singh et al. 1994; Stein and Rudolph 2007), and would increase the relative importance of natural emissions as compared to anthropogenic ones.

Numerical uncertainties can be large. As a result, more precise evaluations should be made, although the potential for seepage as a global ethane and propane source is evident. As for the first studies of geological methane, this finding was viewed with scepticism and the atmospheric chemistry community did not adequately examine the results. In a modelling study, Pozzer et al. (2010) ignored the geological source because its emission distribution was hastily misjudged to be unknown. The results of model simulations did not need extra sources in addition to the three "canonic" ones (fossil-fuels, biomass burning, and oceans). As discussed in Chap. 2, the seepage emission distribution is actually well-known, and a geographical analysis of the potential sources of ethane and propane could be made on the basis of recent seep datasets (e.g., GLOGOS). The erroneous claim by Pozzer et al. (2010) that geological ethane and propane emissions are due to volcanoes, which in reality represent very insignificant contributions, as shown in Table 6.4, reveals a superficial understanding of this unconventional argument. New scientific ideas are often not quickly recognised and accepted, and that is normal. What matters is inspiring future research that may eventually demonstrate, not a priori, that a given hypotheses is actually erroneous.

6.5 Natural Seepage and CO_2 Geological Sequestration

Carbon Capture and Storage (CCS) is an integrated process aimed at capturing the CO_2 produced by various combustion and industrial processes and storing it in deep geological formations or below the sea floor (Hitchon et al. 1999; Bachu 2002; Metz et al. 2005). The final aim of CCS is to reduce climate changes induced by industrial CO_2 emissions. The process includes CO_2 capture, transport, and storage. The injection and storage of CO_2 in geological formations can be performed in the following types of systems: (a) deep saline aquifers, (b) productive petroleum (oil and gas) reservoirs, (c) depleted petroleum reservoirs, and (d) deep coal seams. The last three systems are clearly characterised by the occurrence of gaseous hydrocarbons and, as discussed in previous chapters, these systems can be a source of natural seepage. What occurs when CO_2 gas is injected into these hydrocarbon-bearing rocks (or potential seepage sources)? Describing and discussing the effectiveness of CCS and its physical-chemical processes, or the scientific debate surrounding the process is not the intention of this chapter. A vast array of literature is available on the arguments and discusses the political, strategic, economic, and environmental pros and cons (for example, see reports by the Metz et al. 2005 and Greenpeace 2008). Only the role that gas seepage can have on CCS is briefly discussed here.

The following two main arguments pose potential environmental risk in relation to gas seepage:

(1) If the hydrocarbon-bearing rocks slated to host CO_2 are not completely sealed and if indigenous reservoir gases can seep to the surface (as frequently occurs, as discussed in this book), injected CO_2 may follow the same pathway of naturally migrating hydrocarbons and again return to the surface.
(2) The injection of CO_2 in reservoir rocks increases fluid pressure within the reservoir. Existing gaseous hydrocarbons can be displaced by CO_2 and pushed into the seepage system and arrive at the surface. The result would be removing a greenhouse gas (CO_2) from the atmosphere while adding another greenhouse gas (CH_4) to the atmosphere that has a global warming potential 28 times higher than that of CO_2 on a per molecule basis.

While point (1), the leakage of injected CO_2, in other words the permanence of CO_2 storage, is the object of a wide variety of studies and discussions (e.g., Metz et al. 2005), point (2) is less considered (e.g., Klusman 2006).

Regarding point (1), several CO_2 storage and monitoring projects have successfully injected millions of tonnes of CO_2 into oil fields without detectable leakage (i.e., IEA GHG 2008). However, technical evaluations indicate the possibility of rapid CO_2 leakages through permeable faults. Expected leakage rates are less likely less than 1 % over 100–1,000 years (Metz et al. 2005), low enough not to induce increases in atmospheric CO_2, although forecasts for the long-term migration of CO_2 have been based on complex numerical simulations and not experimental data. Metz et al. (2005) actually acknowledge that experience with geological storage is limited and that leakage risks must be better assessed. Several studies have indicated the importance of assessing the presence of natural baseline seepage in areas where CCS is planned (e.g., Klusman 2011). Here, microseepage has been shown to be a diffuse and widely occurring process in all petroliferous basins. Even large and productive gas-oil fields are not completely sealed. As stated in Chap. 1, perfect sealing is not necessary for a commercial reservoir. The Petroleum Seepage System is an integral part of the Total Petroleum System (TPS). Therefore, it is not improbable that the petroleum reservoirs, still productive or depleted, selected for CO_2 storage have a seepage system. The concepts of TPS and frequent microseepage are, likely, not adequately considered in CCS evaluations. In fact, microseepage has been shown to exist in some oil-gas fields that are the object of Enhanced Oil recovery (EOR) and CO_2 storage programmes, where CO_2 is injected to achieve greater oil recovery. An example is that of Rangely Field in Colorado that, although selected for an EOR-CO_2 disposal project, is characterised by diffuse microseepage, mainly along a fault, with total emissions to the atmosphere of approximately 400 metric tonnes of methane every year from an area of ~ 78 km^2 (Klusman 2005, 2006).

Substantial overpressurisation is required to store appreciable amounts of CO_2 in hydrocarbon reservoirs. Overcoming hydrostatic pressure, as well as the consequences, is described in Chap. 3. Gases in a reservoir will tend to migrate by advection, vertically or laterally, along any permeable pathway in response to

pressure. At the depth of CO_2 storage, CO_2 will be a supercritical fluid, less dense than water, and will tend to dissolve in formation water, to react with carbonate minerals, and to precipitate solid phases. However, some CO_2 at the top of the gas cap may remain gaseous and rapidly leak through cap rocks.

Concerning point (2), it must also be noted that in case of effective CO_2 entrapment, methane seepage can be triggered. Methane is much less soluble and remains gaseous at high pressures. As a result, the overpressurisation induced by CO_2 will tend to drive insoluble buoyant methane upward. Additionally, CO_2-rich water is corrosive and can dissolve some minerals, possibly compromising the sealing of cap rocks, well casings, and cement plugs. The process can create new fractures and avenues for CO_2 and CH_4 to escape. The triggering of methane seepage in CCS would be the opposite process of what occurs with the extraction of oil and gas that, as discussed in Chap. 8, induces a decrease in seepage due to the lowering of reservoir fluid pressures.

In any case, in the absence of present seepage, it is very difficult to be sure that CO_2 or CH_4 will not leak in the future. Leakage occurring many years after gas storage in subsurface reservoirs has been documented (Coleman et al. 1977; Araktingi et al. 1984; AAPG Explorer 2002), although most of this data is proprietary company data that cannot be published for legal reasons. The 2008 Greenpeace report outlined a series of problems regarding CCS, as well as its risks and effectiveness for mitigating climate change. A key point, concerning the potential seepage of gas was that "even a tiny rate of leakage could undermine any putative climate benefit of CCS. A leakage rate of just 1 % on 600 Gt of stored carbon (2,160 $GtCO_2$ or about 100 years' worth of CO_2 emissions from fossil fuels), could release as much as 6 Gt of carbon (21.6 $GtCO_2$) per year back into the atmosphere. This is roughly equivalent to current total global CO_2 emissions from fossil fuels" (Greenpeace 2008).

References

AAPG Explorer (2002) Cores got to root of Kansas problem. http://archives.aapg.org/explorer/2002/07jul/core_preserv_side.cfm. Accessed Dec 2014

Araktingi RE, Benefield ME, Bessinyei Z, Coats KH, Tek MR (1984) Leroy storage facility, Uinta County, Wyoming: a case history of attempted gas-migration control. J Pet Technol 36:132–140

Archer D, Buffet B, Brovkin V (2009) Ocean methane hydrates as a slow tipping point in the global carbon cycle. Proc Natl Acad Sci USA 106:20596–20601

Bachu S (2002) Sequestration of CO_2 in geological media in response to climate change: road map for site selection using the transform of the geological space into the CO_2 phase space. Energy Convers Manag 43:87–102

Baciu C, Etiope G, Cuna S, Spulber L (2008) Methane seepage in an urban development area (Bacau, Romania): origin, extent and hazard. Geofluids 8:311–320

Bradley ES, Leifer I, Roberts DA, Dennison PE, Washburn L (2011) Detection of marine methane emissions with AVIRIS band ratios. Geophys Res Lett 38:L10702

Brunskill GJ, Burns KA, Zagorskis I (2011) Natural flux of greenhouse methane from the Timor Sea to the atmosphere. J Geophys Res 116:G02024

Burton MR, Sawyer GM, Granieri D (2013) Deep carbon emissions from volcanoes. Rev Mineral Geochem 75:323–354

Chang HC, Sung QC, Chen L (2010) Estimation of the methane flux from mud volcanoes along Chishan Fault, southwestern Taiwan. Environ Earth Sci 61:963–972

Chao H-C, You C-F, Sun C-H (2010) Gases in Taiwan mud volcanoes: chemical composition, methane carbon isotopes, and gas fluxes. Appl Geochem 25:428–436

Chilingar GV, Endres B (2005) Environmental hazards posed by the Los Angeles Basin urban oilfields: an historical perspective of lessons learned. Environ Geol 47:302–317

Ciais P, Sabine C, Bala G, Bopp L, Brovkin V, Canadell J, Chhabra A, DeFries R, Galloway J, Heimann M, Jones C, Le Quéré C, Myneni RB, Piao S, Thornton P (2013) Carbon and other biogeochemical cycles. In: Stocker TF et al (eds) Climate change 2013: the physical science basis. Contribution of working group I to the fifth assessment report of IPCC, Cambridge University Press, Cambridge

Cicerone RJ, Oremland RS (1988) Biogeochemical aspects of atmospheric methane 1978–1983. J Atmos Chem 4:43–67

Ciotoli G, Etiope G, Florindo F, Marra F, Ruggiero L, Sauer PE (2013) Sudden deep gas eruption nearby Rome's airport of Fiumicino. Geophys Res Lett 40:5632–5636

Clark JF, Washburn L, Schwager K (2010) Variability of gas composition and flux intensity in natural marine hydrocarbon seeps. Geo-Mar Lett 30:379–388

Coleman DD, Meents WF, Liu DL, Keogh RA (1977) Isotopic identification of leakage gas from underground storage reservoirs—a progress report. Report 111, Illinois state geological survey

Dando PR, Jensen P, O'Hara SCM, Niven SJ, Schmaljohann R, Schuster U, Taylor LJ (1994) The effects of methane seepage at an intertidal/shallow subtidal site on the shore of the Kattegat, Vendsyssel, Denmark. Bull Geol Soc Den 41:65–79

Darrah TH, Vengosh A, Jackson RB, Warner NR, Poreda RJ (2014) Noble gases identify the mechanisms of fugitive gas contamination in drinking-water wells overlying the Marcellus and Barnett Shales. Proc Natl Acad Sci USA 111:14076–14081

Day SJ, Dell'Amico M, Fry R, Javarnmard Tousi H (2013) Fugitive methane emissions from coal seam gas production in Australia. In: International conference on coal science and technology, Penn State University, Pennsylvania

Denman KL, Brasseur G, Chidthaisong A, Ciais P, Cox PM, Dickinson RE, Hauglustaine D, Heinze C, Holland E, Jacob D, Lohmann U, Ramachandran S, da Silva Dias PL, Wofsy SC, Zhang X (2007) Couplings between changes in the climate system and biogeochemistry. In: Solomon S, Qin D, Manning M et al (eds) Climate change 2007: the physical science basis. Cambridge University Press, Cambridge, pp 499–587

Dimitrov L (2002) Mud volcanoes – the most important pathway for degassing deeply buried sediments. Earth Sci Rev 59:49–76

Duffy M, Kinnaman FS, Valentine DL, Keller EA, Clark JF (2007) Gaseous emission rates from natural petroleum seeps in the upper Ojai Valley, California. Environ Geosci 14:197–207

EEA (2004) Joint EMEP/CORINAIR atmospheric emission inventory guidebook, 4th edn. European Environment Agency, Copenhagen. http://reports.eea.eu.int/EMEPCORINAIR4/eni

Emeis K-C, Brüchert V, Currie B, Endler R, Ferdelman T, Kiessling A, Leipe T, Noli-Peard K, Struck U, Vogt T (2004) Shallow gas in shelf sediments of the Namibian coastal upwelling ecosystem. Cont Shelf Res 24:627–642

EMEP/EEA (European Monitoring and Evaluation Programme/EEA) (2009) EMEP/EEA air pollutant emission inventory guidebook—2009. Technical guidance to prepare national emission inventories, EEA technical report no 6/2009, European Environment Agency, Copenhagen. doi:10.2800/23924

Etiope G (2009) Natural emissions of methane from geological seepage in Europe. Atmos Environ 43:1430–1443

Etiope G (2010) Geological methane. Chapter 4. In: Reay D, Smith P, van Amstel A (eds) Methane and climate change, Earthscan, London, pp 42–61

Etiope G (2012) Methane uncovered. Nature Geosci 5:373–374

Etiope G, Ciccioli P (2009) Earth's degassing—a missing ethane and propane source. Science 323:478

Etiope G, Klusman RW (2002) Geologic emissions of methane to the atmosphere. Chemosphere 49:777–789

Etiope G, Klusman RW (2010) Microseepage in drylands: flux and implications in the global atmospheric source/sink budget of methane. Global Planet Change 72:265–274

Etiope G, Milkov AV (2004) A new estimate of global methane flux from onshore and shallow submarine mud volcanoes to the atmosphere. Environ Geol 46:997–1002

Etiope G, Schoell M (2014) Abiotic gas: atypical but not rare. Elements 10:291–296

Etiope G, Caracausi A, Favara R, Italiano F, Baciu C (2002) Methane emission from the mud volcanoes of Sicily (Italy). Geophys Res Lett 29. doi:10.1029/2001GL014340

Etiope G, Feyzullaiev A, Baciu CL, Milkov AV (2004) Methane emission from mud volcanoes in eastern Azerbaijan. Geology 32:465–468

Etiope G, Papatheodorou G, Christodoulou D, Favali P, Ferentinos G (2005) Gas hazard induced by methane and hydrogen sulfide seepage in the NW Peloponnesus petroliferous basin (Greece). Terr Atmos Ocean Sci 16:897–908

Etiope G, Papatheodorou G, Christodoulou D, Ferentinos G, Sokos E, Favali P (2006) Methane and hydrogen sulfide seepage in the NW Peloponnesus petroliferous basin (Greece): origin and geohazard. AAPG Bull 90:701–713

Etiope G, Martinelli G, Caracausi A, Italiano F (2007a) Methane seeps and mud volcanoes in Italy: gas origin, fractionation and emission to the atmosphere. Geophys Res Lett 34:L14303. doi:10.1029/2007GL030341

Etiope G, Fridriksson T, Italiano F, Winiwarter W, Theloke J (2007b) Natural emissions of methane from geothermal and volcanic sources in Europe. J Volcanol Geotherm Res 165:76–86

Etiope G, Lassey KR, Klusman RW, Boschi E (2008) Reappraisal of the fossil methane budget and related emission from geologic sources. Geophys Res Lett 35:L09307. doi:10.1029/2008GL033623

Etiope G, Zwahlen C, Anselmetti FS, Kipfer R, Schubert CJ (2010) Origin and flux of a gas seep in the northern Alps (Giswil, Switzerland). Geofluids 10:476–485

Etiope G, Nakada R, Tanaka K, Yoshida N (2011a) Gas seepage from Tokamachi mud volcanoes, onshore Niigata Basin (Japan): origin, post-genetic alterations and CH_4-CO_2 fluxes. Appl Geochem 26:348–359

Etiope G, Schoell M, Hosgormez H (2011b) Abiotic methane flux from the Chimaera seep and Tekirova (Turkey): understanding gas exhalation from low temperature serpentinization and implications for Mars. Earth Planet Sci Lett 310:96–104

Etiope G, Christodoulou D, Kordella S, Marinaro G, Papatheodorou G (2013a) Offshore and onshore seepage of thermogenic gas at Katakolo Bay (western Greece). Chem Geol 339:115–126

Etiope G, Drobniak A, Schimmelmann A (2013b) Natural seepage of shale gas and the origin of eternal flames in the northern Appalachian Basin, USA. Mar Pet Geol 43:178–186

Friedrich J, Janssen F, Aleynik D, Bange HW, Boltacheva N, Çağatay MN, Dale AW, Etiope G, Erdem Z, Geraga M, Gilli A, Gomoiu MT, Hall POJ, Hansson D, He Y, Holtappels M, Kirf MK, Kononets M, Konovalov S, Lichtschlag A, Livingstone DM, Marinaro G, Mazlumyan S, Naeher S, North RP, Papatheodorou G, Pfannkuche O, Prien R, Rehder G, Schubert CJ, Soltwedel T, Sommer S, Stahl H, Stanev EV, Teaca A, Tengberg A, Waldmann C, Wehrli B, Wenzhöfer F (2014) Investigating hypoxia in aquatic environments: diverse approaches to addressing a complex phenomenon. Biogeosciences 11:1215–1259

Frunzeti N, Baciu C, Etiope G, Pfanz H (2012) Geogenic emission of methane and carbon dioxide at Beciu mud volcano (Berca-Arbanasi hydrocarbon-bearing structure, Eastern Carpathians, Romania). Carpathian J Earth Environ Sci 7:159–166

GEIA-ACCENT database (2005) An international cooperative activity of AIMES/IGBP, sponsored by the ACCENT EU network of excellence. http://www.geiacenter.org and http://www.accent-network.org

Greenpeace (2008) False hope. Why carbon capture and storage won't save the climate. Amsterdam, the Netherlands, Greenpeace. http://www.greenpeace.org/international/press/reports/false-hope. Accessed October 2014

Guliyev IS, Feizullayev AA (1997) All about mud volcanoes. Baku Pub House, NAFTA-Press, Baku, p 120

Hitchon B, Gunter WD, Gentzis T, Bailey RT (1999) Sedimentary basins and greenhouse gases: a serendipitous association. Energy Convers Manag 40:825–843

Hong WL, Etiope G, Yang TF, Chang PY (2013) Methane flux of miniseepage in mud volcanoes of SW Taiwan: comparison with the data from Europe. J Asian Earth Sci 65:3–12

Hornafius JS, Quigley D, Luyendyk BP (1999) The world's most spectacular marine hydrocarbon seeps (Coal Oil Point, Santa Barbara Channel, California): quantification of emissions. J Geophys Res 20(C9):20703–20711

Hovland M, Judd AG (1988) Seabed pockmarks and seepages: impact on geology, biology and the marine environment. Graham and Trotman, London, p 293

Hovland M, Judd AG, Burke RA Jr (1993) The global flux of methane from shallow submarine sediments. Chemosphere 26:559–578

IEA GHG (2008) Geologic storage of carbon dioxide—staying safely underground. International Energy Agency Greenhouse Gas R&D Programme, Cheltenham. http://www.ieagreen.org.uk/glossies/geostoragesfty.pdf

Jackson RB, Vengosh A, Darrah TH, Warner NR, Down A, Poreda RJ, Osborn SG, Zhao K, Karr JD (2013) Increased stray gas abundance in a subset of drinking water wells near Marcellus shale gas extraction. Proc Natl Acad Sci USA 110:11250–11255

Jessen GL, Pantoja S, Gutierrez MA, Quiñones RA, Gonzalez RR, Sellanes J, Kellermann MY, Hinrichs K-U (2011) Methane in shallow cold seeps at Mocha Island off central Chile. Cont Shelf Res 31:574–581

Jones VT (2000) Subsurface geochemical assessment of methane gas occurrences. Playa Vista development. First phase project. Los Angeles, CA. Report by Exploration Technologies, Inc. http://eti-geochemistry.com/Report-04-2000

Judd AG (2004) Natural seabed seeps as sources of atmospheric methane. Environ Geol 46:988–996

Judd AG, Davies J, Wilson J, Holmes R, Baron G, Bryden I (1997) Contributions to atmospheric methane by natural seepages on the UK continental shelf. Mar Geol 137:165–189

Judd AG, Hovland M, Dimitrov LI, Garcia Gil S, Jukes V (2002) The geological methane budget at continental margins and its influence on climate change. Geofluids 2:109–126

Kanakidou M, Singh HB, Valentin KM, Crutzen PJ (1991) A 2-dimensional study of ethane and propane oxidation in the troposphere. J Geophys Res 96:15395–15413

Kessler JD, Reeburgh WS, Southon J, Varela R (2005) Fossil methane source dominates Cariaco Basin water column methane geochemistry. Geophys Res Lett 32:L12609

Kessler JD, Valentine DL, Redmond MC, Du M, Chan EW, Mendes SD, Quiroz EW, Villanueva CJ, Shusta SS, Werra LM, Yvon-Lewis SA, Weber TC (2011) A persistent oxygen anomaly reveals the fate of spilled methane in the deep Gulf of Mexico. Science 331:312–315

Klusman RW (2005) Baseline studies of surface gas exchange and soil-gas composition in preparation for CO2 sequestration research: Teapot Dome, Wyoming. AAPG Bull 89:981–1003

Klusman RW (2006) Detailed compositional analysis of gas seepage at the national carbon storage test site, Teapot Dome, Wyoming, USA. Appl Geochem 21:1498–1521

Klusman RW (2011) Comparison of surface and near-surface geochemical methods for detection of gas microseepage from carbon dioxide sequestration. Int J Greenhouse Gas Control 5:1369–1392

Klusman RW, Jakel ME (1998) Natural microseepage of methane to the atmosphere from the Denver-Julescburg basin, Colorado. J Geophys Res 103(D21):28041–28045

Klusman RW, Jakel ME, LeRoy MP (1998) Does microseepage of methane and light hydrocarbons contribute to the atmospheric budget of methane and to global climate change? Assoc Petrol Geochem Explor Bull 11:1–55

Klusman RW, Leopold ME, LeRoy MP (2000) Seasonal variation in methane fluxes from sedimentary basins to the atmosphere: results from chamber measurements and modeling of transport from deep sources. J Geophys Res 105(D20):24661–24670

Kopf A, Delisle G, Faber E, Panahi B, Aliyev CS, Guliyev I (2009) Long-term in situ monitoring at Dashgil mud volcano, Azerbaijan: a link between seismicity, pore-pressure transients and methane emission. Int J Earth Sci 99:227–240 (and erratum 99:241)

Kvenvolden KA, Rogers BW (2005) Gaia's breath—global methane exhalations. Mar Pet Geol 22:579–590

Kvenvolden KA, Lorenson TD, Reeburgh W (2001) Attention turns to naturally occurring methane seepage. EOS 82:457

Lacroix AV (1993) Unaccounted-for sources of fossil and isotopically enriched methane and their contribution to the emissions inventory: a review and synthesis. Chemosphere 26:507–557

Lassey KR, Lowe DC, Smith AM (2007) The atmospheric cycling of radiomethane and the fossil fraction of the methane source. Atm Chem Phys 7:2141–2149

Leifer I, Patro RK (2002) The bubble mechanism for methane transport from the shallow sea bed to the surface: a review and sensitivity study. Cont Shelf Res 22:2409–2428

Lelieveld J, Crutzen PJ, Dentener FJ (1998) Changing concentration, lifetime and climate forcing of atmospheric methane. Tellus 50B:128–150

LTE (2007) Phase II Raton Basin gas seep investigation Las Animas and Huerfano Counties, Colorado, project #1925 oil and gas conservation response fund. http://cogcc.state.co.us/Library/Ratoasin/Phase%20II%20Seep%20Investigation%20Final%20Report.pdf

Lundegard PD, Sweeney RE, Ririe GT (2000) Soil gas methane at petroleum contaminated sites: forensic determination of origin and source. Environ Forensics 1:3–10

MacDonald IR, Sassen ILR, Stine P, Mitchell R, Guinasso NJ (2002) Transfer of hydrocarbons from natural seeps to the water column and atmosphere. Geofluids 2:95–107

Mazzini A, Etiope G, Svensen H (2012) A new hydrothermal scenario for the 2006 Lusi eruption, Indonesia. Insights from gas geochemistry. Earth Planet Sci Lett 317–318:305–318

McGinnis DF, Greinert J, Artemov Y, Beaubien SE, Wüest A (2006) Fate of rising methane bubbles in stratified waters: how much methane reaches the atmosphere? J Geophys Res 111:C09007

Metz B, Davidson O, de Coninck HCM et al (eds) (2005) IPCC special report on carbon dioxide capture and storage. Prepared by working group III of the intergovernmental panel on climate change. Cambridge University Press, Cambridge, p 442

Molofsky LJ, Connor JA, Wylie AS, Wagner T, Farhat SK (2013) Evaluation of methane sources in groundwater in northeastern Pennsylvania. Groundwater 51:333–349

Monteiro PMS, van der Plas A, Mohrholz V, Mabille E, Pascall A, Joubert W (2006) Variability of natural hypoxia and methane in a coastal upwelling system: oceanic physics or shelf biology? Geophys Res Lett 33:L16614. doi:10.1029/2006GL026234

Mörner NA, Etiope G (2002) Carbon degassing from the lithosphere. Global Planet Change 33:185–203

Nagao M, Takatori T, Oono T, Iwase H, Iwadate K, Yamada Y, Nakajima M (1997) Death due to a methane gas explosion in a tunnel on urban reclaimed land. Am J Forensic Med Pathol 18:135–139

Olivier JGJ, Bouwman AF, van der Maas CWM, Berdowski JJM, Veldt C, Bloos JPJ, Visschedijk AJJ, Zandveld PYJ, Haverlag JL (1996) Description of EDGAR version 2.0: a set of global inventories of greenhouse gases and ozone-depleting substances for all anthrophogenic and most natural sources on a per country 1×1 grid, RIVM Rep. 771060002, Rijksinstituut, Bilthoven, The Netherlands

Osborn SG, Vengosh A, Warner NR, Jackson RB (2011) Methane contamination of drinking water accompanying gas-well drilling and hydraulic fracturing. Proc Natl Acad Sci USA 108:8172–8176

Paull CK, Brewer PG, Ussler W III, Peltzer ET, Rehder G, Clague D (2003) An experiment demonstrating that marine slumping is a mechanism to transfer methane from seafloor gas-hydrate deposits into the upper ocean and atmosphere. Geo-Mar Lett 22:198–203

Pozzer A, Pollmann J, Taraborrelli D, Jöckel P, Helmig D, Tans P, Hueber J, Lelieveld J (2010) Observed and simulated global distribution and budget of atmospheric C_2-C_5 alkanes. Atmos Chem Phys 10:4403–4422

Prather M, Ehhalt D, Dentener F, Derwent RG, Dlugokencky E, Holland E, Isaksen ISA, Katima J, Kirchhoff V, Matson P, Midgley PM, Wang M (2001) Chapter 4. Atmospheric chemistry and greenhouse gases. In: Houghton JT et al (eds) Climate change 2001: the scientific basis, Cambridge University Press, Cambridge, pp 239–287

Ryan S, Dlugokencky EJ, Tans PP, Trudeau ME (2006) Mauna Loa volcano is not a methane source: implications for Mars. Geophys Res Lett 33:L12301. doi:10.1029/2006GL026223

Schmale O, Greinert J, Rehder G (2005) Methane emission from high-intensity marine gas seeps in the Black Sea into the atmosphere. Geophys Res Lett 32:L07609. doi:10.1029/2004GL021138

Schneider von Deimling J, Rehder G, Greinert J, McGinnnis DF, Boetius A, Linke P (2011) Quantification of seep-related methane gas emissions at Tommeliten, North Sea. Cont Shelf Res 31:867–878

Shakhova N, Semiletov I, Salyuk A, Yusupov V, Kosmach D, Gustafsson O (2010) Extensive methane venting to the atmosphere from sediments of the east Siberian Arctic shelf. Science 327:1246–1250

Singh HB, O'Hara D, Herlth D, Sachse W, Blake DR, Bradshaw JD, Kanakidou M, Crutzen PJ (1994) Acetone in the atmosphere: distribution, sources, and sinks. J Geophys Res 99:1805–1819

Sobkowicz JC, Morgenstern NR (1984) The undrained equilibrium behavior of gassy sediments. Can Geotech J 21:439–448

Solomon EA, Kastner M, MacDonald IR, Leifer I (2009) Considerable methane fluxes to the atmosphere from hydrocarbon seeps in the Gulf of Mexico. Nat Geosci 2:561–565

Spulber L, Etiope G, Baciu C, Malos C, Vlad SN (2010) Methane emission from natural gas seeps and mud volcanoes in Transylvania (Romania). Geofluids 10:463–475

Stein O, Rudolph J (2007) Modeling and interpretation of stable carbon isotope ratios of ethane in global chemical transport models. J Geophys Res 112:D14308. doi:10.1029/2006JD008062

Tang J, Yin H, Wang G, Chen Y (2010) Methane microseepage from different sectors of the Yakela condensed gas field in Tarim Basin, Xinjiang, China. Appl Geochem 25:1257–1264

Tassi F, Fiebig J, Vaselli O, Nocentini M (2012) Origins of methane discharging from volcanic-hydrothermal, geothermal and cold emissions in Italy. Chem Geol 310–311:36–48

Thielemann T, Lucke A, Schleser GH, Littke R (2000) Methane exchange between coal-bearing basins and the: the Ruhr Basin and the lower Rhine Embayment, Germany. Org Geochem 31:1387–1408

U.S. Environmental Protection Agency (2010) Methane and nitrous oxide emissions from natural sources, EPA Rep. 430-R-10-001. Off. of Atmos. Programs, Washington, DC

Vidic RD, Brantley SL, Vandenbossche JM, Yoxtheimer D, Abad JD (2013) Impact of shale gas development on regional water quality. Science 340. doi:10.1126/science.1235009

Walter Anthony KM, Anthony P, Grosse G, Chanton J (2012) Geologic methane seeps along boundaries of Arctic permafrost thaw and melting glaciers. Nat Geosci 5:419–426

Warner NR, Jackson RB, Darrah TH, Osborn SG, Down A, Zhao K, White A, Vengosh A (2012) Geochemical evidence for possible natural migration of Marcellus formation brine to shallow aquifers in Pennsylvania. Proc Natl Acad Sci USA 109:11961–11966

Warner NR, Kresse TM, Hays PD, Down A, Karr JD, Jackson RB, Vengosh A (2013) Geochemical and isotopic variations in shallow groundwater in areas of the Fayetteville Shale development, north-central Arkansas. Appl Geochem 35:207–220

Weber TC, Mayer L, Jerram K, Beaudoin J, Rzhanov Y, Lovalvo D (2014) Acoustic estimates of methane gas flux from the seabed in a 6000 km2 region in the northern Gulf of Mexico. Geochem Geophys Geosyst 15:1911–1925

Wuebbles DJ, Hayhoe K (2002) Atmospheric methane and global change. Earth-Sci Rev 57:177–210

Yamamoto A, Yamanaka Y, Tajika E (2009) Modeling of methane bubbles released from large sea-floor area: condition required for methane emission to the atmosphere. Earth Planet Sci Lett 284:590–598

Yang TF, Yeh GH, Fu CC, Wang CC, Lan TF, Lee HF, Chen CH, Walia V, Sung QC (2004) Composition and exhalation flux of gases from mud volcanoes in Taiwan. Environ Geol 46:1003–1011

Chapter 7
Seepage in Serpentinised Peridotites and on Mars

Thus far, this book has mainly addressed the classical seepage of natural gas of biotic (microbial and thermogenic) origin in sedimentary rocks. However, it is also known that methane and other light hydrocarbons can be abiotically produced (i.e., by chemical reactions that do not directly involve organic matter). Abiotic production may occur over a wide range of temperatures and pressures and within a variety of geological systems. Two main classes of abiotic CH_4 generation processes can be distinguished, magmatic and gas-water-rock interactions. For details, the reader is referred to the review of Etiope and Sherwood Lollar (2013). Here, it is important to keep in mind that while magmatic or mantle-derived CH_4 is abiotic, not all abiotic CH_4 is mantle derived. Magmatic and high temperature hydrothermal processes in volcanic and geothermal systems produce a gas mixture that is mainly composed of carbon dioxide (CO_2), while abiotic methane is a very minor component. Indeed, field observations suggest that the majority of abiotic gas on Earth's surface is produced by low-temperature, gas–water–rock reactions. Of particular interest are the Fischer-Tropsch Type (FTT) reactions, the mechanism most widely invoked for explaining large quantities of abiotic CH_4 seeping to the surface. In the sub-chapters that follow, only CH_4-rich abiotic gas seeping to the surface is considered. Such seepage generally occurs in serpentinised ultramafic rocks (peridotites). Serpentinisation (the hydration of olivine and pyroxene minerals, which leads to the formation of H_2 and the subsequent production of CH_4 through FTT synthesis) is considered a fundamental step in the origin of life, representing the primordial passage from inorganic to organic chemistry (Russell et al. 2010). Serpentinisation can also be a source of methane in atypical petroleum systems where hydrocarbon reservoirs are formed by or are adjacent to igneous rocks (Sect. 7.1.2), and a potential source of methane on other planets, such as Mars (Sect. 7.2).

G. Etiope, *Natural Gas Seepage*, DOI 10.1007/978-3-319-14601-0_7

7.1 Seeps and Springs in Active Serpentinisation Systems

7.1.1 Where Abiotic Methane Is Seeping

Abiotic methane seeps have been discovered in an increasing number of countries, beginning from the 1980s with the pioneering work of Abrajano et al. (1988) and Lyon et al. (1990) who reported unusual gas, with large concentrations of CH_4 and H_2, issuing from ultramafic rocks in the Philippines (the Los Fuegos Eternos of Zambales) and New Zealand (Poison Bay). Similar gas was then reported in Oman (Fritz et al. 1992; in the Semail ophiolite springs) and in Turkey (Hosgormez et al. 2008; Etiope et al. 2011b; in Chimaera fires; Fig. 7.1). Recent isotopic analyses have also indicated a dominant abiotic origin for methane seeping from serpentinised

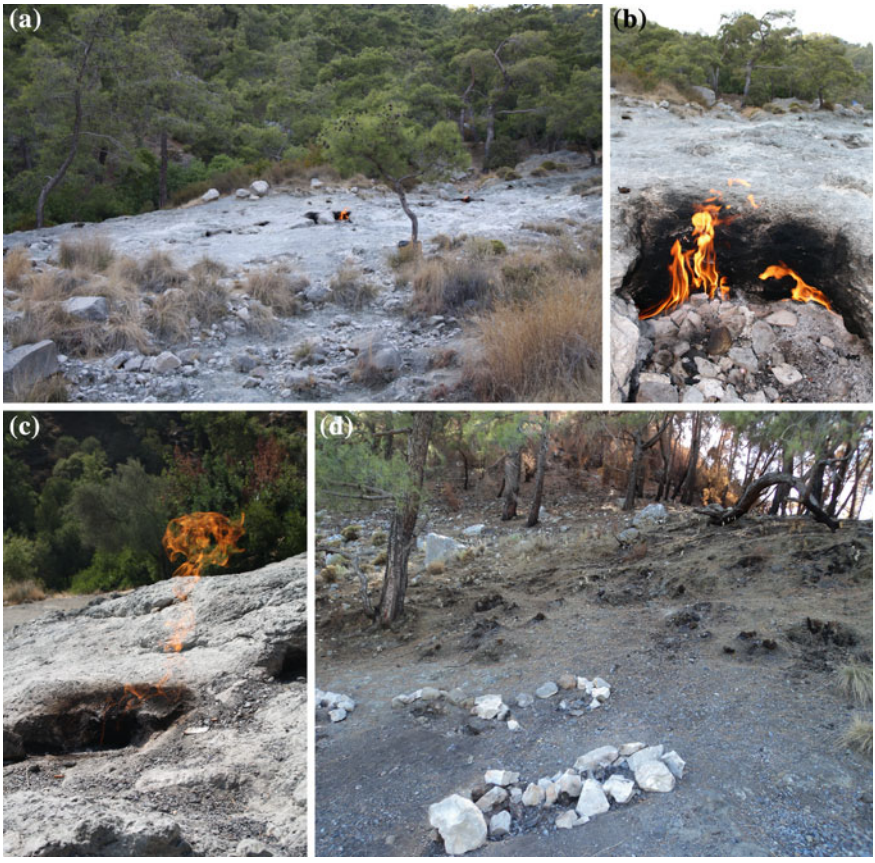

Fig. 7.1 The burning gas seep of Chimaera, near Cirali (Turkey). **a** A general view of the peridotite outcrop with the natural flames; **b–c** two perennial flames from fractured ground; **d** a second seepage site, with burned trees, on the Olympos Mountain a few hundreds meters north of Chimaera

peridotites in Italy (Boschetti et al. 2013; the Genova hyperalkaline springs, Fig. 7.2d), Greece (Etiope et al. 2013b; the Othrys ophiolite), Portugal (Etiope et al. 2013c; the Cabeço de Vide springs), Japan (Suda et al. 2014; the Hakuba-Happo springs), Spain (Etiope et al. 2014; the Ronda peridotites; Fig. 7.2b–c), the United Arab Emirates (Etiope et al. 2015; Fig. 7.2a), and again in Turkey (Yuce et al. 2014; Amik Basin) and New Zealand (Pawson et al. 2014; Dun Mountain ophiolite). Gas in similar serpentinised rocks has also been reported in Serbia (Milenic et al. 2009; the Zlatibor ophiolite), Norway (Okland et al. 2012; the Leka ophiolite), Canada (Szponar et al. 2013; the Tablelands), California (Morrill et al. 2013; The Cedars springs), New Caledonia (Monnin et al. 2014; Prony Bay), and Costa Rica (Sanchez-Murillo et al. 2014; the Santa Elena ophiolite). However, the isotopic data required

Fig. 7.2 Gas-bearing springs **a** in the United Arab Emirates (Al Farfar; photo by J. Judas), **b–c** in the Ronda peridotite massif, Spain (Del Puerto Spring with bubble plumes; photos by I. Vadillo), and **d** near Genova, Italy (the bubbling vent at Acquasanta; photo by M. Whiticar)

Table 7.1 A list of land-based serpentinisation sites where methane seepage (or transport by hyperalkaline waters) has been documented (updated December, 2014)

Country	Site	Setting	References
Methane C–H isotopes determined			
Greece	Othrys Mt. (Archani, Ekkara)	Ophiolite	Etiope et al. (2013b)
Italy	Voltri-Genova (e.g., Acquasanta)	Ophiolite	Boschetti et al. (2013)
Japan	Hakuba-Happo	Orogenic massif	Suda et al. (2014)
New Zealand	Poison Bay	Ophiolite	Lyon et al. (1990)
New Zealand	Red Hills, Dun Mountain	Ophiolite	Pawson et al. (2014)
Oman	Semail (e.g., Al Khaoud, Nizwa)	Ophiolite	Fritz et al. (1992), Boulart et al. (2013)
Philippines	Zambales (Los Fuegos Eternos)	Ophiolite	Abrajano et al. (1988)
Portugal	Cabeço de Vide	Igneous intrusion	Etiope et al. (2013c)
Spain	Ronda peridotites	Orogenic massif	Etiope et al. (2014)
Turkey	Chimaera	Ophiolite	Etiope et al. (2011b)
Turkey	Amik Basin (Kurtbagi, Tahtakopru)	Ophiolite	Yuce et al. (2014)
U.A.Emirates	Al Farfar	Ophiolite	Etiope et al. (2015)
Incomplete or missing C–H isotope analyses			
Canada	Tablelands	Ophiolite	Szponar et al. (2013)
Costa Rica	Santa Elena	Ophiolite	Sanchez-Murillo et al. (2014)
New Caledonia	Prony Bay Fiordland	Ophiolite	Monnin et al. (2014)
Norway	Leka	Ophiolite	Okland et al. (2012)
Philippines	Zambales (Manleluag)	Ophiolite	Meyer-Dombard et al. (2013)
Philippines	Palawan (Brooke's Point)	Ophiolite	Meyer-Dombard et al. (2013)
Serbia	Zlatibor	Ophiolite	Milenic et al. (2009)
US—California	The Cedars	Ophiolite	Morrill et al. (2013)

for CH_4 origin assessments are missing or incomplete (for some of these studies only the stable carbon isotopic composition of CH_4 is available). The list of known methane-bearing serpentinisation seeps and springs, updated for 2014, is reported in Table 7.1. Geographic distribution of those for which the abiotic origin of CH_4 is suspected at least on the basis of the C and H isotopic composition, is shown in Chap. 2, Fig. 2.8.

Land-based peridotites generally belong to an ophiolite (mantle rock obducted on continents), an orogenic peridotite massif, or a batolith intrusion. Abiotic gas can reach the surface while dissolved in groundwater (with concentrations on the order of 0.1–10 mg CH_4/L in springs or in shallow groundwater boreholes), or as a free phase in gas seeps (up to 87 vol.%) and microseepage in the soil (see below). Groundwater is typically of meteoric origin, of the calcium hydroxide (Ca^{2+}–OH^-) hydrochemical type and hyperalkaline, with a pH > 9; these are specific features of active serpentinisation systems resulting from the liberation of OH^- and Ca^{2+} during the hydration of olivine and pyroxenes. The hydrochemistry details of these serpentinisation waters have been reported, for example, in Barnes and O'Neil (1969), Bruni et al. (2002), and Marques et al. (2008). Emissions of abiotic gas related to serpentinisation have also been discovered at a few deep-sea hydrothermal sites located in the Mid-Atlantic Ridge (the Lost City, Logatchev, Rainbow, Ashadze), the Central Indian Ridge (Kairei), and the Mariana Forearc (Charlou et al. 2002; Proskurowski et al. 2008; Schrenk et al. 2013), although the complete C and H isotopic composition of CH_4, at the time this chapter was written, is only available for the Lost City and Logatchev. Abiotic methane is also known to occur in deep boreholes within Precambrian crystalline shields (e.g., Sherwood Lollar et al. 1993) although seepage to the surface has, thus far, not been reported.

In practice, most abiotic methane seeps have been observed on land in correspondence with serpentinised ultramafic rocks along the Alpine-Himalayan orogenic belt (Jurassic-Cretaceous), the Western Pacific and Cordilleran ophiolite belts (Paleozoic-Tertiary), and the Paleozoic plutons. The following chapters refer to the methane observed in these environments, not to gas located in high temperature deep-sea serpentinisation settings for which the reader may refer to the review paper of Schrenk et al. (2013).

7.1.2 How Abiotic Methane in Land-Based Serpentinisation Systems Is Formed

Abiotic methane formation was first recognized in the laboratory in 1913 when Paul Sabatier received the Nobel Prize for discovering that methane can be generated by reacting CO_2 and H_2 with metal catalysts. In 1925, Franz Fischer and Hans Tropsch succeeded in synthesizing more complex hydrocarbons using CO and H_2. The Sabatier reaction, also known as "hydrogenation of CO_2", and the Fischer-Tropsch reaction (with CO) are today cumulatively termed *Fischer-Tropsch Type* (FTT) reactions.

The origin of abiotic gas in serpentinisation systems is generally attributed to these FTT reactions, involving H_2 and a carbon-bearing compound (CO_2, CO, HCOOH), as discussed in a wide array of scientific literature (Etiope and Sherwood Lollar 2013; McCollom 2013, and references therein). A general form of the FTT reaction is the following:

$$nCO + (2n + 1)H_2 \rightarrow C_nH_{(2n+2)} + nH_2O \quad (7.1)$$

or for CO_2, in aqueous solutions:

$$CO_2(aq) + (2 + m/2n)H_2(aq) = (1/n)C_nH_m + 2H_2O \quad (7.2)$$

and in the gas-phase:

$$CO_2 + 4H_2 = CH_4 + 2H_2O \quad (7.3)$$

The last reaction is also known as the Sabatier reaction. H_2 is directly produced via serpentinisation, peridotite (olivine and pyroxene) hydration driven by seawater (in submarine environment) or meteoric water (on land) (e.g., McCollom and Seewald 2007; Schrenk et al. 2013). An alternative mechanism for CH_4 production could be the one occurring via the hydration of olivine in the presence of CO_2, without the initial mediation of H_2; such a process is theoretically possible (Oze and Sharma 2005; Etiope et al. 2013b; Suda et al. 2014) but not easily identifiable (Whiticar and Etiope 2014a) and has not, to date, been demonstrated in the laboratory.

The abiotic synthesis of methane following serpentinisation is considered to be a fundamental step in the prebiotic chemistry and origin of living matter (Russell et al. 2010). Serpentinisation during the Archean may have provided the necessary reducing and high-pH conditions and the relatively low temperatures appropriate for supporting early life. Methane, in particular, was an effective energy source (electron donor) for the development of biomolecules and microrganisms on early Earth. Whether this occurred in ocean floor hydrothermal systems or in continental rocks is an open question.

FTT reactions take place on the surface of a metal (catalyst), lowering the activation energy needed for the reaction (Fig. 7.3); the higher the temperature, the easier methane production.

Many metals (Fe, Ni, Co, and Cr) are known to effectively catalyse the reaction at high temperatures, generally above 200 °C (e.g., Horita and Berndt 1999; Taran et al. 2007; McCollom 2013). FTT reactions are very sluggish in aqueous solutions. As a result, high temperatures are even more important for water saturated rocks. Nevertheless, land-based serpentinisation rock systems are characterised by relatively low temperatures, generally below 100 °C (Bruni et al. 2002; Etiope et al.

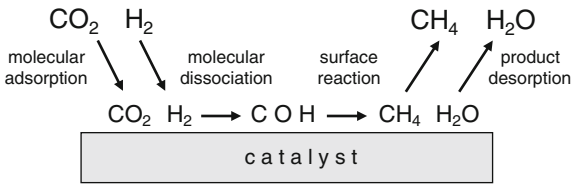

Fig. 7.3 Sketch of methane production via Sabatier reaction, between CO_2 and H_2, catalysed on a metal surface

2013b; Suda et al. 2014; Monnin et al. 2014). The thickness of ophiolite nappes, for example, is generally on the order of a few km, up to 4–5 km, and low geothermal gradients, typical of these areas, suggest maximum temperatures at the deepest ultramafic rock sectors of 100–120 °C. The maximum temperature, at the base of the 3-km deep Tekirova ophiolite in Turkey (where the Chimaera seep is located), is 80 °C (Etiope et al. 2011b). FTT reactions and methane production at such low temperatures are not obvious. Therefore, the following series of questions arise:

(a) Was methane produced at higher temperatures (>200 °C) when peridotites were still influenced by ocean hydrothermal conditions (and the gas was preserved after peridotite obduction or emplacement in the orogen)?
(b) Was methane produced at higher temperatures (>200 °C) during the early stages of peridotite emplacement on land, for example, near the high-temperature "metamorphic sole" (the shear zone) at the base of the ophiolite?
(c) If methane was, instead, formed after the peridotites were emplaced on the continent, at present-day temperatures, did the FTT reaction take place in dry rock or in an aqueous solution?
(d) And, if so, what catalyst was capable of supporting the reaction at temperatures <100 °C?

At present, conclusive answers cannot be determined, although some reasoning is outlined below.

Some land-based peridotites, in ophiolites, orogenic massifs, or intrusions, may conserve the residual gases formed or those that were present during hydrothermal conditions for mantle extrusion on the ocean floor. Such gases such as helium and methane of magmatic origin and methane from high temperature, water-rock-interactions, today, may be found in certain fluid inclusions within the minerals of continental peridotites or within the surrounding mafic rocks (e.g., Sachan et al. 2007). Gas in these inclusions are, in fact, well protected and may survive inside peridotite during obduction or orogenic tectonisation and fracturing. Gas dispersed in peridotite fractures on the ocean floor hardly remained; and it is difficult to imagine that the large amounts of gas observed today in land-based peridotites derived from fluid inclusions alone, or are, in any way, the same gas formed in ancient oceanic hydrothermal systems. A more plausible explanation is that the abundant methane today observed in seeps was formed during the initial stages of ophiolite formation when the "metamorphic sole" (the shear zone at the base of the ophiolite above the sedimentary crust) was still "warm". Detailed studies on ophiolite cooling following obduction are necessary for evaluating such a possibility. However, if such is the case, methane would not be genetically related to low temperature (<100 °C) serpentinisation and the hydrogen identified in many land-based peridotites.

If, instead, methane was formed during present-day low temperature conditions, we need to understand how low-temperature FTT reactions can occur. Below 100 °C, FTT reactions in aqueous solutions are extremely sluggish. Some scholars have assumed, however, that CH_4 is formed in the hyperalkaline waters observed on the seafloor or in onshore springs. Analyses of the radiocarbon contained in CH_4

(^{14}C-CH_4) have indicated that, generally, the carbon is older than 50,000 years (percent of modern carbon ~0; Abrajano et al. 1990; Etiope and Schoell 2014; Whiticar and Etiope 2014b; Etiope et al. 2014), while carbon in the hyperalkaline waters is typically a few thousand years old (e.g., Marques et al. 2008; Whiticar and Etiope 2014b). As a result, methane was formed from carbon that is not related to that occurring in the waters. Furthermore, for high pH, CO_3^{2-} is the only available carbon source dissolved in the water, and the aqueous reaction would be (e.g., Mottl et al. 2004):

$$4H + CO_3^{2-} = CH_4 + H_2O + 2OH^- \quad (7.4)$$

The problem, experts of catalysis say, is that CO_3^{2-} does not significantly react with H_2 on metals, especially at low temperatures. The easiest way to produce CH_4 at temperatures below 100 °C is through the Sabatier reaction in a dry system (reaction 7.3). CH_4 could derive from the H_2 and fossil, ^{14}C-free CO_2 that originate in different, separate systems. H_2 would come from serpentinisation in peridotites. Fossil CO_2 may derive from limestone, any C-bearing rock, mantle or even ancient (older than 50,000 years) atmospheric air. The source rock of abiotic methane would then be a rock that offers the best conditions for FTT reactions, i.e. abundant catalysts (metals) and the mixing of H_2 and CO_2. What are these "magic" rocks and catalysts that allow low temperature CO_2 hydrogenation?

The only catalysts known to be effective below 100 °C, at least on laboratory time scales, are rhodium (Rh) (Jacquemin et al. 2010) and ruthenium (Ru) (Thampi et al. 1987). Rhodium is extremely rare and dispersed in parts-per-billion concentrations within ultramafic rocks. Ruthenium is rare in submarine hydrothermal systems (Pasava et al. 2007) but within the chromitites of many continental ophiolites and igneous complexes it is a dominant Platinum Group Element (PGE), reaching parts-per-million concentration levels (e.g., Economou-Eliopoulos 1996). Ru is mainly found in the form of sulphur minerals such as laurite (RuS_2) or ruthenian pentlandite ($(Ni,Fe)_8RuS_8$), or as Ru-Ir-Os alloys or oxides (RuO_2) (Garuti and Zaccarini 1997). All these Ru forms are found in either stratiform or podiform chromitites with Ru concentrations typically in the range of 0.1–1 ppm (relative to mass chromitite) and up to several ppm in Cr-rich veins (e.g., Page and Talkington 1984; Bacuta et al. 1990). In ophiolite sequences, Ru-enrichments are preferentially located within tectonite and Moho transition zones, particularly in crustal dunite (Prichard and Brough 2009; Mosier et al. 2012). As a result, there is a surprising coincidence between the location of Ru-rich chromitites and the presence of methane. Most of the land-based serpentinisation seeps documented thus far are adjacent to chromite mines or located above ultramafic rocks hosting Ru-enriched chromitites. Examples include the Chimaera fires in Turkey, located near the ancient chrome mines of Cirali (Juteau 1968), the Semail ophiolite in Oman (Page et al. 1982), the Othrys ophiolite in Greece (Garuti et al. 1999), the Zambales in the Philippines (Bacuta et al. 1990), Newfoundland in Canada (Page and Talkington 1984), and the Cabeço de Vide in Portugal (Dias et al. 2006). Deep boreholes, providing abiotic gas from crystalline Precambrian rocks at Sudbury in Canada (Sherwood Lollar et al. 2008), are located

in one of the richest Ru mines in North America (Ames and Farrow 2007). Furthermore, large amounts of methane leading to explosions have been reported in what is likely the world's largest Ru mine complex, Bushveld, located in South Africa (Cook 1998). Recent laboratory experiments have demonstrated that abiotic methane can actually be produced by the Sabatier reaction at temperatures below 100 °C (even at room temperature, 20–25 °C) using ruthenium at concentrations equivalent to those occurring in chromitites in ophiolites or in igneous complexes (Etiope and Ionescu 2014). Therefore, Ru-enriched chromitites are good candidates for inorganic source rocks in land-based serpentinisation systems. Alternatively, we may assume that traditional and more abundant catalysts, Fe, Ni, and Cr are also effective on longer, geological time scales, although this cannot be experimentally confirmed in the laboratory.

In summary, it seems that the most logical answers to the questions above are as follows:

(a) Methane could be produced at high temperatures (>200 °C) during the early stage of ophiolite emplacement near the metamorphic sole, but not under seafloor hydrothermal conditions; and methane is not related to low T serpentinisation and hydrogen.
(b) Methane could be produced at low temperatures (<100–150 °C) and on geological time scales with the support of traditional catalysts (Fe, Ni, and Cr), but this process could not be demonstrated in human time-scale laboratory experiments.
(c) Methane could be produced more rapidly at low temperatures (<100 °C) with the support of ruthenium-based catalysts in chromitites, as already demonstrated in the laboratory.

If these inorganic source rocks occur within or adjacent to a Total Petroleum System (see the definition provided in the Introduction), it is possible that portions of the generated abiotic gas may migrate and mix with biotic natural gas in sedimentary rocks. Since serpentinisation produces microfracturing and increases the permeability of peridotite, these igneous rocks can also directly act as hydrocarbon reservoirs in atypical and deep petroleum systems (Farooqui et al. 2009; Schutter 2003). Serpentinised rocks, for example, form reservoirs for oilfields in Texas and Cuba (Smith et al. 2005). Petroleum pools have also been suggested to incorporate trace metals from reservoir igneous rocks (Szatmari et al. 2011), implying the exchange of material between hydrocarbon fluids and the hosting minerals. The occurrence of minor amounts of abiotic gas in commercial fields has been suggested in China, for example, in the Songliao Basin (Dai et al. 2005; Ni et al. 2009) and in the United States (Jenden et al. 1993). Until the early 1990s, commercial accumulations of abiotic CH_4 have not been identified by the petroleum industry and far less than 1 % of the CH_4 in most oil and gas fields is abiotic (Jenden et al. 1993). However, as shown in Sect. 7.1.3, abiotic methane may have a carbon isotopic composition that overlaps that of biotic gas, and minor amounts of abiotic gas mixed with biotic gas may not be recognised using C and H isotopes. In addition, as suggested by recent laboratory experiments (Etiope and Ionescu 2014),

low temperature FTT reactions can produce CH_4 with a large C isotope fractionation between CO_2 and CH_4, leading to relatively "light" (^{13}C-depleted) CH_4, resembling microbial gas. As a result, the origins of gas, within atypical petroleum systems characterised by igneous rocks, should be re-examined using modern geochemical interpretative techniques (Etiope and Sherwood Lollar 2013).

7.1.3 How to Distinguish Abiotic and Biotic Methane

As described in Chap. 1, combining stable carbon and hydrogen isotopes of CH_4 is the first, basic step for determining the origin of methane. Until a few years ago and based on a limited amount of data, the isotopic composition of abiotic gas was considered to be typically enriched in ^{13}C, when $\delta^{13}C$ values are above −25 ‰. Today, a wide set of data is available that allows us to draw a new isotopic picture of abiotic methane. The $\delta^{13}C$ of methane in land-based serpentinised ultramafic rocks can have values of up to −37 ‰, while the methane from Precambrian shields can be even lighter (Etiope and Sherwood Lollar 2013). Figure 7.4a provides an updated diagram of $\delta^{13}C$ versus $\delta^{2}H$ for the methane released from land-based serpentinisation seeps or springs. Figure 7.4b compares this methane with that found in the following four types of geological settings: Precambrian crystalline shields, Mid-Ocean Ridge serpentinisation, inclusions in intrusive alkaline rocks, and volcanic and geothermal fluids. The isotopic distinction between biotic and abiotic is quite clear. The diagram, however, is only the first step for determining the abiotic origin of gas and cannot be revealed if the methane is completely abiotic or mixed with some biotic components. Additional interpretative tools are necessary and may include the use of noble gases (helium isotopes), Schulz-Flory distribution tests, the molecular and isotopic composition of associated gases (other hydrocarbons and CO_2), and methane vs. ethane mixing plots (Etiope and Sherwood Lollar 2013). In any case, knowledge of the geological context is an essential precondition for final interpretations.

Figure 7.4a–b indicates that methane seeping from land-based serpentinisation sites may have a wide range of C and H isotopic composition. The result is likely due to the variety in the isotopic composition of the carbon feedstocks involved in the production of CH_4 (CO_2 or other C-bearing molecules that may derive from the mantle, limestone, the atmosphere, or metasedimentary rocks), the temperature of the CH_4 generation mechanism, isotopic fractionations in the presence of H_2O (especially for $\delta^{2}H_{CH4}$), and the degree of the reaction itself (Etiope and Ionescu 2014).

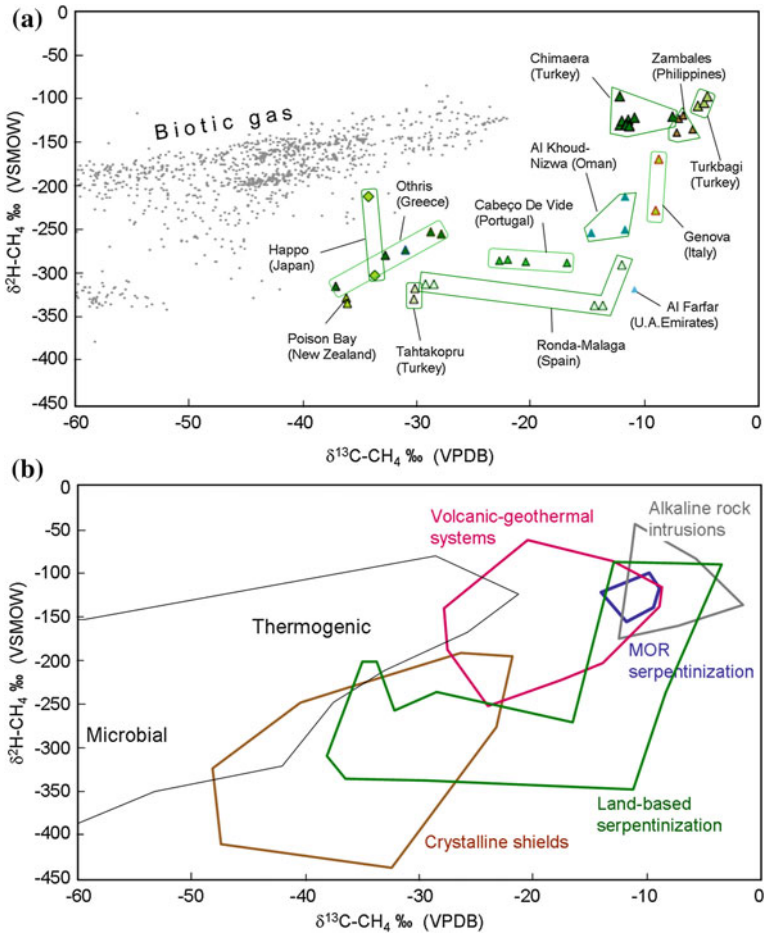

Fig. 7.4 **a** The C and H isotopic diagram for methane discharged in seeps and springs in land-based serpentinised peridotites, as listed in Table 7.1. **b** An isotopic diagram distinguishing fields relative to the abiotic methane shown in (**a**) from other abiotic methane documented in Mid-Ocean Ridges (MOR) (i.e., the Lost City and Logatchev), Precambrian crystalline shields (South Africa, Canada, and Scandinavia), volcanic-hydrothermal systems (e.g., the East Pacific Rise, the southwestern Indian Ridge, Socorro, and Milos), and inclusions in intrusive alkaline rocks (Lovozero, Khibina, and Illimaussaq). Biotic (thermogenic and microbial) data refer to a global dataset of gases in petroleum fields (also see Etiope et al. 2013a; Etiope and Schoell 2014). Diagrams were updated according to Etiope and Sherwood Lollar (2013), Etiope et al. (2013c), and Etiope and Schoell (2014); with additions from Etiope et al. (2014; Spain), Yuce et al. (2014; Turkey, Tahtakopru and Kurtbagi in the Amik Basin) and Etiope et al. (2015; the United Arab Emirates)

7.1.4 Seepage to the Surface

While the exact origin of abiotic methane is sometimes difficult to understand, the story is less cryptic as far as gas seepage is concerned. As revealed by gas flux data acquired at various sites in Italy, Turkey, Greece, and Spain, the relationship between seeps or springs and local geology is quite clear. Abiotic gas seeps or spring sites all have the following characteristics in common:

(a) the seep or spring is typically located in correspondence with a fault or at the intersection of more faults;
(b) the faults are in tectonic contact between ultramafic rocks and carbonate-rich rocks (limestones, flysch, metasedimentary rocks);
(c) gas miniseepage (see the definition in Chap. 2) is frequently observed surrounding visible seeps or springs; and
(d) microseepage also exists along faults, even far from macro-seeps and springs.

The amount of methane detected in land-based serpentinisation seeps and water springs is considerable. CH_4 concentrations in these waters range from 0.01 to 14 mg/L (normal water in equilibrium with the atmosphere has 0.00003 mg CH_4/L). With water flow rates on the order of one litre per second (as for the springs in Greece and Italy), the total amount of CH_4 transported to the surface by a single spring outlet can reach hundreds of kilograms per year. Dry seeps, without water discharge, have CH_4 concentrations of approximately 20 vol.% (as for the seeps in New Zealand) to ~50 vol.% (as for the Zambales seeps located in the Philippines), and up to ~90 vol.% (as for the Chimaera seep in Turkey). Gas flux has been measured at the Chimaera seep and surrounding hyperalkaline and bubbling springs in Greece, Italy, and Spain.

Chimaera, near Çiraly in the Antalya Gulf, is likely the largest terrestrial abiotic gas seep on Earth. Gas burns in at least 20 large flames that are up to half a meter in height (Fig. 7.1a–c). Gas escapes from visible vents in rock fractures and in the form of invisible seepage throughout peridotite outcrops, approximately 5,000 m^2 wide, along the flank of the Olympos Mountain. Based on closed-chamber measurements (see Chap. 4) at least 190 tonnes of CH_4 are released to the atmosphere each year from this main macro-seep (Etiope et al. 2011b). Additional emissions of gas, likely on the same order of magnitude of the Chimaera seep site, occur in a second peridotite outcrop recently discovered on the top of the mountain (Etiope and Schoell 2014). Here, there are two actively burning gas vents and numerous burned trees over an area of at least 2,000 m^2. As suggested by the surrounding burned soil, the trees were likely killed by episodic combustion of gas from the ground (Fig. 7.1d). The total gas flux from the two seepage sites is certainly higher than that of any other land-based serpentinisation seep or spring.

Additionally, methane microseepage, with fluxes up to 1,040 mg $m^{-2}day^{-1}$, was measured along a fault approximately 3 km from the Chimaera seep site at another

peridotite outcrop along Çirali Beach (Etiope et al. 2011b). Radiocarbon (^{14}C) analyses of CH_4 demonstrated that the carbon of Chimaera methane is older than 50,000 years (the percent of modern carbon is ~ 0; Etiope and Schoell 2014). Considering that "eternal flames" have been active for at least two millennia (they were documented by Pliny the Elder in *Naturalis Historia, <79 AD*), the continuous release of hundreds of tonnes of gas per year must be driven by high pressure gradients. The result is only possible if a pressurised gas accumulation exists, by analogy with observations of thermogenic gas seeps. Simple calculations suggest that the total amount of methane emitted thus far would be on the order of 400 Mm^3. Thus, the initial amount of methane stored in the reservoir (the ultimate reserve) could have been on the order of thousands of millions of cubic meters, similar to a conventional biotic gas field. Therefore, it is difficult to imagine that this gas formed during hydrothermal serpentinisation on the ocean floor and has been preserved throughout ophiolite obduction.

At the hyperalkaline water springs in Italy (the Voltri ophiolite, near Genova; Boschetti et al. 2013), Greece (the Othrys ophiolite; Etiope et al. 2013b), and Spain (the Ronda peridotite massif, between Ronda and Malaga; Etiope et al. 2014), gas is transported to the surface both by water and by autonomous gas-phase seepage, either as bubble plumes in water pools or as miniseepage and microseepage from the ground (see the definitions in Chap. 2). Methane fluxes from individual bubble trains, with bubbles having diameters of approximately 1 cm, are on the order of 1–2 kg/day. Methane miniseepage surrounding the springs is on the order of several hundreds of mg CH_4 m^{-2} day^{-1}. Microseepage, measured even at distances of approximately 100 m from the bubble-spring site, generally has fluxes on the order of tens of mg CH_4 m^{-2} day^{-1}. Springs, bubble streams, and microseepage locations in all areas appear to be strictly controlled by faults. Interesting to note is that gas microseepage can be measured even in the absence of organic soil, directly from peridotite outcrops that are apparently unfractured and homogeneous (Etiope et al. 2013a). Given the significant fluxes and rapid pressure build-up in closed-chambers, gas movement in rock is mainly due to advection driven by pressure gradients (Darcy's law), rather than diffusion which is controlled by concentration gradients (Fick's law) (see Chap. 3). Exhalation must take place through pervasive microfractures in rocks. In general, the small-scale permeability of partially serpentinised peridotites is comparable to the permeability of shaley materials. However, olivine hydration generates large volume changes and, thus, high local strains and stresses with episodic cracking (Macdonald and Fyfe 1985). Micro-scale fractures are pervasive throughout peridotite outcrops and are often mineralised by carbonates. As a result of tectonic overthrusting above sedimentary Mesozoic and Cenozoic sequences, ophiolite outcrops can also be characterised by larger joints and faults. Serpentinisation-related microfractures and tectonic fractures are, therefore, important escape pathways for the methane generated inside ultramafic rocks.

7.1.5 Is Abiotic Gas Seepage Important for the Atmospheric Methane Budget?

Section 6.4 discusses global emissions of geological methane to the atmosphere, including microbial and thermogenic gas from all types of seeps, onshore and offshore, in sedimentary basins, and gases of mixed origin, biotic and abiotic, in geothermal systems. Today, as stated in the latest IPCC assessment report, total geological CH_4 emissions are approximately 54 Mt CH_4/y (60 Mt CH_4/y are suggested in Chap. 6) and represent the second natural source of atmospheric methane after wetlands (Ciais et al. 2013). Also of note is that this emission estimate does not include abiotic gas seepage from serpentinised ultramafic rocks. Nevertheless, as widely reported above, such abiotic gas seepage is not rare and in some places is quite considerable. Can it be a significant additional global component of the geologically derived atmospheric budget of methane? At present, no sufficient data exists to fully answer this question. Specific studies and a wider dataset of flux measurements are necessary to better evaluate emission factors and, above all, to estimate at least the order of magnitude of the global area where this type of abiotic gas seepage exists. Today, we know that abiotic methane (also mixed with biotic gas) reaches the Earth's surface from seeps in at least 16 countries (see Table 7.1). Hyperalkaline springs, where methane is yet to be documented, although very likely to occur, are also found in Bosnia and Cyprus. Rather than visible gas emissions from spring sites, invisible seepage, miniseepage, and microseepage, which may extend over wide areas, are likely more important for global methane emissions to the atmosphere. That this invisible seepage is also widespread in other ophiolitic or ultramafic rocks massifs, where hyperalkaline springs and seeps do not exist, cannot be excluded. For example, abiotic microseepage may occur throughout serpentine soils, a special type of soil derived from ultramafic rock bedrock and characterised by unusual plant associations adapted to extreme soil conditions, such as low calcium-to-magnesium ratios, a lack of nutrients such as nitrogen, potassium, and phosphorous, and high concentrations of nickel and chromium (e.g., Proctor and Woodell 1975). These types of ultramafic rock soils occupy approximately 1 % of the global land surface (i.e., $\sim$148,000 km^2; Garnier et al. 2009) but at least 3 % of the Earth's surface is made up of serpentinised peridotite (Guillot and Hattori 2013). Presently, any estimate or guess of the portion of this area that actually hosts microseepages of abiotic gas produced in underlying peridotites, as well as the attribution of an average microseepage flux in this portion, are highly speculative and inappropriate. However, the argument deserves to be studied.

An interesting link exists between such a potential methane emission and carbon dioxide consumption. Due to their capacity for the conversion of CO_2 gas into solid carbonate minerals, peridotite outcrops are, in fact, also potential sinks of atmospheric CO_2. For example, CO_2 uptake by the near surface carbonation of mantle peridotite during weathering consumes $\sim 10^3$ tons per km^3 per year in Oman (Kelemen and Matter 2008) and, by pumping greenhouse gas within peridotites, has been proposed to exploit this process for artificially storing atmospheric CO_2.

Studying how much of the injected CO_2 could react with H_2 and produce CH_4 (a greenhouse gas much more powerful than CO_2) would be an interesting endeavour.

7.2 Potential Methane Seepage on Mars

7.2.1 Looking for Methane on Mars

The information acquired in studies of gas seepage on Earth represents a fundamental reference for the recognition and understanding of possible gas seepage on other planets known to have methane within their atmospheres or the ground. One of the most studied planets in this respect is Mars. Serpentinised ultramafic rocks and hydrated silicates also exist on Mars (Mustard et al. 2008; Ehlmann et al. 2010) and have been considered a plausible source of methane (Oze and Shama 2005; Atreya et al. 2007; Etiope et al. 2013a). The possible existence of methane on Mars has enormous implications because, as for Earth, methane could, in theory, have originated from microbes or could have been an energy source for some microbial organisms or even for prebiotic mechanisms germane to the origin of life. In these cases, methane could be a proxy for life on Mars.

At the time of writing this chapter, the presence of methane on Mars is still being debated because previous reports of methane in the atmosphere are not unequivocal. The first telescopic measurements reporting 10–20 ppb of methane in the martian atmosphere (Mumma et al. 2003; Formisano et al. 2004; Krasnopolsky et al. 2004) suggested the existence of an active gas source. The CH_4 plume observed in the martian region called Northern Summer 2003, indicates emissions from the ground of 19,000 tons CH_4 $year^{-1}$ (Mumma et al. 2009) or 150,000 tons CH_4 $year^{-1}$ (Lefevre and Forget 2009), and possibly up to 570,000 tons CH_4 $year^{-1}$ (Chizek et al. 2010). Although possibly a coincidence, elevated CH_4 concentrations have been detected in correspondence with olivine-bearing rocks, frequently serpentinised, in the martian regions of Syrtis Major, Terra Sirenum, and Nili Fossae (Hoefen et al. 2003; Ehlmann et al. 2010).

The occurrence of CH_4 on Mars has, however, been questioned because atmospheric photochemistry and transport models make short-lived methane plumes implausible and because ground-based observations of methane are heavily affected by telluric interference (Zahnle et al. 2011). In addition, plumes of methane have not been reported since the original report in 2009. However, the Curiosity lander seems to have recently found traces of methane, up to 7.2 ppbv, near the martian surface (Webster et al. 2014), although the location of the measurement (the Gale Crater) is not a favourable place for abiotic methane production due to the lack, at least on the surface, of serpentinised rocks. In any case, the special nature of the processes generating and transporting methane to the surface (i.e. seepage) may not allow detection in the atmosphere 1 m above the ground, a notion supported by

observations of low flux seepage in serpentinised rocks on Earth, where amounts of methane decline rapidly with distance above the surface.

Macro-seeps, like Chimaera in Turkey or Los Fuegos Eternos in the Philippines, are improbable on Mars, as they require considerable amounts of gas and pressurised reservoirs; at least on Earth, Chimaera seep represents a rare phenomenon. Rather, microseepage would be an easier and a more plausible degassing scenario on Mars, whereby minor amounts of dispersed gas can diffusely and slowly migrate to the surface. A diffuse flux of 100–1,000 mg m^{-2} day^{-1} from an area of 500–5,000 km^2 would be sufficient to support the martian CH_4 emissions estimated by Mumma et al. (2009) and Lefevre and Forget (2009). If the entire 30,000 km^2 of the olivine-rich outcrop at Nili Fossae (Hoefen et al. 2003) is assumed to exhale, then a microseepage of 15 mg m^{-2} day^{-1} (i.e. 4–5 times lower than the minimum detected in the ophiolites in Turkey) could account for the observed martian CH_4 plume observed by Mumma et al. (2009). Models of CH_4 release on Mars indeed suggest that the Northern Summer 2003 plume was formed by a broad source rather than a point emission (Mischna et al. 2011). Microseepage can either be episodic (as required by the martian model of Mischna et al. 2011), seasonal (as required by Geminale et al. 2008), or quasi-permanent depending on underground gas pressure gradients, migration mechanisms, and changes in exogenic (atmospheric) factors (Etiope and Klusman 2010). The crux of the query is that low levels of microseepage may not be detected by measurements in air. On Earth, in most cases, methane microseepage cannot be detected a few cm above the soil due to winds and large dilutions of small amounts of leaking CH_4. For example, for proof of geological abiotic CH_4 on Mars, attempts to measure such gas should be concentrated in regions with olivine-bearing rocks (e.g., Syrtis Major, Terra Sirenum Nili Fossae, Claritas Fossae; Fig. 7.5) ideally by drilling deep into the soil, or using accumulation chambers on the ground,

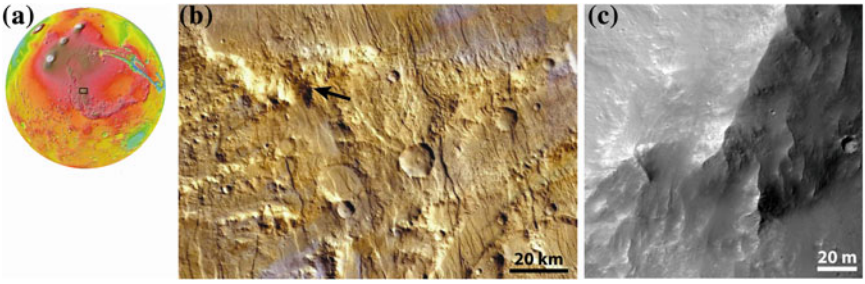

Fig. 7.5 Serpentine occurs in Mars' ancient Noachian terrains, in, for example, the Claritas Fossae highlands on the southern end of Mars' Tharsis Region (26.8 s, 101.2 W). **a** A Mars Orbiter Laser Altimeter (MOLA) topographic map of a location in the Claritas Rise. **b** A high resolution stereo camera color image of the fractured, ancient terrain. **c** Serpentine occurs in the select rock outcrops pictured here in High Resolution Imaging Science Experiment (HiRISE) data and originally detected using visible/near infrared imaging spectrometer data (Ehlmann et al. 2010). Images kindly provided by B. Ehlmann (Caltech/JPL)

preferably above or near tectonic faults. Without these tests, we cannot infer that methanogenic processes related to serpentinisation do not exist on Mars.

7.2.2 A Theoretical Martian Seepage

The potential surface release of methane produced in the martian subsurface depends on the physical properties of the substrate, including water occurrence, permeability, porosity, and pressure and thermal gradients, all of which can affect advection and diffusion migration processes, as discussed in Chap. 3. In general, martian terrains seem to have good gas-transport properties. Vapour–ice deposition models for ice distribution predict that the upper tens to hundreds of meters of Mars' subsurface exchange with the atmosphere, and large-scale aquifer models predict fluid migration through pores at several kilometers in depth (Mellon et al. 1997; Grimm and Painter 2009). Due to repeated meteorite impacts and fracturing during the cooling of lavas, the martian crust is also known to be fractured on multiple scales. As mentioned above, additional fracturing can be due to serpentinisation. Therefore, olivine-bearing rocks may have a relatively high secondary permeability which could enhance the potential for microseepage to the surface.

In such fractured rocks, gas advection, the most important mechanism of gas migration in the subsoil on Earth, can occur in two forms depending on the presence of water, as described in Chap. 3. In dry porous or fractured media, gas flows through interstitial or fissure spaces (gas-phase advection). In saturated porous or fractured media, two possible phenomena may be distinguished: gas dissolves and is transported by groundwater (water-phase advection) or gas flows, displacing water (gas-phase advection). In the equatorial and mid-latitudes on the surface of Mars today, water is typically only stable in the vapour phase (Haberle et al. 2001). However, near-surface salts and thin-film type weathering point to small amounts of liquid water on the surface within the geological recent past (Arvidson et al. 2010). The availability of subsurface water remains a subject of active research, though it is generally believed that subsurface liquid water was available in the past, causing chemical alterations (Ehlmann et al. 2010). Radar investigations have not revealed any present subsurface aquifer, although the modern seepage of brines indicates the potential for episodic subsurface water occurrence in some places on Mars (McEwen et al. 2011). Liquid water could exist today as a brine at depths shallower than 4 km (Oze and Sharma 2005). Subsurface ice may act as a barrier for the advection of gases to the surface; however, evidence for seasonal melting/sublimation offers a mechanism whereby gases of any origin could be trapped by ice-filled pore spaces can occasionally be released. Therefore, the most common form of gas advection on Mars, at least at relatively shallow depths, could be the gas-phase in dry fractured media. Under these conditions, gas velocity may range on the order of 10^0–10^3 m/day for highly permeable, fractured rocks whose fracture aperture or voids are on the order of several mm (see Chap. 3). A simple, first-order

estimation of a gas-advection model suggests that methane fluxes on the order of several mg m^{-2} day^{-1}, similar to the microseepage observed in terrestrial peridotites (as described above), could occur in martian rocks (Etiope et al. 2013a). Overall, serpentinised ultramafic rocks on Mars are likely to have both the necessary chemical constituents for methane production and the fractures that would allow seepage of gas to the atmosphere, similar to serpentinised ultramafic rocks on Earth.

However, in addition to serpentinised ultramafic rocks, methane seepage on Mars could also take place in other regions of the planet characterised by extensive faults and fractures, or regions with particular morphological structures (Fig. 7.6), such as the mounds in the Acidalia Planitia, which have been compared to terrestrial, methane-seeping mud volcanoes (Oehler and Allen 2010; Etiope et al. 2011a), possible ancient springs in Arabia Terra associated with faults and dipping

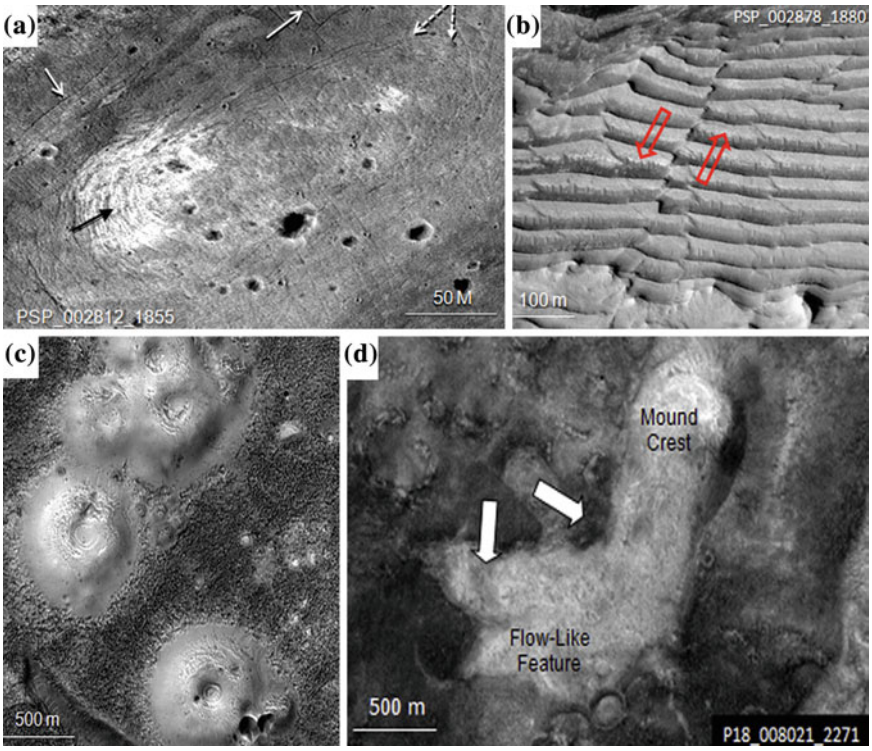

Fig. 7.6 Potential seepage structures on Mars. **a** An elliptical tonal anomaly in Arabia Terra, interpreted as an ancient spring mound (Allen and Oehler, 2008). *Solid white arrows* point to linear fractures; *dashed arrows* point to circumferential faults associated with elliptical features; the *black arrow* points to possible terracing. **b** Faulted sediments in Arabia Terra. As indicated by the warping of layered sediments on either side of the fault, arrows indicate the direction of relative movement across the fault. **c** The mounds in Acidalia Planitia, interpreted as relicts of mud volcanoes. **d** The flow-like extension (*arrow*) of the high-albedo material of the mound. HiRISE images prepared by D. Oehler (NASA/JPL/University of Arizona)

beds (Allen and Oehler 2008), and large-scale polygonal fractures (often called, "giant polygons") in Chryse and Acidalia.

The latter martian polygonal fractures, in particular, appear to be similar to fluid-bearing polygonal faults discovered on Earth thanks to 3D seismic images (e.g., Goulty 2008; Oehler and Allen 2012; Allen et al. 2013). The development of large scale fracture systems could provide both a source of subsurface fluids and migration pathways for those fluids. These polygonal fractures are additionally often associated with mud volcanoes and methane seepage Similarly, the martian "giant polygons" are frequently associated with mounds that have been compared to terrestrial mud volcanoes. Therefore, areas on Mars having both the "giant polygons" and the associated mounds could be important sites for future searches for methane occurrences and evidence of past life (Oehler and Allen 2012).

References

Abrajano TA, Sturchio NC, Bohlke JK, Lyon GL, Poreda RJ, Stevens CM (1988) Methane-hydrogen gas seeps, Zambales Ophiolite, Philippines: deep or shallow origin? Chem Geol 71:211–222

Abrajano TA, Sturchio NC, Kennedy BM, Lyon GL, Muehlenbachs K, Bohlke JK (1990) Geochemistry of reduced gas related to serpentinization of the Zambales Ophiolite, Philippines. Appl Geochem 5:625–630

Allen CC, Oehler DZ (2008) A case for ancient springs in Arabia Terra, Mars. Astrobiology 8:1093–1112

Allen CC, Oehler D, Etiope G, van Rensbergen P, Baciu C, Feyzullayev A, Martinelli G, Tanaka K, Van Rooij D (2013) Fluid expulsion in terrestrial sedimentary basins: a process providing potential analogs for giant polygons and mounds in the martian lowlands. Icarus 224:424–432

Ames DE, Farrow CEG (2007) Metallogeny of the sudbury mining camp, Ontario. In: Goodfellow, WD (ed) Mineral deposits of Canada: a synthesis of major deposit-types, district metallogeny, the evolution of geological provinces, and exploration methods. Geological Association of Canada, Mineral Deposits Division, pp 329–350, Special Publication No. 5

Arvidson RE, Ruff SW, Morris RV, Ming DW, Crumpler LS, Yen AS, Squyres SW, Sullivan RJ, Bell III JF et al (2010) Spirit mars rover mission: overview and selected results from the northern home plate winter haven to the side of Scamander crater. J Geophys Res 115:E00F03. http://dx.doi.org/10.1029/2008JE003183

Atreya SK, Mahaffy PR, Wong A-S (2007) Methane and related trace species on Mars: origin, loss, implications for life, and habitability. Planet Space Sci 55:358–369

Bacuta GC, Kay RW, Gibbs AK, Bruce RL (1990) Platinum-group element abundance and distribution in chromite deposits of the Acoje Block, Zambales ophiolite complex, Philippines. J Geochem Explor 37:113–143

Barnes I, O'Neil JR (1969) The relationship between fluids in some fresh Alpine-type ultramafics and possible modern serpentinization, Western United States. Geol Soc Am Bull 80:1947–1960

Boschetti T, Etiope G, Toscani L (2013) Abiotic methane in hyperalkaline springs of Genova, Italy. Procedia Earth Planet Sci 7:248–251

Boulart C, Chavagnac V, Monnin C, Delacour A, Ceuleneer G, Hoareau G (2013) Differences in gas venting from ultramafic-hosted warm springs: the example of Oman and Voltri ophiolites. Ofioliti 38:143–156

Bruni J, Canepa M, Cipolli F, Marini L, Ottonello G, Vetuschi Zuccolini M (2002) Irreversible water–rock mass transfer accompanying the generation of the neutral, Mg–HCO_3 and high-pH, Ca–OH spring waters of the Genova province, Italy. App Geochem 17:455–474

Charlou JL, Donval JP, Fouquet Y, Jean-Baptiste P, Holm N (2002) Geochemistry of high H2 and CH4 vent fluids issuing from ultramafic rocks at the Rainbow hydrothermal field (36°14′N, MAR). Chem Geol 191:345–359

Chizek MR, Murphy JR, Kahre MA, Haberle RM, Marzo GA (2010) A shortlived trace gas in the martian atmosphere: a general circulation model of the likelihood of methane. Lunar Planet Sci 41 Abstract 1527

Ciais P, Sabine C, Bala G, Bopp L, Brovkin V, Canadell J, Chhabra A, DeFries R, Galloway J, Heimann M, Jones C, Le Quéré C, Myneni RB, Piao S, Thornton P (2013) Carbon and other biogeochemical cycles. In:Stocker TF et al (eds) Climate change 2013: the physical science basis. contribution of working group i to the fifth assessment report of IPCC, Cambridge Univ Press, Cambridge, UK and New York, NY, USA

Cook AP (1998). Occurrence, emission and ignition of combustible strata gases in Witwatersrand gold mines and Bushveld platinum mines, and means of ameliorating related ignition and explosion hazards, part 1: literature and technical review. Safety in mines research advisory committee, GAP 504 (report)

Dai J, Yang S, Chen H, Shen X (2005) Geochemistry and occurrence of inorganic gas accumulations in Chinese sedimentary basins. Org Geochem 36:1664–1688

Dias PA, Leal Gomes C, Castelo Branco JM, Pinto Z (2006) Paragenetic positioning of PGE in mafic and ultramafic rocks of Cabeço de Vide—alter do Chão Igneous Complex. Book of abstracts, VII Congresso Nacional de Geologia, pp 1007–1010

Economou-Eliopoulos M (1996) Platinum-group element distribution in chromite ores from ophiolite complexes: implications for their exploration. Ore Geol Rev 11:363–381

Ehlmann BL, Mustard JF, Murchie SL (2010) Geologic setting of serpentine deposits on Mars. Geophys Res Lett 37:L06201. http://dx.doi.org/10.1029/2010GL042596

Etiope G, Ionescu A (2014) Low-temperature catalytic CO_2 hydrogenation with geological quantities of ruthenium: a possible abiotic CH_4 source in chromitite-rich serpentinized rocks. Geofluids. doi: 10.1111/gfl.12106 (first published online)

Etiope G, Klusman RW (2010) Microseepage in drylands: flux and implications in the global atmospheric source/sink budget of methane. Global Planet Change 72:265–274

Etiope G, Schoell M (2014) Abiotic gas: atypical but not rare. Elements 10:291–296

Etiope G, Sherwood Lollar B (2013) Abiotic methane on Earth. Rev Geophys 51:276–299

Etiope G, Ehlmann B, Schoell M (2013a) Low temperature production and exhalation of methane from serpentinized rocks on Earth: a potential analog for methane production on Mars. Icarus 224:276–285

Etiope G, Oehler DZ, Allen CC (2011a) Methane emissions from Earth's degassing: Implications for Mars. Planet Space Sci 59:182–195

Etiope G, Schoell M, Hosgormez H (2011b) Abiotic methane flux from the Chimaera seep and Tekirova ophiolites (Turkey): understanding gas exhalation from low temperature serpentinization and implications for Mars. Earth Planet Sci Lett 310:96–104

Etiope G, Tsikouras B, Kordella S, Ifandi E, Christodoulou D, Papatheodorou G (2013b) Methane flux and origin in the Othrys ophiolite hyperalkaline springs, Greece. Chem Geol 347:161–174

Etiope G, Vance S, Christensen LE, Marques JM, Ribeiro da Costa I (2013c) Methane in serpentinized ultramafic rocks in mainland Portugal. Mar Pet Geol 45:12–16

Etiope G, Vadillo I, Whiticar MJ, Marques JM, Carreira P, Tiago I, Benavente J, Jiménez P, Urresti B (2014) Methane seepage at hyperalkaline springs in the Ronda peridotite massif (Spain). AGU 2014 Fall Meeting Abstracts

Etiope G, Judas J, Whiticar MJ (2015) First detection of abiotic methane in the eastern United Arab Emirates ophiolite aquifer. Arab J Geosci (in press)

Farooqui MY, Hou H, Li G, Machin N, Neville T, Pal A, Shrivastva C, Wang Y, Yang F, Yin C, Zhao J, Yang Z (2009) Evaluating volcanic reservoirs. Oilfield Rev 21:36–47

Formisano V, Atreya S, Encrenaz T, Ignatiev N, Giuranna M (2004) Detection of methane in the atmosphere of Mars. Science 306:1758–1761

Fritz P, Clark ID, Fontes J-C, Whiticar MJ, Faber E (1992) Deuterium and ^{13}C evidence for low temperature production of hydrogen and methane in a highly alkaline groundwater

environment in Oman. In: Kharaka YK, Maest AS (eds), Proceedings of 7th int symp water–rock interaction: low temperature environments, vol 1. Balkema, Rotterdam, pp 793–796
Garnier J, Quantin C, Guimaraes E, Garg VK, Martins ES, Becquer T (2009) Understanding the genesis of ultramafic soils and catena dynamics in Niquelandia, Brazil. Geoderma 151:204–214
Garuti G, Zaccarini F (1997) In situ alteration of platinum-group minerals at low temperature: evidence from serpentinized and weathered chromitite of the Vourinos complex, Greece. Can Miner 35:611–626
Garuti G, Zaccarini F, Economou-Eliopoulos M (1999) Paragenesis and composition of laurite from chromitites of Othrys (Greece): implications for Os-Ru fractionation in ophiolitic upper mantle of the Balkan peninsula. Min Deposit 34:312–319
Geminale A, Formisano V, Giuranna M (2008) Methane in martian atmosphere: average spatial, diurnal, and seasonal behaviour. Planet Space Sci 56:1194–1203
Goulty NR (2008) Geomechanics of polygonal fault systems: a review. Petrol Geosci 14:389–397
Grimm RE, Painter SL (2009) On secular evolution of groundwater on Mars. Geophys Res Lett 36:L24803
Guillot S, Hattori K (2013) Serpentinites: essential roles in geodynamics, arc volcanism, sustainable development, and the origin of life. Elements 9:95–98
Haberle RM, McKay CP, Schaeffer J, Cabrol NA, Grin EA, Zent AP, Quinn R (2001) On the possibility of liquid water on present-day Mars. J Geophys Res 106(E10):23317–23326
Hoefen TM, Clark RN, Bandfield JL, Smith MD, Pearl JC, Christensen PR (2003) Discovery of olivine in the Nili Fossae region of Mars. Science 302:627–630
Horita J, Berndt ME (1999) Abiogenic methane formation and isotopic fractionation under hydrothermal conditions. Science 285:1055–1057
Hosgormez H, Etiope G, Yalçın MN (2008) New evidence for a mixed inorganic and organic origin of the Olympic Chimaera fire (Turkey): a large onshore seepage of abiogenic gas. Geofluids 8:263–275
Jacquemin M, Beuls A, Ruiz P (2010) Catalytic production of methane from CO_2 and H_2 at low temperature: insight on the reaction mechanism. Catal Today 157:462–466
Jenden PD, Hilton DR, Kaplan IR, Craig H (1993) Abiogenic hydrocarbons and mantle helium in oil and gas fields. In: Howell D (ed) Future of energy gases, USGS Professional paper, vol 1570, pp 31–35
Juteau T (1968) Commentaire de la carte geologique des ophiolites de la region de Kumluca (Taurus lycien, Turquie meridionale): cadre structural, modes de gisement et description des principaux fades du cortege ophiolitique. MTA Bull 70:70–91
Kelemen PB, Matter JM (2008) In situ carbonation of peridotite for CO_2 storage. Proc Nat Acad Sci USA 105(17):295–17,300
Krasnopolsky VA, Maillard JP, Owen TC (2004) First detection of methane in the martian atmosphere: evidence for life? Icarus 172:537–547
Lefevre F, Forget F (2009) Observed variations of methane on Mars unexplained by known chemistry and physics. Nature 460:720–723
Lyon G, Giggenbach WF, Lupton JF (1990) Composition and origin of the hydrogen rich gas seep, Fiordland, New Zealand. EOS Trans V51D(10):1717
Macdonald AH, Fyfe WS (1985) Rate of serpentinization in seafloor environments. Tectonophysics 116:123–135
Marques JM, Carreira PM, Carvalho MR, Matias MJ, Goff FE, Basto MJ, Graça RC, Aires-Barros L, Rocha L (2008) Origins of high pH mineral waters from ultramafic rocks, Central Portugal. App Geochem 23:3278–3289
McCollom TM (2013) Laboratory simulations of abiotic hydrocarbon formation in Earth's deep subsurface. Rev Min Geochem 75:467–494
McCollom TM, Seewald JS (2007) Abiotic synthesis of organic compounds in deep-sea hydrothermal environments. Chem Rev 107:382–401
McEwen AS, Ojha L, Dundas CM, Mattson SS, Byrne S, Wray JJ, Cull SC, Murchie SL, Thomas N, Gulick VC (2011) Seasonal flows on warm martian slopes. Science 333:740–743

Mellon MT, Jakosky BM, Postawko SE (1997) The persistence of equatorial ground ice on Mars. J Geophys Res 102:19357–19369

Meyer-Dombard DR, Woycheese KM, Cardace D, Arcilla C (2013) Geochemistry of Microbial Environments in Serpentinizing Springs of the Philippines. AOGS 2013, Brisbane. Abstract # IG19-D2-PM2-P-007

Milenic D, Dragisic V, Vrvic M, Milankovic D, Vranjes A (2009) Hyperalkaline mineral waters of Zlatibr ultramafic massif in Western Serbia, Europe. Abstract proceedings of the AWRA International Water Congress—Watershed Management for Water systems, Seattle, USA

Mischna MA, Allen M, Richardson MI, Newman CE, Toigo AD (2011) Atmospheric modelling of Mars methane surface releases. Planet Space Sci 59:227–237

Monnin C, Chavagnac V, Boulart C, Ménez B, Gérard M, Gérard E, Quéméneur M, Erauso G, Postec A, Guentas-Dombrowski L, Payri C, Pelletier B (2014) The low temperature hyperalkaline hydrothermal system of the Prony bay (New Caledonia). Biogeosciences Discuss 11:6221–6267

Morrill PL, Gijs Kuenen J, Johnson OJ, Suzuki S, Rietze A, Sessions AL, Fogel ML, Nealson KH (2013) Geochemistry and geobiology of a present-day serpentinization site in California: the Cedars. Geochim Cosmochim Acta 109:222–240

Mosier DL, Singer DA, Moring BC, Galloway JP (2012) Podiform chromite Deposits—database and grade and tonnage models. U.S. Geological Survey Scientific Investigations, Report, pp 2012–5157

Mottl MJ, Wheat C, Frier P (2004) Decarbonateion, serpentinization, abgiogenic methane, and extreme pH beneath the Mariana Forearc. AGU Fall Meeting 2004, abstract V13A-1441

Mumma MJ, Novak RE, DiSanti MA, Bonev BP (2003) A sensitive search for methane on Mars. Am Astron Soc Bull 35:937–938

Mumma MJ, Villanueva G, Novak RE, Hewagama T, Bonev BP, DiSanti MA, Mandell AM, Smith MD (2009) Strong release of methane on Mars in Northern summer 2003. Science 323:1041–1045

Mustard JF, Murchie LS, Pelkey SM et al (2008) Hydrated silicate minerals on Mars observed by the Mars Reconnaissance Orbiter CRISM instrument. Nature 454:305–309

Ni Y, Dai J, Zhou Q, Luo X, Hu A, Yang C (2009) Geochemical characteristics of abiogenic gas and its percentage in Xujiaweizi Fault Depression, Songliao Basin, NE China. Petrol Explor Dev 36:35–45

Oehler DZ, Allen CC (2010) Evidence for pervasive mud volcanism in Acidalia Planitia, Mars. Icarus 208:636–657

Oehler DZ, Allen CC (2012) Giant polygons and mounds in the lowlands of Mars: signatures of an ancient ocean? Astrobiology 12:601–615

Okland I, Huang S, Dahle H, Thorseth IH, Pedersen RB (2012) Low temperature alteration of serpentinized ultramafic rock and implications for microbial life. Chem Geol 318–319:75–87

Oze C, Sharma M (2005) Have olivine, will gas: serpentinization and the abiogenic production of methane on Mars. Geophys Res Lett 32:L10203. doi:10.1029/2005GL022691

Page NJ, Talkington RW (1984) Palladium, platinum, rhodium, ruthenium and iridium in peridotites and chromitites from ophiolite complexes in Newfoundland. Can Miner 22:137–149

Page NJ, Pallister JS, Brown MA, Smewing JD, Haffty J (1982) Palladium, platinum, rhodium, iridium and ruthenium in chromite-rich rocks from the Samail ophiolite, Oman. Can Miner 20:537–548

Pašava J, Vymazalová A, Petersen S (2007) PGE fractionation in seafloor hydrothermal systems: examples from mafic- and ultramafic-hosted hydrothermal fields at the slow spreading Mid Atlantic Ridge. Min Deposita 42:423–431

Pawson JF, Oze C, Etiope G, Horton TW (2014) Discovery of new methane-bearing hyperalkaline springs in the serpentinized Dun Mountain Ophiolite, New Zealand. AGU 2014 Fall Meeting Abstracts

Prichard HM, Brough CP (2009) Potential of ophiolite complexes to host PGE deposits. In: Chusi L, Ripley EM (eds) New developments in magmatic Ni-Cu and PGE Deposits. Geological Publishing House, Beijing, pp 277–290

Proctor J, Woodell SRJ (1975) The ecology of serpentine soils. Adv Ecol Res 9:255–365

Proskurowski G, Lilley MD, Seewald JS, Früh-Green GL, Olson EJ, Lupton JE, Sylva SP, Kelley DS (2008) Abiogenic hydrocarbon production at lost city hydrothermal field. Science 319:604–607

Russell MJ, Hall AJ, Martin W (2010) Serpentinization as a source of energy at the origin of life. Geobiology 8:355–371

Sachan HK, Mukherjee BK, Bodnar RJ (2007) Preservation of methane generated during serpentinization of upper mantle rocks: evidence from fluid inclusions in the Nidar ophiolite, Indus Suture Zone, Ladakh (India). Earth Planet Sci Lett 257:47–59

Sanchez-Murillo R, Gazel E, Schwarzenbach E, Crespo-Medina M, Schrenk MO, Boll J, Gill BC (2014) Geochemical evidence for active tropical serpentinization in the Santa Elena Ophiolite, Costa Rica: an analog of a humid early Earth? Geochem Geophys Geosyst 15:1783–1800

Schrenk MO, Brazelton WJ, Lang S (2013) Serpentinization, carbon and deep life. Rev Min Geochem 75:575–606

Schutter SR (2003) Occurrences of hydrocarbons in and around igneous rocks. In: Hydrocarbons in crystalline rocks. Geol Soc London, Spec Pub 214:35–68

Sherwood Lollar B, Frape SK, Weise SM, Fritz P, Macko SA, Welhan JA (1993) Abiogenic methanogenesis in crystalline rocks. Geochim Cosmochim Acta 57:5087–5097

Sherwood Lollar B, Lacrampe-Couloume G, Voglesonger K, Onstott TC, Pratt LM, Slater GF (2008) Isotopic signatures of CH_4 and higher hydrocarbon gases from precambrian shield sites: a model for abiogenic polymerization of hydrocarbons. Geochim Cosmochim Acta 72:4778–4795

Smith NJP, Sheperd TJ, Styles MT, Williams GM (2005) Hydrogen exploration: a review of global hydrogen accumulations and implications for prospective areas in NW Europe. In: Doré´ AG, Vining BA (eds) Petroleum geology: North-West Europe and global perspectives, Proceedings of 6th petroleum geology conference, 349–358

Suda K, Ueno Y, Yoshizaki M, Nakamura H, Kurokawa K, Nishiyama E, Yoshino K, Hongoh Y, Kawachi K, Omori S, Yamada K, Yoshida N, Maruyama S (2014) Origin of methane in serpentinite-hosted hydrothermal systems: the CH_4–H_2–H_2O hydrogen isotope systematics of the Hakuba Happo hot spring. Earth Planet Sci Lett 386:112–125

Szatmari P, da Fonseca TCO, Miekeley NF (2011) Mantle-like trace element composition of petroleum—contributions from serpentinizing peridotites. In: Closson D (ed) Tectonics, InTech, 3:332–358

Szponar N, Brazelton WJ, Schrenk MO, Bower DM, Steele A, Morrill PL (2013) Geochemistry of a continental site of serpentinization in the Tablelands ophiolite, gros morne national park: a Mars analogue. Icarus 224:286–296

Taran YA, Kliger GA, Sevastyanov VS (2007) Carbon isotope effects in the open-system Fischer-Tropsch synthesis. Geochim Cosmochim Acta 71:4474–4487

Thampi KR, Kiwi J, Grätzel M (1987) Methanation and photo-methanation of carbon dioxide at room temperature and atmospheric pressure. Nature 327:506–508

Webster CR, Mahaffy PR, Atreya SK plus 26 others and the MSL Science Team (2014) Mars methane detection and variability at Gale crate. Science doi:10.1126/science.1261713

Whiticar MJ, Etiope G (2014a) Hydrogen isotope fractionation in land-based serpentinization systems. In:Suda et al. (eds) Comment on "Origin of methane in serpentinite-hosted hydrothermal systems: the CH_4–H_2–H_2O hydrogen isotope systematics of the Hakuba Happo hot spring". Earth Planet Sci Lett 386 (2014) 112–125, Earth Planet Sci Lett 401:373–375

Whiticar MJ, Etiope G (2014b) Methane in land-based serpentinized peridotites: new discoveries and isotope surprises. AGU 2014 Fall Meeting Abstracts

Yuce G, Italiano F, D'Alessandro W, Yalcin TH, Yasin DU, Gulbay AH, Ozyurt NN, Rojay B, Karabacak V, Bellomo S, Brusca L, Yang T, Fu CC, Lai CW, Ozacar A, Walia V (2014) Origin and interactions of fluids circulating over the Amik Basin (Hatay-Turkey) and relationships with the hydrologic, geologic and tectonic settings. Chem Geol 388:23–39

Zahnle K, Freedman RS, Catling DC (2011) Is there methane on Mars? Icarus 212:493–503

Chapter 8
Gas Seepage and Past Climate Change

Chapter 6 described the important role of gas seepage in the current budget for atmospheric greenhouse gases (methane), photochemical pollutants, and ozone precursors (ethane and propane). Global methane emissions (anthropogenic and natural) contribute approximately one-third of the total direct and indirect radiative forcing from all long-lived greenhouse gases (i.e., ~ 1 W/m^2 of 3 W/m^2; Ciais et al. 2013). Today, total geological methane emissions represent the second largest natural source of methane, following wetlands, and are comparable, in terms of magnitude, to other anthropogenic sources (see Fig. 6.7). Totals for the geological methane source do not include abiotic gases, as discussed in Chap. 7. Such is the current state, which is more or less blurry, of our present understanding. To understand what happened in the past and whether or not seepage influenced pre-anthropogenic climate change, two important considerations must be taken into account. The first consideration is whether or not it is logical to assume, in the absence of man-made methane sources before the industrial revolution and during pre-anthropogenic time periods (>5,000 years ago), that gas seepage was the second largest methane source in absolute terms and therefore, as was the case for wetland emissions, constituted a major control on variations in atmospheric methane burden. The second consideration is whether or not seepage has been constant over geological time periods. Using specific references to Late Quaternary changes, this chapter discusses how seepages, as a result of geological factors that change over time, may have influenced global climate. The discussion is based on the main concepts proposed in Etiope et al. (2008), and for the longer Cenozoic geological time scale on the main concept of "sedimentary carbon mobilization" as outlined by Kroeger et al. (2011). Figure 8.1 provides a schematic of the conceptual structure of the argument. Beginning from pre-existing gas accumulations, Quaternary changes refer to variations in the magnitudes of gas seepage. The Cenozoic perspective considers the entire process and the timing of carbon burial, gas generation, accumulation, and leakage. We obtain a sense of the potential impact of gas seepage on climate over long geological time scales if seepage is considered to be a part of a dynamic carbon cycle, which includes a gigantic reservoir (ca. 10^{16} tonnes C) of organic carbon buried in sedimentary basins. Hydrocarbon seepage is the transfer of this buried carbon to the atmosphere in the form of greenhouse gases (CH_4).

G. Etiope, *Natural Gas Seepage*, DOI 10.1007/978-3-319-14601-0_8

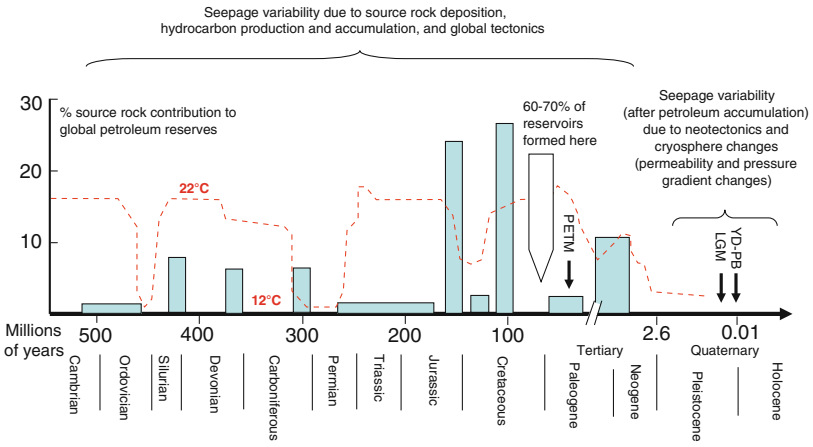

Fig. 8.1 A conceptual scheme for examining the possible effects of past seepage on climate. On long geological time scales seepage may be considered to be the result of the periodical mobilization of hydrocarbons following several major events of source rock deposition (*blue rectangles*) and reservoir formation (e.g., with the *white arrow* representing the formation of 60–70 % of the conventional reservoirs presently produced; from Kroeger et al. 2011 and Klemme and Ulmishek 1991). On shorter geological time scales, such as for the Quaternary, seepage is examined beginning with accumulated hydrocarbons and looking at geological and exhogene changes that may have induced variations in rock permeability and pressure gradients, the two main factors driving seepage (Chap. 3). The PETM (Paleocene-Eocene Thermal Maximum), the LGM (Last Glacial Maximum), and the YD-PB (Younger Dryas and Preboreal transition) are specific climate events studied in relation to seepage and discussed in this chapter. *Dashed red lines* indicate the estimated average temperature variations of C.R. Scotese, http://www.scotese.com/climate.htm, for visualizations of long-term climate variability, not for comparisons with source rock formations

The carbon reservoir is not stable and is mobilized over time. In other words, seepage is much more dynamic than many other geological processes would suggest (Kroeger et al. 2011). However, studies such as these are still in their infancy, and there are no "smoking guns" that demonstrate that hydrocarbon gas seepage actually influenced climates in the past. Therefore, this chapter will provide information regarding the "potential" of hydrocarbon gas seepage, as well as, the difficulties and limitations of possible interpretations.

8.1 Past Seepage Stronger than Today

As a starting point, it is important to consider that it is very likely that methane fluxes from seepage related to deep hydrocarbon reservoirs and migration pathways (e.g., Etiope and Klusman 2002, 2010) were greater during pre-industrial times than they are today, i.e., before petroleum exploitation began in the middle of the 19th century. As discussed in Chap. 2, more than 75 % of the world's petroliferous basins contain surface seeps. A large number of surface gas or oil manifestations from the

Alpine-Himalayan, Pacific Ocean, and Caribbean sedimentary belts, as described in 20th century petroleum geology literature (e.g., Link 1952), have now disappeared or greatly diminished. In many cases, the gas flux from hydrocarbon seeps decreased as a consequence of petroleum extraction from reservoirs in the region. This is possibly due to decreases in reservoir formation pressures, i.e. pressure gradients, related to petroleum production. For example, natural seeps in Azerbaijan were more common and likely released more gas and oil prior to intensive oil exploitation over the last century. Many natural "eternal" fires disappeared following years of petroleum extraction from nearby wells. Gas fluxes from the Coal Oil Point seeps, located off of the California (USA) coast, clearly decreased after 1973 as a result of petroleum production at nearby Platform Holly (Quigley et al. 1999). In Italy, most mud volcanism and gas seeps along the Adriatic and Sicilian passive margins became inactive following petroleum production that began in the 1950s and 1960s. Geographers in the early 1800s reported a small mud volcano in central Italy, near Pineto along the Adriatic coast, which has been actively bubbling and ejecting fresh mud for centuries (Colli and De Ascentiis 2003). Vigorous gas bubbling was observed there until 2005, then, in 2006, bubbling became weaker; the same year, a hydrocarbon well was drilled roughly 4 km away and a gas field was discovered. The well, located $\sim$2,000 m deep in Pliocene sediments, produces almost pure methane, similar to that released by the mud volcano. Isotope analyses of the gas indicated a microbial origin (Etiope et al. 2007). In the years following drilling, mud volcanic activity decreased significantly and ceased almost entirely after 2012 when gas production commenced. Although less likely, an alternative explanation could be that this reduction of activity is temporary and related to multi-year cycles of fluid pressure build-up and discharge. Observations such as these need to be conducted in a systematic way by monitoring the activity of mud volcanoes and other types of seeps, and if possible microseepage, prior to and following petroleum well drilling within the same petroleum system.

8.2 Potential Proxies of Past Seepage

Past gas seepage can be investigated by looking at geochemical and geological features in stratigraphic sequences or ice cores that are related to ancient local seeps or mud volcanoes and their activity.

For example, mud volcanism events can be recognised by abundant mud breccia composed of mud and rock fragments that markedly differ in age and physical properties from surrounding sediments. Both mud volcanoes and pockmarks significantly modify the morphology of the surface and seafloor. Therefore, buried mud volcanoes and other expulsion features can be identified in seismic reflection sections, in boreholes, or in outcrops (Fowler et al. 2000; Huseynov and Gulyiev 2004). The spatial relationships between allochthonous mud volcanic sediments or erosional surfaces created by pockmarks and hosting sediments can be used to date episodes of enhanced seepage. A significant portion of modern mud volcano

activity appears to be a result of the compression of rapidly deposited Pliocene–Pleistocene sediments, leading to overpressurisation, diapirism, and fluid flow within the subsurface (Milkov 2000). The analyses of mud volcanism proxies in Azerbaijan, in particular, indicate that a maximum extension for fluid emission activity occurred during the Upper Quaternary (Etiope et al. 2008).

Methane-derived authigenic carbonate deposits (MDACs) that are enriched in ^{12}C compared with conventional carbonates, form over extensive areas within modern sites of hydrocarbon discharge (Greinert et al. 2001). They also formed abundantly in the past, and those dating to Early Miocene times, i.e., fossilised chemosynthesis-based ecosystems, have been used to trace past seepage events (e.g., Conti et al. 2004; Campbell 2006).

Land-based travertines deposited at CH_4-bearing hydrothermal vents or surrounding hyperalkaline springs in serpentinised ultramafic rocks may provide useful indications of former enhanced gas discharges. The preliminary radiocarbon dating of European travertines suggests that their most extensive deposition occurred during the Mid-Holocene (5,000–10,000 years ago, Pentecost 1995). More detailed studies are necessary to determine the age and distribution of travertines, specifically those related to methane-rich waters, and to estimate the amount of released gas required to precipitate observed travertine deposits.

One of the most studied proxies of past methane emissions is the carbon and hydrogen isotope composition of CH_4 extracted from air trapped in Greenland and Antarctic ice cores. Different natural sources, including wetlands, clathrates, biomass burning, and natural gas seepage have been considered to release methane, each with a distinctive "average" isotope signature, which is not completely correct. The story is not as simple as often assumed. A specific critical discussion of this argument is offered in Sect. 8.3.4, with a reference to Late Quaternary climate changes.

8.3 Methane and Quaternary Climate Change

8.3.1 Traditional Models: Wetlands versus Gas Hydrates

A series of rapid increases in atmospheric methane concentrations during the late Quaternary (the last ~400,000 years) appears to have been accompanied by periods of rapid warming (Brook et al. 1996; Blunier and Brook 2001). Variations in atmospheric methane concentrations can result from changes in either sources and/or sinks of methane. Quaternary changes in tropospheric oxidation by abstraction with OH radicals (the major methane sink) only varied by approximately 17 % between glacial and interglacial episodes (Thompson et al. 1993; Crutzen and Bruhl 1993), while methane concentrations often doubled (Petit et al. 1999). Therefore, some change in methane sources must have been the main cause of variations. Theoretically, an alternative is that there could have been, for some reason, large amounts of other species in the troposphere that competed for OH, resulting in a longer residence time for methane (Whiticar, personal communication).

Two main hypotheses have been proposed to explain rapid increases in methane concentrations accompanying late Quaternary glacial terminations: (a) emissions from tropical wetlands and (b) emissions from submarine gas hydrates (clathrates). The first hypothesis is based on the assumption that wetlands expanded in response to sudden increases in precipitation and temperature (Chappellaz et al. 1993; Maslin and Thomas 2003). The second hypothesis invokes sudden and significant emissions of methane from gas hydrates in shallow sediments on the ocean floor that decompose in response to oscillations of intermediate water temperatures; the hypothesis is often called the "clathrate gun hypothesis" (Kennett et al. 2003). Methane from a catastrophic release reaching the atmosphere would have contributed to the greenhouse effect, causing the temperature to rise. That, in turn, would have led to further gas hydrate decomposition. Therefore, there would have been positive feedback mechanisms inducing the release of large amounts of methane into the atmosphere. The clathrate gun hypothesis is a part of a more general model called the "methane-led hypothesis" (Nisbet 2002) which infers that methane released through the ocean floor precedes and causes temperature increases (Fig. 8.2a). In contrast, the wetland hypothesis states that increased methane emissions were a consequence, not a cause, of climate change (Chappellaz et al. 1990).

Both hypotheses have some weak points. For example, the wetland hypothesis suffers from a lack of geological evidence for the wide and rapid development of wetlands during the late Quaternary, which is necessary to explain the rapid rate of methane concentration increase. Wetlands needed too long to form (several hundreds years) and therefore were too sluggish to result in the fast CH_4 concentration changes. Additionally, it appears that negligible wetland ecosystems existed during the last glacial episode as a result of global aridity, low sea level, and low water tables. Kennett et al. (2003) argued that large (up to –6 ‰) and brief carbon isotopic excursions during the last 60,000 years as recorded in benthic foraminifera from the Santa Barbara Basin may be explained by the release of methane from decomposing gas hydrates. However, there are numerous reasons to doubt this "clathrate gun hypothesis". For example, measurements from modern seeps indicate that the carbon shells of foraminifera living near methane discharges have isotopic properties similar to those living in non-venting pelagic sediments (Torres et al. 2003; Etiope et al. 2014). Even if the excursions are related to methane (Hinrichs et al. 2003), there is no evidence that this methane was derived from gas hydrates. Direct measurements of methane concentrations in marine sediments (Dickens et al. 1997; Milkov et al. 2003) suggest that gas hydrate concentrations in most of the sediments of continental margins do not exceed 1–2 % of porosity over the gas hydrate stability zone (GHSZ). Moreover, relatively moderate stadial-interstadial temperature shifts of 2–3.5 °C are not sufficient to completely eliminate the GHSZ, and most of the methane released at the base of the GHSZ would re-crystallize as new gas hydrates within the GHSZ (Milkov and Sassen 2003). Isotope evidence from ice cores, as discussed in more detail below, is also against the hydrate hypothesis (e.g., Schaefer et al. 2006). Finally, a significant portion of methane released from gas hydrate decomposition is likely to be consumed by micro-organisms, sequestered as authigenic carbonates on the seafloor (Greinert et al. 2001), and oxidized in

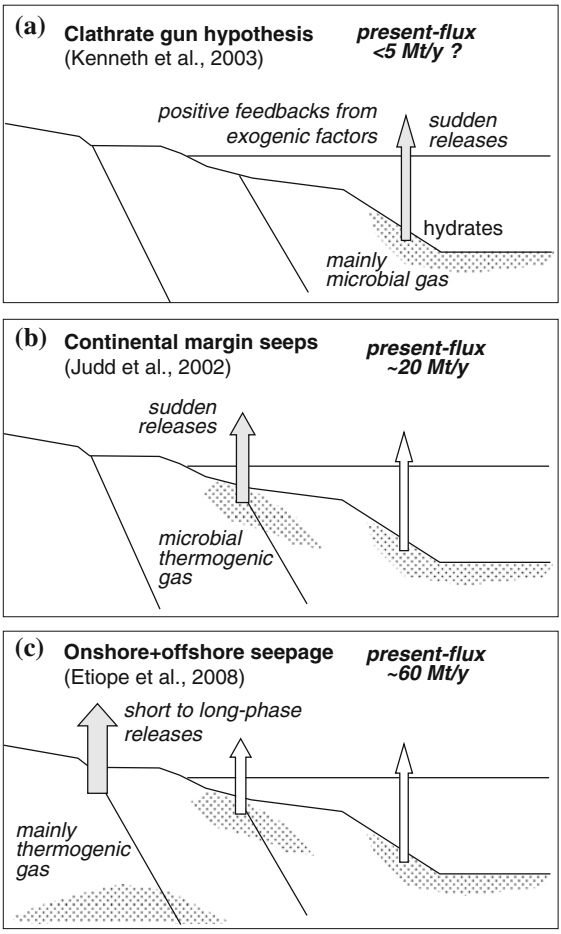

Fig. 8.2 The three hypotheses of climate control by global methane emission from **a** hydrates, **b** submarine seeps, and **c** onshore + offshore seepage in total

the water column (Valentine et al. 2001). In this scenario, gas hydrates would not contribute to the atmospheric budget. As discussed in Chap. 6, since the majority of the methane released from deep sea melting hydrates is dissolved and oxidised in the water column, it does not reach the atmosphere. Therefore, a clear need exists to continue the search for a plausible mechanism to explain increases of methane concentrations during the late Quaternary.

8.3.2 Adding Submarine Seeps

Judd et al. (2002) indicated that in addition to gas hydrates, marine seeps related to various reservoirs and pathways should be incorporated into wider models, providing both positive and negative feedbacks for global warming and cooling

(Fig. 8.2b) during the late Quaternary. For example, glacial periods are characterised by sea-level lowering, producing a decrease in hydrostatic pressure, the subaerial exposure of seafloor seeps, and gas hydrate destabilization in deeper seafloors. All three processes would enhance gas release which, in turn, would lead to "greenhouse" warming (negative feedbacks). However, glacial periods also lead to the advancement of ice sheets, sea ice, and gas hydrate stabilization in high latitudes, which inhibit gas mobility and release (positive feedback). In their work, Judd et al. (2002) stated support for a prevailing negative feedback, largely due to gas hydrate destabilization within the deep sea. We must note, anyway, that deep sea destabilization would be so slow that methanotrophs could likely keep up and consume all methane. Only slope failures could allow the methane to enter the water column fast enough. In addition, deeper water seafloors generally have too little organic carbon to produce "climatically significant" quantities of methane.

However, as mentioned above (and in Chap. 6), measurements within the water column indicate that most of the methane from deep marine seeps becomes dissolved and oxidized within the water column and does not reach the atmosphere. As outlined by Luyendyk et al. (2005), shallow marine seeps and episodic sub-aerial exposure, following sea-level drops, would be more important. Moreover, the model of Judd et al. (2002) assumes that onshore seepage is unaffected by glacial or interglacial changes. As discussed below, such a supposition is only partially true because onshore gas seepage can be influenced by crustal deformations induced by glacial advances and retreats.

All "methane-led hypotheses" refer to marine seepage using a basic concept that methane emissions are controlled by surface conditions, such as the extent of ice sheets, eustatic sea-level, and ocean bottom-water temperatures. Today, we know that submarine seeps are only a component of global gas seepage and that, presently, gas hydrates are not significantly (measurably) contributing to tropospheric greenhouse gas budgets. The amount of methane emitted from contemporary onshore geological sources is likely greater than that from offshore sources. Due to the exposure of continental shelves during low sea level, onshore seepage areas are likely to have been more widespread during glacial periods (Luyendyk et al. 2005). Therefore, wider modelling that includes all geological methane sources, either onshore or offshore, is required to obtain insight into possible Quaternary methane-climate links.

8.3.3 Considering Onshore and Offshore Seepage in Total

A series of theoretical considerations and some proxy analyses suggested that there is no a priori reason why the impact of all geological methane emissions, onshore and offshore (Fig. 8.2c), should be disregarded, at least on the Quaternary time scale (Etiope et al. 2008).

Gas seepage, in general, is largely controlled by endogenic and, in some cases, exhogenic factors (e.g., cryosphere changes), which are not constant over

geological, millennial, and secular time scales. After hydrocarbons are produced in source rocks and accumulated in reservoirs, seepage is modulated by a series of variable geodynamic and petroleum geology processes that can create pathways (increase permeability) and, in some cases, increase pressure gradients. The processes include fracturing by neotectonics, basin uplifting, seismicity, changes of pressure due to propagation and the retreat of ice sheets, and evolving volcanism and magmatism that may increase heat flow in adjacent petroleum systems and, thus, gas pressure. Seepage variations on shorter time scales, years, and seasons, can also occur in response to hydrogeologic and exogenous factors, both climatic and meteorologic.

As discussed in Sect. 3.1, gas seepage basically follows advection Darcy's Law, whereby gas flux is sensitive to the variations of pressure gradients (gas pressure build-up and discharge) and rock permeability (fracturing and sealing). Depending on the gas migration forms described in Sect. 3.2, the mobility of gas, and hence its potential to enter the atmosphere, depends on the intrinsic effective permeability of the rock, the fracture aperture, the bubble or slug radius, the gas viscosity, and the gas density. As determined from studies of mud volcanism, e.g., Mellors et al. (2007), variations of permeability and fracture aperture over time can be induced by seismic activity. Neotectonic faults and fractures in Pleistocene sediments have been recognised as migration pathways for fluids rising from diapirs and hydrocarbon accumulations (e.g., Milkov 2000; Revil 2002). Salt tectonics itself is a powerful factor that is capable of creating crustal weakness zones that are very effective as gas migration routes (Etiope et al. 2006). Basically, any change in mechanical-geological conditions (basin loading, compaction, extension, and the fracturing of rocks) and physical-chemical conditions (variations in temperature, pressure, chemical reactions, and mineral precipitation) can lead to seepage variations. Changes can also be cyclic, e.g., gas pressure build-up and discharge. Additionally, dynamic links exist between certain endogenic and exogenic processes. For example, major glacial advances and retreats may be accompanied by appreciable crustal deformations (Stewart et al. 2000). Interglacial episodes may be characterized by relatively greater earthquake activity than during glacial episodes (Stewart et al. 2000). Large faults appear to have become activated during post-glacial times in many regions, including in Fennoscandia and Canada (Morner 1978; Wu et al. 1999). During ice sheets retreat the consequent pressure release can also trigger enhanced gas seepage. Significant methane emissions, up to 100 Tg of CH_4, have been estimated to be driven by this process in the Michigan Basin alone (Formolo et al. 2008). Therefore, it is possible to hypothesise that the correlation between interglacial warm episodes, the increased methane concentrations within the atmosphere, and the enrichment of ^{13}C in atmospheric methane (typical for geogenic methane) could be explained by increased endogenic activity and the resulting enhancement of seepage during interglacials.

However, because cryosphere disintegration and resultant ice sheet retreat may induce the opposite effect on gas seepage at different time scales, depending on the depth of the gas source, the story is not so simple. Cryosphere formation (ice sheet propagation) may also increase seepage (e.g., Lerche et al. 1997). For gas in

shallow sediments, the removal of ice sheets has the effect of removing a sealing cap, and the result (seepage to the atmosphere) may be rapid, at scales of decades or centuries. However, for deeper gas (thermogenic) accumulations, the effect can be different and operate on much longer time scales. Deglaciations may perturb the hydrodynamic conditions of petroleum systems in sedimentary basins. Cryosphere disintegration may lead to isostatic uplift. Such an uplift may reduce the pore pressure of sediments, which, in turn, may increase the exsolution of gas dissolved in deep water, causing accumulations in reservoir rocks. At the same time, the decrease of pressure may reduce the gas flux by reducing the pressure of already existing reservoirs so that the pressure gradient decreases upward. For example, Lerche et al. (1997) claim that it is overpressure (cryosphere formation) that may lead to the fracturing of sediments, causing the leakage of water, oil, and gas. On the other hand, there is also an indirect effect for seismicity such that deglaciation and isostatic rebounding seismicity (and related seepage) may increase. Basically, there is no univocal relationship between deglaciation and seepage.

It is important to consider that catastrophic or abrupt methane releases, such a massive hydrate dissociation may not be a prerequisite for changes in atmospheric methane concentrations. Continuous enhanced degassing and/or secular phases of intense seepage may lead to significant increases in methane concentrations within the atmosphere.

8.3.4 CH_4 Isotope Signatures in Ice Cores

The multi-isotope composition of methane ($\delta^{13}C$, $\delta^{2}H$, and ^{14}C) in tropospheric air trapped and recorded in ice cores from Greenland and Antarctica is used to trace various natural sources that may have contributed to the late Quaternary greenhouse gas effect and climate change. The assumption used in main reference works such as Kennett et al. (2003), Sowers (2006), Schaefer et al. (2006), Whiticar and Schaefer (2007), Petrenko et al. (2009), Bock et al. (2010), Melton et al. (2011) and Möller et al. (2013) is that natural sources, including wetlands, clathrates, biomass burning, and gas seeps produce methane with different isotopic compositions (Table 8.1). Wetland methane is considered to be microbial, ^{13}C-depleted, ^{2}H-depleted, and relatively modern; in other words with measurable ^{14}C. Clathrates are considered to be substantially microbial, ^{13}C-depleted, ^{2}H-depleted, and fossil; in other words ^{14}C-free. Biomass burning is considered to be unequivocally ^{13}C-enriched. Natural gas seeps are generally considered to be only thermogenic, ^{13}C-enriched, ^{2}H-enriched and fossil; in other words ^{14}C-free. In practice, an increase of ^{13}C-depleted methane in the atmosphere has typically been associated with emissions from wetlands or clathrates. Seeps have been considered to release only ^{13}C-enriched methane. In reality, the picture is more complicated, as the carbon isotope ratios of methane hydrates, wetlands, and, in particular, seeps can vary widely. The clathrate $\delta^{13}C$ values measured to date range from –74.0 to –39.6 ‰, and global averages based on various datasets range from −67 ‰ (Milkov 2005) to −63 ‰ (Whiticar and Schaefer 2007).

Table 8.1 Average $\delta^{13}C$ and $\delta^{2}H$ values of methane from natural sources and related present global CH_4 emissions to the troposphere

Source	$\delta^{13}C$ ‰ (VPDB)	$\delta^{2}H$ ‰ (VSMOW)	Emission (Mt y^{-1})
Tropical wetlands	−59	−360	175–217
Boreal wetlands	−62	−380	
Termites	−63	−390	11
Wild animals	−60	−330	15
Wild fires	−25	−225	3
Hydrates	−63	−190	6 (?)
Geological (WS)	−41.8	−200	–
Geological (updated)	–	–	60
Onshore seeps and mud volcanoes	−48.8 (−26 to −82)	−188 (−114 to −292)	13–24
Microseepage	−25 to −45	–	10–25
Geothermal (abiotic-biotic)	−5 to −30	–	2.5–6.3
Marine seepage	−20 to −60	–	20
Abiotic (serpentinisation)	−6 to −35	−198 (−109 to −333)	?

Isotope ratios of natural sources, including those for "Geological WS", are from Whiticar and Schaefer (2007). Isotope ratios for "Onshore seeps and mud volcanoes" and "Abiotic" are derived from the GLOGOS dataset (see Chap. 2), based on ∼600 data points. Isotope ratios for microseepage, and geothermal and marine seepage are preliminary ranges reported in Etiope et al. (2008). Emissions of natural sources from Ciais et al. (2013), and those of geological sources from Table 6.3 in Chap. 6

Clathrates composed of ^{13}C-enriched methane occur in many localities where the gas flux from deep petroleum systems converges along mud volcanoes and faults (Milkov and Sassen 2002). Methane at such high gas flux sites has a global average $\delta^{13}C$ value of approximately –58 ‰. However, the global average $\delta^{13}C$ of methane in all submarine gas hydrates is more negative than −60 ‰. In a similar manner, the methane released from wetlands is depleted in ^{13}C, but tropical and boreal wetlands produce methane with different $\delta^{13}C$ values. Both marine gas hydrates and natural gas have a relatively higher D/H ratio ($\delta^{2}H_{CH4} > -250$ ‰) as compared to wetland gas (<−250 ‰). However, the main problem has been the attribution of thermogenic C and H isotopes to natural gas seepage. In Chap. 5 (see Fig. 5.5 in particular), it was noted that seeping methane is not only of a thermogenic type and that approximately 10 % of seeps release pure microbial methane whose $\delta^{13}C$ is similar to that of wetlands and most gas hydrates, and approximately 30 % of the gas is mixed, with $\delta^{13}C$ from −50 to −60 ‰. Additionally, abiotic methane (Chap. 7) is ^{13}C-enriched ($\delta^{13}C$ values heavier than −35 ‰) but its $\delta^{2}H$ values can be ^{2}H-depleted (isotopically lighter), frequently on the order of −200 and −300 ‰, resembling microbial gas (Etiope and Sherwood Lollar 2013). Globally, emissions of this abiotic methane are still unknown. Therefore, its potential in the past remain speculative, but it represents an additional unknown factor in the exercise of distinguishing wetlands and seepage. The crux of the discussion is that the average value of seeping natural gas (including

thermogenic, microbial and mixed gas), based on available data (e.g., see the GLOGOS data-set discussed in Chap. 2) is approximately −49 ‰, a bit lower than present and past atmospheric values (−47.3 ‰ today and approximately −46 ‰ before the Holocene). Therefore, even huge emissions of thermogenic gas may not change atmospheric CH_4 isotope ratios. This uncertainty and re-evaluations of gas seepage isotopic compositions should be considered in order to improve paleo-CH_4 budget models, such as those by Whiticar and Schaefer (2007).

At present, atmospheric methane has a mean $\delta^{13}C$ value of −47.3 ‰, implying a mixture of microbial methane (∼70 %, mainly by methyl-type fermentation in terrestrial environments) depleted in ^{13}C relative to the mean atmospheric value, thermogenic methane (∼20 %) commonly enriched in ^{13}C, and methane from biomass burning (∼10 %) significantly enriched in ^{13}C. This atmospheric value ($\delta^{13}C_{CH4} \sim -47.3‰$), does not correspond to the isotope ratio of the integrated inputs due to the isotope effects associated with the hydroxyl abstraction removal of tropospheric methane. This photochemical reaction enriches residual tropospheric methane in ^{13}C by ca. 5 ‰ (e.g., Cantrell et al. 1990, Saueressig et al. 2001). As discussed in Sect. 6.4.1.4, it is also important to keep in mind that the source for roughly 30 % of atmospheric methane is fossil and radiocarbon-free.

With an assumption that seepage is represented only by thermogenic ^{13}C-enriched and ^{2}H-enriched methane, most methane source identifications for the Late Quaternary have been made for the Younger Dryas, a glacial period at the end of Pleistocene (11,400–12,800 years BP), and its ending phase, the transition to the Preboreal Holocene (YD-PB, from 11,400 to 11,600 years BP). The YD-PB transition corresponds to an abrupt warming, with global temperatures rising to 10 °C over 20–50 years (Severinghaus et al. 1998) and with methane increasing rapidly from approximately 450 ppbv to over 850 ppbv. Various authors have emphasised certain aspects rather than others, so overall interpretations regarding the possible links between methane and warming are still open to revision and the uncertainties are quite large.

It seems that for the YD period, before the YD-PB transition, tropospheric methane was relatively constant but systematically ^{13}C-enriched and ^{2}H-depleted as compared to the present day ($\delta^{13}C$: –46 ‰ and $\delta^{2}H$: –95 ‰, i.e. ∼ +1 ‰ and −9‰ relative to the present day, respectively). The stable isotope record also indicates that in the first part of the YD, both $\delta^{13}C$ and $\delta^{2}H$ increased and then, during the second portion of the YD, both $\delta^{13}C$ and $\delta^{2}H$ decreased (Whiticar and Schaefer 2007). Then, at the YD-PB transition, CH_4 concentration increased abruptly but at this interval the $\delta^{13}C$ was essentially constant, while the $\delta^{2}H$ decreased. The trends are schematized in Fig. 8.3.

The trend at the transition may be explained by assuming that the rise in CH_4 concentration was either just a proportional increase in the same sources during the entire interval, or that changes in the sources and/or sinks were well balanced. Sowers (2006) suggested that a constant $\delta^{13}C$ at periods when CH_4 increased could be compatible with the addition of wetland emissions. The suggestion was later supported by radiocarbon (^{14}C), analyses of CH_4 in Pakitsoq ice on Greenland (Petrenko et al. 2009). This work attributed most of the YD-PB CH_4 rise to

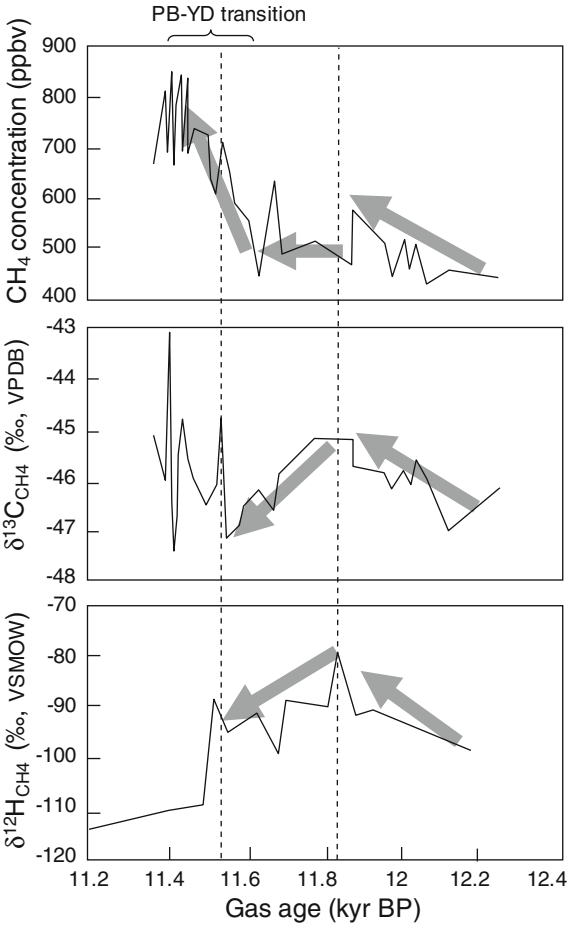

Fig. 8.3 Trends of CH_4 concentration and its stable isotope composition across the YD–PB transition as measured in the Greenland ice sheet (redrawn and modified after Whiticar and Schaefer 2007)

wetlands, not to marine gas hydrates. The argument against massive marine gas hydrate release is consistent with the $\delta^{13}C_{CH_4}$ of Pakitsoq ice (Schaefer et al. 2006; Melton et al. 2011).

However, corresponding C- and H-isotope mass balances for the YD suggested fluctuating emissions of thermogenic gas (Whiticar and Schaefer 2007). Decreasing δ^2H values at the YD-PB transition suggest that gas hydrates were either stable or not present in significant amounts. In any case, a massive microbial gas hydrate release, proposed by the 'clathrate gun hypothesis' does not seem responsible for methane increases at the YD–PB transition. The gradual, non-catastrophic, release of thermogenic hydrate occurring during the first part of the YD is feasible, but not the later. The release of thermogenic gas could also be conventional, thermogenic natural gas seepage (Whiticar and Schaefer 2007).

Another well-studied period during the Quaternary is the Last Glacial Maximum (LGM) that occurred from 18,000 to 26,000 years BP. Here, δ^2H_{CH4} significantly

increased, becoming ~20 ‰ higher than early Holocene values, considered to be coherent with increased emissions from natural gas seeps (Sowers 2006). $\delta^{13}C$ was also found to be quite high during the LGM. Fischer et al. (2008) attributed ^{13}C-enrichment to a shutdown of boreal wetland sources, accompanied by little or no change in biomass burning sources. The LGM has been a benchmark interval for understanding glacial-interglacial CH_4 isotopic shifts. The LGM demonstrates the dependency on variable sources, but also, and in some cases predominantly, on variable tropospheric sinks such as CH_4 oxidation by atomic chlorine (Levine et al. 2011). Today, it is clear that past atmospheric methane emissions can only be constrained using methane isotope records from ice cores if changes to source signatures and sink isotope effects with varying environmental and climatic conditions are accurately known. Even when they are known, considering that ^{13}C-depleted and ^{2}H-depleted CH_4 may also come from geological sources, the uncertainties in the attribution of several sources increase. Many large petroleum systems (and petroleum seepage systems, as defined in Chap. 1), with current active seeps contain microbial methane. Examples include the Illinois Basin (Coleman et al. 1988), the Transylvanian Basin (Spulber et al. 2010), the Po Basin (Etiope et al. 2007), and, certainly, the world's largest gas accumulation, the Urengoy gas field in the West Siberian Basin. The methane in this field has a $\delta^{13}C_{CH_4}$ from −48 to −54 ‰ and a $\delta^{2}H_{CH4}$ as low as −227 ‰ (Cramer et al. 1999). Many large mud volcanoes release gas that is a mixture of thermogenic and microbial sources (Etiope et al. 2009). Examples include the southeastern Caspian Basin, Turkmenistan ($\delta^{13}C$ up to −56 ‰, $\delta^{2}H$ up to −216 ‰), the Makran Basin in Pakistan ($\delta^{13}C$ up to −59 ‰), and the New Papua Guinea ($\delta^{13}C$ up to −72 ‰, $\delta^{2}H$ up to −230 ‰). If these basins experienced major degassing due to Pleistocene-Holocene neotectonics, including recent basin uplifts, in concert with episodes of enhanced microbial gas emissions in these regions, then their combined carbon isotope signature could be difficult to interpret. In particular, if only $\delta^{13}C$ values are examined in the ice records, then such mixed isotope values could clearly be confused with ^{13}C-depleted methane emissions from clathrates and from wetlands.

8.4 Longer Geological Time Scale Changes

8.4.1 The Concept of Sedimentary Organic Carbon Mobilization

When expanding the geological time scale it is important to consider not only variations of seepage following hydrocarbons generation and accumulation, but also variations in hydrocarbon generation after organic carbon accumulation and burial. This perspective is discussed by Kroeger et al. (2011).

Oil and gas are the "quintessence" of a huge carbon reservoir in sedimentary rocks, amounting to roughly 10^{16} tonnes. The carbon that comprise oil and gas was buried with variable intensities and rates over time. It is instructive to learn that petroleum

(oil and gas) was not produced in equal measure in the geological past. More than 50 % of conventional reservoired oil and gas was generated by source rocks formed within two relatively short geological time periods, i.e., between 144 and 169 Myrs ago (Upper Jurassic) and between 88 and 119 Myrs ago (Aptian-Turonian) (Klemme and Ulmishek 1991). Both the Upper Jurassic and Mid-Cretaceous were special periods characterised by the break-up of Gondwana and enhanced marine transgressions, with the formation of wide continental shelves and epicontinental seas that were favourable basins for the deposition of organic-rich sediments. For example, Upper Jurassic source rocks produced much of the petroleum within the Arabian Basin, North Sea, Siberia, and Gulf of Mexico. After source rock (the "kitchen") is created, kerogen maturation and petroleum generation evolves dependent on the thermal history of the sedimentary basin. The process can be variable over time, depending on continental tectonic changes (e.g., basin thickening, subsidence, extensions, orogenesis with mountain and foredeep building). In theory, the thermal maturation of kerogen can also be affected by global atmospheric and ocean warming (Kroeger et al. 2011). An increase in surface temperature may, in fact, increase subsurface temperatures within the basin on geological time scales. For an average gradient of 3°/100 m, it has been estimated that a 10 °C increase in surface temperatures can result in source rock warming with an upward shift of oil and gas windows by approximately 300 m (Allen and Allen 2006). This is an example of an external (exogenous) influence on petroleum generation.

Oil and gas migrates and accumulates in reservoirs. In this case, tectonic changes modulate the formation of suitable reservoirs and traps. Approximately 65–70 % of conventional reservoirs were formed between 80 and 90 Myrs ago (Fig. 8.1). From this point onward the story is the one discussed in Sect. 8.3 and it is important to consider that migration and seepage occur within geologically short time intervals following the onset of the main petroleum generation phase (Mathews 1996). Seepage becomes focused over geological time and is intermittent due to pressure build-ups and discharges within accumulations. For a geological time scale perspective, however, it is clear that given the large size of sedimentary carbon inventory, only slight changes in remobilization could have a significant impact on seepage and the atmosphere. The remobilization of 1 % of sedimentary carbon would be equivalent to 150,000 Gt of carbon as a seepage feedstock.

8.4.2 Paleogene Changes

Climate changes recorded throughout the Cenozoic include either long-lasting or sudden warming periods (hyperthermals) that may be related to changes in geological gas emissions. The Paleocene-Eocene Thermal Maximum (PETM) has garnered considerable scientific interest. The PETM provides an excellent analogue for understanding the impacts of global warming and massive carbon input to the ocean and atmosphere. The PETM is characterized by extreme changes in Earth's surface occurring approximately 55.8 million years ago and lasting $\sim$170,000 years. Global

temperatures rose by ~6 °C. Warming extended from the tropics to high latitudes and to the deep ocean (~4–5 °C in bottom ocean waters over ~20,000 years; e.g., Higgins and Schrag 2006). The PETM is also marked by a prominent negative excursion in carbonate carbon stable isotope ($\delta^{13}C_{carb}$) records from across the globe; specifically, a large decrease (from ca 2 to 6‰) in the $^{13}C/^{12}C$ ratio of marine and terrestrial carbonates depending on the location. Strong evidence for the cause/source of the abnormal amounts of ^{13}C-depleted carbon during the PETM has been the topic of intense speculation. Svensen et al. (2004) proposed that this isotopically light carbon may have been due to the emission of large volumes of methane (up to several 1,000s Gt of carbon), formed in metamorphic aureoles surrounding volcanic sill intrusions in organic-rich sedimentary basins. Methane hydrates were initially the most popular explanations, but since the hydrate reservoir at that time was likely smaller than today and since increases in atmospheric CO_2 due to methane release were not sufficient to trigger the warming (Higgins and Schrag 2006), additions from catastrophic methane hydrate decomposition (Dickens et al. 1997) are less plausible. However, 4,000 Gt of carbon would have been sufficient if the carbon was related to methane of thermogenic origin (Kroeger et al. 2011). Such emissions may not only have been effective during hyperthermals, such as the PETM, but may have been operating over longer time scales, on the order of millions of years. In fact, it is possible that a general increase in heat flow due to enhanced magmatic activity during the Eocene (Svensen et al. 2004) accelerated the maturation of buried organic matter into hydrocarbons. This type of general enhanced thermogenic hydrocarbon production (with $\delta^{13}C$ between −50 and −25 ‰) may have resulted in increased seepage, which may explain extensive negative $\delta^{13}C$ excursions during the Early Eocene Climate Optimum (EECO). Increased thermogenic methane fluxes could also have been related to the following: (a) the greatest hydrocarbon production in Earth's history, occurring in Upper Jurassic and Aptian-Turonian source rocks; (b) regional and global tectonic changes; and (c) expansion of the "thermogenic" window due to the climate warming discussed above (Kroeger et al. 2011). However, these are only potential processes. More precise evaluations of causal-effect links and global methane emissions over several geological periods can only be obtained through specific Earth system models linking the atmosphere, hydrosphere, and geosphere on different time scales.

References

Allen PA, Allen JR (2006) Basin analysis. Blackwell, Oxford, 549 pp

Blunier T, Brook E (2001) Timing of millenial-scale climate changes in antarctica and greenland during the last glacial period. Science 291:109–112

Bock M, Schmitt J, Möller L, Spahni R, Blunier T, Fischer H (2010) Hydrogen isotopes preclude marine hydrate CH_4 emissions at the onset of Dansgaard-Oeschger events. Science 328:1686–1689

Brook E, Sowers T, Orchardo J (1996) Rapid variations in atmospheric methane concentration during the past 110,000 years. Science 273:1087–1091

Campbell KA (2006) Hydrocarbon seep and hydrothermal vent paleoenvironments: past developments and future research directions. Palaeogeogr Palaeoclimatol Palaeoecol 232:362–407

Cantrell CA, Shetter RE, McDaniel AH, Calvert JG, Davidson JA, Lowe DC, Tyler SC, Cicerone RJ, Greenberg JP (1990) Carbon kinetic isotope effect in the oxidation of methane by the hydroxyl radical. J Geophys Res 95:22,455–22,462

Chappellaz J, Barnola JM, Raynaud D, Korotkevich YS, Lorius C (1990) Ice-core record of atmospheric methane over the past 160,000 years. Nature 345:127–131

Chappellaz J, Fung IY, Thompson AM (1993) The atmospheric CH4 increase since the last glacial maximum (1) source estimates. Tellus 45B:228–241

Ciais P, Sabine C, Bala G, Bopp L, Brovkin V, Canadell J, Chhabra A, DeFries R, Galloway J, Heimann M, Jones C, Le Quéré C, Myneni RB, Piao S, Thornton P (2013) Carbon and other biogeochemical cycles. In: Stocker TF et al (eds) Climate change 2013: the physical science basis. Contribution of working group i to the fifth assessment report of IPCC. Cambridge University Press, Cambridge, UK and New York, NY, USA

Coleman DD, Liu C-L, Riley KM (1988) Microbial methane in the shallow paleozoic sediments and glacial deposits of illinois, U.S.A. Chem Geol 71:23–40

Colli B, De Ascentiis A (2003) Il Cenerone: vulcanello di fango di Pineto. De rerum natura. Periodico di informazione sull'ambiente, n.35–36, anno XI

Conti S, Fontana D, Gubertini A, Sighinolfi G, Tateo F, Fioroni C, Fregni P (2004) A multidisciplinary study of middle miocene seep-carbonates from the northern apennine foredeep (Italy). Sedim Geol 169:1–19

Cramer B, Poelchau HS, Gerling P, Lopatin NV, Litke R (1999) Methane released from groundwater—The source of natural gas accumulations in northern West Siberia. Mar Pet Geol 16:225–244

Crutzen PJ, Bruhl C (1993) A model study of atmospheric temperatures and the concentrations of ozone, hydroxyl, and some other photochemically active gases during the glacial, the preindustrial holocene and the present. Geoph Res Lett 20:1047–1050

Dickens GR, Paull CK, Wallace P (1997) The ODP leg 164 scientific party direct measurement of in situ methane quantities in a large gas-hydrate reservoir. Nature 385:426–428

Etiope G, Feyzullayev A, Baciu CL (2009) Terrestrial methane seeps and mud volcanoes: a global perspective of gas origin. Mar Pet Geol 26:333–344

Etiope G, Klusman RW (2002) Geologic emissions of methane to the atmosphere. Chemosphere 49:777–789

Etiope G, Klusman RW (2010) Microseepage in drylands: flux and implications in the global atmospheric source/sink budget of methane. Global Planet Change 72:265–274

Etiope G, Papatheodorou G, Christodoulou D, Ferentinos G, Sokos E, Favali P (2006) Methane and hydrogen sulfide seepage in the NW Peloponnesus petroliferous basin (Greece): origin and geohazard. AAPG Bull 90:701–713

Etiope G, Martinelli G, Caracausi A, Italiano F (2007) Methane seeps and mud volcanoes in Italy: gas origin, fractionation and emission to the atmosphere. Geoph Res Lett 34:L14303. doi:10.1029/2007GL030341

Etiope G, Milkov AV, Derbyshire E (2008) Did geologic emissions of methane play any role in Quaternary climate change? Global Planet Change 61:79–88

Etiope G, Panieri G, Fattorini D, Regoli F, Vannoli P, Italiano F, Locritani M, Carmisciano C (2014) A thermogenic hydrocarbon seep in shallow Adriatic Sea (Italy): gas origin, sediment contamination and benthic foraminifera. Mar Pet Geol 57:283–293

Etiope G, Sherwood Lollar B (2013) Abiotic methane on Earth. Rev Geoph 51:276–299

Fischer H, Behrens M, Bock M, Richter U, Schmitt J, Loulergue L, Chappellaz J, Spahni R, Blunier T, Leuenberger M, Stocker TF (2008) Changing boreal methane sources and constant biomass burning during the last termination. Nature 452:864–867

Formolo MJ, Salacup JM, Petsch ST, Martini AM, Nusslein K (2008) A new model linking atmospheric methane sources to Pleistocene glaciation via methanogenesis in sedimentary basins. Geology 36:139–142

Fowler SR, Mildenhall J, Zalova S (2000) Mud volcanoes and structural development on Shah Deniz. J Pet Sci Eng 28:189–206
Greinert J, Bohrmann G, Suess E (2001) Methane venting and gas hydrate-related carbonates at the hydrate ridge: their classification, distribution and origin. In: Paull CK, Dillon WP (eds) Natural gas hydrates: occurence, distribution, and detection. Geophysical Monograph, vol 124. American Geophysical Union, Washington, DC, pp 99–113
Higgins JA, Schrag DP (2006) Beyond methane: towards a theory for the paleocene-eocene thermal maximum. Earth Planet Sci Lett 245:523–537
Hinrichs K-U, Hmelo LR, Sylva SP (2003) Molecular fossil record of elevated methane levels in late pleistocene coastal waters. Science 299:1214–1217
Huseynov DA, Guliyev IS (2004) Mud volcanic natural phenomena in the South Caspian Basin: geology, fluid dynamics and environmental impact. Environ Geol 46:1012–1023
Judd AG, Hovland M, Dimitrov LI, Garcia Gil S, Jukes V (2002) The geological methane budget at continental margins and its influence on climate change. Geofluids 2:109–126
Kennett JP, Cannariato KG, Hendy IL, Behl RJ (2003) Methane hydrates in quaternary climate change. The clathrate gun hypothesis. American Geophysical Union, Washington, DC, p 216
Klemme HD, Ulmishek GF (1991) Effective petroleum source rocks of the world: stratigraphic distribution and controlling depositional factors. AAPG Bull 75:1809–1851
Kroeger KF, di Primio R, Horsfield B (2011) Atmospheric methane from organic carbon mobilization in sedimentary basins—The sleeping giant? Earth-Sci Rev 107:423–442
Lerche I, Yu Z, Torudbakken B, Thomsen RO (1997) Ice loading effects in sedimentary basins with reference to the Barents Sea. Mar Pet Geol 14:277–339
Levine JG, Wolff EW, Jones AE, Sime LC (2011) The role of atomic chlorine in glacial-interglacial changes in the carbon-13 content of atmospheric methane. Geoph Res Lett 38:L04801. doi:10.1029/2010GL046122
Link WK (1952) Significance of oil and gas seeps in world oil exploration. AAPG Bull 36:1505–1540
Luyendyk B, Kennett J, Clark JF (2005) Hypothesis for increased atmospheric methane input from hydrocarbon seeps on exposed continental shelves during glacial low sea level. Mar Pet Geol 22:591–596
Maslin MA, Thomas E (2003) Balancing the deglacial global carbon budget; the hydrate factor. Quatern Sci Rev 22:1729–1736
Mathews MD (1996) Migration—a view from the top. In: Schumacher D, Abrams MA (eds) Hydrocarbon migration and its near-surface expression. AAPG Memoir, vol 66. Penn Well Publishing, Tulsa, pp 139–155
Mellors R, Kilb D, Aliyev A, Gasanov A, Yetirmishli G (2007) Correlations between earthquakes and large mud volcano eruptions. J Geophys Res 112:B04304. doi:10.1029/2006JB004489
Melton JR, Whiticar MJ, Eby P (2011) Stable carbon isotope ratio analyses on trace methane from ice samples. Chem Geol 288:88–96
Milkov AV (2000) Worldwide distribution of submarine mud volcanoes and associated gas hydrates. Mar Geol 167:29–42
Milkov AV (2005) Molecular and stable isotope compositions of natural gas hydrates: a revised global dataset and basic interpretations in the context of geological settings. Org Geochem 36:681–702
Milkov AV, Sassen R (2002) Economic geology of offshore gas hydrate accumulations and provinces. Mar Pet Geol 19:1–11
Milkov AV, Sassen R (2003) Two-dimensional modeling of gas hydrate decomposition in the northwestern Gulf of Mexico: Significance to global change assessment. Global Planet Change 36:31–46
Milkov AV, Claypool GE, Lee Y-J, Dickens GR, Xu W, Borowski WS (2003) The ODP Leg 204 Scientific Party. In situ methane concentrations at Hydrate Ridge offshore Oregon: new constraints on the global gas hydrate inventory from an active margin. Geology 31:833–836

Möller L, Sowers T, Bock M, Spahni R, Behrens M, Schmitt J, Miller H, Fischer H (2013) Independent variations of CH_4 emissions and isotopic composition over the past 160,000 years. Nat Geosci 6:885–890

Morner NA (1978) Faulting, fracturing and seismicity as functions of glacioisostasy in Fennoscandia. Geology 6:41–45

Nisbet EG (2002) Have sudden large releases of methane from geological reservoirs occurred since the Last Glacial Maximum, and could such releases occur again? Phil Trans R Soc London 360:581–607

Pentecost A (1995) The Quaternary travertine deposits of Europe and Asia Minor. Quat Sci Rev 14:1005–1028

Petit JR, Jouzel J, Raynaud D, Barkov NI, Barnola JM, Basile I, Bender M, Chappellaz J, Davis M, Delaygue G, Delmotte M, Kotlyakov VM, Legrand M, Lipenkov VY, Lorius C, Pepin L, Ritz C, Saltzman E, Stievenard M (1999) Climate and atmospheric history of the past 420,000 years from the Vostok ice core, Antarctica. Nature 399:429–436

Petrenko VV, Smith AM, Brook EJ, Lowe D, Riedel K, Brailsford G, Hua Q, Schaefer H, Reeh N, Weiss RF, Etheridge D, Severinghaus JP (2009) $^{14}CH_4$ measurements in Greenland Ice: investigating Last Glacial Termination CH_4 sources. Science 324:506–508

Quigley DC, Hornafius JS, Luyendyk BP, Francis RD, Clark J, Washburn L (1999) Decrease in natural marine hydrocarbon seepage near Coal Oil Point, California, associated with offshore oil production. Geology 27:1047–1050

Revil A (2002) Genesis of mud volcanoes in sedimentary basins: a solitary wave-based mechanism. Geophys Res Lett 29:15-1–15-4

Saueressig G, Crowley JN, Bergamaschi P, Bruehl C, Brenninkmeijer CA, Fischer H (2001) Carbon 13 and D kinetic isotope effects in the reactions of CH_4 with O(1D) and OH: new laboratory measurements and their implications for the isotopic composition of stratospheric methane. J Geophys Res 106:23127–23138

Schaefer H, Whiticar MJ, Brook EJ, Petrenko VV, Ferretti DF, Severinghaus JP (2006) Ice record of $\delta^{13}C$ for atmospheric CH_4 across the Younger Dryas-Preboreal transition. Science 313:1109–1112

Severinghaus JP, Sowers T, Brook EJ, Alley RB, Bender ML (1998) Timing of abrupt climate change at the end of the Younger Dryas interval from thermally fractionated gases in polar ice. Nature 391:141–146

Sowers T (2006) Late Quaternary atmospheric CH_4 isotope record suggests marine clathrates are stable. Science 311:838–840

Spulber L, Etiope G, Baciu C, Malos C, Vlad SN (2010) Methane emission from natural gas seeps and mud volcanoes in Transylvania (Romania). Geofluids 10:463–475

Stewart I, Sauber J, Rose J (2000) Glacio-seismotectonics: ice sheets, crustal deformation and seismicity. Quatern Sci Rev 19:1367–1389

Svensen H, Planke S, Malthe-Sørenssen A, Jamtveit B, Myklebust R, Eidem T, Rey SS (2004) Release of methane from a volcanic basin as a mechanism for initial Eocene global warming. Nature 429:542–545

Thompson AM, Chappellaz JA, Fung IY, Kucsera TL (1993) The atmospheric CH_4 increase since the Last Glacial Maximum (2). Interactions with oxidants. Tellus 45B:242–257

Torres ME, Mix AC, Kinports K, Haley B, Klinkhammer GP, McManus J, de Angelis MA (2003) Is methane venting at the seafloor recorded by $\delta^{13}C$ of benthic foraminifera shells? Paleoceanography 18, 1062, doi:10.1029/2002PA000824

Valentine DL, Blanton DC, Reeburgh WS, Kastner M (2001) Water column methane oxidation adjacent to an area of active hydrate dissociation, Eel river Basin. Geochim Cosmochim Acta 65:2633–2640

Whiticar MJ, Schaefer H (2007) Constraining past global tropospheric methane budgets with carbon and hydrogen isotope ratios in ice. Philos Trans R Soc London Ser. A 365:1793–1828

Wu P, Johnston P, Lambeck K (1999) Postglacial rebound and fault instability in Fennoscandia. Geophy J Int 139:657–670

Chapter 9
Seeps in the Ancient World: Myths, Religions, and Social Development

The final chapter completes the discussion on natural hydrocarbon seepage by reporting engaging information regarding the significance and importance of seeps in the ancient world. Gas and oil seeps have, in fact, had a special role in ancient cultures, driving mythological legends, religious traditions, and contributing to human civilisation. As it is mainly the domain of historians and archaeologists, these concepts are poorly understood in the geological academic community. Descriptive information, not exhaustive, extensive, or critical (since the correctness of certain statements in the literature referenced are not addressed), is provided here. Examinations of facts are left to experts in the fields of history and archaeology. However, it is important to outline that in addition to an interest in archaeological and anthropological studies, historical reports of gas-oil manifestations are formidable evidence of the extreme longevity and persistence of seepage over time. Knowing that a certain "eternal fire" observed today was active at least in Biblical times indicates that it was not triggered by the recent drilling and production of petroleum (on the contrary, as mentioned in Chap. 8, petroleum extraction has often reduced natural seepage). What can be measured today (for example, the gas composition and its flux to the atmosphere), is probably also valid, at least in terms of orders of magnitude, for the past, and is very important for the discussions provided in Chaps. 6 and 8. Knowing present-day gas fluxes from a seep and knowing that a seep was active and vigorous two thousands years ago, we can estimate the total amount of gas that has been released to the atmosphere thus far. Such information may not only be relevant for atmospheric methane budget studies but may also be important for understanding the leaking potential of petroleum systems, whether or not they are commercial. The problem is understanding when seeps actually formed prior to being documented in historical or archaeological reports.

9.1 Seeps in Mythology and Religion

The impact of geological phenomena (earthquakes, volcanoes, and tsunamis) on ancient cultures is widely studied in archaeology and ancient history under the specific term "geomythology", as coined by the geologist Dorothy Vitaliano

G. Etiope, *Natural Gas Seepage*, DOI 10.1007/978-3-319-14601-0_9

(Vitaliano 1973). In this framework, petroleum (oil and gas) seeps have a peculiar role, as they have been the source of mythological tales, and Biblical and historical events (e.g., Yergin 1991; Piccardi and Masse 2007). Ancient historians and naturalists such as Pliny the Elder (AD 23–AD 79) were fundamental in converting myth into chronicles of observations and natural interpretation of gas-oil seeps in the Mediterranean area. A leading example is that of the Chimaera seep, as described in Chap. 7 (Fig. 2.2, Hosgormez et al. 2008; Etiope et al. 2011). Chimaera is a large burning gas seep near Cirali in ancient Lycia (Antalya Gulf, Turkey). The seep is adjacent to the ruined temple to Hephaestus, the Greek god of fire (2nd century BC, Hellenistic period). The name "Chimaera" refers to the legendary monstrous female fire-breathing creature killed by Bellerophon (Homer 2004). Since it was reported by Pliny the Elder in his *Historia Naturalis*, the existence of "Chimaera" fires issuing from the ground dates back at least two millennia. More recently, Spratt and Forbes (1847) tell about their travel in 1842:

> April 15th—Not far from the Deliktash, on the side of a mountain, Captain Beaufort discovered the yanar or perpetual fire, famous as the Chimaera of many ancient authors. We found it as brilliant as when he visited it, and also somewhat increased; for besides the large flame in the corner of the ruins described by him, there were small jets issuing from crevices in the sides of a crater-like cavity, five or six feet deep. At the bottom of this was a shallow puddle of sulphureous and turbid water, regarded by the Turks as a sovereign remedy for all skin diseases. We met here two old Turks attended by two black slaves, who has come from a distance to procure some of the soot deposited from the flames, valued as efficacious in the cure of sore eye-lids, and also as a dye for the eyebrows. They had been enjoying themselves by this ancient fireside for 2 days, cooking their meals and boiling their coffee on the flames of Chimaera.

Anyone who has visited Chimaera today can understand the truth in this story. The only difference today is that the puddle with turbid water does not currently exist. However, it is very likely that the water was hyperalkaline, of the same type found in similar serpentinised ultramafic rocks (see Chap. 7). The water was "a *sovereign remedy for all skin diseases*", exactly as claimed today in modern spas built at the methane-bearing hyperalkaline springs in Genova (Italy) and Cabeço de Vide (Portugal) (Boschetti et al. 2013; Etiope et al. 2013). Interestingly, recent papers (Yargicoglu 2012; Meyer-Dombard et al. 2014) reported the occurrence of a small discharge of hyperalkaline (pH: 11.9) water close to a burning gas vent of Chimaera, which could be a trace of the *turbid water* mentioned by Spratt and Forbes (1847).

Another link between mythology and gas seepage is that of the Delphi oracle in ancient Greece. The Sanctuary of Delphi is considered to be the most important religious location of the ancient Greek world. The Sanctuary was the pole of attraction for pilgrims for ~11 centuries, between 700 BC and AD 400. Pythia, a Delphic woman, was seated upon a tripod placed over a chasm in the *Adyton* (an inaccessible place inside the temple) (Fig. 9.1a–c). Plutarch, who served as a priest in the Oracle for many years, wrote that intoxicating vapors were released from the chasm and induced in Pythia a mantic state that enabled her to be the intermediary of the prophet god (Holland 1933). Two scientific articles (Piccardi 2000; De Boer et al. 2001) have proposed a link between faults, gas occurrence,

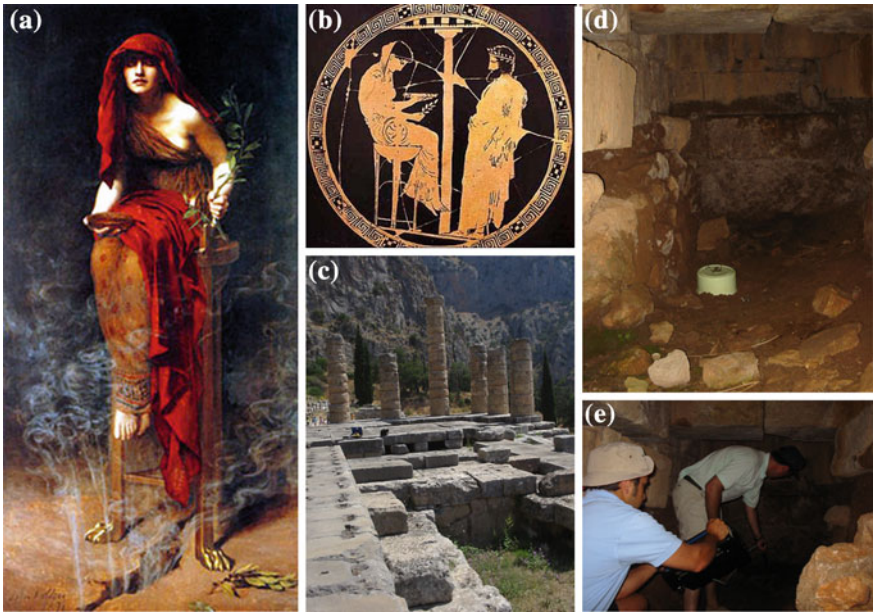

Fig. 9.1 **a** The *Priestess of Delphi* (1891) by John Collier. **b** The Delphic Oracle Kylix, a type of wine-drinking cup, by the painter Kodros, c. 440–430 BC (from the collection of Joan Cadden). **c** The Apollo Temple of Delphi. **d–e** In search of gas seepage in the temple undergrounds using closed-chambers and gas sniffers (Etiope et al. 2006; *photos* by G. Etiope and G. Papatheodorou)

and the Pythia prophetic properties. De Boer et al. (2001), in particular, suggested that the Temple of Apollo is located exactly above the intersection of two faults and that ethylene, a sweet-smelling hydrocarbon gas, exhaled from the rocks, inducing neurotoxic effects, trance, and delirium in the woman sitting in the *Adyton*. Geochemical investigations have successively indicated that the possibility of significant ethylene emissions is not obvious (Etiope et al. 2006). Ethylene could neither be produced in the present nor in the past within the deep carbonatic rocks of Delphi in sufficient amounts (hundreds of ppmv) to produce smelling vapors. Ethylene can only be found in very low amounts (some ppmv) in shallow clastic sediments with microbial gas, and there is no known way of forming hundreds of ppmv of ethylene seeping from accumulations in the subsurface. The geological framework of Delphi is characterised by a carbonate platform with a relatively high thermal regime that causes the advanced maturation (catagenetic) of sapropelic kerogen. Methane (not microbial) and ethane with a ratio of $C_1/C_2 < 100$ (as measured by Etiope et al. 2006) and bitumens are all typical products of this environment. However, the study actually found weak seepage for methane underground in the Apollo Temple (Fig. 9.1d, e). As indicated by the formation of travertine, whose isotopic composition ($\delta^{13}C \sim -18$ ‰) suggests CO_2 precipitation originating from CH_4 oxidation, CH_4 release must have been much greater thousands of years ago (Etiope et al. 2006). If any gas-linked neurotoxic effect of Pythia

must be invoked as suggested by historical tradition, it could be searched for in the possibility of oxygen depletion due to CH_4 exhalation in the enclosed and non-aerated *Adyton*, possibly accelerated by the use of a coal-burner with essential oils, perfumes, or drugs, leading to the production of carbon monoxide.

Most seeps, especially "everlasting fires", were initially directly documented in association with religious practices. Many are examples of the origin of sanctuaries (of all religions) linked to gas and flame emissions. The symbol of an eternal flame is a common concept in several religions. The discussion provided may touch the sensibility of many believers (an old proverb says: "play with the soldiers but do not touch the saints", in other words "don't mix the sacred with the profane"). However, the question is not whether geological phenomena discredit or prove that some ancient religious miracles were false (one could also argue that supernatural manifestations may be expressed through natural processes). The point is that, somehow, petroleum (gas and oil) seeps have influenced human social and cultural activity and behaviour in history; the issue is not a banal one. A few important examples are addressed in the following discussion.

Ancient fires in Iran and Azerbaijan (such as the *Yanardag*; Fig. 2.2d) were worshipped by the Zoroastrians. The "Pillars of Fire" near modern Baku became a centre of worship and pilgrimage (Fig. 9.2). The modern word Azerbaijan has its root in the word *Aberbadagan* (garden of fire). Pliny the Elder also observed "eternal fires" in Persia and Turkmenistan. In Iraq, the Baba Gurgur seep (Fig. 2.2d) was probably the "burning fiery furnace" into which Nebuchadnezzar cast the Jews (Yergin 1991).

Fig. 9.2 The "eternal flame" at the Zoroastrian Ateshgah "Fire Temple" near Baku, Azerbaijan. The temple was built over natural burning seeps that are today extinct. The flame in the photo is now artificially fed via a gas pipe. Active natural flames are instead found at Yanardag, located approximately 9 km NE (see Fig. 2.2) (photo by G. Etiope)

In the village of Manggarmas in Java, Indonesia, an eternal flame named Mrapen has been active at least since the 15th century's Demak Sultanate era. The Mrapen flame is considered sacred in Javanese culture and is used in the annual Buddhist ceremony. A similar burning gas seep, located within the Jwalamukhi Devi Temple in India (Himachal Pradesh State), is dedicated to the goddess Jwalamukhi, the deity of flaming mouth or light. The flame is worshiped as a deity by millions of pilgrims.

A legend of ancient Rome reports a stream of crude oil issuing from the ground in the centre of the city, around 38 BC during Augustus' rule. The local Jewish community interpreted it as "a sign that God's grace would soon flow into the world". The place became a meeting spot for the first Roman converts to Christianity and a church, today the Basilica of Santa Maria in Trastevere, was later built. The mysterious event was given the Latin name *fons olei* ("oil source" or "oil fountain"). Old chronicles report that the oil "for the time length of one day and one night, like a broad river reached the banks of the Tiber" (Rendina and Paradisi 2004). The inscription "fons olei" is today visible near the main altar of the church (Fig. 9.3).

Not far from this site in the centre of Rome, another church, San Giovanni de' Fiorentini, was apparently built in correspondence with gas exhalations from the ground near the Tiber River bank (Bersani et al. 2013). In the ancient Roman epoch (VI century, BC), a pagan altar, dedicated to *Ditis Patris et Proserpinae*, the Roman gods of the underworld, was located at this site. The site, named *Tarentum*, was associated by Roman writers (Valerius Maximus) to hot springs and gas exhalations, which led to the belief that an entrance to the lower world existed at the site and is the reason for the establishment of the cult of Dis Pater and Proserpina (Platner and Ashby 1929).

In northern Italy, close to the city of Genova (in the Ligurian region), the hyperalkaline springs of Acquasanta also have a link with ancient religious episodes. The water originated in serpentinised peridotites and has high concentrations of methane. The process is described in Sect. 7.1. Also, in this case a church, a sanctuary dedicated to the Virgin S. Mary, was built in place of a pagan altar for the cult of a nymph (the female nature deity typically associated with springs). According to tradition, sometime before 1400, a group of shepherds saw a "light" from the rocks in the river near the ruins of the pagan temple. The shepherds also found a small statue of S. Mary in the river. Afterward, the Christian sanctuary was built. Interestingly, this place is characterised by gas bubbling (see Fig. 7.2), with methane concentrations that can reach combustion levels (Boschetti et al. 2013). The "light" could have been a flame produced by gas burning.

9.2 Seeps in Social and Technological Development

In addition to cultural (mythological, literary, or religious) impact, hydrocarbon seeps have influenced the social and technological development of many ancient populations, thus contributing to global civilisation and, sometimes, to the outcome of wars.

Fig. 9.3 The inscription "fons olei" (*above*) and its explanation (*bottom*) near the main altar of the Basilica of Santa Maria in Trastevere, Roma (photo by G. Etiope)

The first evidence for petroleum usage is likely that of the natural bitumen found on stone tools from Neanderthal sites located in Syria dating from ~40,000 years ago (Connan 1999). Oil seeps and asphalts have been known and mined in the Dead Sea region since Neolithic times, 11,000–12,000 years ago (Forbes 1938; Mithen 2003). Ancient Persia (part of Iran) was, then, likely the territory in the ancient world with the highest exploitation of seeps. *Naft* (naphtha), a Persian-Arabic word for petroleum, was derived from the Akkadian-Assyrian *Napatu*, which means "to flare up". Heavy oil and asphalt seeps were used to build the palaces of Ur in Mesopotamia (3000 B.C.)

and all of the populations that successively remained within the seep-rich valleys of the Middle East, the Sumerians, Akkadians, Assyrians, Medes, and Persians, found multiple uses for petroleum products (Owen 1975). Oil and bitumen were used in various ways in ancient Iran: (1) as mortar in ziggurats (tower temples), city walls, and water gutters; (2) to caulk boats and to manufacture water-proof containers; (3) in fireworks; (4) in lamps; (5) to lubricate wheels; (6) to glue and cement gemstones in artefacts and decorations; (7) to remove dirty stains from clothes; (8) to heat and cook; and (9) as a medicine (Sorkhabi 2005). The Bible in Genesis 14:10 refers to wells of tar or slime as the basis for the wealth of Sodom and Gomorrah. Oil pits were mined near Ardericca, not far from Babylon, today Hillah, ~85 km south of Baghdad, where seeps are still active today. Ancient Egyptians used oil and bitumen for mummification and the word "mummy" is derived from the Arabic *mūmiyyah* (bitumen) or Persian *mum* (wax). Oil was also used as a medicine, a wound dressing, a liniment, and a laxative. As a result, the ancient literature of Greece and Rome contains many references to oil and gas. Herodotus (c. 484–425 BC) described the production of oil and salt from springs and the use of natural asphalt for construction of the walls and towers of Babylon.

As early as the 9th century BC, numerous incendiary and flaming weapons were produced by the Assyrians using oil seeps, culminating in the terrible "Greek fire" of the Eastern Roman Empire (Partington 1999). The weapon was likely invented by Kallinikos, a Greek or Syrian architect (ca. 672 AD), using a mixture of petroleum, sulphur, and other ingredients. Most modern scholars agree that the Greek fire was based on petroleum, either crude or refined, collected by the Byzantines from numerous seeps in the Taman peninsula. An ancient Greek text known as *De Administrando Imperio* (Moravcsik 1967) reported the following:

> Outside the city of Tamatarcha are many wells (springs) yielding naphtha. In Zichia, near the place called Pagi, which is in the region of Papagia and is inhabited by Zichians, are nine wells yielding naphtha, but the oils of the nine wells are not of the same colour, some of them being red, some yellow, some blackish. In Zichia, in the place called Papagi, near which is a village called Sapaxi, which means "dust", there is a spring yielding naphtha.

Tamatarcha, belonging to the Greek colony of Hermonassa, is located in modern Tmutarakan, near Krasnodar in the Taman peninsula. Archaeological work recovered the so-called "Tmutarakan pitchers" containing traces of hydrocarbons on their inner surfaces. The pitchers have been associated with shipments or exports of oil, collected in local seeps, and delivered to Constantinople to be used in the "Greek fire" weapon. Zichia was located at the southern boundary of Tamatarcha (Fig. 9.4). Both areas were, and still are today, characterised by the presence of numerous mud volcanoes with active oil seepage (e.g., Kikvadze et al. 2010). The GLOGOS data-set, as described in Chap. 2, lists 31 mud volcanoes within the Taman region.

The flammable liquid was generally used in siege warfare. However, the Byzantines were the first to apply it in naval wars against the Arabs. The fluid was stored in the bladders of warships, then pumped on the deck into nozzles or tubular projectors (*siphōn*) and ignited, creating a long jet of flame directed towards enemy ships. The Greek fire was practically an early weapon of mass destruction and

Fig. 9.4 **a** Map of the ancient territories north of the *Black Sea*, including the Taman peninsula, where petroleum was collected from seeps for use in the "Greek fire". Map by Guillelmo Del'Isle (1715?), Paris, from the David Rumsey Map Collection, www.davidrumsey.com. **b** The location of modern seeps (mud volcanoes) located in the same area, as extracted from the GLOGOS dataset and as described in Chap. 2

allowed for destruction of the Arab-Egyptian fleet by the Byzantine navy in a series of battles that decided the destiny of Europe.

Native Americans used oil seeps for more peaceful purposes, generally as a medicine. Spanish accounts indicate that local Indians bathed in oil springs to cure rheumatisms. Indians produced a gelatinous material of olefin hydrocarbons and applied it to human and animal skin in order to protect wounds, stimulate healing, and keep the skin moist. By many populations in America, Europe, and Asia, oil was used as a base for paints and to seal boats.

The usage of gas seeps for technical purposes has been widely reported in ancient Iraq and China. In Assyria, today the northeastern sector of Iraq, dozens of centuries before Christ, methane seeps were burned to heat bathwater. In 500 BC, the Chinese used seeps and near-surface gas pockets of flammable gas, with the support of bamboo pipes, to boil seawater, trap salt, and supply freshwater. These systems were the first water desalinisers. Methane was also used to cook food and feed lamps (Temple 2007).

An interesting fact is that "natural gas" technology was widely developed in Asia but not in Europe, at least until the 17th century, likely due, at least in part, to the fact that wood and coal were largely available for combustion applications in England, France, Germany, Poland, Russia, and Scandinavia. As a result of wood and coal availability, there was no need to use gas from seeps that were then, and are today, only abundant in Italy, Romania, and the Crimea and Taman peninsulas (see Fig. 2.8). Major understanding regarding the technical potential of natural gas was largely due to the studies of the Flemish chemist Jan Baptist van Helmont in the early 17th-century, and, a century later, by the British physician William Brownrigg and Italian physicist Alessandro Volta.

van Helmont was the founder of "pneumatic chemistry" and coined the word "gas" (from a phonetic transcription of the Greek word χάος, *Chaos,* following Paracelsus's terminology for "ultra-rarefied water", or from the Flemish word *gheest* or the Old English word *gast*, meaning ghost or spirit). van Helmont was the first to understand that there are different gaseous species distinct from atmospheric air. From 1737 to 1742, Brownrigg studied the burning gas occurring in coal mines in more detail and recognised its origin from Earth's interior. As outlined in the following excerpt, Brownrigg understood that large amounts of gas ("elastick exhalations") emanate from the Earth and enter the atmosphere (Tomory 2010):

> "From considering therefore the vast quantities of damps and elastic exhalations which are everywhere generated in the bowels of the earth, and from thence continually expire into the atmosphere, it seems highly reasonable to believe that that large and constant expanse of air absorbed from the atmosphere by vegetables and animals, and consumed by fire an by various other ways continually reduced to a fixed state, is, in a great measure, again repaired by those elastic exhalations which continually arise from the subterraneal regions of the earth".

The excerpt above is likely the first scientific discussion about seepage and its impact on the environment. A few years later, from 1776 to 1780, Alessandro Volta recognised "inflammable air from marshes", in other words methane. During his

holidays on Lake Maggiore (in Northern Italy), Volta observed gas bubbles from the muddy bottom of the water lake. He successively studied gas from the burning seeps of Pietramala in Tuscany (a thermogenic gas, see Table 5.1) and understood the combustion and explosive potential of the gas after electrical sparking. He then invented an inflammable air gun, called Volta's Pistol, and a "Perpetual Lamp".

The examples above, from the ancient world to the modern era, indicate that the discovery of technical and energy qualities of petroleum material, either fluid, semisolid, or solid have had a considerable impact on the development of human communities in different fields, from the urbanization of cities to transport, marketing, and military power, to the improvement of individual and social wellness. The passage from seeps to underground reservoirs, mainly within the first wells drilled in China (in the 13th century) and then in Azerbaijan, Poland, Romania, and North America (1800s), which triggered the industrial revolution, was a logical follow-up. Our technological progress and daily life is deeply dependent on the use of hydrocarbons and the availability of their resources is, as well known, a basic factor affecting our present and future.

References

Bersani P, Nisio S, Pizzino L (2013) Mineral waters, gaseous emissions and seismicity in the area between Rome and its Southern seashore: historical data and new contributions. Mem Descr Carta Geol It XCIII:409–438 (in Italian)

Boschetti T, Etiope G, Toscani L (2013) Abiotic methane in hyperalkaline springs of Genova, Italy. Procedia Earth Planet Sci 7:248–251

Connan J (1999) Use and trade of bitumen in antiquity and prehistory: molecular archaeology reveals secrets of past civilizations. Philos Trans R Soc London 354:33–50

De Boer JZ, Hale JR, Chanton J (2001) New evidence for the geological origins of the ancient Delphic oracle (Greece). Geology 29:707–710

Etiope G, Papatheodorou G, Christodoulou D, Geraga M, Favali P (2006) The geological links of the ancient Delphic Oracle (Greece): a reappraisal of natural gas occurrence and origin. Geology 34:821–824

Etiope G, Schoell M, Hosgormez H (2011) Abiotic methane flux from the Chimaera seep and Tekirova ophiolites (Turkey): understanding gas exhalation from low temperature serpentinization and implications for Mars. Earth Planet Sci Lett 310:96–104

Etiope G, Vance S, Christensen LE, Marques JM, Ribeiro da Costa I (2013) Methane in serpentinized ultramafic rocks in mainland Portugal. Mar Pet Geol 45:12–16

Forbes RJ (1938) Petroleum and bitumen in antiquity. Ambix 2:68–92

Holland LB (1933) The mantic mechanism at Delphi. Am J Archaeol 37:201–214

Homer (2004) The Iliad (trans: Fitzgerald R). Farrar, Straus and Giroux, New York, p 632

Hosgormez H, Etiope G, Yalçın MN (2008) New evidence for a mixed inorganic and organic origin of the Olympic Chimaera fire (Turkey): a large onshore seepage of abiogenic gas. Geofluids 8:263–275

Kikvadze O, Lavrushin V, Pokrovskii B, Polyak B (2010) Gases from mud volcanoes of western and central Caucasus. Geofluids 10:486–496

Meyer-Dombard DR, Woycheese KM, Yargicoglu EN, Cardace D, Shock EL, Güleçal-Pektas Y, Temel M (2014) High pH microbial ecosystems in a newly discovered, ephemeral,

serpentinizing fluid seep at Yanartaş (Chimaera), Turkey. Front Microbiol 5:723 doi:10.3389/fmicb.2014.00723
Mithen SJ (2003) After the ice: a global human history, 20,000–5,000 bc. Weidenfeld & Nicolson, London, p 622
Moravcsik G (ed) (1967) Constantine VII Porphyrogenitus, De Administrando Imperio, vol 1. Greek text (Eng. Trans: Jenkins RJH). Dumbarton Oaks Center for Byzantine Studies, Washington D.C
Owen EW (1975) The earliest oil industry: Chapter 1. In: Trek of the oil finders: a history of exploration for petroleum. AAPG, Tulsa, pp xv, 1647
Partington JR (1999) A history of Greek Fire and gunpowder. Johns Hopkins University Press, Baltimore, pp xxxiv + 381
Piccardi L (2000) Active faulting at Delphi, Greece: seismotectonic remarks and a hypothesis for the geological environment of a myth. Geology 28:651–654
Piccardi L, Masse WB (eds) (2007) Myth and Geology. Geological Society, London, Special Pub, 273
Platner SB, Ashby T (1929) A topographical dictionary of ancient Rome. Humphrey Milford. Oxford University Press, London
Rendina C, Paradisi D (2004) Le strade di Roma. Newton & Compton Editori, Roma (in Italian)
Sorkhabi R (2005) Pre-modern history of bitumen, oil and gas in Persia (Iran). Oil-Ind Hist 6:153–177
Spratt TAB, Forbes E (1847) Travels in Lycia, Milyas and the Cibyratis, in company with the Late Rev. E.T. Daniell. London (Van Voorst J) p 332
Temple R (2007) The genius of China: 3,000 years of science. Discovery & Invention, Inner Traditions, p 288
Tomory L (2010) William Brownrigg's papers on fire-damps. Notes Rec R Soc 64:261–270
Vitaliano D (1973) Legends of the Earth: their geological origins. Indiana University Press, Bloomington
Yargicoglu EN (2012) Experimental verifications of metabolic potential in deeply-sourced springs in western Turkey. Dissertation, University of Illinois at Chicago, http://hdl.handle.net/10027/9716
Yergin D (1991) The prize: the epic quest for oil, money, and power. Simon & Schuster, New York, p 912

Epilogue

Hydrocarbons are natural substances with the highest energy potential known. Following formation in deep crustal sedimentary and igneous rocks, their ascent to Earth's surface has had a primary role in the evolution of the biosphere and its inhabitants. The initial transformation of carbon dioxide (CO_2) into methane (CH_4), via the Sabatier reaction, marked the primordial transition from inorganic to organic chemistry, opening the way to biotic processes and life on Earth. Methane emissions on the ocean's floors have fuelled microbial and chemosynthetic-based benthic communities. For the geological past, methane emissions to the atmosphere have likely contributed to certain modifications of the climate. Since the dawn of human civilization, "technological man" has understood the practical benefit of hydrocarbon seeps for wellness and defence; "spiritual man" glimpsed a supernatural message; and poets have been inspired while imagining mythological creatures. Many, including myself, have been enchanted by the charm and natural beauty of some of these manifestations. Over the years, since they may pose some risks, may pollute the ground and natural waters, and may contribute, via the greenhouse effect, to global climate change, mankind has had to learn how to live with seeps. Mankind has also learned that geological sources feed hydrocarbon seeps, and that these sources have enormous value as an energy resource. Today this resource, for better or for worse, greatly influences global economies, politics, technologies, and the global environment; but has certainly improved our individual and social life style and wellness. Within this holistic perspective, natural gas seepage, the Earth's hydrocarbon degassing, appears to be a multifaceted, far-reaching and vital phenomenon. In this respect, I truly see a sense of coherence in the beliefs of worshippers who express their gratitude to an "eternal flame".

G. Etiope, *Natural Gas Seepage*, DOI 10.1007/978-3-319-14601-0

Index

G. Etiope, *Natural Gas Seepage*, DOI 10.1007/978-3-319-14601-0